Tissue engineering of the liver

Wung, Nelly

Award date:
2017

Awarding institution:
University of Bath

Tissue Engineering of the Liver

Nelly Wung

A thesis submitted for the degree of Doctor of Philosophy

University of Bath

Department of Biology & Biochemistry

September 2016

"A dreamer is one who can only find his way by moonlight, and his punishment is that he sees the dawn before the rest of the world."

Oscar Wilde

Abstract

Currently, the only cure for liver failure is orthotopic liver transplantation. However, there are insufficient donor organs available to treat every patient on the transplant list and many die before they are able to receive a liver transplant. The bioartificial liver (BAL) device is a potential extracorporeal treatment strategy utilising hepatocytes or hepatocyte-like cells (HLCs) within a bioreactor to recapitulate normal liver function and therefore 'bridge' a patient with liver failure until they receive a transplant. The work in this thesis utilised tissue engineering methods to develop novel approaches to BAL device design through development and characterisation of a polymer membrane scaffold ("PX") for hollow fibre bioreactor (HFB) culture and a HLC source generated from the transdifferentiation of pancreatic AR42J-B13 (B13) cells. A flat sheet membrane model was used for the development of asymmetrical, hydrophobic polystyrene (PS) phase inversion membranes. Oxygen plasma significantly increased PS membrane surface wettability through addition of oxygen functional groups to create an environment conducive for cell culture. The treated membrane was henceforth referred to as "PX". The culture medium HepatoZYME^{+} was investigated for its ability to induce transdifferentiation of B13 cells to HLCs and maintain the hepatic phenotype. Overall, HepatoZYME^{+}-cultured cells experienced viability loss. A diluted version, "50:50", showed induction of the hepatic markers carbamoylphosphate synthetase-1 (CPS-1) and HNF4α, as well as a change towards a HLC morphology. When using 50:50 as a maintenance medium, transdifferentiated HLCs retained loss of pancreatic amylase and also induction of hepatic markers, with comparable serum albumin secretion to the established Dex + OSM treatment. However, culture viability in 50:50 was still compromised. Therefore, HepatoZYME^{+} based media were deemed unsuitable for induction and maintenance compared to Dex-based protocols. PX flat sheet membranes were able to support culture of B13 cells and also the human osteosarcoma cell line, MG63, demonstrating improved cell attachment over non-surface treated PS membranes. PX membranes supported transdifferentiation of B13 cells to HLCs, presenting with loss of pancreatic amylase, induction of the hepatic markers transferrin, GS and CPS-1 and serum albumin secretion. Furthermore, PX showed no change in mass or loss of culture surface area over 15 days in culture conditions. Together, the novel membrane material and the media formulation and feeding regime developed have strong potential to be translated to a HFB setting and guide future BAL device design.

Acknowledgements

Firstly, I would like to thank my supervisors, Prof David Tosh and Dr Marianne Ellis for their continuous help, support and encouragement throughout my time at the University of Bath, and also for the opportunity to work in such an intriguing, multidisciplinary research area. I have learned so much from the both of you.

I would also like to thank the University of Bath and the Biotechnology and Biological Sciences Research Council for the funding provided for this PhD research.

Special thanks go to the members of the technical staff at the University of Bath for their assistance throughout this project. I would like to thank Dr Marianne Harkins, Dr Dan Lou-Hing, Dr Alex Ciupa and Fernando Acosta of the Department of Chemical Engineering; and Ursula Potter and Dr John Mitchels of the Microscopy and Analysis Suite for their technical support. I am very grateful to Dr Naoko Sano of the NEXUS facility at Newcastle University for the X-ray photoelectron spectroscopy analyses of my samples.

To the friends and colleagues of the labs I had the great pleasure of being part of in the Departments of Biology and Biochemistry and Chemical Engineering – thank you for all the help, advice, support and laughter throughout the years, as well as our truly memorable shared experiences both in and out of the lab.

From the Department of Biology and Biochemistry, I would like to thank Dr Zoë Burke, Dr Caroline Sangan, Dr Yu Chen "Cherry", James Corbett, Dr Leonard Griffiths, Dr Chris Brimson, Abdullah Alaqel, Dr Silvia Muñoz Descalzo, Elena Corujo Simon and Stephen Weston.

From the Department of Chemical Engineering, I would like to thank Dr Ian Benzeval, Dr Mike Storm, Sam Acott, Jaspreet Kular, Dr Iain Argyle and Dr Kim Luetchford.

Finally, I would like to thank my parents and my sister for their constant love, support and encouragement through this journey.

Declaration of Work in Conjunction with Others

Chapter 4, Section 4.2.5

X-ray photoelectron spectra were obtained at the National EPSRC XPS Users' Service (NEXUS) at Newcastle University, an EPSRC Mid-Range Facility by Dr Naoko Sano.

Contents

List of Figures

List of Tables

Abbreviations

2D	Two dimensional
3D	Three dimensional
2-Me	2-mercaptoethanol
AMC-BAL	Amsterdam Medical Centre Bioartificial Liver
ANOVA	Analysis of variance
AFM	Atomic force microscopy
ATR-FTIR	Attenuated total reflectance Fourier transform infrared
B13	Rat pancreatic cell line AR42J-B13
BAL	Bioartificial liver
BD	Bile duct
BLSS	Bioartificial Liver Support System
BMP-2	Bone morphogenetic protein-2
BSA	Bovine serum albumin
C	Carbon
CO_2	Carbon dioxide
cDNA	Complimentary DNA
C/EBPβ	CCAAT/enhancer-binding protein beta
CPS	Counts per second
CPS-1	Carbamoylphosphate synthetase-1
CYP	Cytochrome P450

DAPI	4', 6-diamidino-2-phenylindole
Dex	Dexamethasone
DEPC	Diethyl pyrocarbonate
DMEM	Dulbecco's Modified Eagle's Medium
DMEM+	Dulbecco's Modified Eagle's Medium with GlutaMAX
DMSO	Dimethyl sulfoxide
DNA	Deoxyribonucleic acid
dsDNA	Double-stranded DNA
ECM	Extracellular matrix
ECS	Extracapillary space
EDTA	Ethylenediaminetetraacetic acid
EGTA	Ethylene glycol-bis(2-aminoethylether)-N,N,N′,N′-tetraacetic acid
ELAD	Extracorporeal Liver Assist Device
ELISA	Enzyme-linked immunosorbent assay
FBS	Foetal bovine serum
FDA	Food and Drug Association
FGF-1	Fibroblast growth factor-1
FITC	Fluorescein isothiocyanate
FOV	Field of view
GIMP	GNU Image Manipulation Program
Gly	Glycine
GS	Glutamine synthetase

H	Hydrogen
H_2O	Water
HA	Hepatic artery
hESC	Human embryonic stem cell
HFB	Hollow fibre bioreactor
HGF	Hepatocyte growth factor
HLC	Hepatocyte-like cell
hMSC	Human mesenchymal stem cell
HNF4α	Hepatocyte nuclear factor 4 alpha
IMS	Industrial methylated spirits
iPSC	Induced pluripotent stem cell
LDH	Lactate dehydrogenase
MARS	Molecular Adsorbant Recirculating System
MELS	Modular Extracorporeal Liver System
MEM-NEAA	Minimum essential medium non-essential amino acids
MTT	3-(4,5-dimethylthiazol-2yl)-2,5-diphenyltetrazolium bromide
MWCO	Molecular weight cut off
N	Nitrogen
NaClO	Sodium hypochlorite
NaPyr	Sodium pyruvate
NEXUS	National EPSRC XPS Users' Service
NHS	National Health Service

NGS	Normal goat serum
NMP	N-methyl 2-pyrrolidinone
O	Oxygen
OSM	Oncostatin M
PBS	Phosphate buffered saline
PCR	Polymerase chain reaction
PERV	Porcine endogenous retrovirus
PFA	Paraformaldehyde
PH3	Phospho-histone H3
PLGA	Poly(D,L-lactide-*co*-glycolide)
PS	Polystyrene
PV	Portal vein
PX	Oxygen plasma treated polystyrene
qRT-PCR	Quantitative real time polymerase chain reaction
RCF	Relative centrifugal force
RF	Radio frequency
RNA	Ribonucleic acid
RT	Reverse transcription
RT-PCR	Reverse transcription polymerase chain reaction
SE	Standard error of the mean
SEM	Scanning electron microscopy
SPAD	Single pass albumin dialysis

TAE	Tris-acetate-EDTA
TCPS	Tissue culture polystyrene
TE	Tris-EDTA
TFN	Transferrin
TTR	Transthyretin
XPS	X-ray photoelectron spectroscopy

Chapter 1
Introduction

The liver is the largest internal organ of the human body and is responsible for a number of essential physiological functions. These include regulation of carbohydrate, fat and protein metabolism, storage, synthesis of proteins and detoxification of xeno- and endobiotics. Although the liver is a highly regenerative organ and is able to restore full organ mass where damage has occurred, if there is over 70% loss of liver function due to acute injury or chronic disease, the regenerative capability of the liver is impaired and it is unable to regain a physiological capacity of functions. This is classed as liver failure, which will cause severe deterioration in health and eventual death if not treated. However, the only cure for liver failure is an orthotopic liver transplant to replace lost liver function. Unfortunately, patients on the transplant waiting list often die before they are able to have a transplant due to lack of available donor livers. The number of deaths from liver failure is also increasing year upon year. Therefore, new therapeutic strategies are required to reduce patient mortality.

The bioartificial liver (BAL) device is a potential interim treatment for patients with liver failure. The principle behind the BAL device is to act as an extracorporeal support through replication of the normal physiological functions of the liver. This is done via the use of hepatocytes or hepatocyte-like cells (HLCs), housed in a bioreactor, thus allowing the patient to be bridged to transplantation or to allow the ailing liver to regenerate. Although there have been BAL devices in clinical trials, there are presently none in clinical usage as the trials do not show conclusively improved survival rates. This is namely due to a lack of a plentiful cell source that can fully function like liver cells and providing an optimum environment for these cells to function and thrive.

To address these issues, the work contained within this thesis presents a novel polystyrene membrane biomaterial (PX) for hollow fibre membrane bioreactor (HFB) design and a novel source of functional hepatocytes – transdifferentiated HLCs – to provide hepatic function, through the use of tissue engineering methods – a combination of molecular cell biology, regenerative medicine and chemical engineering theories and techniques.

This thesis can broadly be divided into two parts – Part I comprises the present Chapter, which gives a summary and background to the work. **Chapter 2** reviews the literature to date, describing liver biology, liver failure, the current status of BAL device designs and potential solutions. The aims and objectives of this thesis are detailed at the end of this chapter. The materials and methods utilised in the experimental work are then presented in **Chapter 3**.

Part II comprises the main body of the thesis and is divided into four Chapters. **Chapter 4** involves the development of a polystyrene phase inversion membrane suitable for hollow fibre bioreactor cell culture. **Chapter 5** investigates a potentially novel induction and maintenance culture medium for the hepatic transdifferentiation of the rat pancreatic cell line, AR42J-B13 (B13) in comparison with established transdifferentiation protocols. **Chapter 6** brings the results from **Chapters 4** and **5** together and examines the biocompatibility of PX flat sheet membranes with regards to its capacity to support cell culture, and most importantly, transdifferentiated HLCS, in comparison to other established biomaterials. Finally, **Chapter 7** provides overall conclusions and suggestions for future work, along with the implications of how these results and conclusions could be used for the development of a clinically viable next-generation BAL device.

Chapter 2
Literature Review

2.1 The human liver

2.1.1 Anatomy of the liver

The liver is the second largest organ of the human body and the largest gland. It is located in the right hypochondrium within the intraperitoneal space. The superior border of the liver extends from the 5th intercostal space and reaches below the costal margin on its inferior border. The liver has a dual blood supply, with 70% coming from the hepatic portal vein and the remaining 30% from the hepatic artery. In the adult human, the mean mass of the liver is 1800 g for men and 1400 g for women [1,2].

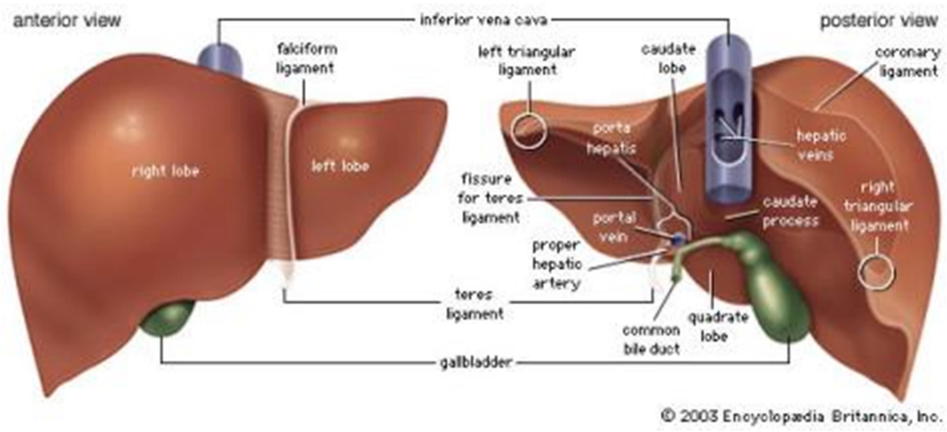

Figure 2.1 Anterior and posterior views of the liver. Image reproduced with permission from [3].

The anatomical division of the liver into lobes – left, right, caudate and quadrate (**Figure 2.1**) does not correlate to a division of liver functions. The lobes are further subdivided into lobules. Each lobule consists of a central vein that is surrounded by hepatocytes in a roughly hexagonal shape [4]. Sinusoids supplied by the hepatic artery separate the hepatocytes from each other, providing oxygen and nutrients, before draining into the central vein. Blood then leaves the liver via the hepatic vein.

There are over 100 billion cells in the liver, wherein 80% of the lobular parenchyma consists of hepatocytes [1]. The remaining non-parenchymal cell population includes ductal cells (cholangiocytes), sinusoidal endothelial cells, Kupffer cells, stellate cells and pit cells [2,5].

2.1.2 Liver physiology

The liver possesses multiple functions that are essential in ensuring that the normal physiological state of the human body is maintained. A summary of hepatic cell functions is described in **Table 2.1**. It is a metabolic organ, able to modulate glucose levels to prevent the body becoming hyper- or hypoglycaemic. This is done by storing glucose as glycogen (glycogenesis) or breaking down glycogen (glycogenolysis) in response to the pancreatic hormones insulin and glucagon respectively. The liver can also produce glucose (gluconeogenesis), particularly in severe starvation [6]. The liver is also involved in the oxidation of fatty acids, production of triglycerides and synthesising cholesterol and lipoproteins.

Table 2.1 Cells of the liver and their functions.

Cell	Function	References
Hepatocyte	Metabolism, synthesis, storage, xenobiotic and ammonia detoxification	[1,2]
Cholangiocyte	Bile transportation, bicarbonate and water secretion	[7]
Sinusoidal endothelial cell	Fenestrated barrier between sinusoidal blood and hepatocytes	[5]
Kupffer cell	Liver macrophages, cytokine production for mediating inflammation	[8]
Stellate cell	Liver regeneration, myofibroblast precursor, Vitamin A and lipid storage	[5,7,9]
Pit cell	Liver lymphocytes (natural killer cells), antitumorigenic, antiviral behaviour	[10]

As well as storing glycogen, the liver acts as a storage organ for vitamins A, B_{12} and D and dietary iron. It removes toxins from the body, an example being the removal of ammonia through conversion to urea, as well as drug detoxification. The production of bile by hepatocytes signifies an excretory role as well as an aid in digesting fats through emulsification. The liver is also able to synthesise blood coagulation factors, plasma proteins and amino acids, as well as remove old and damaged erythrocytes via phagocytosis [2].

2.1.3 The hepatocyte

The hepatocyte is the main functional unit of the liver. Hepatocytes make up the cellular majority of the liver parenchyma [1,2]. Morphologically, hepatocytes form irregular polyhedral shapes ranging between 20-30 μm in size, with the age, location and regenerative capability of the cell being the causes of size and shape variability [1]. 25% of hepatocytes also exhibit binuclearity [1]. Cellular volume adapts to changes in blood flow and osmotic load through the liver sinusoid. Increased cellular volume due to large solute quantities such as glucose, amino acids and bile acids consequently stimulates bile flow, exocytosis and protein and glycogen synthesis. Conversely, this causes the inhibition of proteolysis and glycogenolysis [1].

Hepatocytes are polarised cells that possess three functionally specialised membrane domains which differ from each other in protein, lipid and receptor compositions. The basolateral or sinusoidal domain is orientated towards the sinusoid, consisting of surface microvilli within the perisinusoidal space, also known as the space of Disse. The canalicular or apical domain forms the bile canaliculi that run between adjacent hepatocytes and the lateral domain extends from the edge of the canalicular domain to the basolateral domain (**Figure 2.1**) [1].

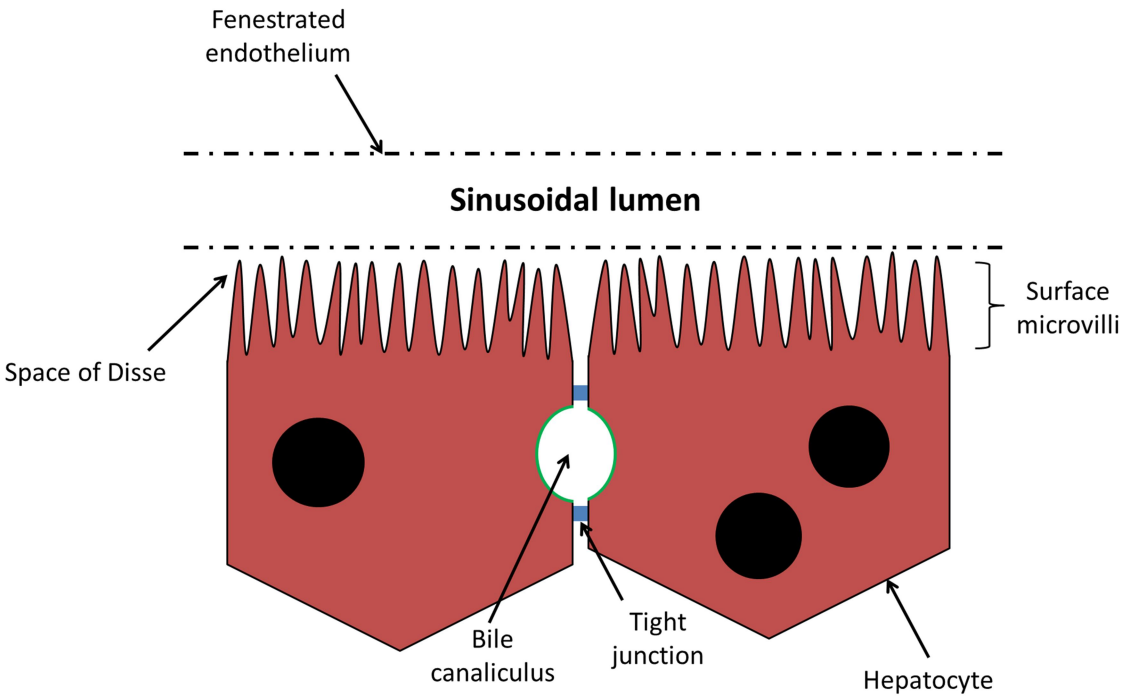

Figure 2.2 Ultrastructure of the hepatocyte. The basolateral domain contains surface microvilli within the space of Disse. Tight junctions (blue) separate the canalicular domain (green) from the lateral domain.

The fenestrated endothelium allows for efficient transfer of molecules from sinusoidal blood to the microvilli of the basolateral domain within the space of Disse, where they are taken up by the hepatocytes. The canalicular domain facilitates the movement of bile via transporter proteins into the bile canaliculus where it is transported to the bile ducts of the portal triad to be stored in the gall bladder, before eventual exit to the small intestine [1].

The distribution of hepatocytes in the liver lobule displays functional heterogeneity through metabolic gradients along the porto-venous axis. The porto-venous axis runs from the portal triad, which includes the hepatic artery, portal vein and bile duct, to the central vein. Hepatocytes that lie closer to the portal triad are classified as being in the periportal region whereas hepatocytes nearer to the central vein are located in the perivenous region. This phenomenon of functional heterogeneity is known as metabolic zonation and applies mainly to hepatocyte activity related to glucose metabolism, ammonia detoxification and xenobiotic metabolism (**Figure 2.3**) [4,11]. Other functions, such as the synthesis of serum transferrin (TFN), transthyretin (TTR) and albumin, are not zonally distributed and occur in all hepatocytes [11].

By reversing the flow of blood and therefore the concentration gradients of oxygen, nutrients and hormones, zonation can be altered. This is observed in glucose metabolism where zonal behaviours of gluconeogenesis and glycolysis are also reversed [12]. However, this behaviour is not a universal occurrence. For example, in the case of the ammonia detoxifying enzymes, carbamoylphosphate synthetase-1 (CPS-1) and glutamine synthetase (GS), reversing the flow of blood has no effect with regards to altering distribution of these enzymes along the porto-venous axis. Zonation of these enzymes is instead modulated by the Wnt/β-catenin signalling pathway [13,14].

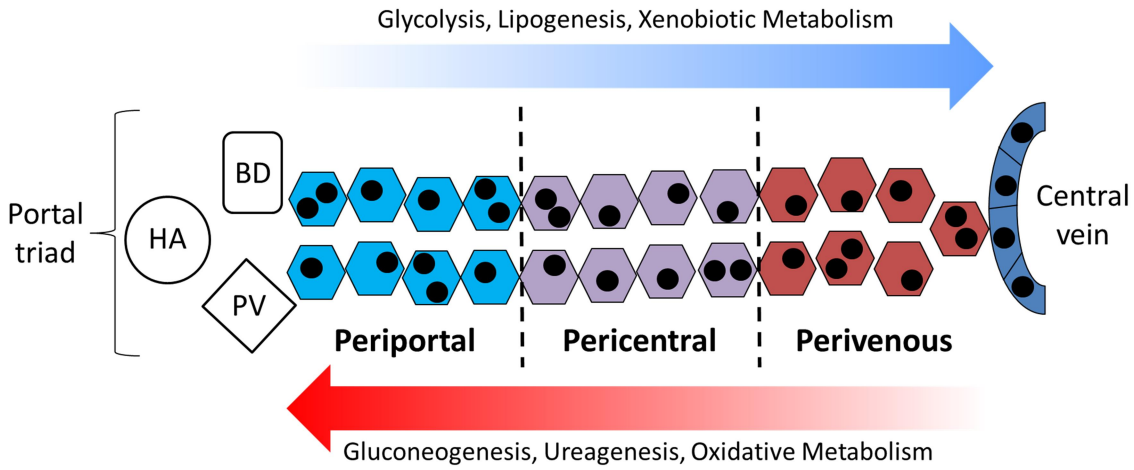

Figure 2.3 Metabolic zonation down the porto-venous axis of the liver. Hepatocytes radiate out from the central vein in 'plates' along with the portal triad. The portal triad consists of the bile duct (BD), hepatic artery (HA) and portal vein (PV). Blood enters the liver sinusoid via the hepatic artery and portal vein and drains into the central vein. Metabolic gradients alter functional expression in hepatocytes [4,11].

2.1.4 Liver failure

Liver failure is defined as over 70% loss of functional mass [1]. The liver is a highly regenerative organ and has the capability of functioning as normal and restoring full organ mass providing the damage does not exceed 70%. Beyond this limit, the liver is unable to regenerate significantly enough to overcome the damage and can no longer function at normal physiological levels and if left untreated, the outlook is poor [15]. Damage to the liver leads to life threatening complications that can cause pathophysiological problems in

other body systems due to the wide ranging functions of the liver, including kidney failure, hepatic encephalopathy, immune derangement, circulatory problems and coagulopathy.

Liver failure can be classed as one of three types – acute, chronic and acute-on-chronic. Acute liver failure is where there is no previous history of liver disease but a sudden loss of liver function occurs, resulting in coagulopathies and encephalopathies [16]. The major causative factor of acute liver failure in the UK and USA is drug-induced, particularly by paracetamol overdose. In developing countries, the predominant cause is due to viral aetiologies [16]. Chronic liver failure consists of deterioration in liver function due to the result of ongoing liver disease. Acute-on-chronic liver failure is a sudden deterioration in chronic liver disease over a period of four weeks due to a direct event (e.g. hepatoxicity) or an indirect event (e.g. infection) [17].

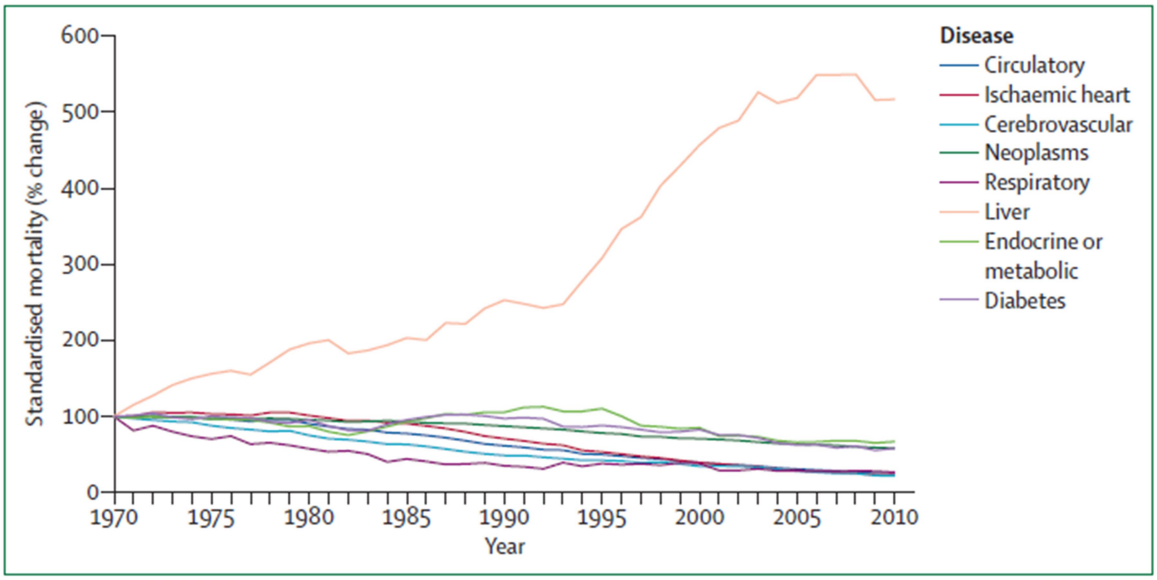

Figure 2.4 Standardised mortality rate percentage change of various diseases in the UK between 1970 and 2010. Data were normalised to 100% in 1970. Mortality from liver disease has increased to over 400% in 2010 since 1970, compared to other diseases which demonstrate an overall decline. Image reproduced with permission from [18].

Deaths from liver disease in the UK have been on the increase, despite other causes of mortality such as diabetes, cancer and respiratory conditions showing a decline between 1971 and 2010 (**Figure 2.4**) [18,19]. In England alone, deaths from liver disease steadily increased from 9,231 to 11,575 between 2001 and 2009. 37% of these deaths were primarily attributable to alcoholic liver disease. The remaining causes of liver failure

mortality were accounted for by liver cancer and other non-alcoholic liver diseases [20]. Notably, due to the extent of obesity, 25% of the general population of the UK is estimated to have non-alcoholic fatty liver disease [18]. The burden on the National Health Service (NHS) of the UK has been estimated at £3.5 billion per year for alcohol-related health problems and £5.5 billion for obesity related diseases [18]. This is likely to increase further if the current trend for liver disease mortality continues.

Orthotopic liver transplantation is currently the only cure for liver failure. As a result of this treatment, the patient is required to take immunosuppressive medication to prevent their body rejecting the donor organ. Although orthotopic liver transplantation is successful in restoring liver functionality in liver failure patients, there are not enough suitable donor organs available for the number of patients on the transplant waiting list that require them. Furthermore, the numbers of patients requiring transplantation in the UK has also been increasing year upon year as of 2015 [21]. Unfortunately, as a result of this mismatch in numbers, many patients deteriorate in condition and die before they can receive a transplant.

The increasing rate of mortality from liver disease has driven interest in developing alternative methods of treatment to ameliorate this rise. One approach for the preservation of remaining liver function and prevention of further organ deterioration is the development of an extracorporeal liver support device. The purpose of the liver support device is to recapitulate the physiological functions of the normal liver and therefore bridge the patient to transplantation. This interim approach of replacing lost liver function and preventing further liver deterioration would also be particularly useful in cases of acute liver failure that have demonstrated regeneration of the liver over time with no subsequent requirement for transplantation [15,22].

2.2 Liver support devices

There are two main approaches to liver support device design – artificial (non-biological) liver support systems and bioartificial (containing a biological component) liver devices. Both of these approaches are reviewed here.

2.2.1 Artificial liver devices

Due to deterioration of physiological liver functionality during liver failure, there is a subsequent increase of water soluble and protein bound toxic substances including ammonia, bilirubin and bile salts within the body. Under normal physiological circumstances, these would be detoxified and removed by the liver. Accumulation of these substances without treatment will eventually lead to pathophysiologies in multiple organ systems, including hepatic encephalopathy, immune impairment with subsequent susceptibility to infections and renal and circulatory dysfunction [23]. The result of these events can eventually lead to multiple organ failure and death if left untreated. Therefore, approaches utilising an artificial liver support device design have sought to take on the detoxification role of the physiological liver with the goal of reducing these pathological events within the body. Approaches to artificial liver device design include haemodialysis, haemofiltration, dilution, charcoal adsorption and blood plasma replacement for the removal of toxins from patient whole blood and plasma [24].

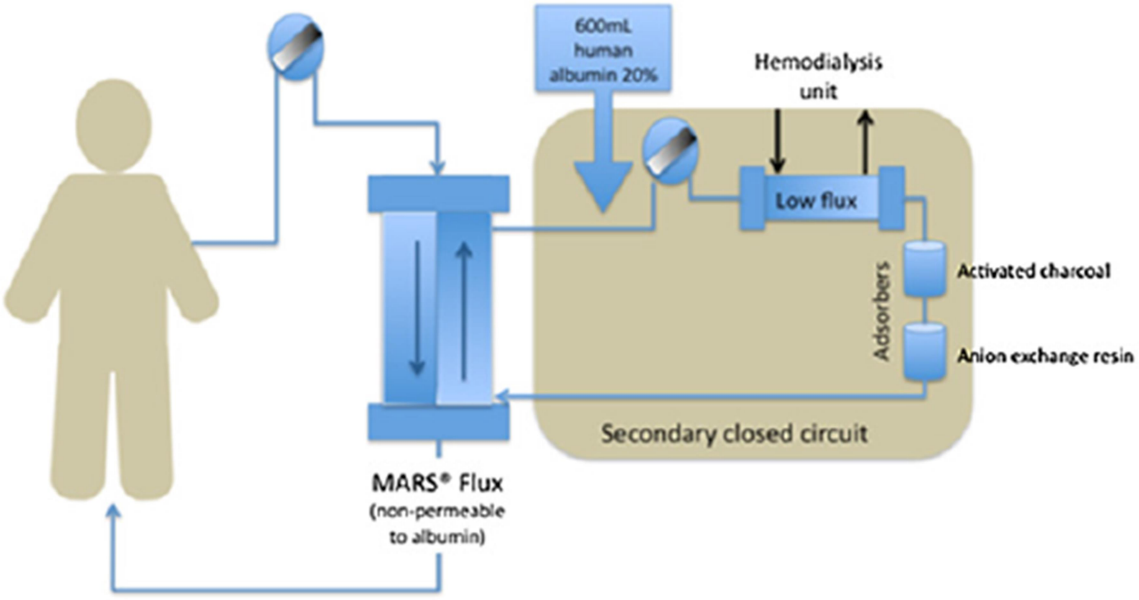

Figure 2.5 Structure of the Molecular Adsorbent Recirculating System (MARS) artificial liver device. The MARS system removes water soluble and protein bound toxins by haemodialysis through a semipermeable membrane into an albumin dialysate, which is further detoxified by activated charcoal and resin adsorption and secondary dialysis prior to recirculation. Image reproduced with permission from [17].

One of the most widely tested artificial liver devices is the Molecular Adsorbent Recirculating System (MARS) (**Figure 2.5**). MARS was originally developed in 1993 and takes the approach of removing water soluble and protein bound toxins from patient blood via haemodialysis using membrane separation techniques [23,25].

Semipermeable, albumin coated high flux polysulfone hollow fibre membranes (MARSFlux) facilitate diffusion of toxins through to a secondary circuit containing an albumin dialysate. The albumin dialysate is circulated through a separate, secondary system, where it is perfused over activated charcoal and anion exchange resin columns to remove albumin bound toxins, and undergoes low flux dialysis prior to recirculation of the regenerated dialysate through the device [23].

The efficacy of using MARS on patients with liver failure to reduce the effects of liver dysfunction has been assessed in several studies. Initial clinical results with a small group of 13 patients suggested that the device was well tolerated by patients and also demonstrated significant decreases in bilirubin, ammonia, serum creatinine and urea [26]. Further studies and a subsequent systematic review have also noted that MARS demonstrates improvement in hepatic encephalopathy [27–29], including a larger multicentre randomised controlled trial in 2007 [30].

However, there have been mixed reports as to whether MARS significantly improves patient survival when compared to standard medical treatment in the long term, particularly with regards to acute-on-chronic liver failure. A large clinical trial in 2013 noted that despite showing significant reductions in serum bilirubin, serum creatinine and improvement of hepatic encephalopathy after treatment with MARS, there was no overall improvement in patient survival coupling MARS with standard medical treatment versus using standard medical treatment alone for acute-on-chronic liver failure patients [31]. Furthermore, neither does it appear to restore the functional capability of native patient albumin [32]. Due to the conflicting reports on patient survival, these findings demonstrate the necessity of further investigations into whether this system is an overall safe benefit compared to current treatments for liver failure and therefore whether it should be utilised as routine therapy.

Single pass albumin dialysis (SPAD) utilises a similar system to MARS but does not involve recirculation of the albumin dialysate; it is constantly replenished with fresh

albumin dialysate. An *in vitro* study comparing the two methods suggested that SPAD was more effective than MARS in reducing ammonia and bilirubin levels whilst having comparable reductions in bile acid [33]. However, an *in vivo* study involving patients with liver failure suggested that MARS was able to eliminate bile acids at greater efficiency than SPAD [34]. This contrast highlights discrepancies between *in vitro* and *in vivo* studies, as the *in vitro* study did not take into account potential ongoing bile acid production and diffusion from tissues experienced in the *in vivo* study [34]. In light of this, further studies using an *in vivo* clinical setting would need to be performed to determine the efficacy of SPAD as a liver failure therapy.

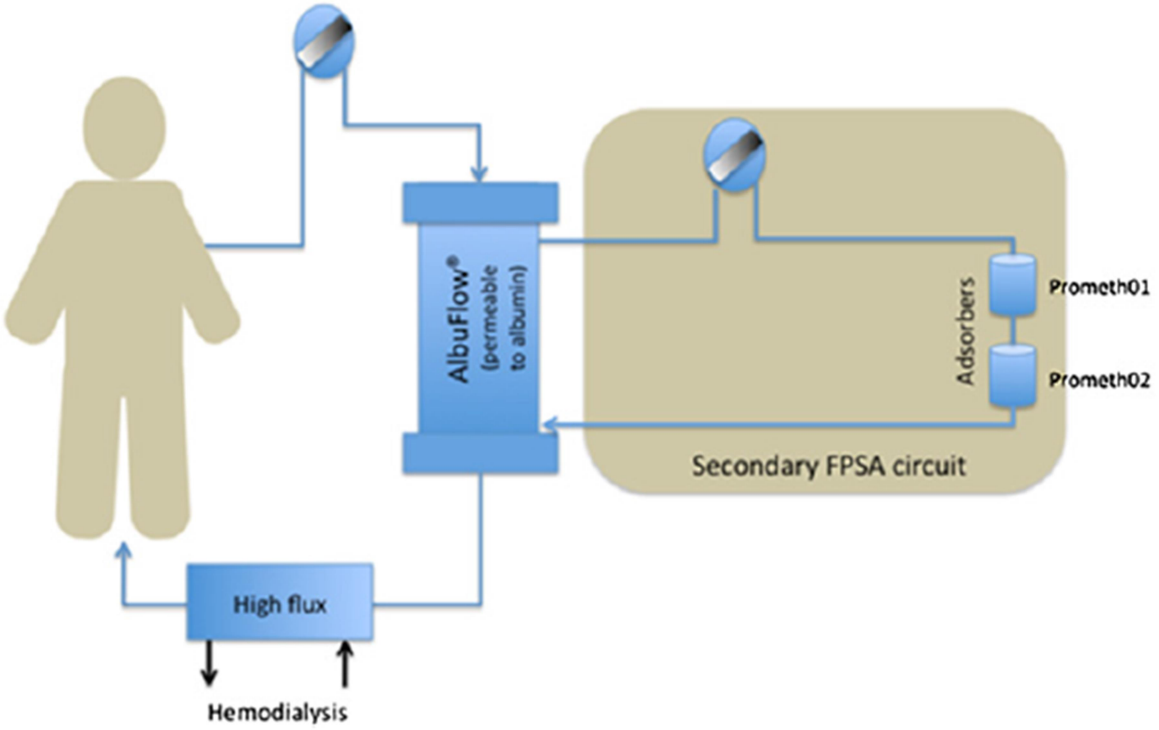

Figure 2.6 Structure of the Fractionated Plasma Separation and Adsorption (PROMETHEUS) artificial liver device. PROMETHEUS utilises plasmaphaeresis to initially filter albumin and low molecular weight plasma proteins. This fraction is purified using resin adsorbers before re-entering the bloodstream. Haemodialysis is then used to remove water soluble toxins from the blood. Image reproduced with permission from [17].

The Fractionated Plasma Separation and Adsorption (PROMETHEUS) artificial liver device offers a different approach to detoxification than that demonstrated by MARS or SPAD. The mechanism of PROMETHEUS utilises plasmaphaeresis, which functions by filtration of patient blood through an albumin permeable membrane (AlbuFlow) (**Figure**

2.6). This filtered fraction is passed through a secondary circuit containing a resin adsorbing agent and anion exchanger prior to re-entering the primary circuit which contains the rest of the patient's blood. To remove water soluble toxins, the blood, with the purified albumin fraction, undergoes haemodialysis prior to re-entering the patient [35]. PROMETHEUS has demonstrated patient safety and has shown utility in reducing total bilirubin, bile acid and ammonia concentrations along with elimination of water soluble toxins [36–41]. However, similarly to MARS, PROMETHEUS was able to clear serum cytokines but neither device significantly reduced the levels of serum cytokines in acute-on-chronic liver failure [42]. Similarly to MARS, when PROMETHEUS was utilised in combination with standard medical treatment in a randomised controlled trial for treatment of acute-on-chronic liver failure, no overall improvement in long term patient survival was found when using this device compared to using standard medical treatment alone [43].

Various meta-analyses assessing artificial liver devices have conflicting conclusions as to whether their therapeutic usage has an overall benefit on patient survival from liver failure. A study in 2004 suggested that there was no improvement in liver failure survival at all after treatment with artificial liver devices [44], although this study did not differentiate between the different types of liver failure and examined only 4 randomised controlled trials. A study from 2011 examined 8 randomised controlled trials where they noted improvement in acute liver failure but not acute-on-chronic liver failure [45], whereas the contrary was reported in a further study in 2013 looking at the results of 19 randomised controlled trials, suggesting improved patient survival in acute-on-chronic liver failure but not acute liver failure [46]. A study in 2015 of 10 randomised controlled trials again found no overall improvement in survival [29]. The mixed reports here are possibly affected by an insufficient number of suitable clinical trials for extensive comparison. Secondly, variance in the specific aetiological events and extent of liver deterioration leading to a patient's liver failure may impact upon the utility of the artificial liver device [47]. Therefore, these factors suggest that there is a great need for additional long term clinical trial data to determine if these devices are effective in improving overall patient survival beyond current medical therapies or only under specific circumstances.

Although artificial liver devices have shown some promise in toxin elimination in liver failure patients, a major limitation with their design is that they focus solely on detoxification and toxin removal. Artificial liver devices therefore do not replicate the full

functionality of the liver and are unable to recapitulate other functions such as synthesis of proteins and metabolism. These factors may contribute to the lack of overall improvement in patient survival when used therapeutically, with regards to reports of additional coagulopathies and metabolic disturbances associated with liver failure affecting overall device efficacy and patient survival [34,48,49].

In the normal physiological liver, such synthetic and metabolic functions are carried out by hepatocytes [50]. The importance of being able to replicate these aspects is demonstrated through the restoration of function in transplanted livers and improved survival. Therefore, to solve this issue, there has been great interest in the development of liver support devices known as bioartificial liver (BAL) devices. These systems incorporate a biological component in the way of hepatocytes or hepatocyte-like cells (HLCs), with the intention of recapitulating lost liver functions to prevent further patient deterioration.

2.2.2 Bioartificial liver devices

BAL devices are hybrid extracorporeal systems that incorporate hepatocytes or HLCs in a synthetically designed bioreactor within a flow system. The whole blood or plasma of the patient with liver failure is perfused through the BAL device, either coming into direct contact with the isolated hepatocytes or allowing a diffusion gradient to be formed between the plasma and hepatocytes separated from the plasma by virtue of being cultured on a semipermeable membrane.

The overarching goal of the BAL device is identical to that of the artificial liver device – to support a patient to transplantation and reduce the effects of liver dysfunction. Where artificial liver devices rely upon detoxification and removal using methods such as adsorption, filtration and dialysis, the BAL device seeks to utilise biological methods via functioning hepatocytes or HLCs to detoxify ammonia and xeno- and endobiotics. Furthermore, the incorporated cells would potentially provide additional liver functionality that is not performed by artificial liver devices, such as protein synthesis and metabolism of carbohydrates and lipids [51]. By recapitulation of these additional liver functions as well as taking on a detoxification and removal role, it is presumed that there will be an improvement in overall patient mortality from using a BAL device. Notably, use of smaller

scale BAL devices has been suggested as potential *in vitro* drug toxicity models, potentially reducing the need for animal models [51].

Various BAL device designs have entered clinical trials, but none are currently in active clinical usage [52,53]. A summary of five BAL devices with their design characteristics is shown in **Table 2.2**. Notably, the majority of these BAL devices utilise hollow fibre membranes as cell scaffolds within a bioreactor.

Table 2.2 Characteristics of five BAL devices that have undergone clinical trials.

BAL device	Bioreactor design	Cell source	Perfusion
HepaMate (previously HepatAssist 2000)	Hollow fibre with charcoal adsorption	Primary porcine hepatocytes	Plasma
Extracorporeal Liver Assist Device (ELAD)	Hollow fibre	C3A human hepatoma cell line	Plasma
Modular Extracorporeal Liver System (MELS)	Hybrid modular system with hollow fibre bioreactor, SPAD and filtration	Primary human liver cells from discarded donor livers	Plasma
Bioartificial Liver Support System (BLSS)	Hollow fibre	Primary porcine hepatocytes	Whole blood
Amsterdam Medical Centre Bioartificial Liver (AMC-BAL)	Perfused bed bioreactor with hollow fibres for gas exchange	Primary porcine hepatocytes (original design) HepaRG human liver progenitor cell line (current design; untested clinically)	Plasma

The HepaMate (formerly HepatAssist 2000) BAL device utilises cryopreserved primary porcine hepatocytes as the cell source attached to collagen coated dextran microcarriers [54]. These cells are housed within a hollow fibre bioreactor (HFB) and cultured on the extraluminal surfaces of semipermeable hollow fibre membranes. Plasma flows through the fibre lumen and is kept separated from the hepatocytes by the hollow fibre membranes, only allowing diffusion of specifically sized molecules across the membrane wall. Additional detoxification is supplied through the presence of a charcoal adsorption column within the system (**Figure 2.7**).

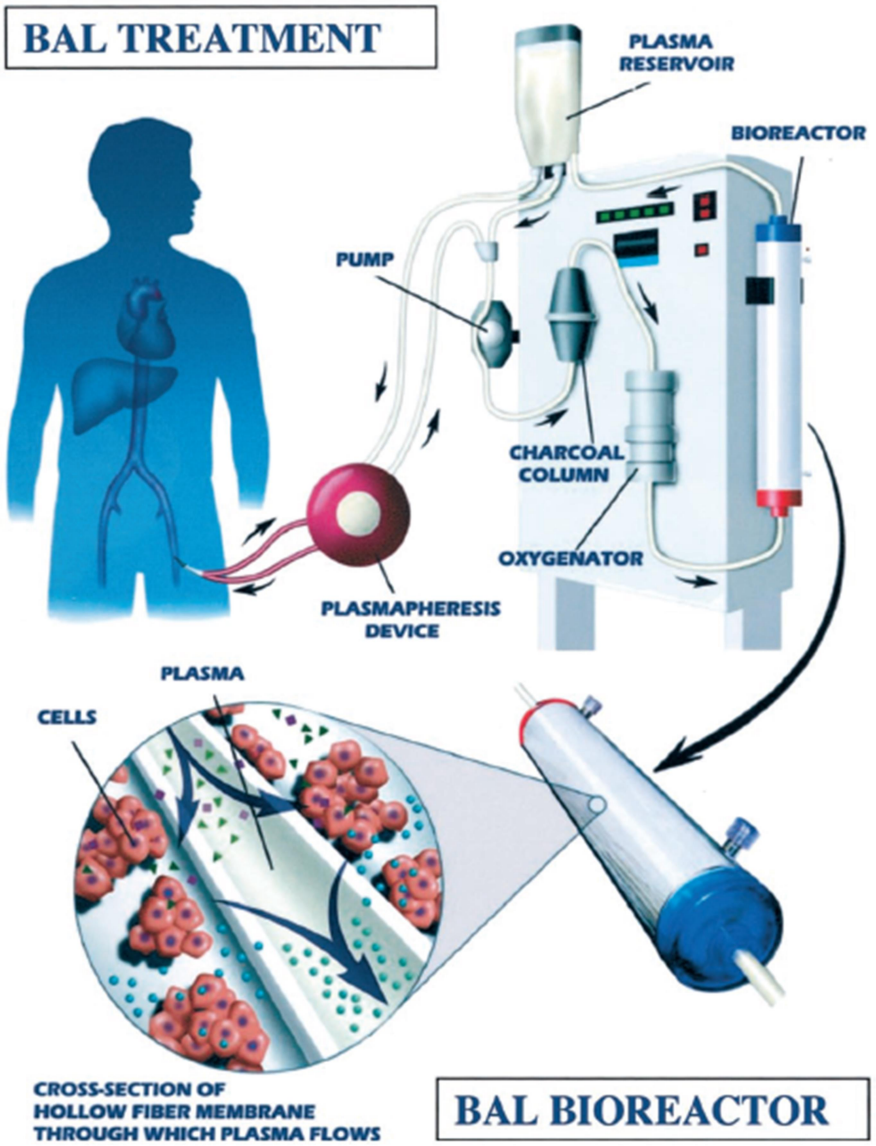

Figure 2.7 Structure of the HepatAssist 2000 BAL device (now HepaMate). This system utilises a hollow fibre bioreactor with primary porcine hepatocytes alongside a charcoal adsorption column. Image reproduced with permission from [55].

As HepatAssist, this BAL device has shown promising results in clinical trials for acute liver failure, demonstrating improvement of neurological symptoms and liver function enzymes, coupled with reduction of plasma ammonia and bilirubin [56,57]. However, a larger multicentre trial in 2004 involving 171 patients with acute liver failure and primary nonfunction following orthotopic liver transplantation failed to show any overall improvement in patient survival after 30 days within the BAL treated group compared to the control group [55]. Only on removal of the primary nonfunction patients from the statistical analysis was HepatAssist deemed to show improvement of survival in acute liver

failure patients, although no such similar analysis appeared to be performed for primary nonfunction patients by removal of acute liver failure patients. The overall efficacy of HepatAssist still remains unclear. Furthermore, the US Food and Drug Association (FDA) deemed that the trial did not demonstrate the efficacy of HepatAssist. Therefore, further clinical trials will be necessary to further clarify whether this device has a positive effect on liver failure patient survival [58].

The Extracorporeal Liver Assist Device (ELAD) utilises a similar HFB system to HepaMate. In contrast to HepaMate, the cells used are the human hepatoma cell line, C3A. The use of an established cell line provides an unlimited resource of HLCs that survive well when cultured *in vitro*. The cells are seeded within four cartridges containing hollow fibre membranes and patient plasma undergoes filtration and treatment with the cell inoculated cartridges prior to re-joining the bloodstream (**Figure 2.8**) [50,59,60].

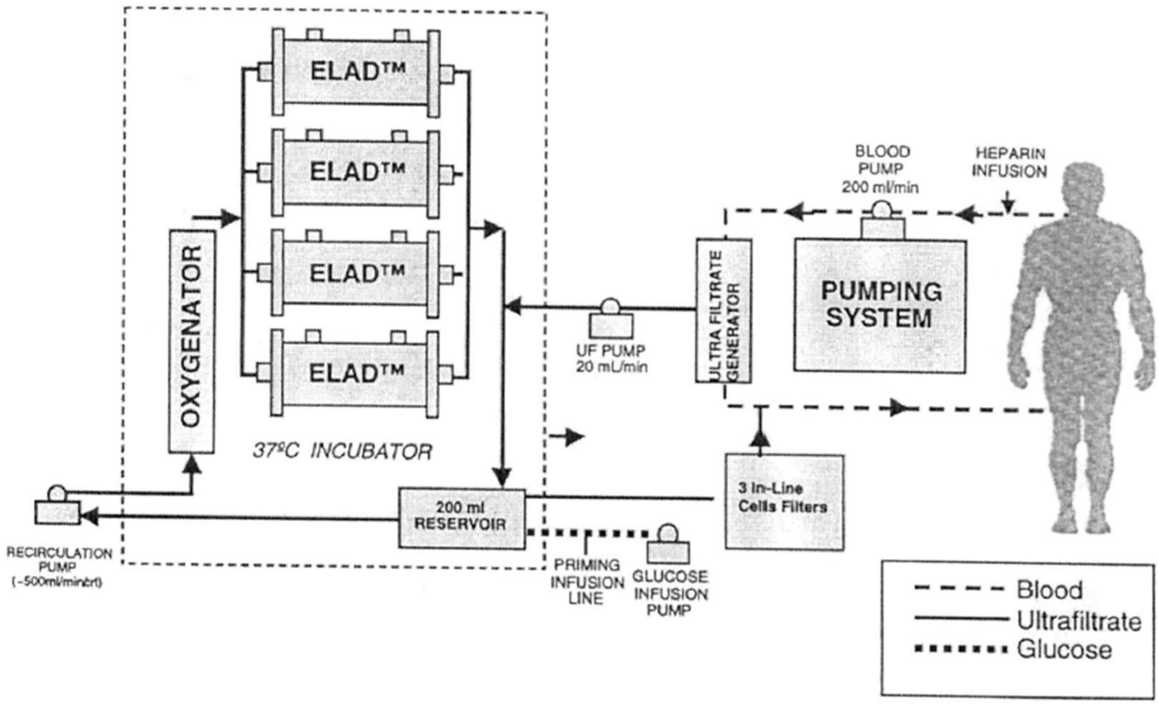

Figure 2.8 Structure of the Extracorporeal Liver Assist Device (ELAD). Plasma is filtered and circulated through the system. The four ELAD cartridges contain hollow fibres seeded with human C3A hepatoma cells. Image reproduced with permission from [60].

However, evidence on whether ELAD improves patient survival is mixed. A pilot study using ELAD to treat patients with acute liver failure suggested that there was some improvement in hepatic encephalopathy and ammonia levels but no significant changes in

blood lactate or serum albumin were found. Overall, survival was no different to that of the control group [61]. A second study examined the performance of ELAD with standard medical treatment in patients with acute-on-chronic liver failure suggesting no improvement at 30 days, but improvement at 90 days compared to standard medical treatment alone [62]. In a study involving patients with severe alcoholic hepatitis, no significant difference was found, although it was noted that patient age, level of renal function and extent of coagulopathies may impact upon the efficacy and overall specificity of this treatment toward a certain patient demographic [63,64].

The Modular Extracorporeal Liver System (MELS) utilises a woven network of 3 hollow fibre bundles (CellModule) for plasma inflow, outflow and gas exchange of oxygen and CO_2 respectively [58]. In addition to the HFB system, MELS can utilise two other modules that are added depending upon patient requirements. MELS incorporates SPAD (DetoxModule) and continuous haemofiltration (DialysisModule) for additional detoxification [65,66]. Therefore, MELS is considered to be a 'hybrid' of artificial and BAL configurations (**Figure 2.9**).

Currently, MELS utilises primary human liver cells sourced from donor livers unsuitable for transplantation comprising a population of parenchymal and nonparenchymal cells [66]. These donor livers include livers discarded due to presence of steatosis, cirrhosis or traumatic injury [66,67].

A Phase 1 clinical study in 2002 demonstrated the safety of MELS and was successful in bridging two patients to transplantation [67]. However, as the sample size was 8 patients, it is not possible to definitively comment on the overall efficacy of the system and comparative patient survival without further clinical studies to confirm the results from this study.

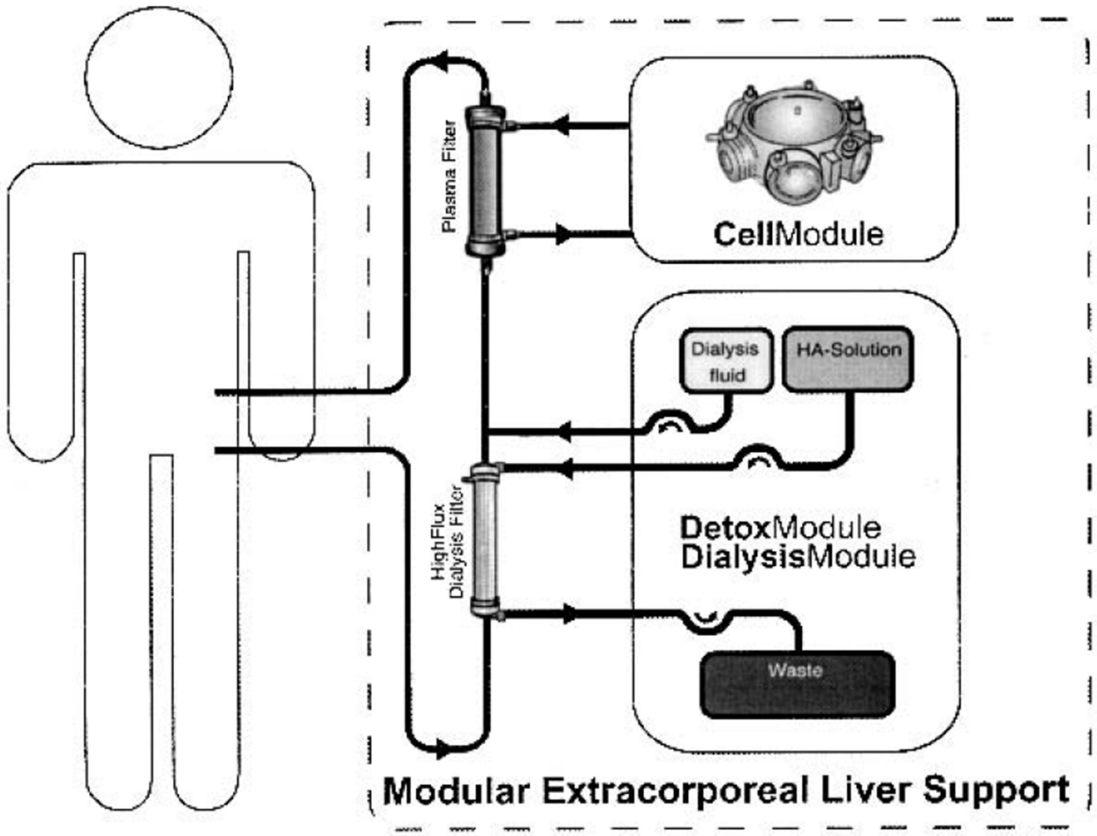

Figure 2.9 Structure of the Modular Extracorporeal Liver Support (MELS) device. The system comprises up to three modules containing primary human liver cells from discarded donor livers (the HFB CellModule), SPAD (DetoxModule) and continuous filtration (DialysisModule) for treatment of liver failure. Image reproduced with permission from [66].

In contrast to the other systems which are primarily perfused by the plasma fraction of patient whole blood, the Bioartificial Liver Support System (BLSS) utilises primary porcine hepatocytes and whole blood within a HFB system, with no separation of plasma (**Figure 2.10**) [68]. A Phase 1 clinical trial looking at the safety of the BLSS noted good tolerance with patients, although the sample size was only 4 [69]. To guide future development of the system, potential issues were highlighted, such as fluid overload due to lack of a haemodialysis or haemofiltration system, as well as potential clot formation within the system due to use of whole blood [69]. However, there is no further data referring to the comparative efficacy of BLSS against standard medical treatment.

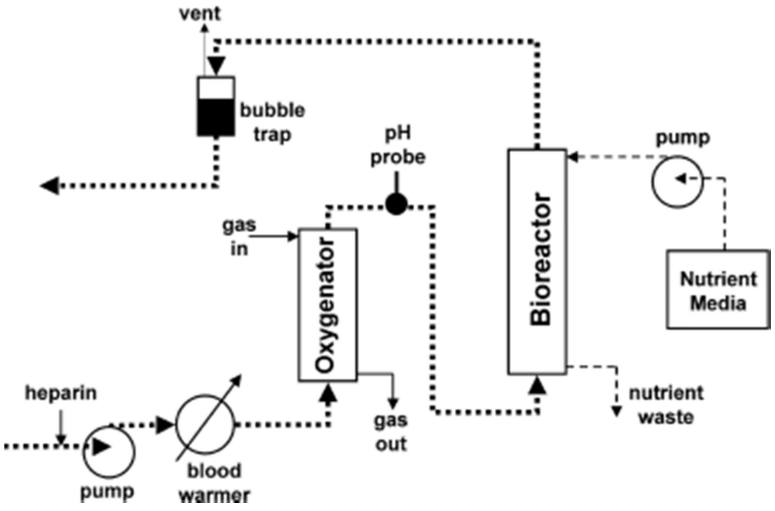

Figure 2.10 Structure of the Biological Liver Support System (BLSS). This system uses a HFB with primary porcine hepatocytes, perfused with the whole blood of the patient. Dotted lines represent the flow of whole blood through the system. Dashed lines represent the path of nutrient media in the system. Solid lines represent direction of gas flow. Image reproduced with permission from [68].

The Amsterdam Medical Centre-Bioartificial Liver Device (AMC-BAL) utilises a different approach to the overall bioreactor design. Unlike the other systems described in this review, which are primarily based upon a HFB system, the AMC-BAL involves direct contact between patient plasma and cells from use of a perfused bed bioreactor in a flow system. Instead of providing a scaffold for cell attachment, the hollow fibres in this device provide oxygenation of the system and removal of CO_2 (**Figure 2.11**) [70–72].

The initial Phase 1 clinical trial in 2002 with acute liver failure patients utilised primary porcine hepatocytes. The trial reported that no severe adverse effects were detected. Reduction of bilirubin and ammonia along with improved neurological symptoms were also found. Furthermore, 6 out of the 7 patients treated were bridged to transplantation, with the seventh not requiring orthotopic liver transplantation [73]. To comply with European Union (EU) standards disallowing use of porcine hepatocytes [70], a more recent iteration of the AMC-BAL utilises the human liver progenitor cell line HepaRG [74]. Although this version of the AMC-BAL has not been tested under a clinical setting, animal studies involving rats with acute liver failure have demonstrated reductions in hepatic encephalopathy progression, kidney failure and ammonia build-up [75].

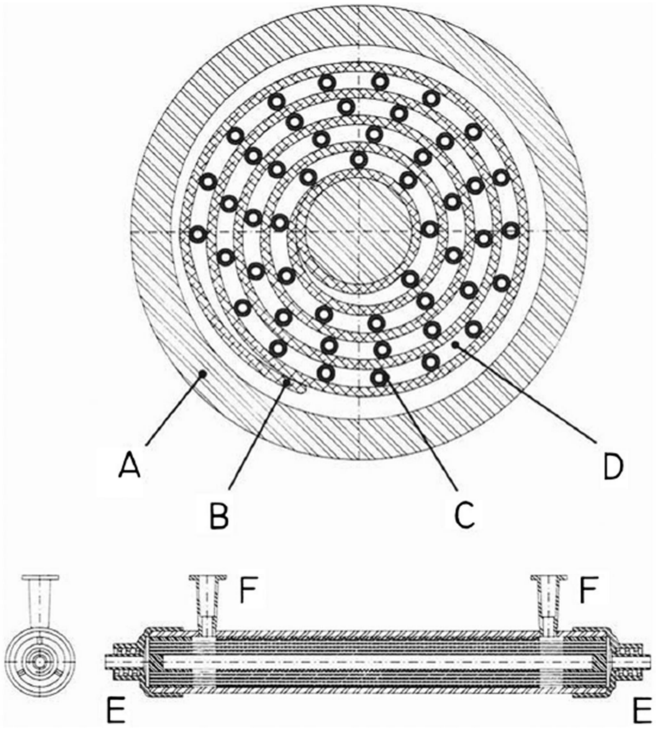

Figure 2.11 Structure of the Amsterdam Medical Centre-Bioartificial Liver (AMC-BAL). Polysulfone housing (**A**) surrounds a non-woven polyester matrix (**B**) for cell culture. Polypropylene hollow fibres (**C**) are utilised for gas exchange with gas perfusion entering via (**E**). Patient plasma enters the system through sideports (**F**) and is perfused through the extracapillary space between the hollow fibres (**D**). Image reproduced with permission from [72].

Notably, there is little data involving direct comparative experimental studies between the different BAL device designs. Comparative clinical studies between BAL devices are difficult due to large variations in overall bioreactor setup and cell source, patient population and data collection methods hampering study design. A study in 2007 compared the AMC-BAL with MELS under *in vitro* conditions utilising primary porcine hepatocytes and found that the devices were essentially comparable in hepatic functions after 7 days, although the AMC-BAL displayed higher ammonia elimination over 7 days [76]. However, MELS demonstrated reduced lactate dehydrogenase (LDH) release over the same time period. LDH release is a marker for reduced cell viability. The LDH reduction in MELS is possibly due to comparatively reduced shear stress on the cells from perfusion due to the presence of the semipermeable hollow fibre membranes separating them from the perfusion compartment in MELS, compared to the direct contact between cells and plasma in the AMC-BAL. Interestingly, this study did not utilise the full modular capability of MELS and only involved the CellModule rather than the additional SPAD

and filtration modules. Therefore, the full capability of the MELS unit was not portrayed in this study. An *in vivo* study utilising a full setup of MELS would provide a more direct comparison between the units.

The data reported from these BAL device designs, although showing the safety of the systems, suffer from lack of comprehensive clinical trial data with regards to determining overall efficacy and improvement to patient survival. The majority of studies are Phase 1 clinical trials, which are primarily to establish device safety under a clinical setting [77]. Similar to the findings with artificial liver devices, subsequent systematic reviews and meta-analyses on extracorporeal BAL device research with regards to overall patient survival are mixed in whether they offer an improvement upon standard medical treatment. A study by Gu et al in 2012 found that after analysis of 31 BAL device studies, of which only two were randomised controlled trials, neurological improvements were found along with improved elimination of ammonia and bilirubin. However, no significant improvement on patient survival was observed [78]. A further systematic review in 2013 suggested that BAL devices only reduced patient mortality with regards to acute liver failure, and not acute-on-chronic liver failure, with the reverse true for artificial liver devices [79]. Again, these conflicting reports highlight the necessity for suitably powered clinical testing of these devices to determine their overall effectiveness as clinical therapy.

BAL devices require further development to ensure greater efficacy, safety and improvement in patient survival before they can be regularly utilised in clinical situations. There are two major challenges to BAL device design that will affect the overall efficacy of the system and its entrance into the clinical setting. Firstly, it is necessary to select a cell source that can recapitulate the physiological functions of human hepatocytes as displayed *in vivo* and as such, can also be obtained in sufficient numbers for safe clinical usage. Secondly, it is important to ensure that the bioreactor can provide a suitable environment for the selected cells to thrive in and therefore function effectively as hepatocytes or HLCs [23,77,80]. As BAL device design is of primary interest in this thesis, further review of the literature will focus on this method of therapeutic liver support.

2.3 Cell sources for bioartificial liver devices

The extent of function of a BAL device is highly dependent on whether the selected cell source is able to behave similarly to the physiological liver. Certainly, orthotopic liver transplantation results in restoration of liver function through replacement of the damaged organ. However, as previously mentioned, suitable donors are scarce. This problem is the driving force behind the search for alternative sources of hepatocytes or cells that are able to function as *in vivo* hepatocytes. As summarised in **Section 2.2.2**, the various BAL devices that have undergone clinical trials utilise different types of hepatocytes or HLCs to replace lost liver functionality. The functional replicability of these cells will impact on how well they perform as a native hepatocyte substitute.

It is similarly imperative to consider as part of the hepatocyte cell source selection criteria the utility of sourcing sufficient quantities of cells. Along with the basic functional capabilities of the chosen cell source, the total number of hepatocytes within the BAL device will heavily impact upon the efficacy of the device. Based on animal studies, Tsiaoussis et al estimated that to provide sufficient support with a BAL device, the quantity of cells required in the system must represent 20% to 40% of the original liver mass [51,81], whereas on data based on surgical resections, this range was lowered to 10% to 30% [82]. Calculations based on theoretical analyses and data from human liver resections suggested a minimum number of approximately 1-2 x 10^{10} viable hepatocytes in the BAL device system for maintenance of normal liver function in a human [65,82,83]. As cells can be affected by the environment they are cultivated in, the overall efficacy of the hepatocyte or HLC efficacy should be, at minimum, equivalent to this cell number. In addition, there is a requirement that a cell source should be easily replenished and thus meet the demands of widespread clinical usage.

A third aspect to consider is the level of risk associated with the cell source. Use of non-human cell sources such as porcine hepatocytes increase the potential for zoonotic transmission of diseases to the patient. The potential for immunological responses from the patient from using non-autologous cells should also be considered, as well as the potential for metastatic formation from usage of cancer cell lines [77].

In summary, an ideal cell source would combine:

1. Replicable human hepatic function.
2. Sufficient supply for clinical requirements.
3. No risk in clinical usage.

2.3.1 Primary human hepatocytes

Primary human hepatocytes would be the gold standard cell line with regards to functionality. However, they suffer from similar issues to donor livers used for transplantation in that they are limited in supply and have low proliferative capacity [51]. Another hindrance with using primary human hepatocytes is that they undergo progressive dedifferentiation with loss of phenotype and functionality when cultured *in vitro*, a significant issue due to the *in vitro* nature of the BAL device [84,85]. Studies addressing this limitation have examined different approaches to countering dedifferentiation. These approaches include addition of differentiating promoting growth factors to the culture medium [85,86]; restoration of extracellular matrix (ECM) interactions through culture with ECM proteins [87,88]; or co-culture with other non-parenchymal hepatic cells such as stellate cells to recapitulate physiological cell-to-cell interactions and improve primary hepatocyte functionality [89,90]. Although these methods have reported improved primary hepatocyte functionality compared to culturing primary hepatocytes alone, no single standard method of solving the dedifferentiation issue is currently utilised. Determination of the optimum strategy is hindered due to issues comparing between systems involving varying lengths of culture time, methods of functional analyses and the differences in the ratio of non-parenchymal cells to hepatocytes utilised [91].

Primary human hepatocytes have been sourced from donor livers rejected for transplantation, notably in MELS [66,67]. However, as these cells are from livers presenting with pathological features such as steatosis and cirrhosis, their overall yield, functionality and viability between batches compared to suitable donor livers are likely to vary in quality [92,93].

The ability to store primary hepatocytes without adversely affecting viability and function is similarly questionable. The method of isolation, cryopreservation and thawing utilised

can also negatively affect the overall usable cell yield as well as their functional capability. Bhogal et al suggested that the critical time point for decreases in quality as part of the isolation process was between initial hepatectomy and subsequent perfusion of the liver slice prior to digestion and should not be longer than 3 hr [92]. A study in 2005 by Terry et al compared the effects of cryopreservation on hepatocytes from suitable and rejected donor livers. The findings from this study were that viability and functional capability with regards to CYP1A1/2 and albumin secretion was significantly reduced in cryopreserved hepatocytes of both sources when compared to freshly isolated hepatocytes [94]. Furthermore, freshly isolated hepatocytes from steatotic liver tissue showed reduced hepatic functionality and viability compared to freshly isolated hepatocytes from non-steatotic tissue [94]. Given these issues, development of a standardised isolation, cryopreservation and thawing protocol that preserves viability and function, and furthermore, preservation of the differentiated hepatocyte state, will be necessary before primary human hepatocytes can see widespread clinical use.

2.3.2 Primary porcine hepatocytes

The increased availability of primary porcine hepatocytes over their human counterpart has made them an attractive source of cells for BAL devices [57]. As described previously, these cells have been utilised in clinical trials for BAL devices with the HepatAssist, BLSS and AMC-BAL devices. Porcine hepatocytes are described as possessing a metabolic capability and efficacy similar to that of humans [80], of which examples include testosterone metabolism [95], albumin secretion and CYP1A activity [96,97]. However, a cross-species incompatibility with regards to activation of parts of the coagulation process in humans has been reported [67,80,98]. In addition, primary porcine hepatocytes display dedifferentiation *in vitro*, similar to primary human hepatocytes, which may affect their overall effectiveness as a cell source [99].

There is a risk of transmissible zoonosis by way of the porcine endogenous retrovirus (PERV) from porcine hepatocytes, particularly if patient blood or plasma comes in direct contact with the cells or if the retrovirus can pass through the separation membrane. There have been studies involving HepatAssist, BLSS and AMC-BAL regarding the potential transmission of PERV within these BAL device designs, although no transmission was

displayed [100–103]. In addition, use of primary porcine hepatocytes in clinical treatment is hampered by regulations banning xenotransplantation in many EU countries, meaning this cell source is not suitable for widespread clinical applications [24].

2.3.3 Hepatocyte cell lines

Hepatocyte cell lines, in contrast to primary hepatocytes, have an unlimited proliferative capacity. This feature solves the issue of producing enough cells for clinical usage. The human hepatoma cell line HepG2 and its subclone, C3A, are readily utilised in laboratory based BAL device studies due to their ease of proliferation and range of hepatic functions [104–107]. However, despite possessing a wide hepatic functionality, the HepG2 cell line has been shown to have reduced metabolic activity in comparison to primary hepatocytes [108,109]. C3A is the cell line of choice for the ELAD system and was selected for its improved capacity for albumin synthesis and metabolic capability over the parent HepG2 line [108]. However, a major issue with both HepG2 and C3A as BAL device cell sources is that they do not possess the full capability of ammonia detoxification displayed by primary hepatocytes. This issue may hinder the efficacy of the BAL device to eliminate toxins from the patient. In studies by Mavri-Damelin et al, it was found that both HepG2 and C3A do not have a functional urea cycle, with absence of the enzymes ornithine transcarbamylase and arginase-1 [110,111].

The AMC-BAL system is now currently utilising the HepaRG human liver progenitor cell line, which demonstrates cytochrome P450 (CYP) activity, ammonia elimination and protein synthesis [112,113]. Comparison with primary human hepatocytes showed that the HepaRG line has a similar level of functionality with regards to ammonia elimination and apolipoprotein A1 production [74]. It has been successfully tested using an *in vivo* rat acute liver failure rat model showing reduction of hepatic encephalopathy, kidney failure and ammonia levels compared to untreated controls [75]. Survival rates were noted to be approximately 50% higher although this was in comparison to untreated rats with acute liver failure rather than a comparison with standard treatment. Therefore, although these findings demonstrate the hepatic activity of the cell line within the system, it is not yet possible to predict survival improvement over current strategies with this experimental model. Clinical trials will be required to characterise the system further.

Notably, an *in vitro* comparison between HepaRG and C3A using this BAL device noted that the HepaRG cell line displayed comparatively improved xenobiotic metabolism, ammonia and lactate elimination over the C3A cell line [114]. However, it has also been reported that the HepaRG cell line possesses a slow growth rate and potentially loses its phenotype at higher cell passage numbers [51]. This may be problematic when producing sufficiently differentiated quantities of cells for use. Furthermore, HepRG has demonstrated greater resilience to hepatotoxic agents in comparison to primary human hepatocytes, suggesting that they may not be fully comparable as a model in drug hepatotoxicity testing [115].

2.3.4 Stem cells

A stem cell is broadly defined as an undifferentiated cell that upon division, either produces a similarly undifferentiated cell or undergoes differentiation to one or more cell types [116]. By utilising methods based upon liver development, human embryonic stem cells (hESCs) and induced pluripotent stem cells (iPSCs) have both been induced to differentiate into HLCs with a range of hepatocyte functions including ammonia elimination, albumin and urea synthesis and CYP activity [117–121]. However, differentiated yields from hESCs and iPSCs are currently not sufficient in numbers to be utilised in a clinical setting, particularly due to the loss of proliferative capacity upon differentiation. hESCs and iPSCs appear to possess a less mature functional phenotype when compared to adult primary hepatocytes, with the overall metabolic profile reminiscent of foetal hepatocytes in the case of albumin secretion and CYP activity [122,123]. Therefore, further work looking into protocols for improvement of phenotype maturation is required to improve comparability of these HLC sources. Furthermore, tumorigenicity and possible metastatic transfer to the patient is a major risk factor with using hESCs and iPSCs within a BAL device [124].

HLCs have also been derived from human mesenchymal stem cells (hMSCs). A study by Aurich et al has shown differentiation to HLCs from hMSCs harvested from bone marrow that displayed urea synthesis and increased glycogen deposition as well as expression of hepatocyte transcripts such as albumin, TFN and CPS-1 [125]. A further study successfully differentiated adipose tissue hMSCs to HLCs [126]. Despite these results, hMSC-derived

HLCs are not fully comparable to primary hepatocytes as there is currently no single protocol that offers a wide range of hepatic functionality [127]. hMSCs have also been reported to display heterogeneity in phenotype, not only dependent upon the tissue of origin, but also within the same tissue type [128]. This heterogeneity may impact on overall effectiveness of these cells. Furthermore, these issues limit potential usage of HLCs from hMSCs due to the requirement for standardisation and reduction of phenotypic variability.

2.3.5 Transdifferentiated hepatocyte-like cells

The use of transdifferentiated HLCs provides an alternative approach to obtaining HLCs suitable for use in a BAL device. Transdifferentiation constitutes the permanent conversion, or cellular reprogramming of one differentiated cell type to another differentiated cell type [129]. In the case of HLCs, an *in vitro* model of pancreatic cell transdifferentiation to HLCs has been developed utilising a rat pancreatic acinar cell line, AR42J-B13 (B13). Under treatment with the synthetic glucocorticoid hormone Dexamethasone (Dex), B13 cells lose their pancreatic phenotype, displaying loss of amylase expression. They eventually display hepatocyte-like morphology and functionality including expression of albumin, CCAAT/enhancer-binding protein beta (C/EBPβ), hepatocyte nuclear factor alpha (HNF4α), GS, CPS-1, glucokinase, production of acute phase proteins and replication of hepatitis B virus within 14 days of culture [130–133].

Use of this glucocorticoid treatment has also been replicated with mouse embryonic pancreas and human foetal and adult pancreatic cells to induce transdifferentiation of pancreatic cells to HLCs, thus demonstrating that it is not a species specific phenomenon [134–136]. Comparative gene expression analysis of markers such as CYP2E1, albumin, C/EBPβ and CPS-1 was similar between adult primary human hepatocytes and adult human pancreatic cells transdifferentiated to HLCs [135]. However, a small percentage of cells display resistance to Dex-based transdifferentiation and do not lose the pancreatic phenotype, producing a heterogeneous population of cells, and the maturity of transdifferentiated HLCs with regards to their metabolic behaviour in comparison to mature primary hepatocytes is not clear [129]. Further examination of the mechanisms involved in transdifferentiation, such as the growth factors and pathways involved will aid

understanding of the developmental background between the two tissue types. In addition, this information can be used to guide optimisation of current transdifferentiation protocols and improve upon the subsequent transdifferentiated HLC phenotype.

The range of hepatocyte functions displayed in transdifferentiated HLCs make them an attractive prospect for supplying a BAL device. Use of the B13 cell line in particular may provide a potentially limitless source of HLCs.

2.4 Bioreactor design for bioartificial liver devices

The bioreactor design and operating parameters can affect the quality of the BAL device due to the relationship the selected cell source has with the environment it is being cultured in [137]. The ideal bioreactor for a BAL device would be able to maintain a suitable growth and metabolic environment for the hepatocytes; allow bidirectional and efficient mass transport between the hepatocytes and blood or plasma; and prevent immunogenicity between the hepatocytes and the patient. The majority of BAL devices that have entered clinical trials utilise the hollow fibre bioreactor (HFB) configuration as their primary design. Other bioreactor designs that have been tested include perfused bed, fluidised bed, and flat membrane [65]. A summary of bioreactor characteristics is shown in **Table 2.3**.

Table 2.3 Characteristics of bioreactors used for hepatocyte culture.

Bioreactor design	Features	References
Perfused bed	Cells are cultured within a porous scaffold, in direct contact with medium flow	[138,139]
Fluidised bed	Cells are encapsulated and fluidised by vertical medium flow against gravity	[107,140,141]
Hollow fibre	Cells are cultured on porous fibre membrane scaffolds, separated from intraluminal medium flow	[142–144]
Flat membrane	Sandwich cell culture within a gel, or flat monolayer culture	[145,146]

HFBs provide a three dimensional (3D) culture system and are composed of semipermeable hollow fibre membranes that form a dual compartment system comprising

the intraluminal and extracapillary spaces. An example configuration for HFB cell culture is shown in **Figure 2.12**. One of the major advantages of using HFBs for cell culture is that they are an improved method of bioprocessing over other culture methods. HFBs have a greatly increased surface area for cell attachment and proliferation, thus allowing for higher density hepatocyte culture within a BAL device. In comparison with a tissue culture flask and stirred tank bioreactor to grow equivalent numbers of cells, HFBs only require 0.1% and 0.5% of their respective volumes [147]. In addition, a 3D culture system provides a more *in vivo* environment for cells to two dimensional (2D) culture as demonstrated by comparison of 2D and 3D scaffolds [148,149].

Common HFB configurations for cell culture involve culturing cells on the internal surface, which exposes the cells directly to perfusion within the lumen; on the outer surface, where the cells are protected from shear stress damage as they are not directly exposed to active perfusion (**Figure 2.12**); or suspension of cells within a gel in the extracapillary space (ECS) [150]. Perfusion may be intra- or extraluminal. Direct exposure of the cells to intraluminal perfusion, similar to perfused bed bioreactor systems, can provide enhanced bidirectional mass transfer between cell and perfusate due to lack of a separating barrier. However, overall cell viability may be compromised due to damage from shear stresses from the active flow [151]. It has been suggested that by cultivating cells internally within a semipermeable biocompatible polymer fibre, the seeded construct can be implanted within a patient and also avoids immune rejection due to control over the molecular weight cut off point of the membrane [152]. For the purposes of BAL device design, seeding internally within the fibre effectively leads to a 2D monolayer culture system. 3D intraluminal cell culture would require additional cell encapsulation [153].

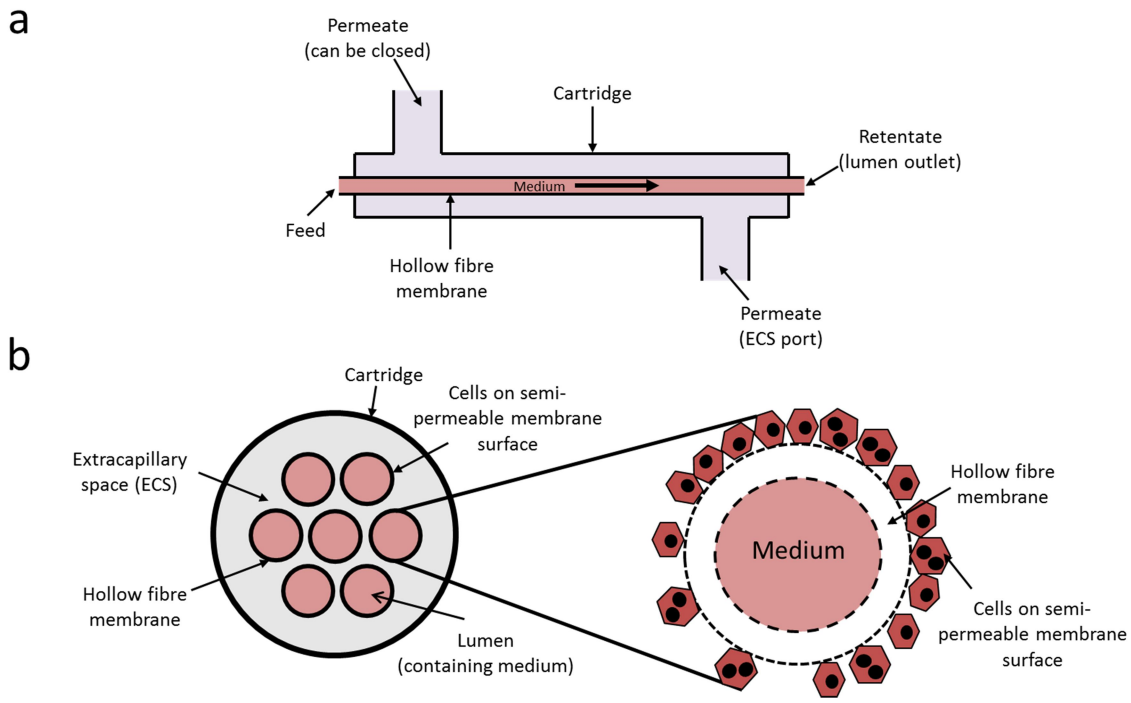

Figure 2.12 An example configuration for a hollow fibre bioreactor used for cell culture. (**a**) Longitudinal view; (**b**) cross sectional view with a close up of a single fibre. In this configuration, cells are seeded directly on to the outer surface (shell) of the hollow fibre membrane. Culture medium is perfused through the lumen of the hollow fibre and kept separate from the cultured cells. The semipermeable nature of the membrane can be tailored to a specific molecular weight cut off point for selective diffusion of nutrients and waste products between the intraluminal and extracapillary compartments.

A 3D culture system structured similarly to that of the physiological liver is provided by HFBs by the culture of cells on the exterior surface of a hollow fibre, within a bundle of similarly seeded fibres within the bioreactor cartridge. By culturing on the fibre outer surface, the cells are separated from the flow of media flowing through the fibre lumen. Shear stress damage on the cells from direct flow is therefore avoided due to the presence of the membrane [154]. The separation of cells from the perfusate is similar to the relationship between blood and hepatocytes within the liver sinusoid. Anatomically, a fenestrated endothelium separates the hepatocytes from sinusoidal blood flow (**Figure 2.2**). Immobilisation or encapsulation of the cells within a biocompatible ECM-like gel, such as collagen, sodium alginate or chitosan, has been shown to promote hepatic phenotype and function in hepatocyte culture [155–157] and could be contained within the ECS of the hollow fibre, thus retaining the dual compartment system described here [158].

The biomaterial utilised for the hollow fibre membranes can directly impact upon the hepatocyte phenotype quality and functionality as well as the replicability of the physiological environment within the system. As part of developmental consideration, these factors must be balanced out with a culture scaffold that is mechanically stable, semipermeable, supplies efficient mass transfer between cell and perfusate and is biocompatible. Hepatocytes are anchorage dependent cells, and for direct scaffold adherence, require a biomaterial that is not cytotoxic and is conducive to allowing sufficient densities of cells to attach and subsequently spread.

Hollow fibre membranes can be fabricated utilising a phase inversion method involving the immersion precipitation of a polymer-solvent dope solution in a suitable nonsolvent (ternary system) via dry-wet or wet-wet spinning to fabricate a polymer fibre membrane with a hollow lumen [154,159]. The precipitate may be porous, nonporous or asymmetrical, with a nonporous top layer and porous substructure [159]. The immersion precipitation technique can also be used to cast flat sheet membranes that can be used as a model system for determining hollow fibre structure. Control over polymer, solvent and nonsolvent selection allows for customisation and tailoring of hollow fibre membrane characteristics for the required purpose. Ideally, with a porous hollow fibre membrane scaffold, the size of the pores should be no larger than 5 μm to ensure that the attached cells do not enter the scaffold substructure [154]. Further tailoring of the molecular weight cut off (MWCO) of the porous membrane would allow selectivity in transfer of molecules across the membrane wall. Previous studies into hollow fibre bioreactor BAL device design have focused upon this method of molecular selection and have demonstrated that a MWCO of between 150 – 400 kDa is sufficient to prevent transfer of larger complement factors and immunoglobulins across the membrane by acting as an immuno-isolation barrier [160]. As the liver protein albumin, which has a molecular weight of 65 – 70 kDa, binds to several waste molecules such as bilirubin, an even lower MWCO of 100 kDa has been shown as sufficient for membrane separation within a HFB system [161].

Cell density within the bioreactor system must be balanced between hepatocyte metabolic capability and the fixed volume limitation of the HFB system. It has been previously reported that a high hepatocyte density within the BAL device is necessary to provide the required functional support for patients with acute liver failure [162]. A study using porcine hepatocytes demonstrated increased and thereafter consistently high urea

production and [^{3}H]-leucine incorporation at higher cell density levels, but conversely showed reduction in glucose-6-phosphatase activity [162]. It has also been observed that a higher hepatocyte density results in a reduction in oxygen consumption rate, potentially due to limitations in oxygen diffusivity, or approximation towards the density within the normal physiological liver leading to reduction in cellular stress [163]. These results show the need for further tailoring of the system to discover optimum hepatocyte functionality. In particular, mathematical modelling of HFB culture systems to determine experimental operating parameters is especially important for tailoring the system to the cell type [164]. Modelling of oxygen transport through the system is one particular example, as different cells types have different oxygen requirements. In the case of hepatocytes, zonation of some hepatic functions is oxygen and nutrient gradient dependent so parameters must be tightly controlled and understood to develop a truly replicable *in vitro* BAL system [53,83,163].

A hydrophobic surface is not considered conducive for hepatocyte cell culture [165], so methods have been developed to improve surface wettability for cell culture, such as surface modification by oxygen plasma treatment or surface grafting of bioactive molecules to promote cell attachment [166,167]. Using a polymer blend incorporating hydrophilic additives such as polyvinyl alcohol or polyethylene glycol can also reduce membrane hydrophobicity [168]. Comparative analysis between rat hepatocytes cultured on polycarbonate, polysulfone, cellulose acetate and polypropylene membranes determined that their metabolic behaviour improved upon more hydrophilic surfaces such as polycarbonate and cellulose acetate. This study demonstrates the importance of characterising the selected polymer membrane for overall biocompatibility and cell function [169].

Depending upon the overall purpose of the hollow fibre, the polymer utilised to fabricate the fibres may be biodegradable or non-biodegradable. The former characteristic is useful for implantation of therapeutic tissue constructs, where the scaffold degrades and leaves behind the cultured cells, such as with poly(D,L-lactide-*co*-glycolide) (PLGA) scaffolds [154,170,171]. For situations where scaffold degradation is unwanted, such as in a BAL device, or where long term culture is required, such as in cell expansion and differentiation, a non-biodegradable scaffold is ideal. Common polymers utilised for HFB cell culture include PLGA, polysulfone, polyethersulfone, cellulose acetate and

polypropylene [105,154,172–174]. Notably, polystyrene (PS), whilst widely established as the traditional biomaterial used in 2D cell culture, has yet to be reported as part of a phase inversion hollow fibre membrane system for cell culture purposes and thus warrants further research in this area.

2.5 Conclusion

The liver is responsible for multiple functions that contribute to the overall normal physiological state of the human body, such as metabolism, detoxification, synthesis of proteins, storage and removal. In the case where the liver is no longer able to perform these functions, such as in liver failure, systemic pathologies can develop, such as kidney failure, hepatic encephalopathy and coagulopathies. The only cure for liver failure is orthotopic liver transplantation, but there are not enough donor organs for the patients that require them. Therefore, many patients die before receiving a transplant. As the number of deaths from liver failure is increasing yearly, it is important to develop new therapeutic strategies to prevent liver failure mortality.

One such strategy is the BAL device. The BAL device intends to bridge patients to transplantation through the recapitulation and maintenance of normal physiological liver functions within the device. The HFB system provides a physical configuration that is similar to liver microanatomy. However, current BAL device designs have not gained clinical acceptance, as currently there is no overall improvement in patient survival over standard treatment procedures from their use. Notably, the two main issues with BAL device design are sourcing hepatocytes or HLCs that can function similarly to that of the normal liver; and secondly, providing a suitable culture environment for the cells so they can perform liver functions effectively.

2.6 Aims and objectives

The primary aim of the research in this thesis is to address the above BAL device design issues through the development of a novel polymer scaffold for HFB cell culture and functional hepatocyte source. Polystyrene has been proposed as a potential candidate for developing phase inversion hollow fibre membranes to be used in a BAL device due to its

known biocompatibility, cost-effectiveness and well documented use as a biomaterial for 2D cell culture. However, its usage to develop phase inversion membranes for cell culture has yet to be reported. A potential cell source for use in a BAL device is transdifferentiated HLCs generated from pancreatic cells. These cells display a wide range of hepatocyte functions and can be generated from an unlimited source through transdifferentiation of the pancreatic B13 cell line. However, further optimisation of the transdifferentiation protocol is required to improve the hepatic phenotype and remove heterogeneity within the culture population.

In summary, the objectives of the work in this thesis are as follows:

- Develop a ternary system for the fabrication of polystyrene phase inversion hollow fibre membranes using a flat sheet membrane model.
- Characterise the resultant membrane through morphology, surface wettability and surface chemistry.
- Investigate and characterise the utility of surface modifying polystyrene membranes with oxygen plasma to increase surface wettability for cell culture.
- Characterise the utility of the culture medium 'HepatoZYME^{+}' for inducing transdifferentiation of the rat pancreatic B13 cell line to HLCs.
- Investigate and characterise the utility of 'HepatoZYME^{+}' as a maintenance medium for transdifferentiated HLCs compared to established Dex-based transdifferentiation media.
- Investigate the utility of oxygen plasma surface modification to affect cell attachment on polystyrene membranes.
- Characterise the biocompatibility of oxygen plasma surface modified polystyrene membranes (PX) with regards to cell attachment and viability of the B13 and MG63 cell lines, relative to tissue culture polystyrene and PLGA.
- Investigate the utility of the B13 cell line to undergo transdifferentiation to HLCs on PX membranes.
- Investigate structural changes to PX membranes kept under culture conditions.

Chapter 3
Materials and Methods

This Chapter describes the Materials and Methods utilised throughout this thesis. Specific details of reagent preparation and methodology can be found in the relevant experimental Chapters.

3.1 Materials

3.1.1 Membrane preparation

Table 3.1 Polymers, solvents, cell culture substrates and membrane sterilisation reagents.

Material	Supplier	Product Number	Working Concentration
Industrial methylated spirits (IMS)	Sigma-Aldrich	458600-25L	70% (v/v) in deionised water
N-methyl 2-pyrrolidinone (NMP)	Acros Organics	127630025	80% (w/w) with specified polymer
Poly(D,L-lactide-*co*-glycolide) (75:25) (PLGA)	Evonik	RESOMER RG 756 S	20% (w/w) with NMP
Polystyrene (PS)	Sigma-Aldrich	182427-500G	20% (w/w) with NMP
Tissue culture polystyrene (TCPS) – 6-well plate	BD Biosciences	353046	n/a
Tissue culture polystyrene (TCPS) – 24-well plate	BD Biosciences	353047	n/a
Antibiotic-antimycotic solution	Sigma-Aldrich	A5955	1% (v/v) in PBS

3.1.2 AR42J-B13 cell culture

Section 3.1.2 describes the culture conditions and additional supplementation for the AR42J-B13 (B13) cell line. B13 cells are a subclone of the parent rat pancreatic cell line AR42J and were provided by Itaru Kojima (Tokyo, Japan).

Table 3.2 AR42J-B13 complete maintenance and proliferation medium.

Material	Supplier	Product Number	Working Concentration
Dulbecco's Modified Eagle's Medium (DMEM)	Sigma-Aldrich	D5546	1X
Foetal bovine serum (FBS)	Gibco	10270-106	10% (v/v)
L-glutamine	Sigma-Aldrich	G7513	1% (v/v)
Penicillin-streptomycin	Sigma-Aldrich	P4333	1% (v/v)

Table 3.3 AR42J-B13 additional complete medium supplements for transdifferentiation to HLCs.

Material	Supplier	Product Number	Stock Concentration	Working Concentration
Dexamethasone (Dex)	Sigma-Aldrich	D4902	1 mM in ethanol	1 μM
Oncostatin-M (OSM)	PeproTech	300-10T	10 μg/ml with 0.1% BSA in PBS	10 ng/ml

Table 3.4 HepatoZYME^{+} complete differentiation medium.

Material	Supplier	Product Number	Stock Concentration	Working Concentration
HepatoZYME-SFM	Gibco	11570536	1X	1X
L-glutamine	Sigma-Aldrich	G7513	100% (v/v)	0.5% (v/v) L-glutamine + 2-Me solution
Hepatocyte growth factor (HGF)	PeproTech	100-39	10 µg/ml with 0.1% BSA in PBS	10 ng/ml
Hydrocortisone	Sigma-Aldrich	H0888	1 mM in PBS	10 µM
2-mercaptoethanol (2-Me)	Sigma-Aldrich	M3148	1X	7 in 5000 (diluted in L-glutamine solution)
Oncostatin-M (OSM)	PeproTech	300-10T	10 µg/ml with 0.1% BSA in PBS	20 ng/ml
Penicillin-streptomycin	Sigma-Aldrich	P4333	100% (v/v)	1% (v/v)

Table 3.5 Additional complete medium supplements and cell culture reagents.

Material	Supplier	Product Code	Stock Concentration	Working Concentration
Dimethyl sulfoxide (DMSO)	Sigma-Aldrich	D8418	100% (v/v)	10% (v/v) in FBS for freezing medium
Phosphate buffered saline (PBS)	Sigma-Aldrich	D5652-50L	1X	1X
Trypsin-EDTA	Gibco	25300-054	0.05% (v/v)	Stock concentration

3.1.3 MG63 cell culture

Section 3.1.3 describes the culture conditions for the MG63 cell line. The MG63 cell line is a human osteosarcoma cell line obtained from ECACC.

Table 3.6 MG63 complete maintenance and proliferation medium.

Material	Supplier	Product Number	Working Concentration
Dulbecco's Modified Eagle's Medium with GlutaMAX (DMEM+)	Gibco	61965-026	1X
Foetal bovine serum (subsequently heat inactivated at 56°C for 30 min) (FBS)	Gibco	10270-106	10% (v/v) in DMEM+
Sodium pyruvate (NaPyr)	Gibco	11360-39	1% (v/v) in DMEM+
Minimum essential medium non-essential amino acids (MEM-NEAA)	Gibco	11140-035	1% (v/v) in DMEM+
Penicillin-streptomycin	Gibco	15140-122	1% (v/v) in DMEM+

Table 3.7 Additional cell culture reagents.

Material	Supplier	Product Number	Working Concentration
Phosphate buffered saline (PBS)	Sigma-Aldrich	D8537	1X
Trypan blue	Gibco	15250-061	1:1 with cell suspension

3.1.4 Immunofluorescence characterisation

Table 3.8 Fixation reagents.

Material	Supplier	Product Number	Working Concentration
Methanol	Sigma-Aldrich	34860	100% (v/v)
Paraformaldehyde (PFA)	Fisher	P/0840/53	4% (v/v) in PBS

Table 3.9 Immunofluorescence reagents.

Material	Supplier	Product Number	Working Concentration
Blocking buffer	Roche	11096176001	2% (w/v) in PBS
Normal goat serum (NGS)	Sigma-Aldrich	G9023	10% (v/v) in PBS
Bovine serum albumin (BSA)	Sigma-Aldrich	A7906	5% (v/v) in PBS
Glycine (Gly)	Sigma-Aldrich	G7403	0.3 M in PBS
4', 6-diamidino-2-phenylindole (DAPI)	Sigma-Aldrich	D9564	1 in 1000 in PBS
Triton X-100	Sigma-Aldrich	T9284	0.1% (v/v) or 1% (v/v) in PBS
Mowiol mounting medium	Calbiochem	475904	n/a

Table 3.10 Primary antibodies.

Primary Antibody	Species	Supplier	Dilution	Fixation	Blocking Buffer	Antigen Retrieval
Albumin	Mouse	Sigma-Aldrich	1 in 100	4% PFA	Roche	n/a
Amylase	Rabbit	Sigma-Aldrich	1 in 100	4% PFA	Roche	n/a
CPS-1	Rabbit	Abcam	1 in 300	Methanol (ice cold)	NGS-BSA-Gly	n/a
GS	Mouse	BD Transduction Laboratories	1 in 300	4% PFA or Methanol (ice cold)	Roche	n/a
HNF4α	Rabbit	Santa Cruz	1 in 100	4% PFA	Roche	n/a
PH3	Rabbit	Milipore	1 in 100	4% PFA	Roche	n/a
TFN	Rabbit	Dako	1 in 100	4% PFA	Roche	n/a

Table 3.11 Secondary antibodies.

Secondary Antibody	Species	Supplier	Dilution
Alexa Fluor 546	Rabbit conjugated	Invitrogen	1 in 500
Alexa Fluor 594	Rabbit conjugated	Invitrogen	1 in 1000
Fluorescein isothiocyanate (FITC)	Mouse conjugated	Vector Laboratories	1 in 100
Fluorescein isothiocyanate (FITC)	Rabbit conjugated	Vector Laboratories	1 in 100

3.1.5 RT-PCR characterisation

Table 3.12 RNA extraction and cDNA synthesis reagents.

Material	Supplier	Product Number
10X DNase I buffer	Ambion	8170G
Chloroform	Sigma-Aldrich	132950
Diethyl pyrocarbonate (DEPC)	Sigma-Aldrich	D5758
rDNase I	Ambion	AM2235
Ethylene glycol-bis(2-aminoethylether)-N,N,N′,N′-tetraacetic acid (EGTA)	Sigma-Aldrich	E3889
Ethanol (absolute)	VWR	20821.330
Isopropanol	Fisher	P/7490/17
Oligo Dt 15 primer	Promega	C110A
Omniscript RT Kit	Qiagen	205113
ReddyMix PCR MasterMix	Thermo Scientific	AB-0575
RNAsin plus	Promega	N261A
Tri-Reagent	Sigma-Aldrich	T9424

Table 3.13 Rat PCR primers.

Primer	Sequence	Annealing temperature (°C)
β-actin	Forward: CCGGACTCATCGTACTCCTGCTTG Reverse: TCATGCCATCCTGCGTCTGGACCT	65
Albumin	Forward: CTTCAAAGCCTGGGCAGTAG Reverse: GCACTGGCTTATCACAGCAA	61
C/EBPβ	Forward: ACAAGCTGAGCGACGAGTAC Reverse: ACAGCTGCTCCACCTTCTTC	55
CPS-1	Forward: TGAGTGGGTCTGCCATGAAC Reverse: TCTGCGTAGGTAGCATCAGT	60
CYP2E1	Forward: TGGTGCATGAGATCCAGAGA Reverse: TGACAGGACTGAGGTCGATA	60
HNF4α	Forward: CTCAACTCATCCAACAGCC Reverse: AAGCACTTCTTGAGCCTGC	58

TFN	Forward: ACAAAACGGTCAAATGGTGC Reverse: AAAACTCTGCTGCCACAGG	58
TTR	Forward: ATGACCAGAGTCATTGGCTG Reverse: GTCCTCTGATGGTCAAAGTC	58

Table 3.14 Gel electrophoresis reagents.

Material	Supplier	Product Number	Working Concentration
Tris-acetate-EDTA (TAE) buffer	National Diagnostics	EC-872	1X
Agarose	Sigma-Aldrich	A9539	2% (w/v) in TAE buffer
100 bp ladder	Norgen	11300	1X
Gel Red	Biotium	41003	1 in 10000 in deionised water

3.1.6 Quantitative cell culture assays

Table 3.15 Quantitative assays and additional reagents.

Material	Supplier	Product Number
LIVE/DEAD Viability/Cytotoxicity Kit	Invitrogen	L3224
Pierce BCA Protein Assay Kit	Thermo Scientific	23225
Pierce LDH Cytotoxicity Kit	Thermo Scientific	88953
Quant-iT Picogreen dsDNA Assay Kit	Invitrogen	P11496
Rat Albumin ELISA Quantitation Set	Bethyl Labs	E110-125
Protease inhibitor cocktail	Sigma-Aldrich	P8340

3.2 Membrane fabrication

3.2.1 Solution preparation

Solutions were prepared at a concentration of 20% (w/w) polymer. Polystyrene (PS) or poly(D,L-lactide-*co*-glycolide) (PLGA) were added to NMP in airtight containers and left overnight at room temperature on a roller mixer to ensure complete dissolution.

3.2.2 Flat sheet membrane fabrication

Membranes were cast using the phase inversion process as previously described [154]. Approximately 5 ml of dope was spread out onto a glass plate using a 1 cm diameter glass rod. A membrane thickness of 200 µm was established by wrapping 200 µm wires either side of the rod where it was in contact with the solution. The coated glass sheet was then submerged in 2 L of either deionised water or 70% (v/v) IMS at 18°C as a nonsolvent. The nonsolvent was replaced at 6 and 24 hr intervals after the initial immersion to remove any residual solvent. The precipitated membrane was removed from the coagulation bath after 3 days and allowed to air dry overnight.

3.2.3 PS membrane surface modification by oxygen plasma to create PX membranes

PX membranes were generated by surface modification of PS membranes by oxygen plasma. Surface modification was performed in a custom built vacuum chamber using inductively coupled plasma generation or a capacitively coupled plasma chamber (Zepto-Diener), both at radio frequencies (RF) of 13.56 MHz. Oxygen gas was used to generate the plasma under vacuum. The membranes were secured to a plastic well plate lid using double-sided tape to ensure that the membrane surface would be completely exposed to the plasma when in the chamber. The membranes were plasma treated for 1 min, 2 min and 5 min respectively in the custom built chamber at a power supply of 30 W or by using the capacitively coupled plasma chamber at a power supply of 25 W for 30 s.

3.3 Membrane characterisation

3.3.1 Membrane morphology

Membrane morphology was examined on both top surface and cross section of untreated and treated PS membranes by scanning electron microscopy (SEM) (JEOL JSM480LV). For surface analysis, the membranes were cut into approximately 5 x 5 mm squares using a scalpel blade and secured to an aluminium stub using double-sided conductive carbon tape. For cross sectional analysis, the membranes were immersed in liquid nitrogen for 5 min using forceps and freeze fractured using a razor blade. The sample was secured to a slanted aluminium stub with the fractured edge of interest exposed on top. After overnight storage in a desiccator, samples were coated in gold using a sputter coater (Edwards S150B) and viewed under vacuum at an accelerating voltage of 10 kV.

3.3.2 Surface wettability

Surface wettability of untreated and plasma treated PS membranes was analysed by measuring water contact angles using the sessile drop method. 2 µl deionised water was pipetted on to the membrane surface using the Dataphysics Contact Angle System OCA goniometer and the contact angle imaged and measured using the integrated camera and program. Measurements were taken from three randomly selected areas of each membrane surface and the means and respective standard errors (SEs) calculated.

3.3.3 Surface chemistry

Detection of additional oxygen functional groups on untreated and treated membrane surfaces was performed using attenuated total reflectance Fourier transform infrared (ATR-FTIR) spectroscopy (Perkin Elmer Frontier FTIR) and X-ray photoelectron spectroscopy (XPS) (Theta Probe). ATR-FTIR spectra were collected through the accumulation of 20 scans at a resolution of 2 cm^{-1} and a data interval of 0.25 cm^{-1}. X-ray photoelectron spectra were obtained at the National EPSRC XPS Users' Service (NEXUS) at Newcastle University, an EPSRC Mid-Range Facility. CasaXPS Version 2.3.16 software was used to determine elemental compositions.

3.4 General cell culture methods

3.4.1 AR42J-B13 (B13) cell line maintenance and passaging

Reagents for rat pancreatic B13 cell culture and experiments are described in **Section 3.4.1**. B13 cells were maintained in complete medium as previously described [130]. Complete B13 medium composition is described in **Table 3.2**. Cells were cultured in a T75 flask. At approximately 70% confluence, the culture medium was aspirated off and the cells washed with 10 ml sterile PBS. The PBS was then removed and 5 ml 0.05% trypsin-EDTA solution added. The flask was incubated at 37°C for 5 min to encourage detachment from the culture surface prior to the addition of 5 ml complete B13 medium to neutralise trypsin-EDTA activity. The cell suspension was then centrifuged at 1000 rpm (151 *g*) for 3 min (ALC PK110 Centrifuge). The supernatant was removed and the resulting pellet re-suspended in 1 ml fresh complete medium. 30 µl cell suspension was added to a fresh T75 flask containing 12 ml fresh complete medium. Cells were incubated at 37°C at 5% (v/v) CO_2 in a humidified incubator. Medium was changed every 2 days.

3.4.2 MG63 cell line maintenance and passaging

Reagents for human osteosarcoma MG63 cell culture and experiments are described in **Section 3.1.3**. MG63 cells were maintained in complete medium as described in **Table 3.6**. Cells were cultured in a T75 flask. Passaging protocol for MG63 cells was the same as that described in **Section 3.4.1** with the following amendments: MG63 cell suspension was centrifuged at 1000 rpm (179 *g*) for 5 min (ALC PK120 Centrifuge). Cells were incubated at 37°C at 5% (v/v) CO_2 in a humidified incubator. Medium was changed every 2 days.

3.4.3 Cell line storage and revival

Liquid nitrogen was used for long term storage of cell lines. Cells were passaged as previously described until after the centrifugation step. After centrifugation and removal of the supernatant, the cell pellet was re-suspended in 1 ml freezing medium (10% (v/v) DMSO, 90% (v/v) FBS). The resulting suspension was transferred to a cryovial and stored overnight at -80°C in a Mr Frosty Freezing Container (Thermo Scientific) before transferring to liquid nitrogen storage.

Cells were revived from liquid nitrogen by the addition of 1 ml respective complete medium pre-warmed to 37°C to the cryovial and rapid thawing at 37°C. The cell suspension was added to 10 ml complete medium and centrifuged at 1000 rpm for 3 min. The supernatant was aspirated off and the resulting cell pellet re-suspended in 12 ml complete medium. The cell suspension was then transferred to a T75 flask and incubated at 37°C at 5% (v/v) CO_2 overnight in a humidified incubator. The medium was replaced with fresh complete medium the following day with subsequent medium changes occurring every 2 days as per cell line maintenance protocols.

3.4.4 Cell seeding

For seeding cells at a specific density, cells were visualised using a 1:1 dilution of cell suspension and trypan blue and counted using a haemocytometer or a Fast Read cell counter as per manufacturer's instructions. The seeding volume per well for the required density was subsequently calculated as follows:

3.4.4.1 Haemocytometer cell count

Cells were counted in 4 grids of the haemocytometer and the cell number per grid noted. The mean cell number per grid was calculated by adding the cell counts per grid together and dividing this total by 4. The seeding volume was then calculated using the following formula:

$$Seeding\ volume\ (\mu l/well) = \frac{Cell\ density\ \times Surface\ area\ of\ culture\ substrate}{Mean\ cell\ number\ per\ grid\ \times 10\ \times 2}$$

3.4.4.2 Fast Read cell counter cell count

The total number of cells contained within the 10 grids of a single counter chamber were counted and a mean cell number per grid calculated by dividing the total cell count by 10. The seeding volume was then calculated using the following formula:

$$Seeding\ volume\ (ml/well) = \frac{Cell\ density\ \times Surface\ area\ of\ culture\ substrate}{Mean\ cell\ number\ per\ grid\ \times 1000\ \times 2}$$

3.4.5 Inducing transdifferentiation of B13 cells to hepatocyte-like cells

B13 cells were cultured as previously described in **Section 3.4.1**. Cells were seeded on to either TCPS, PS or PLGA membranes or 22 x 22 mm glass coverslips at a density of 3,125 cells/cm^2 (30000 cells in a single well of a 6-well plate) and incubated at 37°C at 95% air/5% CO_2 in a humidified incubator overnight in complete medium. The following day, medium was removed and complete medium supplemented with either 1 μM Dex only or 1 μM Dex and 10 ng/ml OSM (**Table 3.3**) was added to the cells. Cells were treated with the transdifferentiation medium for a minimum of 14 days as previously described [130] unless otherwise specified in the experimental method. Medium was changed every 2 days.

3.5 Treatment of B13 cells with different media

3.5.1 Treatment of B13 cells with HepatoZYME$^+$ complete culture medium

B13 cells were cultured as previously described in **Section 3.4.1**. Cells were seeded in 6-well plates at a density of 3,125 cells/cm^2 either directly on to TCPS or on 22 x 22 mm glass coverslips. Cells were incubated at 37°C at 5% (v/v) CO_2 in a humidified incubator overnight. The following day, medium was removed and complete medium supplemented with either 1 μM Dex only, 1 μM Dex and 10 ng/ml OSM, HepatoZYME$^+$ differentiation medium (**Table 3.4**) or a 50:50 dilution of HepatoZYME$^+$ with complete medium (henceforth referred to as "50:50") was added to the cells. Detailed experimental conditions can be found in **Chapter 5**.

3.6 Membrane biocompatibility characterisation

3.6.1 Bioreactor construction

PS and PLGA flat sheet membranes were fabricated as described in **Section 3.2** with minimum dimensions of 85 x 128 mm, comparable with the dimensions of a well plate. PS membranes were oxygen plasma treated using a Zepto Diener plasma chamber as described in **Section 3.2.3**. Membranes were tightly screwed into autoclaved custom designed 24-well plate polycarbonate bioreactor modules with silicon gaskets. This left a membrane surface area of 1.9 cm^2 per well exposed for cell culture which is comparable to a single well of a commercial 24-well plate (**Figure 3.1**). Membranes were sterilised as

previously described [175]. Membranes were incubated in 1% (v/v) antibiotic-antimycotic solution in PBS at 4°C for 24 hr then rinsed 3 times with PBS. Module construction and membrane sterilisation was performed inside a Class II laminar flow biohood. Specific membrane compositions for biocompatibility experiments are described in more detail in **Chapter 6**.

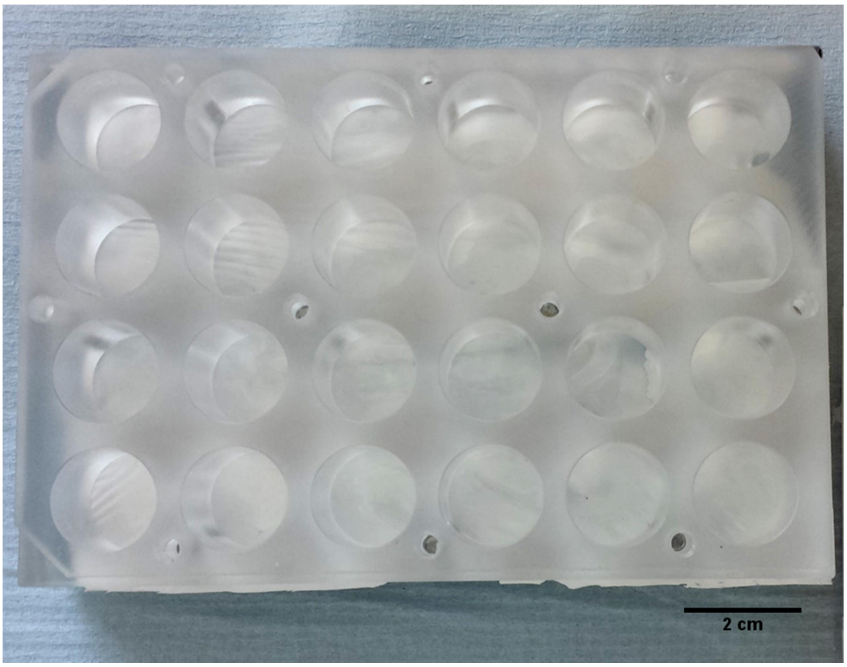

Figure 3.1 Custom 24-well plate polycarbonate bioreactor module for flat sheet membrane cell culture. Exposed membrane surface area per well = 1.9 cm^2. Scale bar = 2 cm.

3.6.2 Cell attachment

Cell attachment on different biomaterial surfaces was quantified by measuring cellular dsDNA content relative to cell density using the Quant-iT Picogreen dsDNA Assay Kit (Invitrogen). Membranes were fixed into custom 24-well plate modules as described in **Section 3.6.1**. TCPS was used as a control culture substrate. Cells were seeded onto the different culture substrates at a density of 20,000 cells/cm^2 using the method described in **Section 3.4.4.2**. Cells were incubated for 6 hr in a humidified incubator at 37°C at 95% air/5% (v/v) CO_2 then removed. The culture medium was removed and the cells were gently washed in PBS. 500 µl 1X TE buffer provided by the assay was added to each well and the plate was incubated at room temperature for 30 min before undergoing 2 freeze-thaw cycles at -80°C. The working Picogreen solution was a 1:200 dilution in 1X TE

buffer from the provided stock solution. The provided λ DNA standard was diluted according to the manufacturer's instructions to create a standard curve correlating mean fluorescence values to dsDNA content (ng). The diluted λ DNA standards and lysed cell samples were added in triplicate 75 µl aliquots to a 96-well plate suitable for fluorospectroscopy. 75 µl of the working Picogreen solution was added to each sample well and the plate gently agitated for 5 min. Fluorescence was measured at an excitation of 485 nm and emission of 528 nm using a Fluorospectrometer BioTek Synergy HT (NorthStar Scientific). dsDNA content in the experimental samples was deduced from the λ DNA standard curve and correlated to cell density (cells/cm^2).

3.6.3 Cell viability

The LIVE/DEAD Viability/Cytotoxicity Kit (Invitrogen) was used to determine the presence of live and dead cells cultured on different biomaterial surfaces. Membrane samples were cut into 22 x 22 mm squares and placed into a well of a 6-well plate. The cut membranes were held down in the well by sterilised cloning rings and sterilised as described in **Section 3.6.1**. Cells were seeded at a density of 20,000 cells/cm^2 using the method mentioned in **Section 3.4.4.1** then incubated for 48 hr in a humidified incubator at 37°C in 5% (v/v) CO_2. After incubation, the cells were washed gently in PBS and 2 ml working live/dead stain solution added, consisting of 1 µM calcein AM and 1 µM ethidium homodimer-1 in PBS. The cells were incubated in the solution at room temperature for 30 min. 100 µl of the working solution was pipetted on to a glass microscope slide and the membrane placed cell side down on the droplet. Green fluorescence of live cells and red fluorescence of dead cells was visualised on an inverted microscope (Olympus IX51, Olympus) and imaged using the CellP software. The number of cells showing green or red fluorescence was counted for 6 random fields of view (FOV) per replicate and normalised against the total number of cells counted in the FOV using ImageJ to determine the percentage number of live and dead cells.

3.6.4 Cytoxicity

The percentage cytotoxicity was analysed by determining lactate dehydrogenase (LDH) activity in the culture medium of cells cultured on different biomaterial surfaces using the

Pierce LDH Cytotoxicity Kit. Membranes were fixed and sterilised in custom 24-well plate modules as previously described (**Section 3.6.1**). TCPS was used as a control culture substrate. Cells were seeded at a density of 3000 cells/well in 3 sets of triplicate wells and incubated at 37°C in 5% (v/v) CO_2 in a humidified incubator for 48 hr. After incubation, 30 µl ultrapure water was added to 1 well per set to form the Spontaneous LDH Activity Control, 30 µl 10x Lysis Buffer was added to the 2nd well per set to form the Maximum LDH Activity Control and 30 µl complete medium were added to the 3rd well per set to form the LDH Activity Sample. LDH activity was measured in the culture medium at absorbances 490 nm and 680 nm using a Fluorospectrometer BioTek Synergy HT (NorthStar Scientific). The percentage cytotoxicity was calculated using the following formula as per manufacturer's instructions:

$$\%\ Cytotoxicity = \frac{Compound\ treated\ LDH\ activity - Spontaneous\ LDH\ activity}{Maximum\ LDH\ activity - Spontaneous\ LDH\ activity} \times 100$$

3.6.5 Membrane bulk changes under cell culture conditions

Membrane bulk changes under cell culture conditions was quantified by percentage weight change and percentage surface area change of membranes after 3, 8 and 15 days under cell culture conditions.

PX and PLGA membranes were fabricated as described in **Section 3.2**. The membranes were then cut into squares approximating 20 mm x 20 mm and their length and width measured using a micrometer with a resolution of 0.01 mm to determine their pre-incubation available culture surface areas. The squares were then weighed on an electronic balance with a resolution of 0.001 g to determine their pre-incubation masses. Following this, the membranes were then transferred to a 6-well plate, held down with cloning rings and sterilised as described in **Section 3.6.1**. After 24 hr incubation at 4°C, the membranes were washed in PBS and 2 ml of complete B13 maintenance medium (**Section 3.1.2**) was added to each well. The membranes were incubated at 37°C at 5% (v/v) CO_2 in a humidified incubator. After 3, 8 or 15 days, the membranes were removed from the incubator and the culture medium aspirated away. The membranes were washed 3 times in PBS then dried in a desiccator overnight. The membranes were then measured again to determine their post-incubation surface areas and masses.

Means for percentage mass change and percentage surface area change and their standard errors (SEs) were calculated for 3 different membranes per time point. Statistical analyses were performed using a paired samples Student's t-test for membranes cast from the same polymer and an independent samples Student's t-test to compare between PX and PLGA membranes.

3.7 Immunofluorescent staining of cell cultures

3.7.1 Cell fixation

B13 cells were cultured for the time as stated in the relevant chapters. At the experimental endpoint, the culture media was removed and the cells washed in PBS. The fixative was selected based upon the target antigen of interest (**Table 3.8** and **Table 3.10**). For 4% PFA fixation, after washing the cells in PBS, 4% PFA solution was added to the cells and incubated at room temperature for 25 min. For methanol fixation, after washing the cells in PBS, methanol chilled to -20°C was added to the cells and incubated at room temperature for 5 min. After fixation, the fixative was then removed and the cells washed 3 times in PBS. The cells were stored in PBS at 4°C prior to immunofluorescent staining.

3.7.2 Immunofluorescent staining

The staining method was dependent on the fixation method. The PBS was first removed from fixed cell cultures. Cells fixed with 4% PFA were permeabilised using 0.1% (v/v) Triton X-100 in PBS and incubated for 20 min at room temperature. Cells fixed with methanol did not require permeabilisation or antigen retrieval.

Following this, blocking buffer was added to the fixed cultures. 2% Roche Blocking Buffer (Roche) was added to cells fixed with 4% PFA. Cells fixed with methanol were blocked using 10% (v/v) normal goat serum, 1% (v/v) BSA and 0.3 M glycine in PBS (NGS-BSA-Gly Buffer). The cells were incubated with their respective blocking buffers at room temperature for 30 min. Primary antibodies were diluted in blocking buffers as described in **Table 3.10** and added to the cells on the culture substrate. Cells were incubated overnight with the antibody-blocking buffer solution at 4°C.

The following day, cells were washed 3 times with PBS and incubated at room temperature in PBS on a rocker for 30 min to remove residual primary antibody. Secondary fluorescently-conjugated antibodies were diluted in blocking buffers as per primary antibodies and added to the cells on the culture substrate (**Table 3.11**). Cells were incubated at room temperature with the antibody-blocking buffer solution, protected from light. Following this, the cells were washed twice with PBS and then incubated in PBS at room temperature on a rocker for 20 min. The PBS was removed and a 1:1000 dilution of DAPI in PBS solution added to the cells. The cells were incubated with this solution on a rocker for 10 min at room temperature, protected from light, before removing the solution and washing the cells in deionised water. Coverslips and membranes were mounted using Mowiol mounting medium on to glass microscope slides. An additional glass coverslip was added to the top of stained membranes to hold the membrane in place. Slides were incubated overnight at room temperature and then stored at 4°C.

For double staining of cells with two primary antibodies, it was ensured that the primary antibodies used had been developed in different species to prevent cross-reactivity.

Cells were visualised on an Olympus IX51 microscope and imaged using CellP software. Post-processing of images was performed using the GNU Image Manipulation Program (GIMP) 2.

3.7.3 Percentage expression quantification

Percentage expression of a marker of interest was calculated by counting the number of cells showing both positive immunofluorescent staining for the marker of interest as well as the DAPI nuclear stain. These cells were counted in 3 random FOVs per replicate and normalised against the total number of DAPI-positive cells counted in the FOV using ImageJ to determine the percentage expression of the marker of interest.

3.8 RT-PCR analysis of gene expression

3.8.1 Total cellular RNA extraction

RNA was extracted from cells at the stated experimental endpoint using the following method. Culture medium was removed and the cells were washed twice in PBS. 500 µl of Tri-Reagent (Sigma-Aldrich) was added per well in 6-well plate cultures; 100 µl per well in 24-well plate cultures. The solution was allowed to incubate for 5 min at room temperature. The lysate was repeatedly pipetted up and down the culture surface to ensure a homogenous solution before it was transferred to an RNase-free Eppendorf tube. Solutions were able to be stored at -80°C until required.

After thawing (if required), 200 µl 100% (v/v) chloroform was added to the solution and the tube gently shaken for 20 s before incubating for 15 min at room temperature. The solutions were then centrifuged at a relative centrifugal force (RCF) of 12,000 *g* at 4°C for 15 min (Eppendorf Centrifuge 5417R). The top aqueous layer was then transferred to a fresh RNase-free Eppendorf tube and 500 µl 100% (v/v) isopropanol added to the tube. The tube was mixed briefly using a vortex mixer and incubated for 10 min at room temperature before centrifugation at a RCF of 12,000 *g* at 4°C for 10 min. The supernatant was removed and 1 ml 75% (v/v) absolute ethanol in DEPC-H_2O cooled to 4°C was added to the tube before centrifuging at a RCF of 7,600 *g* at 4°C for 5 min. The supernatant was removed and the resultant RNA pellet allowed to dry on a heat block at 37°C. The pellet was re-suspended in 20 µl DEPC-H_2O and heated at 60°C on a heat block for 10 min then placed on ice. Extracted RNA concentration (µl/ml) and purity (A260/A280) was measured using the GeneFlow NanoPhotometer.

3.8.2 DNase treatment of extracted RNA

To remove contamination of extracted RNA samples by genomic DNA, the working mass of RNA in solution and volume required for DNase treatment was calculated to be between 50 ng and 2 µg, based on the sensitivity of the Omniscript RT Kit (Qiagen). The maximum volume of RNA sample was 7.5 µl. DNase treatment reagents can be found in **Table 3.12** with required volumes in **Table 3.16**.

Table 3.16 Reagents for DNase treatment of one extracted RNA sample.

Reagent	Volume (µl)
Extracted RNA in solution	Dependent on working mass of RNA in solution
10x DNase I buffer	1.0
rDNase I	1.0
RNAsin plus	0.5
DEPC-H_2O	7.5 – Volume of extracted RNA in solution
TOTAL	**10.0**

Samples were briefly spun in a centrifuge then incubated at 37°C for 30 min. The DNase reaction was stopped by the addition of 1 µl 20 mM EGTA and samples incubated at 65°C for 10 min. For long-term storage, DNase-treated RNA samples were then stored at -80°C until required.

3.8.3 Reverse transcription (RT)

cDNA synthesis from DNase-treated RNA was done using the Omniscript RT Kit (Qiagen). The reagent components are stated in **Table 3.12** with quantities in **Table 3.17**. The reaction mixture was briefly spun in a centrifuge then incubated at 37°C for 1 hr. Samples were then kept on ice for 1 min. For long-term storage, cDNA was frozen at -20°C until required.

Table 3.17 Reaction mixture reagents for reverse transcription of RNA to cDNA.

Reagent	Volume (µl)
DNase-treated RNA	11.0
10X RT buffer (Omniscript RT Kit)	2.0
5 mM dNTP (Omniscript RT Kit)	2.0
Oligo dT	1.0
RNAsin plus	0.2
RT omniscript (Omniscript RT Kit)	1.0
RNase-free H_2O (Omniscript RT Kit)	2.8
TOTAL	**20.0**

3.8.4 Polymerase chain reaction (PCR) and gel electrophoresis

Expression of specific genes was determined using the polymerase chain reaction (PCR) and visualised using gel electrophoresis. For PCR, species specific forward and reverse primers were used to highlight specific genes of interest. Primers, sequences and annealing temperatures are listed in **Table 3.13**. The PCR reaction mixture and quantities per sample are stated in **Table 3.18**.

Table 3.18 PCR reaction mixture for one cDNA sample.

Reagent	Volume (µl)
cDNA	1.0
Forward primer (10 µM)	0.4
Reverse primer (10 µM)	0.4
2X ReddyMix PCR MasterMix	10.0
DEPC-H_2O	8.2
TOTAL	**20.0**

The samples were spun down briefly in a centrifuge and the PCR reaction was performed in a TC-412 Techne Thermal Cycler (Jencons Pls) under the following conditions: initialisation at 95°C for 2 min, denaturation at 95°C for 25 s, amplification at the specified primer annealing temperature for 35 s and extension at 72°C for 1 min. The number of cycles of denaturation to extension was 25 for β-actin and 30 for all other primers, followed by a final extension step at 72°C for 5 min on the final cycle. All PCR reactions included a cDNA-negative control.

PCR products were analysed using gel electrophoresis. Products were run on a 2% agarose gel in 1X TAE buffer alongside a 100 bp ladder. Samples were run at 90 V for 30 min. Gels were subsequently stained with Gel Red and visualised under ultraviolet light. Images were captured using a Chemi-DocIt^2 Imager.

3.9 Quantitative cell assays

B13 cells were quantified for serum albumin production in culture media (**Section 3.9.2**). Data were normalised against total cell number or total cellular protein content for serum

albumin production. Total cellular protein quantification is detailed in **Section 3.9.1**. Total cell number quantification is detailed in **Section 3.6.2**.

3.9.1 Total cellular protein quantification

Total cellular protein content was quantified using the Pierce BCA Protein Assay Kit (Thermo Fisher). The Working Reagent was prepared as per manufacturer's instructions. 25 µl of cellular protein lysate from 1% (v/v) Triton X-100 treated B13 cells were added in duplicate to a 96-well plate. 200 µl of the Working Reagent was added to each well and the contents mixed thoroughly on a shaker for 30 seconds. The plate was protected from light and incubated at 37°C for 30 min before being cooled to room temperature. Absorbance was measured at 562 nm using a Synergy Plate Reader (Biotek).

3.9.2 Serum albumin production

Serum albumin in culture media used in the treatment of B13 cells was quantified using the Rat Albumin ELISA Quantitation Set (Bethyl Labs). B13 cells were seeded on a specified culture substrate at 3,125 cells/cm^2 and treated with a specified culture medium for 13 or 20 days. On day 13 or 20 of treatment, the medium was removed and the cells gently washed in PBS. For the cultures in **Chapter 5** utilising TCPS 6-well plates, the cells were then treated with 1 ml serum-free treatment medium for 1 day. The cultures utilising the custom 24-well plate bioreactor in **Chapter 6** were treated with 500 µl serum-free treatment medium for 1 day. Following this, the culture medium was then removed from the cells and stored at -20°C. For protein quantification, the cells were washed in PBS and 500 µl 1% (v/v) Triton X-100 in PBS containing a 1:100 dilution of protease inhibitor cocktail added to the cells to extract cellular protein. The subsequent lysate was collected and stored at -80°C. For cell number quantification, the cells were washed in PBS and 500 µl 1X TE buffer added to the cells and incubated at room temperature for 30 min before following the protocol stated in **Section 3.6.2** for cell lysis and analysis.

Serum albumin was then quantified in the removed culture medium. The rat albumin ELISA was performed using Nunc F96 Maxisorp plates. Plates were coated and washed in preparation for standards and samples as per the manufacturer's guidelines. All standards

and samples were transferred to the ELISA plate in volumes of 100 µl and incubated at room temperature for 60 min before washing.

The HRP Detection Antibody was diluted 1:20,000 in Sample/Conjugate Diluent and 100 µl added per well, before incubation for 60 min at room temperature prior to washing. 100 µl TMB substrate solution was then added to each well and incubated at room temperature for 15 min before adding 100 µl 0.18 M H_2SO_4 to each well to stop the solution.

Absorbance was measured at 450 nm using a Synergy Plate Reader (Biotek). Normalisation was either done versus total protein content using the Pierce BCA Protein Assay Kit (Thermo Scientific) or per million cells via the Quant-iT Picogreen dsDNA Assay Kit (Invitrogen).

3.10 Microscopy and image processing

Flat sheet membrane morphology was analysed using a JEOL JSM480LV scanning electron microscope at an accelerating voltage of 10 kV and imaged using the installed software.

Transmitted light images of cells in culture were visualised using a Leica DM IRB microscope and imaged using NIS Elements software or GXCapture 7 software.

Fluorescently stained cells were visualised using a Leica DMRB microscope with images taken using an Olympus XM10 or visualised using an Olympus IX51 microscope with images taken using CellP software.

Image-based quantification, including relative proportions of integrated intensity of fluorescence, image-based cell counts and measurements of cell diameter was done using Image J.

Post-processing of images for brightness and contrast and figure labelling were performed using GIMP 2 and Microsoft PowerPoint.

3.11 Statistical analysis

For statistical analysis, experiments were performed a minimum of 3 times independently of each other (n = 3) and where applicable, a mean and respective standard error (SE) was calculated. Further statistical analyses were performed using SPSS 22 for Windows. Statistical tests were selected based on whether the data were determined to be parametric or non-parametric following a Shapiro-Wilk normality test. Where the data was judged to be normally distributed, comparison of differences in mean between stated data sets was performed either using an independent samples Student's t-test for comparison of 2 independent samples, a paired samples Student's t-test where samples were compared before and after treatments or via a one-way ANOVA with Tukey's post-hoc tests for a minimum of 3 samples. Differences between means in compared data sets were considered to be statistically significant where $p < 0.05$.

Chapter 4
Development of polystyrene flat sheet membranes for cell culture

4.1 Introduction

4.1.1 Phase inversion membranes as a cell culture substrate

To replicate a physiological environment in an *in vitro* setting such as a bioartificial liver (BAL) device, it is necessary to tailor the culture system to the specific cell type to ensure that functionality is maintained as closely to *in vivo* as possible. Two BAL devices that have reached clinical trials have utilised a hollow fibre bioreactor (HFB) system in different configurations, such as culturing the cells on the outer surface of the fibre (ELAD) or by culturing the cells on collagen-coated dextran microcarriers in the extracapillary space of the hollow fibre cartridge (HepatAssist) [23,52]. In both systems, the cells are separated from the flow of medium through the fibre lumen by the wall of a semipermeable hollow fibre membrane. This set-up bears great similarity to the anatomy of the liver sinusoid, where the microvilli of the hepatocyte in the space of Disse are separated from sinusoidal blood flow by a fenestrated endothelium.

Based on the normal liver anatomy, the construction of suitable hollow fibres requires the development of semipermeable membranes. These scaffolds are selective barriers that allow nutrients in medium flowing intraluminally to diffuse across the membrane to cells cultured upon the extraluminal surface, limited by molecular weight. The membrane must be constructed from a mechanically stable, biocompatible material, where the cells are able to attach, thrive and function as normal; and also must be porous, to facilitate sufficient mass transfer to cells whilst preventing transfer of larger molecules and cells themselves into the membrane substructure and lumen.

Phase inversion membranes have previously been used in HFBs for cell culture [154,171–173] and are favoured for their efficient mass transfer capabilities and potentially porous nature. Membranes are cast via a ternary, immersion precipitation method [159,176]. Here,

a polymer is dissolved in a solvent, and the resulting dope solution introduced to a secondary solvent, termed the nonsolvent. The solvent dissolves in the nonsolvent, creating a binary liquid phase and therefore precipitating a membrane in the solid phase. Membrane characteristics including structure, MWCO, surface chemistry and wettability will vary depending upon the mutual affinity and miscibility between the chosen polymer, solvent and nonsolvent [159]. Phase inversion membranes can be porous or nonporous in structure, or form an asymmetrical structure where a nonporous top skin layer forms on top of a porous sublayer [159,177,178]. This is dependent upon the rate of liquid-liquid demixing that occurs in a polymer-solvent-nonsolvent system [159]. Flat sheet membranes fabricated using the immersion precipitation method of phase inversion are a suitable model system to identify potential hollow fibre membrane structural attributes. In the case of flat sheet membrane casting, the demixing occurs at the interface between the dope solution and nonsolvent through immersion. During hollow fibre membrane formation, demixing occurs from both the shell (fibre exterior) and bore (spinneret needle bore) side where the dope solution is exposed to nonsolvent from the coagulation bath (fibre exterior) and also the spinneret needle bore (fibre interior) [159,179]. As the nonsolvents examined in this Chapter via the flat sheet membrane model would also be used in the coagulation bath and the spinneret needle under hollow fibre conditions respectively, the structural features observed from flat sheet membrane casting could be translated to a hollow fibre membrane setting. This translation is due to similar dope solution-nonsolvent interfaces occurring at the demixing stage during hollow fibre membrane fabrication.

4.1.2 Polystyrene as a potential biomaterial for hollow fibre bioreactor cell culture

A novel candidate polymer for the development of hollow fibre membranes for 3D bioreactor cell culture is polystyrene (PS). PS is a non-biodegradable thermoplastic **(Figure 4.1)**. It is highly resistant to photodegradation [180] and does not lose structural integrity at 37°C as it possesses a glass transition temperature of approximately 100°C [181] and a melting point of 240°C [182]. The durable and long lasting nature of PS means that it is an ideal candidate for use in BAL devices. A polymer such as PLGA, whilst useful for tissue graft implantation and removal of the graft scaffold by biodegradation, would not be suited for long term maintenance of adherent cells that require a constant

scaffold presence. Outside of BAL device design, this biomaterial could also be utilised for long term cell expansion in a HFB setting to produce a large quantity of therapeutically useful cells.

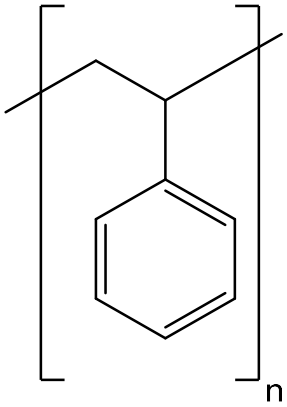

Figure 4.1 Chemical structure of polystyrene. Polystyrene is the result of the polymerisation of styrene monomers and consists of a repeating unit of a phenyl group attached to a hydrocarbon chain.

PS is biocompatible, inexpensive to mass produce and readily utilised as a culture scaffold [183] in the form of tissue culture plastic-ware. 3D porous PS scaffolds have also been used to culture the HepG2 human hepatocellular carcinoma cell line [149] and research into electrospun PS fibres has also shown good cell attachment of human bladder smooth muscle cells [184]. However, the use of phase inversion PS flat sheet or hollow fibre membranes for cell culture or BAL device design has not been previously reported in the literature.

4.1.3 Selecting a suitable ternary system for casting phase inversion membranes

As previously described in **Section 4.1.1**, the ternary system chosen for casting phase inversion membranes can affect the characteristics of the resultant product. This is particularly dependent upon the mutual affinities between the system components.

N-methyl-pyrrolidinone (NMP) is an FDA-approved solvent that has previously been used in the manufacture process of pharmaceutical agents and also as part of solutions in controlled release drug delivery devices [185]. NMP is of particular interest in bone tissue

engineering as it has been shown to enhance the effects of bone morphogenetic protein-2 (BMP-2) in bone cell maturation [186]. It has been previously used in casting PLGA phase inversion flat sheet and hollow fibre membranes, which were able to support human bone cell culture [154,171,172], and also in phase inversion cast polysulfone membranes for the culture of human hepatocytes [187]. Furthermore, given its miscibility with water, relative safety and history of usage in medical device design, NMP was therefore chosen as the polymer dissolution solvent for this study.

The selected polymer concentration in the casting dope is vital to successful hollow fibre membrane fabrication. Insufficient polymer concentration can prevent precipitation of a mechanically stable membrane. A 1987 study by Eenink and Feijen using poly(L-lactide) stated that polymer concentrations below 10% (w/w) would not be sufficient for casting hollow fibres [188]. However, a polymer concentration that is too high will result in decreased membrane porosity, particularly at the surface interface between dope and nonsolvent [159]. Other polymer-NMP concentrations previously utilised for casting hollow fibre membranes have included poly(ε-caprolactone) at 15% (w/w) [189], PLGA at 20% (w/w) [175] and 25% (w/w) [154,189] and polyethersulfone at 30% (w/w) and 35% (w/w) [190]. Previous work in this laboratory has utilised a 20% (w/w) concentration (Personal communication from Marianne Ellis). From this, a 20% (w/w) PS-NMP solution was selected as the initial experimental concentration for a hollow fibre membrane casting dope and thus the concentration used for casting flat sheet membranes.

As the demixing process during phase inversion casting can determine whether a porous membrane is formed, deionised water and a solution of 70% (v/v) industrial methylated spirits in water (70% (v/v) IMS) were chosen as candidate nonsolvents for the ternary system due to their miscibility with NMP, immiscibility with PS and relative safety. In addition, 70% (v/v) IMS is already utilised as a common sterilising agent to ensure aseptic conditions for tissue culture.

4.1.4 Developing membrane surface treatments to produce a suitable cell culture surface

Adherent cell culture in a HFB system requires the hollow fibre membrane surface to be conducive to cell attachment and also porous, to allow for the diffusion of nutrients and

waste products between intraluminal medium flow and cells cultured upon the outer membrane surface. However, it is difficult to find a material that possesses all of these characteristics for optimum effect. Efficacy of cell attachment to biomaterial surfaces is affected by the membrane surface chemistry, and given that phase inversion cast membranes can be porous or nonporous, it may be the case that additional surface treatments post-casting must be applied to create a more compatible biomaterial for the required purpose.

Surface modification via plasma treatment allows for versatile alteration of surface chemistry depending on the gas utilised. The sample is contained within a vacuum chamber and exposed to plasma at a specific power for a certain length of time. This allows for additional functional groups to be added to the sample surface and can also change the surface topography as the surface is modified by reactive species present in the plasma. PS is a hydrophobic material, thus making it less conducive for cell attachment. Therefore, oxygen plasma treatment was selected as a potential method for altering the culture surface wettability and surface topography. The effectiveness of increasing hydrophilicity was then analysed and membrane morphology assessed.

4.1.5 Experimental aims and objectives

The experimental research described in this Chapter focuses on the development of phase inversion cast PS flat sheet membranes and subsequent morphological and chemical characterisation. Membranes were cast either by using water or 70% (v/v) IMS as the nonsolvent. Initially, the effects of inductively coupled oxygen plasma and subsequently, capacitively coupled oxygen plasma as membrane surface treatments were then investigated to determine parameters for the subsequent development of a novel substrate (PX) that could potentially be utilised for the fabrication of cell culture hollow fibre membranes.

Characterisation of untreated and treated membranes was achieved through analyses of: (i) surface and cross sectional morphologies using scanning electron microscopy (SEM); (ii) surface wettability via the sessile drop method and finally (iii) surface chemistry via attenuated total reflectance Fourier transform infrared (ATR-FTIR) spectroscopy and X-ray photoelectron spectroscopy (XPS).

4.2 Results

4.2.1 Polystyrene flat sheet membrane morphology

Phase inversion cast flat sheet membranes were used as a model experimental setup to determine a suitable polymer-solvent-nonsolvent ternary system for spinning hollow fibre membranes and subsequent parameters for surface treatments. Flat sheet membranes can be cast using comparatively smaller volumes of polymer dope and nonsolvent and require less preparation time than spinning hollow fibre membranes. They form two surface interfaces during the casting process – one that is directly exposed to the nonsolvent, which is representative of surfaces formed during spinning of hollow fibre membranes, which would be the surface that the cells would be cultured upon, and a second surface that interfaces with the glass casting plate. The former surface is the surface of interest for this study.

PS flat sheet membranes were cast as described in **Section 3.2**, with the 20% (w/w) PS in NMP mixture dissolving to form a homogenous dope solution. Two nonsolvents were used to fabricate the membranes – deionised water and 70% (v/v) IMS. Both nonsolvent conditions generated white precipitates as part of the casting process. Membranes cast in deionised water precipitated and lifted off the glass casting plate after 2 seconds following immersion of the dope solution in the nonsolvent. This was in contrast to membranes cast in 70% (v/v) IMS, which took over 5 min to coagulate and lift off the glass plate.

SEM imaging was used to visualise membrane surface and cross sectional morphologies. Micrographs of PS membrane morphologies are shown in **Figure 4.2**.

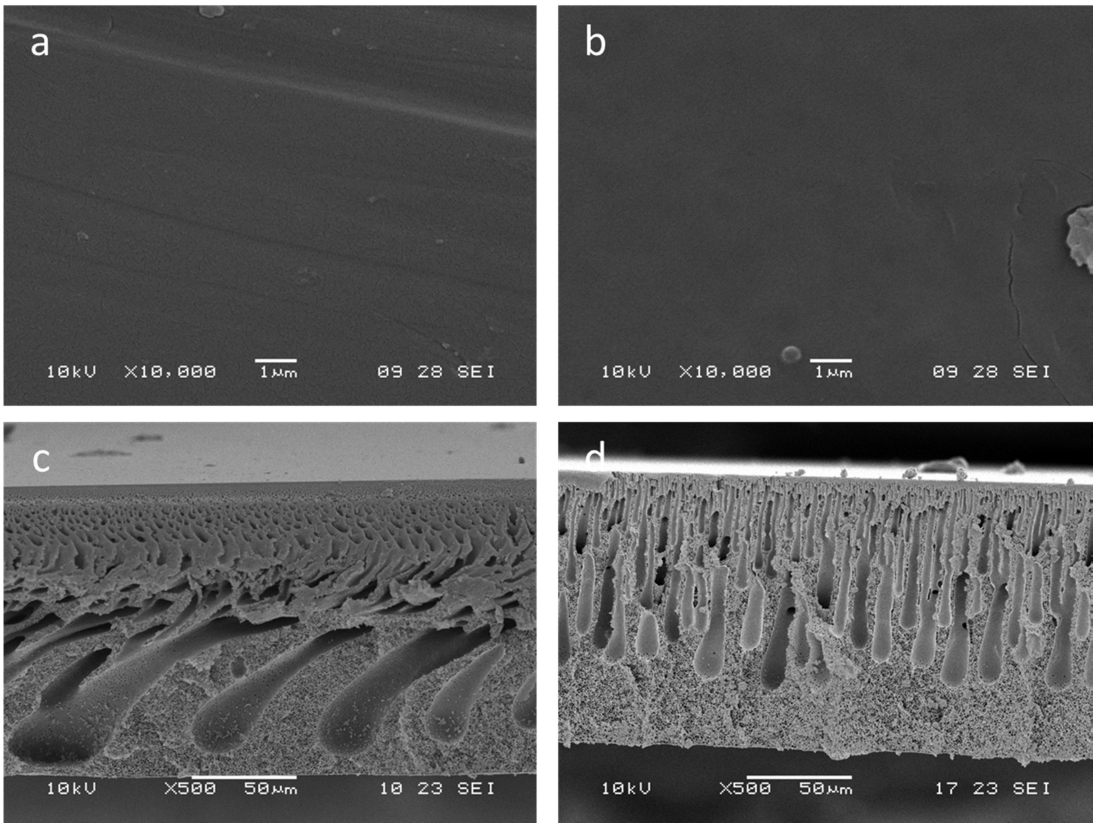

Figure 4.2 Morphology of PS flat sheet membrane top surfaces and cross sections. Membranes were cast from a solution of 20% (w/w) PS in NMP. (**a**) Deionised water nonsolvent, surface; (**b**) 70% (v/v) IMS nonsolvent, surface; (**c**) deionised water nonsolvent, cross section; (**d**) 70% (v/v) IMS nonsolvent, cross section. Scale bar = 1 µm (surface) or 50 µm (cross section).

Regardless of the nonsolvent used, the fabricated PS membranes presented with an asymmetrical structure, consisting of a smooth nonporous surface skin layer on top of a highly porous substructure. Long finger like macrovoids running perpendicular to the surface layer were present in both membranes. Furthermore, these macrovoids were surrounded by a sponge-like layer consisting of smaller pore substructures.

4.2.2 Morphology of inductively coupled oxygen plasma treated PS membranes

Both water and 70% (v/v) IMS cast PS membranes were then exposed to oxygen plasma under a vacuum with the intention of modifying the surface to become conducive to adherent cell culture. Initially, a custom built vacuum chamber using inductively coupled plasma was used to treat the membrane surfaces. These treated PS membranes (PX

membranes) were exposed to the oxygen plasma treatment for 1 min, 2 min and 5 min under experimental conditions as described in **Section 3.2.3**. The surface morphologies of each treatment condition are shown in **Figure 4.3** and **Figure 4.4**.

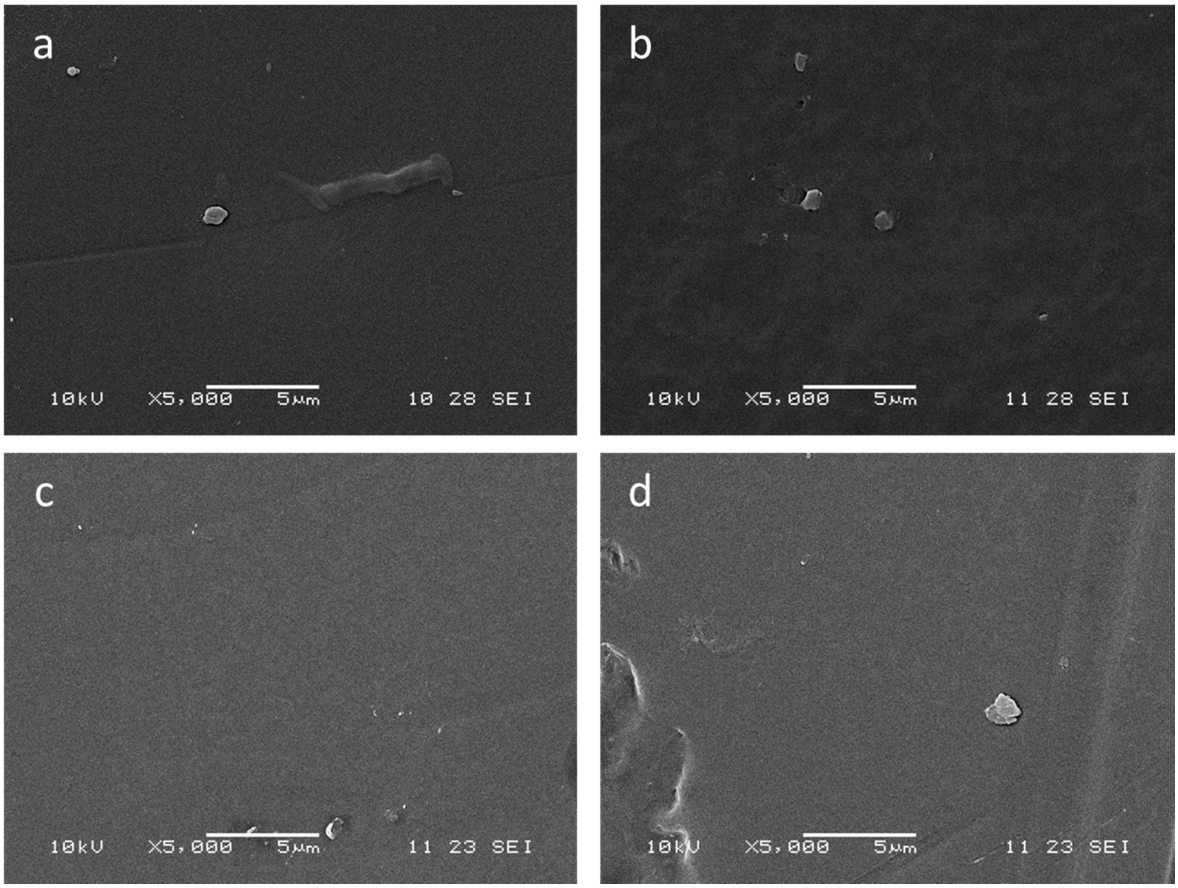

Figure 4.3 Morphology of untreated PS and inductively coupled oxygen plasma treated PX membrane surfaces cast in deionised water. Membranes were cast using a solution of 20% (w/w) polymer in NMP with deionised water as the nonsolvent. Membranes were either untreated (PS) (**a**) or treated (PX) through exposure to oxygen plasma at 30 W power for 1 min (**b**), 2 min (**c**), or 5 min (**d**) in a vacuum. Scale bar = 5 µm.

PX membranes originally cast using deionised water showed no visible differences in surface morphology after surface treatment compared to the untreated control PS membrane (**Figure 4.3**). Surfaces appeared to be smooth and nonporous. In contrast, where 70% (v/v) IMS was used as the nonsolvent during casting, there was no visible increase in surface porosity up to 2 min, but after 5 min of treatment, the membrane presented with a highly porous surface with pore diameters measuring less than 1 µm (**Figure 4.4d**).

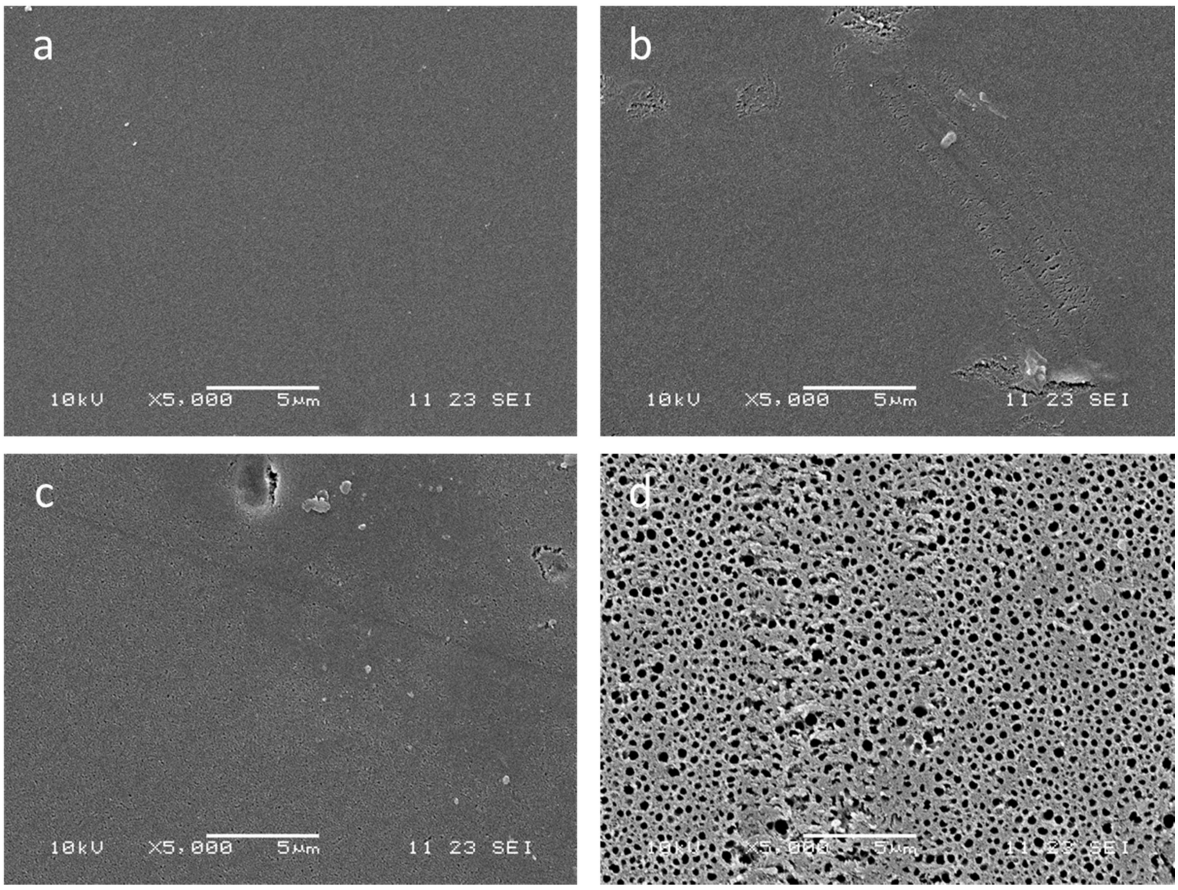

Figure 4.4 Morphology of untreated PS and inductively coupled oxygen plasma treated PX membrane surfaces cast in 70% (v/v) IMS. Membranes were cast using a solution of 20% (w/w) polymer in NMP with 70% (v/v) IMS as the nonsolvent. Membranes were either untreated (PS) (**a**) or treated (PX) through exposure to oxygen plasma at 30 W power for 1 min (**b**), 2 min (**c**), or 5 min (**d**) in a vacuum. Scale bar = 5 µm.

Cross sectional analysis 5 min post-treatment is shown in **Figure 4.5**. Similar to their untreated counterparts, the substructure contained macrovoids surrounded by a sponge-like porous network. Treated membranes showed no visual deterioration of the porous substructure.

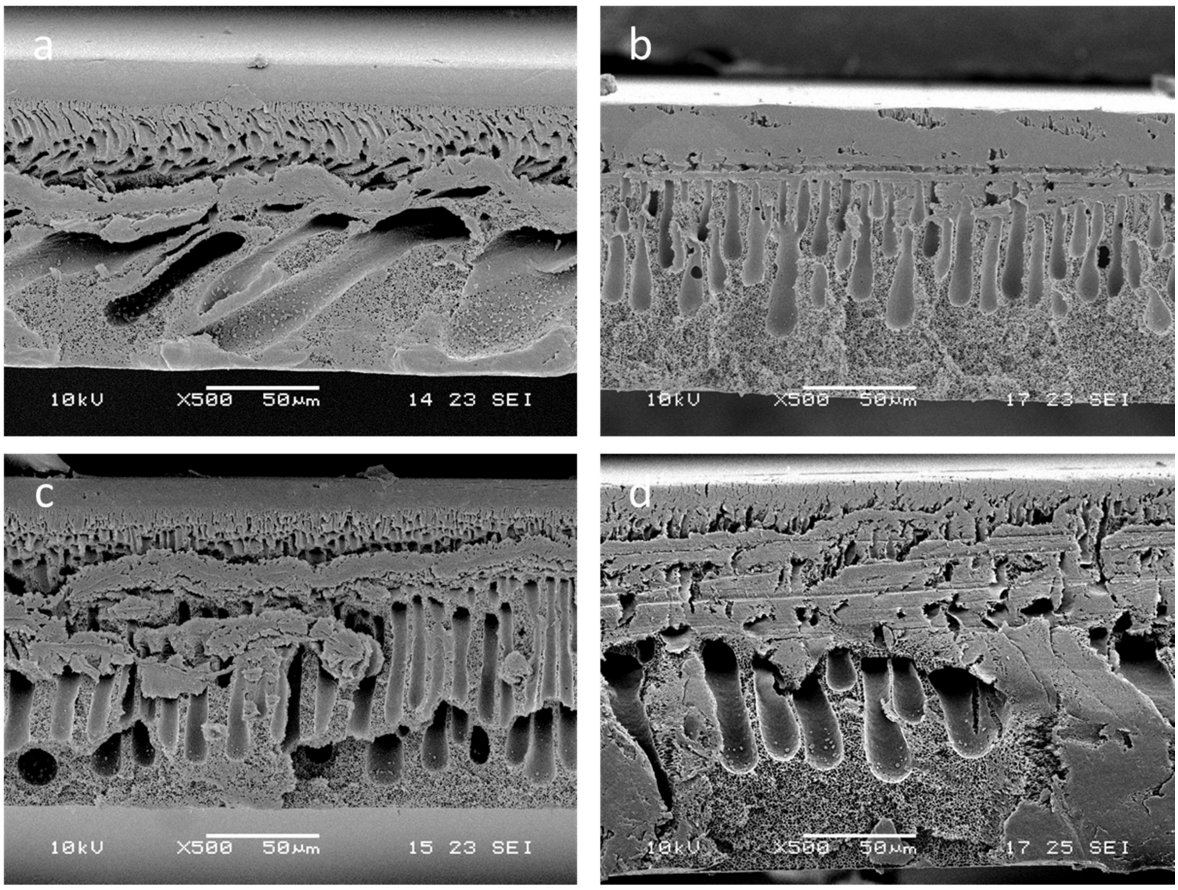

Figure 4.5 Morphology of untreated PS and inductively coupled oxygen plasma treated PX membrane cross sections. Membranes were cast using a solution of 20% (w/w) polymer in NMP. Deionised water (**a** & **c**) or 70% (v/v) IMS (**b** & **d**) was used as the nonsolvent. Membranes were either untreated (PS) (**a** & **b**) or treated (PX) through exposure to oxygen plasma at 30 W power for 5 min (**c** & **d**) in a vacuum. Scale bar = 50 µm.

4.2.3 Surface wettability of PS and PX flat sheet membranes

To investigate the effect of oxygen plasma treatment upon PS membrane surfaces, it was necessary to determine whether the method for surface modification had altered the membrane surface wettability. A wettable surface, otherwise termed hydrophilic, is conducive for cell attachment to the surfaces of biomaterials, whereas untreated PS is hydrophobic, therefore not providing a suitable environment for cell attachment. To assess the wettability of PX membranes, the sessile drop method was utilised with experimental conditions as described in **Section 3.3.2**.

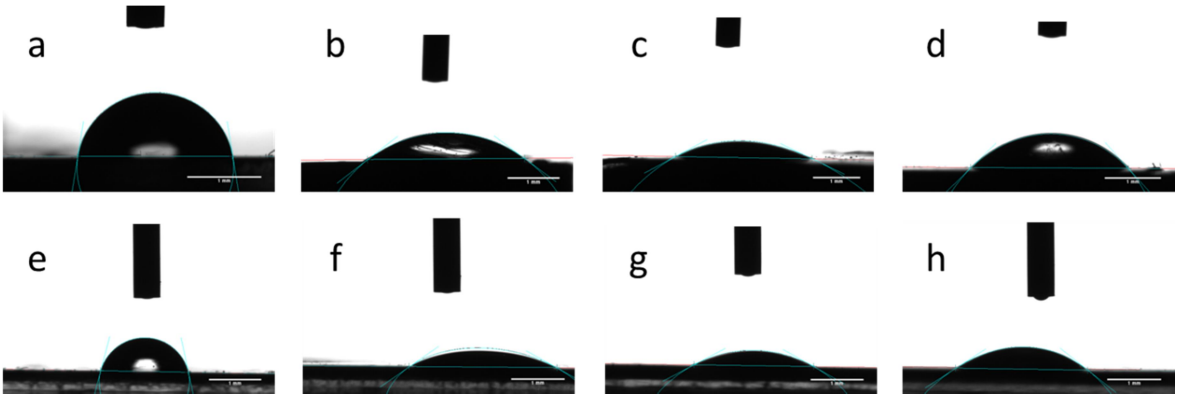

Figure 4.6 Images of water droplets on untreated PS and inductively coupled oxygen plasma treated PX membranes. Membranes were cast in either deionised water (**a** to **d**) or 70% (v/v) IMS (**e** to **h**). Analysis was via the sessile drop method measuring static water contact angles against the membrane surface. PX membranes were exposed to inductively coupled oxygen plasma at 30 W power for 1 min (**b** & **f**), 2 min (**c** & **g**) or 5 min (**d** & **h**). Untreated PS membrane surfaces were used as a control (**a** & **e**). Scale bar = 1 mm.

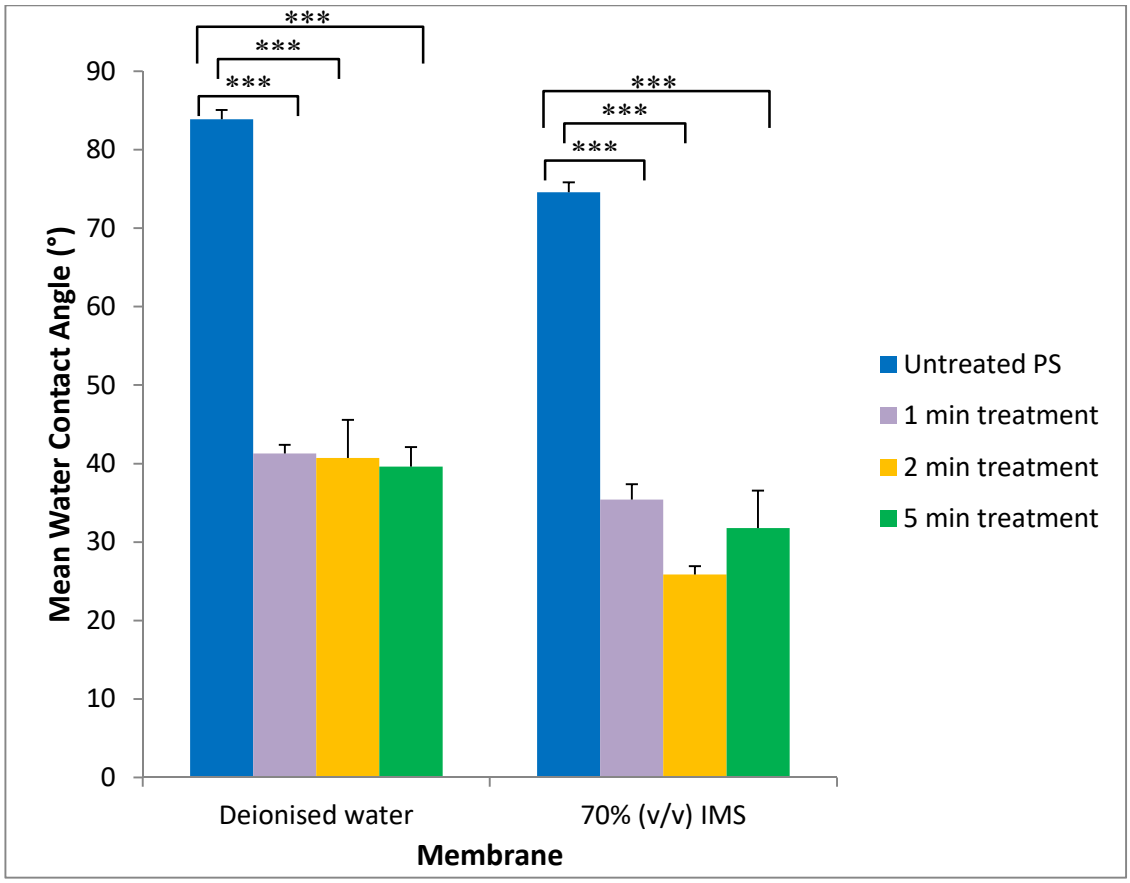

Figure 4.7 Mean water contact angles for untreated PS and inductively coupled oxygen plasma treated PX membrane surfaces. Statistical analysis was by a one-way ANOVA with Tukey's post-hoc tests. Error bars = + 1 SE; n = 3; *** = $p < 0.001$.

Static water contact angles were measured for untreated control PS flat sheet membranes cast in either deionised water or 70% (v/v) IMS and treated PX membranes exposed to oxygen plasma for 1 min, 2 min or 5 min. All PX membranes visually displayed a decrease in water contact angle compared to the untreated control PS membranes (**Figure 4.6**).

Comparative statistical analyses via a one-way ANOVA with Tukey's post-hoc tests were then performed to examine whether there were significant differences in mean water contact angle between a) untreated and plasma treated surfaces for membranes cast with the same nonsolvent for increasing time periods and b) membranes cast using different nonsolvents with the same surface treatment applied.

There were statistically significant differences between all treated surfaces compared to the untreated surfaces where membranes were cast with the same nonsolvent. However, there was no significant difference upon increasing treatment exposure time beyond 1 min. There was also no significant difference in contact angle between the different nonsolvents used for membrane fabrication, regardless of treatment exposure time (**Figure 4.7**).

4.2.4 Surface chemistry of PS and PX flat sheet membranes

Surface wettability is governed by chemical structures present on the surface of a material. In the case of developing a suitable cell culture surface, the side of the membrane exposed for cell attachment should not be hydrophobic. Culture media containing FBS or similar supplementation to aid cell attachment possess proteins such as fibronectin or vitronectin, which deposit upon the culture substrate and aid in cell attachment through cell adhesion proteins, known as integrins. A hydrophilic surface has been shown to facilitate this protein adsorption [169,191,192].

Changes in surface wettability from surface modification may signify differences in surface chemistry from untreated surfaces. ATR-FTIR spectroscopy was utilised to assess whether exposure to oxygen plasma had physically altered the chemical structure of PS membrane surfaces. This was assessed on membranes that had been cast in deionised water and also in 70% (v/v) IMS.

Figure 4.8 and **Figure 4.9** show ATR-FTIR spectra of untreated PS and inductively coupled oxygen plasma treated PX membranes, cast in deionised water and in 70% (v/v)

IMS respectively. All membranes regardless of treatment showed a strong absorption peak at around 700 cm^{-1}, which is indicative of the presence of C-H bonds within a benzene ring. Smaller absorption peaks at approximately 2920 and 3020 cm^{-1} signified C-H alkane bonds, and a small peak at 1600 cm^{-1} suggested the presence of aromatic C-C bonds. However, there was a medium peak at around 1700 cm^{-1} and a small peak between 3080 and 3650 cm^{-1} only in the membranes that had been exposed to oxygen plasma. These peaks suggested the presence of C=O bonds in the form of aldehyde and ketone structures as well as O-H bonds in the form of carboxylic acid groups respectively. These oxygen functional groups were not present in the spectra of the untreated control membranes.

Furthermore, there was no detectable difference in spectra between membranes cast using the two different nonsolvents, nor were there differences where oxygen plasma treatment time was extended beyond 1 min.

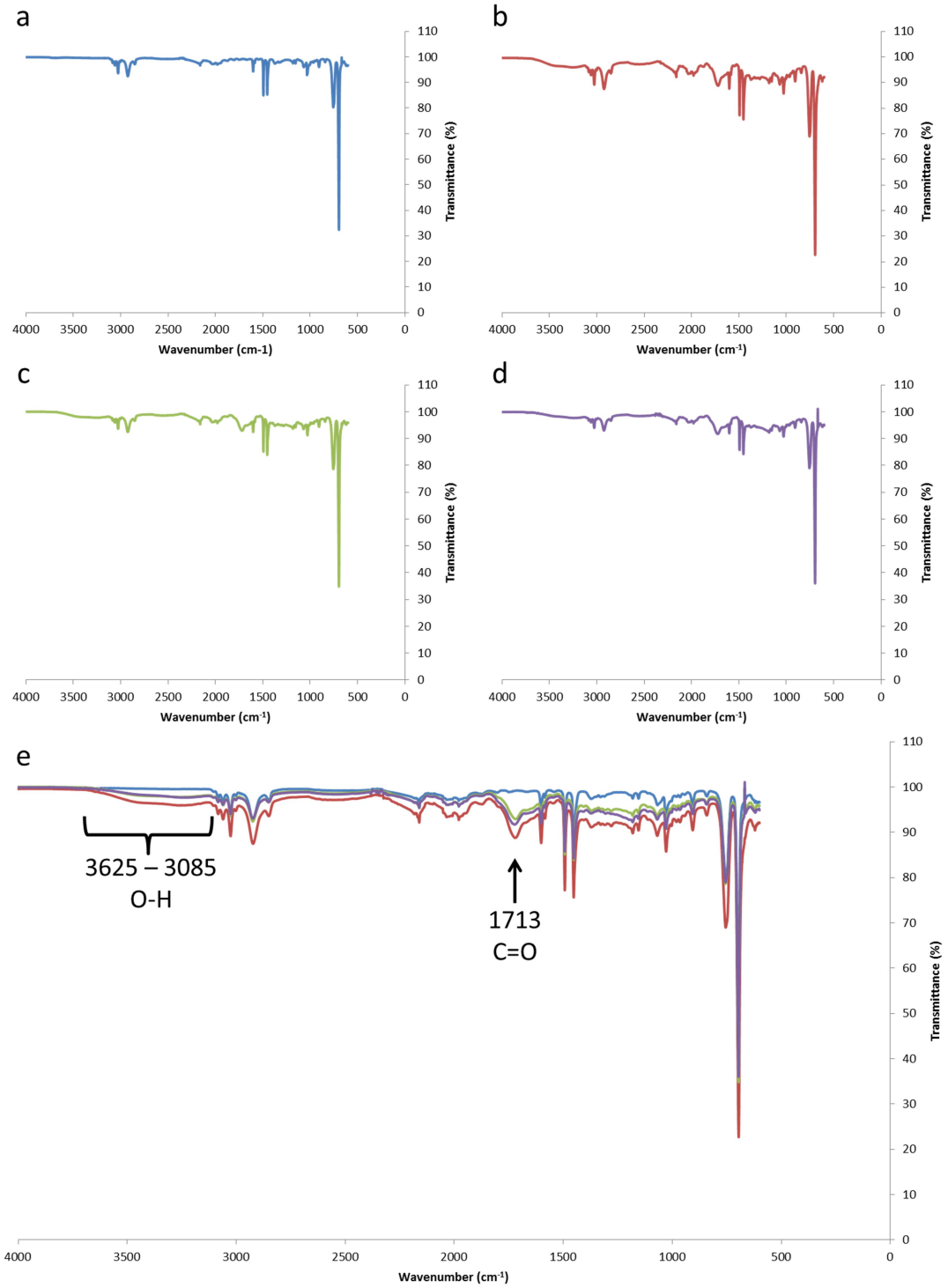

Figure 4.8 ATR-FTIR spectra of untreated PS and inductively coupled oxygen plasma treated PX membranes cast in deionised water. Membranes were either untreated (**a**) or treated with inductively coupled oxygen plasma for 1 min (**b**), 2 min (**c**) or 5 min (**d**). Arrows in the overlay spectra (**e**) depict presence of oxygen functional groups in the treated membranes only.

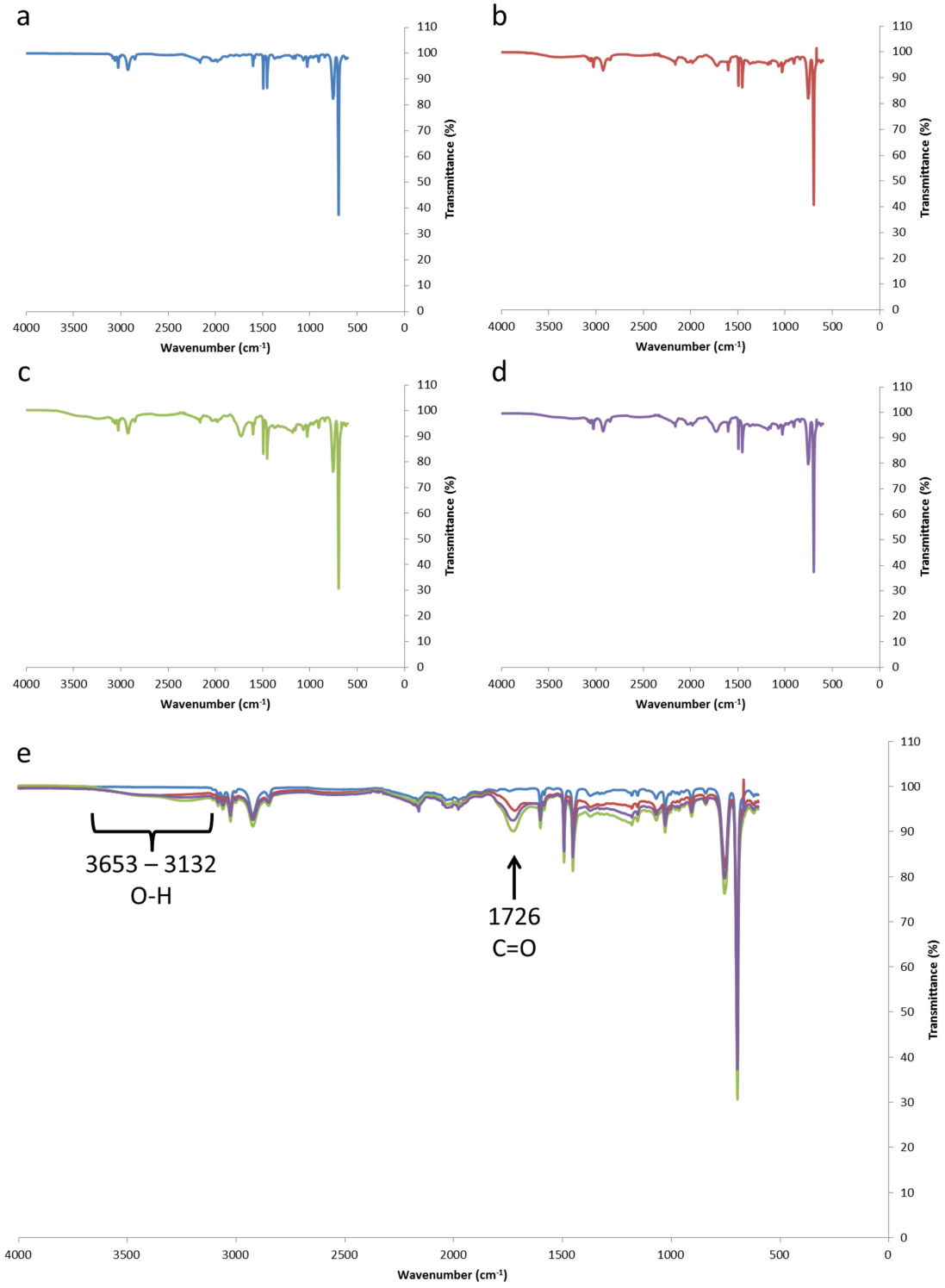

Figure 4.9 ATR-FTIR spectra of untreated PS and inductively coupled oxygen plasma treated PX membranes cast in 70% (v/v) IMS. Membranes were either untreated (**a**) or treated with inductively coupled oxygen plasma for 1 min (**b**), 2 min (**c**) or 5 min (**d**). Arrows in the overlay spectra (**e**) depict presence of oxygen functional groups in the treated membranes only.

4.2.5 Membrane surface treatment with capacitively coupled oxygen plasma

PS membranes investigated in this part of the study were exposed to oxygen plasma using a commercial Zepto Diener capacitively coupled plasma chamber as described in **Section 3.2.3**. Therefore, it was necessary to confirm that the increased surface hydrophilicity and changes to surface chemistry observed with the inductively coupled plasma chamber were replicable and comparable with this system. Further wettability studies with statistical analysis were performed. ATR-FTIR spectroscopy and XPS were also performed to determine any changes between the membrane surfaces in surface chemistry. Further visualisation by SEM was utilised to determine any changes to surface morphology. Plasma power was set at 25 W and exposure time at 30 s due to no significant reduction in hydrophobicity or changes in surface chemistry or morphology seen beyond these parameters (data not shown).

The surface morphology of capacitively coupled oxygen plasma treated PX membranes compared to untreated PS membrane controls is shown in **Figure 4.10**. All treated membranes presented with a smooth, nonporous surface indistinguishable from the untreated controls regardless of the nonsolvent used for casting. Further visualisation of membranes treated at 50 W power for 10 min also showed no changes in surface morphology compared to the untreated controls (data not shown).

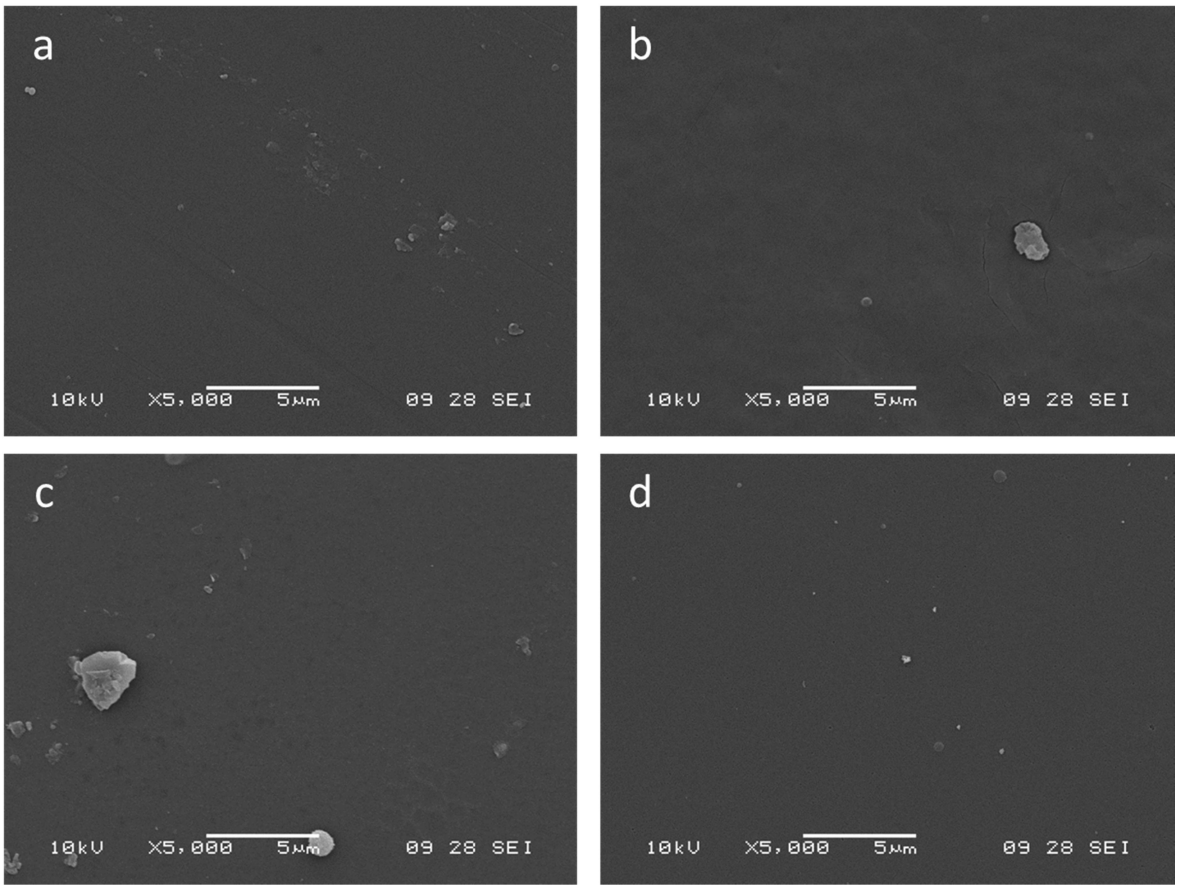

Figure 4.10 Morphology of untreated PS and capacitively coupled oxygen plasma treated PX membrane top surfaces. Membranes were cast using a solution of 20% (w/w) polymer in NMP. Membranes were either untreated (PS) or treated (PX) through exposure to capacitively coupled oxygen plasma at 25 W power for 30 s in a vacuum. (**a**) Deionised water nonsolvent, untreated; (**b**) 70% (v/v) IMS nonsolvent, untreated; (**c**) deionised water nonsolvent, treated; (**d**) 70% (v/v) IMS nonsolvent, treated. Scale bar = 5 µm.

Figure 4.11 depicts static water droplets on the surfaces of untreated control PS and surfaces treated by exposure to oxygen plasma using the capacitively coupled plasma chamber for 30 s. All treated membranes demonstrated a reduction in static water contact angle compared to the untreated controls with the water droplet visibly spreading across the membrane surface, suggesting an increase in hydrophilicity similar to that observed previously in **Figure 4.6**.

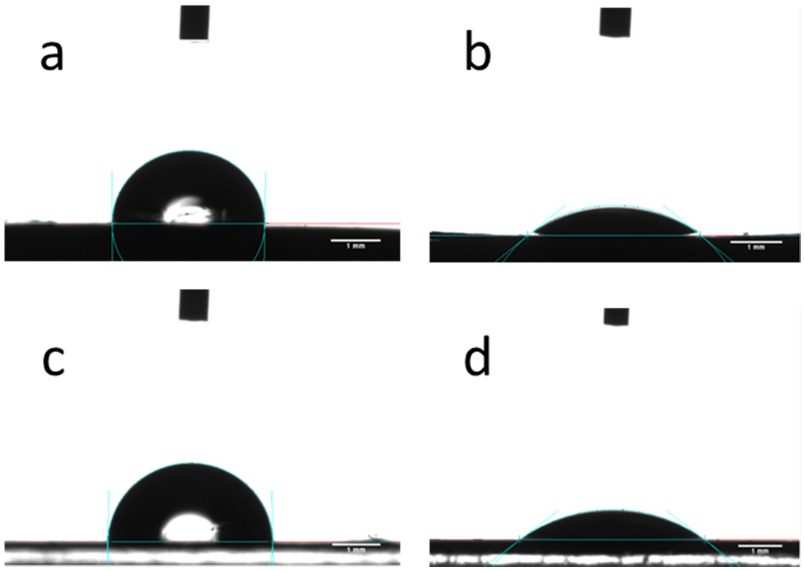

Figure 4.11 Images of water droplets on untreated PS and capacitively coupled oxygen plasma treated PX membranes. Analysis was via the sessile drop method measuring static water contact angles against the membrane surface. PX membranes were exposed to capacitively coupled oxygen plasma at 25 W power for 30 s. Untreated PS membrane surfaces were used as a control. (**a**) Deionised water nonsolvent, untreated; (**b**) deionised water nonsolvent, treated; (**c**) 70% (v/v) IMS nonsolvent, untreated; (**d**) 70% (v/v) IMS nonsolvent, treated. Scale bar = 1 mm.

In addition, analysis between the untreated and treated membranes samples determined that there was a statistically significant difference between the static water contact angles of the two treatment conditions regardless of the nonsolvent used to originally cast the membranes (**Figure 4.12**). This behaviour was also demonstrated previously with the inductively coupled plasma treatment (**Figure 4.7**).

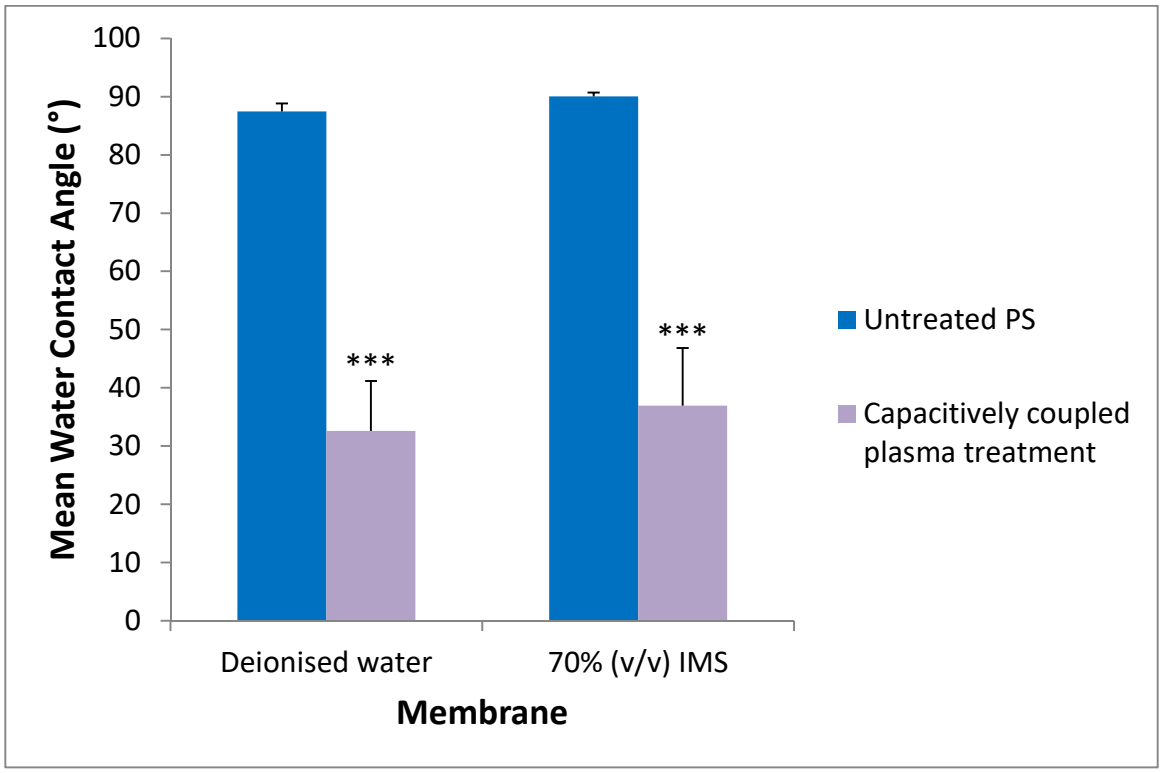

Figure 4.12 Mean water contact angles for untreated PS and capacitively coupled oxygen plasma treated PX membrane surfaces. Membranes were either untreated or exposed to capacitively coupled oxygen plasma at a power of 25 W for 30 s. Statistical analysis was by an independent samples Student's t-test. Error bars = + 1 SE; n = 3; $p < 0.001$.

A further statistical comparison between the two oxygen plasma treatment methods is shown in **Figure 4.13**. The capacitively coupled plasma treatment appears to result in a reduced mean water contact angle when compared to the inductively coupled plasma treatment. However, statistical comparison via an independent samples Student's t-test determined that there was no significant difference between the treatment types for either membrane casting method, suggesting that the two methods are comparable in affecting PS membrane surface wettability.

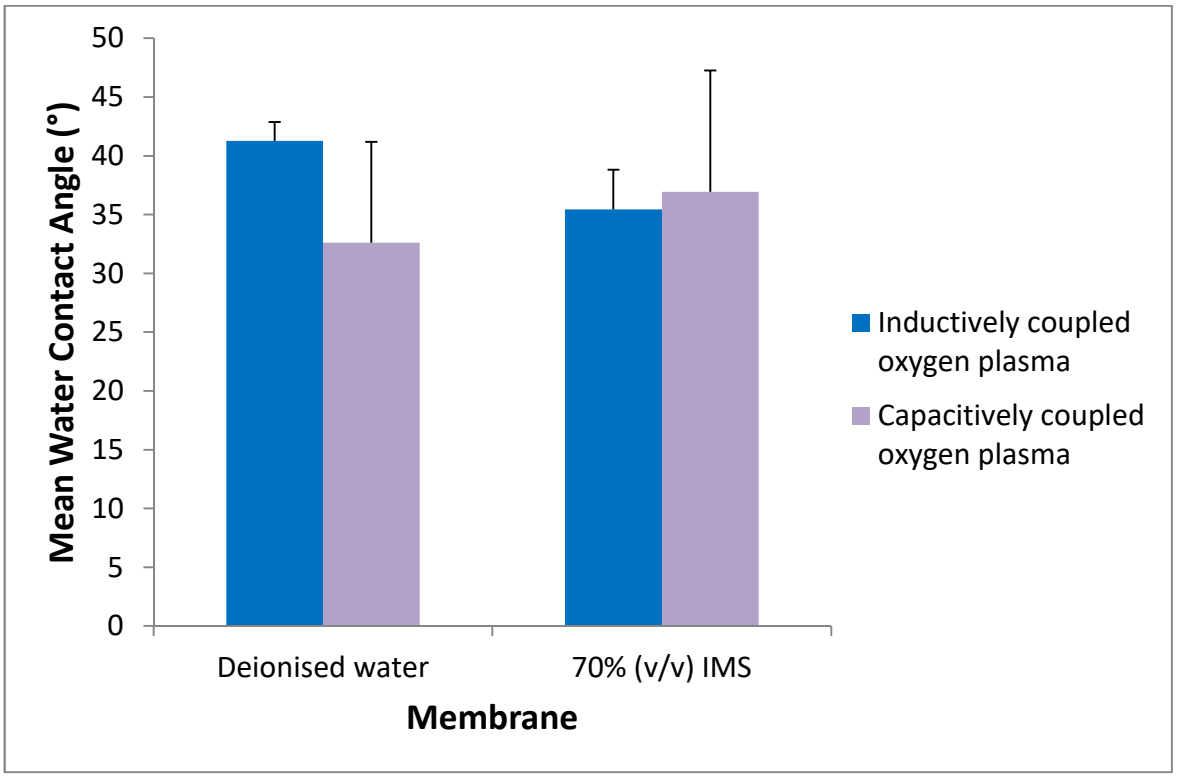

Figure 4.13 Comparison between mean water contact angles for inductively coupled and capacitively coupled oxygen plasma treated PX membrane surfaces. Membranes were either exposed to inductively coupled oxygen plasma at a power of 30 W for 1 min or capacitively coupled oxygen plasma at a power of 25 W for 30 s. Statistical analysis was by an independent samples Student's t-test. Error bars = + 1 SE; n = 3; $p > 0.05$.

ATIR-FTIR analyses of untreated and treated membrane surfaces are shown in **Figure 4.14** for deionised water cast membranes and **Figure 4.15** for 70% (v/v) IMS cast membranes. As previously observed in **Figure 4.8** and **Figure 4.9**, all untreated and treated membranes showed a strong peak at 700 cm^{-1} indicative of benzene ring C-H bonds, further alkane C-H bonds with peaks at approximately 2900 and 3000 cm^{-1} and C-C bonds with a minor peak at 1600 cm^{-1}.

Both treated membranes showed a medium peak at approximately 1700 cm^{-1} and a wide peak between 3110 and 3650 cm^{-1}, relating to the presence of C=O and O-H bonds. The capacitively coupled oxygen plasma treated spectra showed presence of oxygen functional groups similar to that seen in membrane surfaces treated using inductively coupled oxygen plasma suggesting that the addition of functional groups between the two methods are comparable.

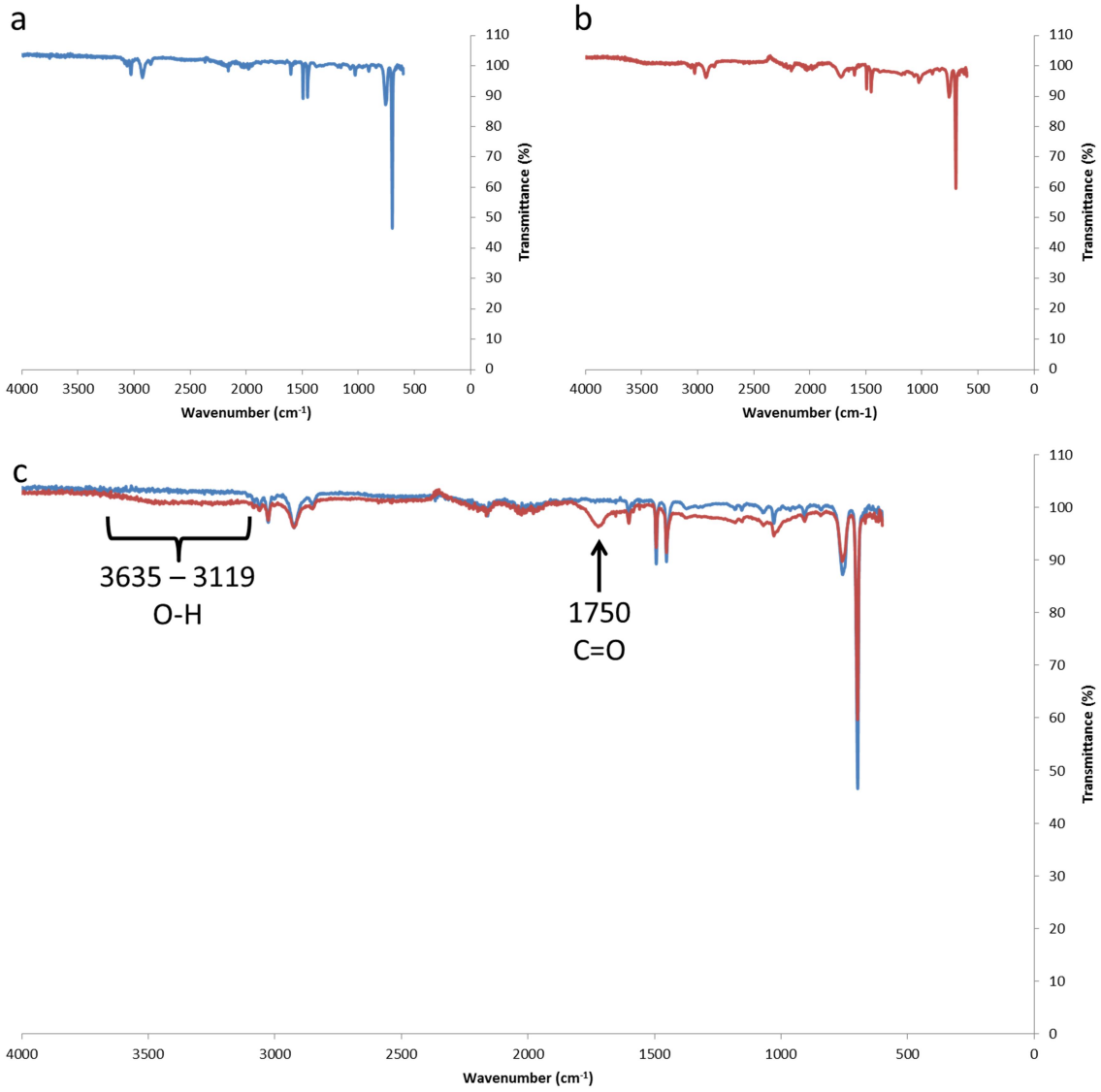

Figure 4.14 ATR-FTIR spectra of untreated PS and capacitively coupled oxygen plasma treated PX membranes cast in deionised water. Membranes were either untreated (**a**) or treated (**b**) with capacitively coupled oxygen plasma at a power of 25 W for 30 s. Arrows in the overlay spectra (**c**) depict presence of oxygen functional groups on the treated membrane surface only.

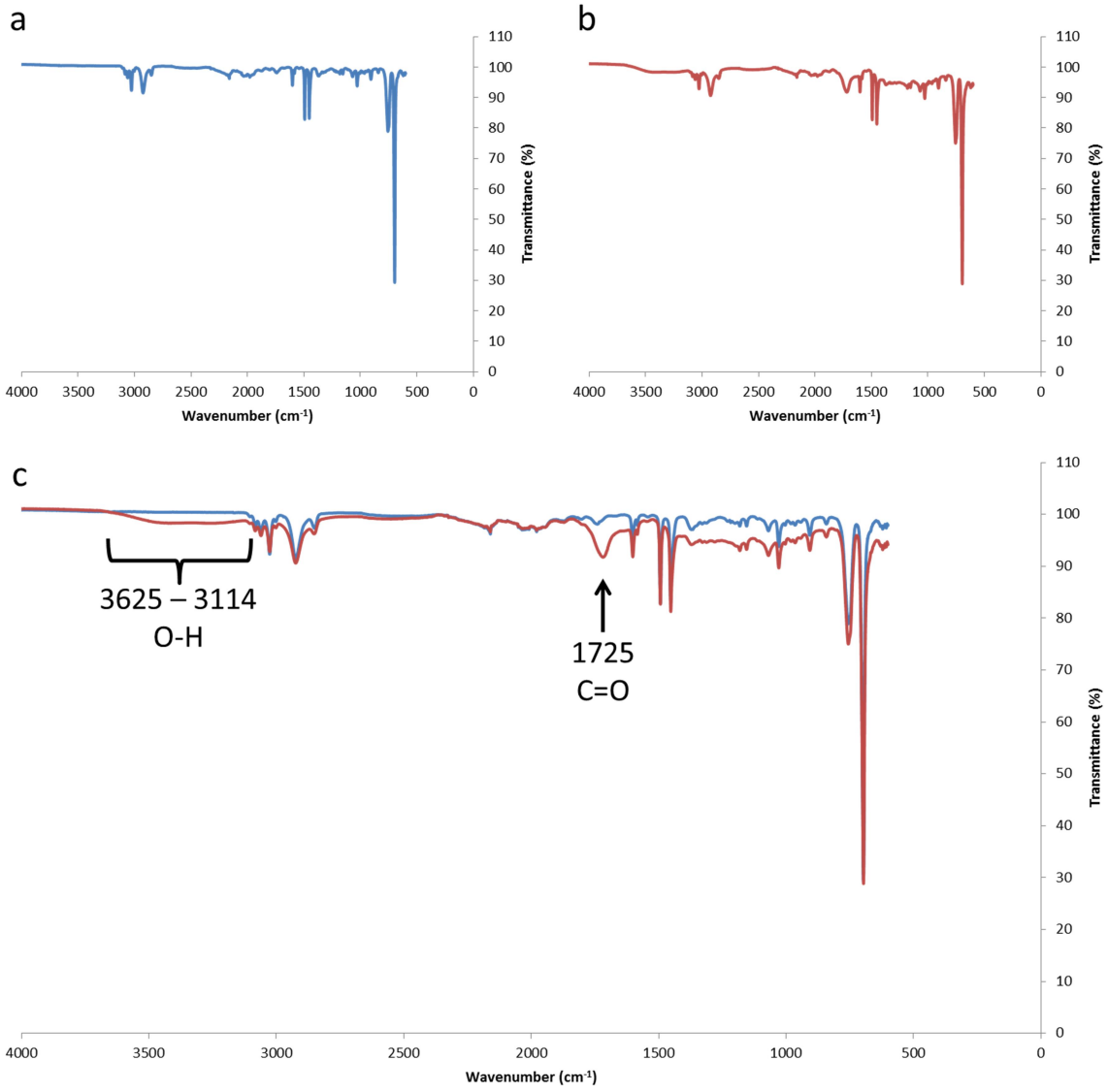

Figure 4.15 ATR-FTIR spectra of untreated PS and capacitively coupled oxygen plasma treated PX membranes cast in 70% (v/v) IMS. Membranes were either untreated (**a**) or treated (**b**) with capacitively coupled oxygen plasma at a power of 25 W for 30 s. Arrows in the overlay spectra (**c**) depict presence of oxygen functional groups on the treated membrane surface only.

Further examination of surface chemistry utilised XPS analysis to quantify the elemental composition of the untreated and oxygen plasma treated membrane surfaces. XPS is able to detect resonance peaks for specific surface atoms dependent on electrons ejected from the sample surface upon irradiation by X-rays. As PS is a hydrocarbon polymer and added oxygen functional groups were apparent from the ATR-FTIR spectra after plasma treatment, the elements particularly of interest were C and O. **Figure 4.16** shows the XPS survey spectra of untreated PS and oxygen plasma treated PX membranes.

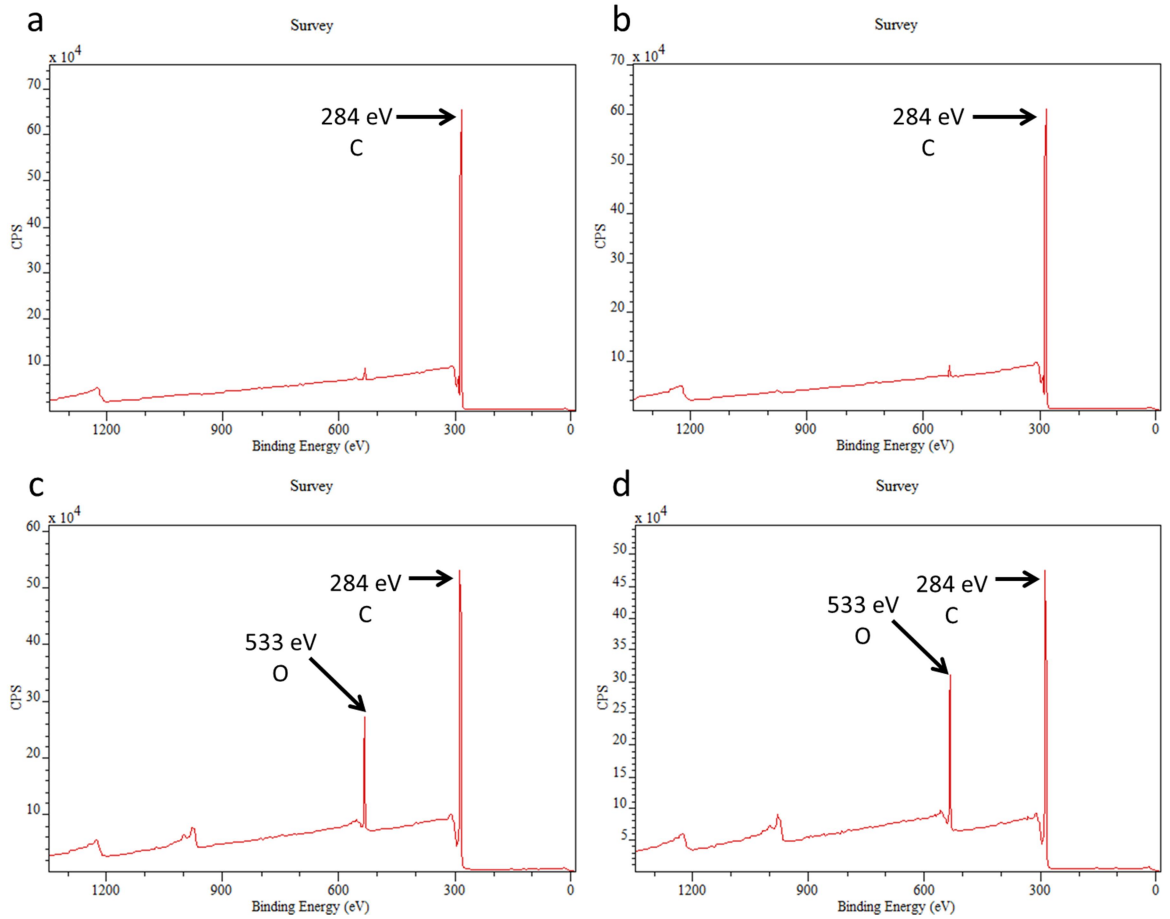

Figure 4.16 XPS survey spectra of untreated PS and capacitively coupled oxygen plasma treated PX membranes. Membranes were either untreated or exposed to capacitively coupled oxygen plasma at a power of 25 W for 30 s. Intensity of binding energy (eV) peaks is shown as counts per second (CPS). (**a**) Deionised water nonsolvent, untreated; (**b**) 70% (v/v) IMS nonsolvent, untreated; (**c**) deionised water nonsolvent, treated; (**d**) 70% (v/v) IMS nonsolvent, treated.

In all conditions, a high intensity peak at 284 eV was detected, which is indicative of a large presence of elemental C. Medium intensity peaks at 533 eV, representative of elemental O, were detected in the oxygen plasma treated membrane surfaces. However, this peak was negligible in the untreated membrane surfaces.

Table 4.1 Mean elemental C and O compositions of untreated PS and capacitively coupled oxygen plasma treated PX membrane surfaces. Statistical analysis was by independent samples Student's t-tests and a one-way ANOVA with Tukey's posthoc tests.

Membrane Nonsolvent	Treatment	Mean [C_{1s}] Atomic %	Mean [O_{1s}] Atomic %
Deionised water	Untreated PS	95.19 ± 1.32 ***	4.81 ± 1.32 ***
	Treated PX	85.91 ± 1.16 ### +++	14.09 ± 0.34 ### +++
70% (v/v) IMS	Untreated PS	98.37 ± 0.34	1.63 ± 1.16
	Treated PX	81.84 ± 0.42 +++	18.17 ± 0.43 +++

± 1SE; n = 3; *** = ($p = 0.001$) (untreated only); ### = ($p < 0.001$) (treated only); +++ = ($p < 0.001$) (untreated vs treated)

The mean atomic % of C and O for each membrane condition is shown in **Table 4.1**, given as the ratio of peak intensity to the total intensity of electrons measured. The O atomic % was higher for all PX membranes compared to untreated membranes. Statistical analyses were then performed to determine whether there were any significant differences between untreated membranes only, treated membranes only and also between untreated membranes and their treated counterparts.

An independent samples Student's t-test was used to compare elemental compositions between untreated deionised water cast and 70% (v/v) IMS cast PS membranes. It was determined that there was a statistical difference between the two untreated membranes with the untreated PS membrane cast in deionised water showing a higher O atomic % than the untreated IMS-cast membrane ($p = 0.001$). There was also a significant difference in O atomic % between treated deionised water cast and 70% (v/v) IMS cast PX membranes ($p < 0.001$).

Further analysis via a one-way ANOVA with Tukey's posthoc tests showed that there was a strong statistical difference in atomic C and O for both PX membranes versus their untreated counterparts ($p < 0.001$).

4.3 Discussion

The research aims for this Chapter were to characterise a method for the development of polystyrene hollow fibre membranes using phase inversion cast flat sheet membranes as a model system. Two potential ternary systems and the subsequent membrane surface treatments with inductively coupled and capacitively coupled oxygen plasmas were examined and characterised to generate a biomaterial suitable for adherent cell culture in a hollow fibre membrane bioreactor system.

4.3.1 Selection of ternary system for casting polystyrene membranes

To successfully cast a membrane, it is necessary to establish polymer dissolution in the chosen solvent, and subsequent precipitation in a suitable nonsolvent. The eventual membrane characteristics are dependent upon the ternary system utilised. The ternary system components analysed in this part of the thesis were selected on the basis of their considerably documented usage in tissue culture, previous phase inversion membrane casting and safety – PS is currently the most widely used cell culture substrate; NMP is an FDA-approved solvent that has previously been utilised to dissolve polymers for membrane fabrication and water and 70% (v/v) IMS are relatively safe nonsolvents frequently used for cell culture. In particular, 70% (v/v) IMS was selected as a potential substitute nonsolvent for water due to its use as a disinfecting agent in aseptic cell culture, with the consideration that the potential membrane would be cast within an environment less conducive to bacterial infection. It has also been previously shown that ethanol-wetted foams can improve wettability upon hydrophobic polymers due to liquid phase mixing within the porous structure between water and a surface pre-wet with ethanol due to their high mutual affinities [193,194]. Furthermore, the formation of a porous membrane is encouraged by a mutual affinity between solvent and nonsolvent as well as the concentration of the polymer in the dope solution.

A 20% (w/w) mixture of PS in NMP dissolved entirely into the liquid phase overnight, forming a homogenous solution. Subsequent immersion of the dope into water or 70% (v/v) IMS caused a white PS precipitate to form. This is a process termed liquid-liquid demixing, occurring due to the addition to the polymer-solvent system of a large volume of nonsolvent such that the binodal point of the ternary system is surpassed [159]. This

generates thermodynamic instability in the polymer-solvent solution, thus causing precipitation of the polymer [159]. In the PS-NMP-water/70% (v/v) IMS ternary system, this behaviour was aided by the miscibility of NMP and comparative immiscibility of PS with both nonsolvents.

PS membrane precipitation behaviour differed depending upon the nonsolvent used. Membranes cast using deionised water precipitated almost immediately and lifted away from the coagulation plate easily, whereas immersion of the dope in 70% (v/v) IMS caused the membranes to precipitate more slowly before lifting away from the plate. The faster precipitation behaviour of water-cast membranes infers a more instantaneous demixing of polymer from solvent, whereas 70% (v/v) IMS-cast membranes demonstrated a more delayed demixing process due to the slower membrane precipitation. This demixing behaviour is linked to the solubility of NMP in the respective nonsolvents – increased solubility of the solvent in the nonsolvent is a factor that favours a more instantaneous form of demixing, suggesting that water has a greater solubility in NMP than 70% (v/v) IMS.

These initial observations show that both ternary systems are able to produce a polymer precipitate. However, the differences in solubility of NMP in deionised water or 70% (v/v) IMS and differing rates of demixing will affect the resultant structure of the membrane. To replicate the physiological environment of the liver *in vitro* it is necessary for the membrane to possess a porous structure, thus allowing diffusion of molecules of a certain molecular weight across the membrane substructure. By adjusting the components of the ternary system involved to alter the rate of demixing, such as the solubility of solvent and nonsolvent, this can aid the formation of surface and substructure pores during membrane fabrication. As cells will be cultured on the membrane surface, it is essential that any pores present on the surface cannot be greater in size than 5 μm as cells may migrate into the substructure [154]. In this case, the top surfaces of both water-cast flat sheet membranes and 70% (v/v) IMS-cast membranes were shown to be very smooth with no visible pores, suggesting that these nonsolvents are unable to produce porous membranes as part of this system.

A line of investigation previously explored in this laboratory had examined the effect on PS flat sheet membrane morphology where the membranes were cast using 20% (w/w) PS in 1, 4-dioxane or dimethylformamide as solvents with deionised water as the nonsolvent.

Both solvents are miscible with water and membranes cast using these solvents had visible surface pores in contrast to the PS-NMP dopes, also with highly porous substructures. However, the surface pores were sparsely present and averaged between 20 – 100 μm in diameter – considerably larger than the required 5 μm diameter [195]. It was also shown that casting of membranes where the PS concentration was reduced to 10% (w/w) in a dope solution with NMP, 1,4-dioxane or DMF in water did not produce a membrane with surface pores [195]. Although a high polymer concentration can result in a less porous top layer, a lower concentration would affect the solution viscosity and therefore the capability of the dope solution to form mechanically stable hollow fibres. It is therefore likely that the polymer itself is the cause of the lack of pore formation on the membrane surface.

The cross sectional membrane substructures were highly porous with long finger-like macrovoids. In the water-cast membranes, these macrovoids presented in the lower third of the substructure, whereas in membranes cast in 70% (v/v) IMS showed macrovoids descending perpendicularly from the surface, approximately two-thirds the depth of the membrane. In both membrane types, the macrovoids were contained within a spongy layer that consisted of smaller porous substructures.

The presence of macrovoids in both systems suggests that the rate of demixing experienced during the phase inversion process is rapid rather than delayed. As previously mentioned, the membranes cast in 70% (v/v) IMS took longer to coagulate than the water-cast membranes, suggesting it had undergone a more delayed demixing. However, a fully delayed demixing process would not generate macrovoids but a spongy layer with small pores. This was shown in a previous study comparing NMP and 1,4-dioxane as solvents in a PLGA phase inversion membrane system with water as the nonsolvent, it was shown that the NMP-cast membranes, which contained macrovoids, tended towards instantaneous demixing. This was a feature absent in 1,4-dioxane-cast membranes, which possessed a spongy substructure due to delayed demixing [154] from the higher affinity of the solvent to the polymer. Therefore, it is likely that although the 70% (v/v) IMS-cast membranes took longer to coagulate, the reduced rate of demixing compared to water-cast membranes was still rapid enough to allow for a similar macrovoid-containing substructure to develop.

Macrovoids are considered to be unfavourable as they can lead to mechanical weaknesses in the membrane structure [159,196]. This is seen in systems operating at higher pressures; for example, in gas separation [159,196]. However, a similar high pressure operating

system is not required for the intended application. A study by Ellis and Chaudhuri in 2007 characterised PLGA phase inversion hollow fibre membranes as tissue engineering scaffolds and suggested that macrovoids in the membrane structure could be considered a positive feature [154]. This is due to reduced flow resistance through the macrovoids, yet still providing suitable support for other porous sublayers [154]. Therefore, the presence of macrovoids in these PS phase inversion membranes should not considered a negative feature.

4.3.2 Surface modification of polystyrene membranes by plasma treatment

To reduce the surface hydrophobicity of polystyrene membranes, both water-cast and 70% (v/v) IMS-cast PS membranes were exposed to oxygen plasma. Plasma treatment allows for changes to surface characteristics such as wettability and chemistry whilst leaving the properties of the bulk material largely unaltered [166]. Where inductively coupled oxygen plasma is generated through an electric field in oxygen gas induced from a magnetic field generated from a running an RF current through a coil wrapped around the plasma chamber, capacitively coupled plasma is generated from an electrical discharge occurring between electrodes in oxygen gas [197]. Both inductively coupled and capacitively coupled methods of plasma generation form low pressure plasmas which have been used to surface treat the membranes investigated in this chapter.

The surface morphology of membranes exposed to inductively coupled oxygen plasma differed between water-cast and IMS-cast membranes dependent upon exposure length. Treated and untreated water-cast membranes all presented with smooth surfaces with no pores visible. For IMS-cast membranes, surface pores were visible post-treatment, increasing in number with greater exposure time, although for both membranes, there was no visual deterioration in the bulk substructure. Increases in surface roughness due to oxygen plasma exposure have been previously seen in PS, PLGA and polypropylene films [198–201]. Therefore, the change in morphology to a more porous surface is attributable to the increased exposure to inductively coupled oxygen plasma. From this, oxygen plasma alone could be potentially used to generate a porous surface without considerably altering the porous substructure. However, the lack of pores in the treated water-cast membrane surfaces and also the capacitively coupled oxygen plasma treated samples even at higher

power and increasing time of exposure suggests that this method may not be entirely relied upon. Previous examples of surface topography change signified by increased surface roughness have been shown in microwave oxygen and argon plasma treated PS culture dishes whilst maintaining the effect of increased hydrophilicity [202]. These changes have also been seen in inductively coupled oxygen plasma treatment of PS films [201,203] so both methods can be utilised for functionalisation of PS substrates to produce a surface altered, less hydrophobic material. The lack of visual change described in this Chapter in PS flat sheet membranes upon exposure to capacitively coupled plasma does not necessarily preclude changes in the surface structure due to limitations with SEM being a visual medium. Further analysis by atomic force microscopy (AFM) would provide a topographic image from which to determine further surface structure differences between untreated and treated membranes, therefore guiding future optimisation of the plasma treatment method to produce a porous surface. AFM can further be used to determine the stiffness of the culture substrate, which is a factor that can affect the behaviour of cultured cells [204]. Further analysis into the stiffness of untreated and treated membranes would also develop characterisation of the biomaterial further. Culture substrate stiffness is an additional factor in determining the ability of cells to attach to the substrate surface and undergo normal cellular functions such as proliferation, differentiation and tissue specific functions [205]. Furthermore, it should also be noted that excessive exposure to plasma etching may penetrate through into the bulk structure and mechanically weaken the membrane so this approach may not be optimal if long sample exposure time or high power is required to generate the plasma [206]. To determine if the plasma treatment has affected the mechanical properties of the biomaterial positively or negatively, further work necessitates comparative measurements of tensile strength and also elasticity of untreated and treated membranes dependent upon the length of exposure to oxygen plasma. This analysis would aid tailoring of the plasma treatment method to ensure that the treated membrane will possess the changes in surface wettability and chemistry with little to no mechanical weakening of the structure. Both PS membranes when treated with oxygen plasma showed reductions in hydrophobicity compared to untreated membranes from static water contact angle measurements. Using inductively coupled plasma, exposure beyond 1 min did not reduce hydrophobicity further, suggesting that there is no added improvement for longer exposure time. Capacitively coupled oxygen plasma showed reduction in hydrophobicity after 30 s exposure. A possible reason for the lack of improvement with

longer exposure times may be due to the method utilised to examine changes in surface energy. Although the sessile drop method and subsequent measurement of static water contact angles are widely used to determine hydrophobicity of a surface, there are limitations with this method that may cause variations in results. Such variations altering the reported contact angle include evaporation of the water droplet or infiltration of the droplet to exposed sections of porous substructure [207,208]. In the case of these results, the contact angle measurement was taken immediately after releasing the droplet, thus minimising any evaporation effect. However, water infiltration of the membrane due to exposure to the porous membrane substructure may have affected contact angle measurement by increasing the difficulty of distinguishing between samples with greatly reduced contact angles with the goniometer, particularly as no statistical differences were found when increasing initial plasma exposure time. Differences in surface chemistry between untreated deionised water-cast and IMS-cast membranes and their treated counterpart were observed. Quantification of surface elemental C and O showed a statistically significant increase in elemental O in untreated deionised water-cast PS membranes compared to untreated IMS-cast membranes. However, this increase did not correlate with detectable presence of added oxygen functional groups in the membrane surface nor a significant improvement in wettability over untreated IMS-cast membranes. Treated membranes were observed to have detectable presence of added oxygen functional groups with the increase in surface elemental O deemed statistically significant, and also between treated deionised water and 70% (v/v) IMS membranes. Furthermore, these changes in surface chemistry in the treated membranes correlate with the reduced water contact angles similarly observed in the treated membranes only, although there were no further differences in wettability between treated membranes cast from different nonsolvents. These alterations in PS surface chemistry have also been observed in previous studies examining oxygen plasma treatment of PS films [209] and non-tissue culture PS dishes [202,210], where wettability was increased and carbonyl and alcohol structures were found to be present upon the treated substrate surface. This therefore suggests that fabricating PS membranes via phase inversion are similarly able to have their hydrophobicity reduced upon treatment with oxygen plasma. Although both ternary systems are suitable for casting hollow fibres, the use of capacitively coupled plasma treatment was unable to replicate the results of the inductively coupled plasma treatment to produce a porous surface on 70% (v/v) IMS cast membranes, even though both methods

are used to produce similar low pressure oxygen plasmas. Therefore, both ternary systems are considered comparable in the case of increased wettability and lack of surface pores when treated with oxygen plasma generated using the capacitively coupled method.

A future experimental approach to take into consideration is the analysis of potential hydrophobic recovery of plasma treated surfaces. Hydrophobic recovery describes the loss of modifications to the surface energy of a treated surface over time, although the extent that this occurs to treated PS surfaces appears to vary within the literature [211,212]. A potential situation that may arise would be an increase in PX membrane hydrophobicity and therefore potentiate a risk that the membrane will revert to being non-conducive to adherent cell culture. A possible approach would be to perform a long-term time-course examination utilising contact angle measurements to determine if wettability is reduced. Furthermore, a time-course assessment of cell attachment would determine the overall long-term efficacy of the biomaterial.

4.4 Conclusion

This Chapter has examined the development and characterisation of phase inversion cast PS membranes that could be used as a cell culture substrate in a hollow fibre membrane setting. Two ternary systems have been developed utilising a 20% (w/w) PS-NMP casting solution and either deionised water or 70% (v/v) IMS as a nonsolvent. Both systems were able to produce asymmetrical membranes possessing a nonporous top skin over a highly porous substructure. The lack of pore structure on the membrane surfaces suggest that the membranes are potentially able to support cell culture without the cells entering the membrane substructure. However, surface pores of no greater than 5 μm diameter are required to ensure the cells do not enter the membrane substructure. Therefore, the phase inversion casting method described here is not sufficient on its own for providing completely porous membranes from surface to substructure. Further work in this area to develop a porous membrane could examine additional surface treatments, such as sodium hypochlorite, or the addition of porogens such as sodium chloride to the casting dope. Utilising an additional method could tailor the pore size further to a specific MWCO.

Subsequent surface treatments with inductively coupled and capacitively coupled oxygen plasma were able to significantly reduce the hydrophobicity of the untreated membranes by

the addition of oxygen functional groups. This could create an environment more conducive to cell attachment as well as possibly providing a method for generating a porous top skin in the case of inductively coupled plasma treatment and 70% (v/v) IMS cast membranes. In addition, this would allow for intra- and extraluminal nutrient diffusion without the loss of cells into the membrane substructure, although further work will be required to optimise a suitable method for developing surface pores. Capacitively coupled oxygen plasma treated deionised water and 70% (v/v) IMS membranes were comparable in their reduction of surface wettability, important for encouraging cell adhesion to the membrane surface.

Further membrane experimental work in this thesis utilises capacitively coupled oxygen plasma treatment to increase surface wettability of membrane surfaces. Although this method was unable to replicate the appearance of surface pores seen when treating 70% (v/v) IMS membranes using inductively coupled plasma, the PS-NMP-water system and PS-NMP-IMS system under capacitively coupled oxygen plasma treatment were comparable with regards to changes to surface wettability and addition of oxygen functional groups. Bearing the scale up costs in mind, from a process point of view, water was selected as a more cost effective nonsolvent to study further with regards to developing a suitable membrane. Therefore, further work in this thesis sought to determine the suitability of the PS-NMP-water system as a biomaterial for supporting cell culture.

Chapter 5
Characterisation of induction and maintenance media for the transdifferentiation of pancreatic cells to hepatocyte-like cells

5.1 Introduction

5.1.1 Transdifferentiated hepatocyte-like cells as a cell source for bioartificial liver devices

An orthotopic liver transplant allows for the restoration of physiological liver function to patients with liver failure. However, a shortage of suitable donor livers means that many patients die whilst waiting on the transplant list. The principle behind the bioartificial liver (BAL) device as a therapeutic biotechnology allows a patient with liver failure to maintain liver function until an organ transplant becomes available. Furthermore, the ability to replicate liver structure and functions is additionally useful as an *in vitro* liver model. The motive behind this would be to use such models as a replacement for animal models which are currently used for drug toxicity testing and also in understanding liver development and functionality.

Given the lack of donor livers it is essential to find a suitable functional substitute that can be sourced from a regular supply. Transdifferentiated hepatocyte-like cells (HLCs) provide a novel approach to sourcing cells for a BAL device. Transdifferentiation (or cellular reprogramming) is defined as the conversion of one differentiated cell type to another, and is considered a type of metaplasia [213,214]. This process has been documented in rats with the appearance of HLCs in the pancreas when fed a copper-deficient diet [215]. Human cases of hepatoid carcinomas occurring in the pancreas demonstrate that this is not solely an animal phenomenon, nor is it purely an *in vivo* occurrence either [216]. An *in*

vitro model was developed utilising the rat pancreatic acinar cell line AR42J-B13 (B13), a subclone of the AR42J line. The B13 subclone has been shown to be more susceptible to differentiation down endocrine lineages than its parent line [130,217]. B13 cells have been shown to readily transdifferentiate into HLCs when cultured with Dexamethasone (Dex) with loss of the pancreatic phenotype [130] and gain of hepatic markers. This involves induction of CCAAT/enhancer binding protein beta (C/EBPβ), considered the 'master switch' for direct conversion; and hepatocyte nuclear factor 4 alpha (HNF4α), essential for hepatic differentiation, within the first 2 days of treatment. This is followed by expression of a range of mature liver markers such as transferrin (TFN), glucose-6-phosphatase and albumin with continued treatment [130–132,218].

Transdifferentiation of pancreatic cells to HLCs using this method has also been demonstrated in mouse embryonic pancreas [136] and primary mouse, rat and human pancreatic cells [134,135,219–221]. The addition of Oncostatin M (OSM) to the culture medium has been shown to enhance the conversion to a hepatic phenotype and upregulate the production of acute phase proteins, essential for the inflammatory response of the immune system [130–132,218]. As well as transdifferentiating to HLCs, the B13 cell line has shown plasticity in its ability to convert to other cell types such as insulin producing β-cells [217] and ductal cells [222], displaying similar functionalities to their primary counterparts.

Characterisation of transdifferentiated HLCs has shown that they possess a wide range of hepatic functions including expression of both ammonia detoxification enzymes glutamine synthetase (GS) and carbamoylphosphate synthetase-1 (CPS-1) in different cell populations, reflecting their zonation along the porto-venous axis [4,14,218]. They also show long term expression of functional cytochrome P450 (CYP) enzymes [223], responsiveness to the xenobiotics ciprofibrate and phenobarbitol [131,218] and can support replication of Hepatitis B virus [133], displaying functional similarity to primary hepatocytes which makes them an ideal candidate for a BAL device cell source. As B13 cells come from an established cell line that can be readily cultured *in vitro*, transdifferentiated HLCs, with their wide range of hepatic functions, also offer a potential, limitless alternative to other cell sources for drug toxicity models. However, an issue with this cell source is that not all B13 cells lose their pancreatic phenotype upon treatment [129]. Furthermore, the functional maturity of transdifferentiated HLCs when compared to

mature hepatocytes is unclear, warranting further investigation into improving the transdifferentiation protocol.

Greater understanding of the mechanisms behind transdifferentiation as a whole can help guide understanding of the factors involved in normal development. For example, transdifferentiated HLCs are also useful as an *in vitro* model for investigating the background behind pancreatic and liver development. The ability of pancreatic cells to convert to hepatocytes belies their similar developmental origins as during embryonic development they originate from the same region of the endoderm [218]. This knowledge can also be translated to guide the development of new cellular therapies utilising stem cell reprogramming. In addition, knowledge of transdifferentiation can aid the understanding behind certain metaplastic events such as in Barrett's metaplasia, as metaplasia is often a precursor to cancer development [224–226].

5.1.2 HepatoZYME^{+} as an induction and maintenance medium for transdifferentiated HLCs

The original method for the transdifferentiation of pancreatic cells to HLCs initially utilised supplementation of the complete B13 culture medium with the glucocorticoid hormone Dex [130]. Initially, treatment of the B13 cell line with Dex would stimulate an upregulation of amylase exocrine function beyond that of naïve cells; similar behaviour to that previously reported in the parent AR42J cell line [217]. It was found that with prolonged glucocorticoid stimulation, this expression decreased over time along with subsequent induction of hepatic markers, displaying a loss of pancreatic phenotype toward a hepatic one [130]. As previously mentioned, additional supplementation with OSM alongside Dex improved the hepatic phenotype beyond that seen from culturing with Dex alone [130–132]. Interestingly, B13 cells express c-Myc, Klf4, Oct4 and Sox2, known as the four pluripotency factors [227]. After glucocorticoid treatment, c-Myc remains as the only one active, and it has been hypothesised that maintenance of a pluripotent phenotype provides the B13 cell line with its ability to transdifferentiate into different cell types [129,227].

The basal culture medium HepatoZYME-SFM is a proprietary serum-free medium that has previously been used for the long term maintenance of hepatic phenotypic expression for

the culture of isolated primary rat and human hepatocytes [228,229]. From a manufacturing process point of view, consistency in the protocol is essential for scale up for clinical usage so that there are no variations in the quality of the product. Serum-free media are attractive as foetal bovine serum (FBS), although commonly used in tissue culture media to aid attachment of adherent cells to culture substrates, suffers from issues such as wide batch-to-batch variability that can affect product optimisation as well as ethical issues with sourcing [230–232].

A protocol supplementing HepatoZYME-SFM with the glucocorticoid Hydrocortisone (10 μM), the cytokines hepatocyte growth factor (HGF) (10 ng/ml) and OSM (20 ng/ml) (HepatoZYME^{+}) reported promising results for improvement of the hepatic phenotype as part of the directed differentiation of human embryonic stem cells (hESCs) and induced pluripotent stem cells (iPSCs) to HLCs over other specialised hepatocyte media [121,233–235]. On the basis of this, the hepatic differentiation and maturation qualities of the serum-free HepatoZYME^{+} medium were of interest as a potentially novel culture medium that could be translated to the B13 transdifferentiated HLC model as a possible inducing agent and maintenance medium.

5.1.3 Experimental aims and objectives

The experimental research in this Chapter involves the characterisation of two potential culture media – HepatoZYME^{+} and 50:50 – for the induction of transdifferentiation of the pancreatic B13 cell line to HLCs in comparison with established Dex-based protocols. The 50:50 culture medium consisted of HepatoZYME^{+} diluted 1 in 2 with the complete B13 culture medium, therefore containing half the supplementation concentrations of HepatoZYME^{+} - Hydrocortisone (5 μM), HGF (5 ng/ml) and OSM (10 ng/ml). The research questions to be answered here were whether HepatoZYME^{+} could a) induce conversion to HLCs in the B13 cell line when compared to Dex-treated cells; and b) produce HLCs with an improved hepatic phenotype beyond that already established by Dex-induced transdifferentiation.

The effects of the culture media on the cell line and transdifferentiated HLCs as potentially novel methods of inducing and maintaining this state were characterised with regards to their morphology and expression of gene and protein markers. The first part of this Chapter

describes the treatment of the B13 cells with the experimental culture media to induce transdifferentiation, and the second part investigates use of the experimental culture media to maintain transdifferentiated HLCs.

Characterisation of untreated and treated cells was done via analyses of (i) morphology by transmitted light microscopy; (ii) protein expression by immunofluorescent staining with fluorescent microscopy; (iii) protein expression quantification and finally (iv) gene expression by RT-PCR.

5.2 Results

5.2.1 Characterisation of transdifferentiation in B13 cells using HepatoZYME^{+}-based media

Prior to treatment, B13 cell cultures were initially maintained in complete B13 culture medium as described in **Section 3.4.1**. The efficiency of transdifferentiation has previously been found to be affected by the initial cell seeding density, where seeding at too high a density demonstrated resistance to conversion toward a hepatic phenotype [236,237] and seeding too sparsely showed low cell growth and conversion rates [236]. Therefore, an initial seeding density of 30,000 cells per well of a standard cell culture 6-well plate (3,125 cells/cm^2) was utilised for the experiments in this Chapter.

24 hr post seeding, the B13 cell culture medium was supplemented with either 1 μM Dex or changed completely to HepatoZYME^{+} or a 50:50 combination of complete B13 culture medium and HepatoZYME^{+}, referred to as "50:50". B13 cells cultured in complete B13 culture medium only were used as an untreated control.

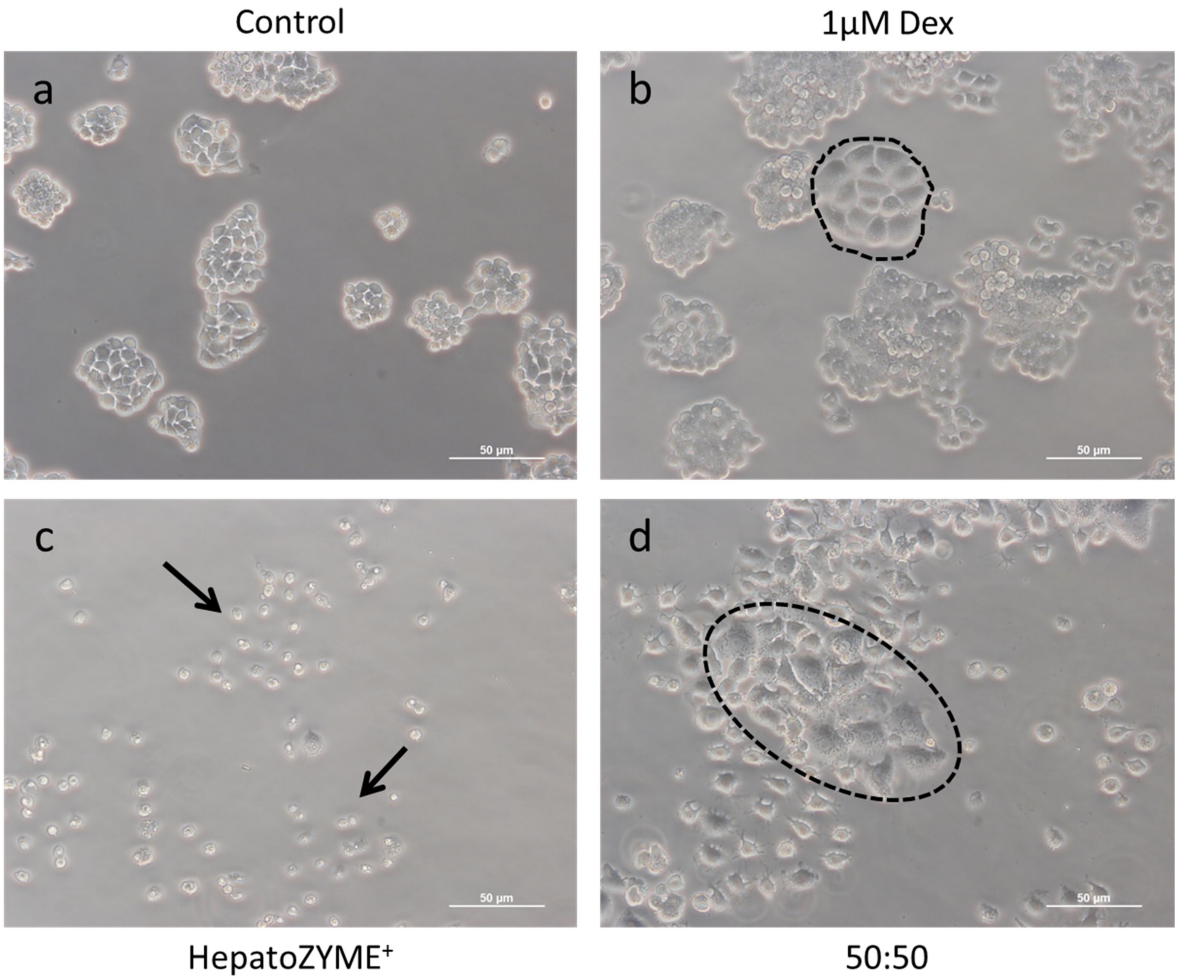

Figure 5.1 Morphology of B13 cells in different induction media over 5 days. Cells were treated without (**a**) or with 1 µM Dex, (**b**) HepatoZYME^{+} (**c**) or 50:50 (**d**). Areas demarcated by dashed lines show cells with an enlarged, flattened, hepatocyte-like morphology (**b** & **d**) compared to the untreated control (**a**). Arrows indicate areas of dead or dying cell colonies (**c**). Scale bar = 50 µm.

Morphological changes in the cells over 5 days of treatment were visualised through transmitted light microscopy as shown in **Figure 5.1**. Compared to the untreated control, a flattening and enlargement of cell morphology was observed in some cells of the Dex-treated and the 50:50-treated cultures, a trait seen previously in the transdifferentiation of B13 cells to a hepatocyte-like phenotype. However, after 5 days, the cells cultured in the HepatoZYME^{+} medium did not exhibit this behaviour. The colonies initially took on a star-shaped morphology after 24 hr of treatment. After 2 days the cells had vacuoles present in the cytoplasm, and at 5 days, the cells had shrivelled in shape and were detaching from the culture surface, with some dead colonies present. Reducing the

concentration of Hydrocortisone to 1 μM did not improve cell survival with similar loss of colony viability over 24 hr (data not shown). Similar shrivelling, cytoplasmic vacuolation and dead colonies were also observed in the 50:50-treated cells, although the rate of occurrence was reduced.

Due to lack of survival of the HepatoZYME^{+} cultures beyond 5 days, further analysis sought to identify whether the thriving cultures containing cells with flattened morphology were tending towards a functioning HLC phenotype rather than a pancreatic one. Immunofluorescent staining was utilised to identify protein expression of pancreatic and liver markers in Dex-treated and 50:50-treated cells after 9 days of culture, with the B13 cells treated under normal maintenance conditions used as a pancreatic control.

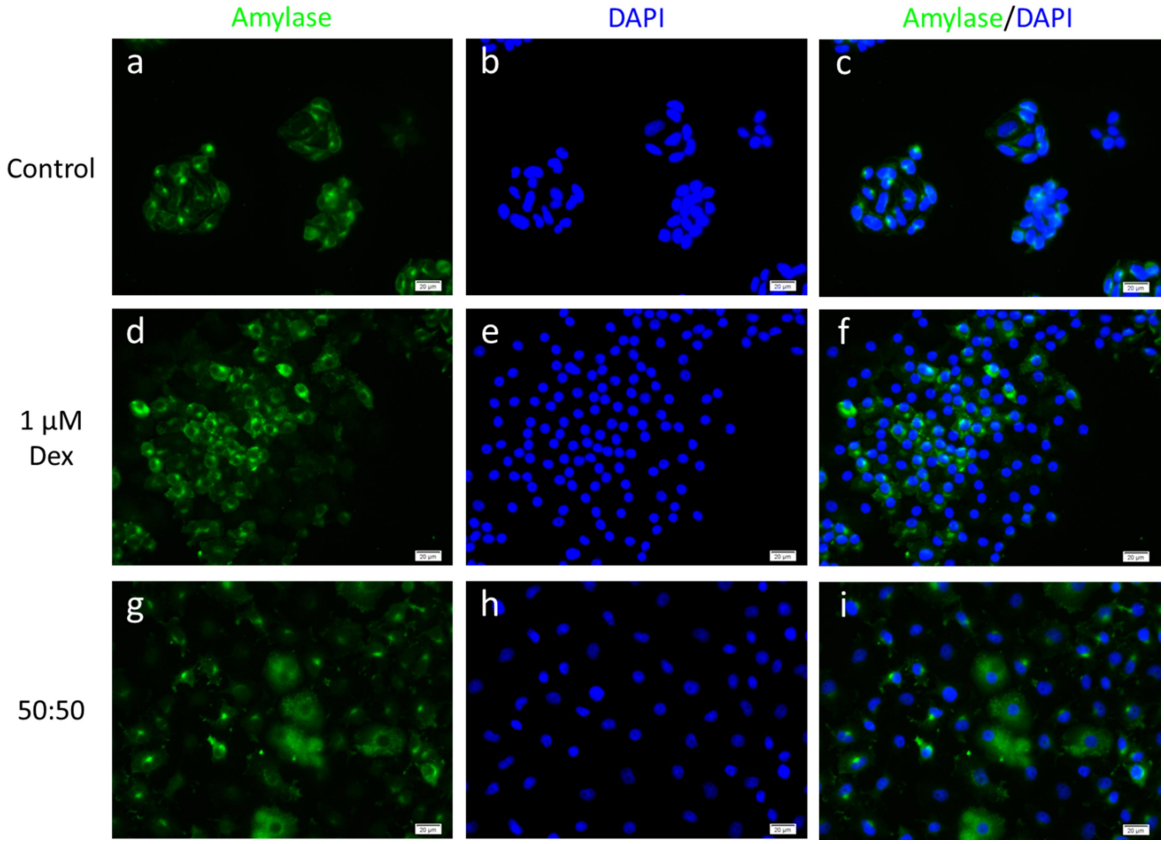

Figure 5.2 Expression of the pancreatic marker amylase in B13 cells cultured in different induction media. Cells were treated without (**a – c**) or with 1 µM Dex (**d – f**) or 50:50 (**g – i**) for 9 days. Cells were stained for the pancreatic marker amylase (green) and nuclei stained with DAPI (blue). Images (**c**), (**f**) and (**i**) are composites of (**a** & **b**), (**d** & **e**) and (**g** & **h**) respectively. Dex and 50:50 cultures showed a reduction in amylase expression compared to the control. Scale bar = 20 µm.

Staining for the pancreatic marker amylase is depicted in **Figure 5.2**. All cultures showed cells positive for amylase expression, although not all the cells in the Dex-treated and 50:50-treated cultures were positive for amylase, in comparison to the B13 controls where all the cells were positive for amylase, suggesting reduced expression in the treated cultures. Amylase also appeared to be present in some of the larger, flatter cells in the 50:50 cultures.

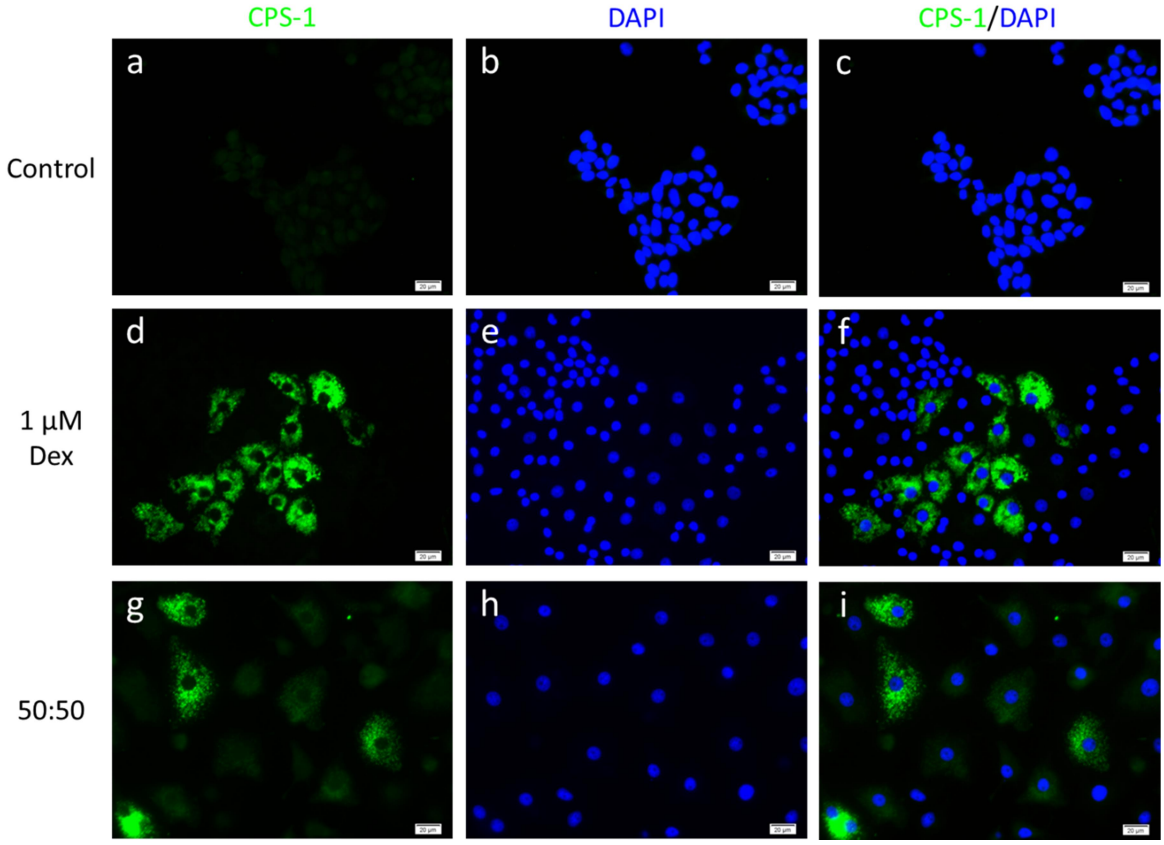

Figure 5.3 Expression of the hepatic marker CPS-1 in B13 cells cultured in different induction media. Cells were treated without (**a – c**) or with 1 µM Dex (**d – f**) or 50:50 (**g – i**) for 9 days. Cells were stained for the ammonia detoxifying liver enzyme CPS-1 (green) and nuclei stained with DAPI (blue). Images (**c**), (**f**) and (**i**) are composites of (**a** & **b**), (**d** & **e**) and (**g** & **h**) respectively. Dex and 50:50-treated cultures contained cells that were positive for CPS-1 expression. Scale bar = 20 µm.

Figure 5.3 and **Figure 5.4** show immunofluorescent staining of the hepatic markers CPS-1 and HNF4α under the different culture conditions. CPS-1 characteristically displays a distinct punctate staining in the cytoplasm and was clearly expressed within some cells in the Dex-treated and 50:50-treated cultures. The Dex-treated and 50:50-treated cultures showed expression of HNF4α in some nuclei, with reduced expression in the 50:50-treated cultures compared to Dex-treated cells. Neither of these liver markers was visible in the B13 cell control cultures.

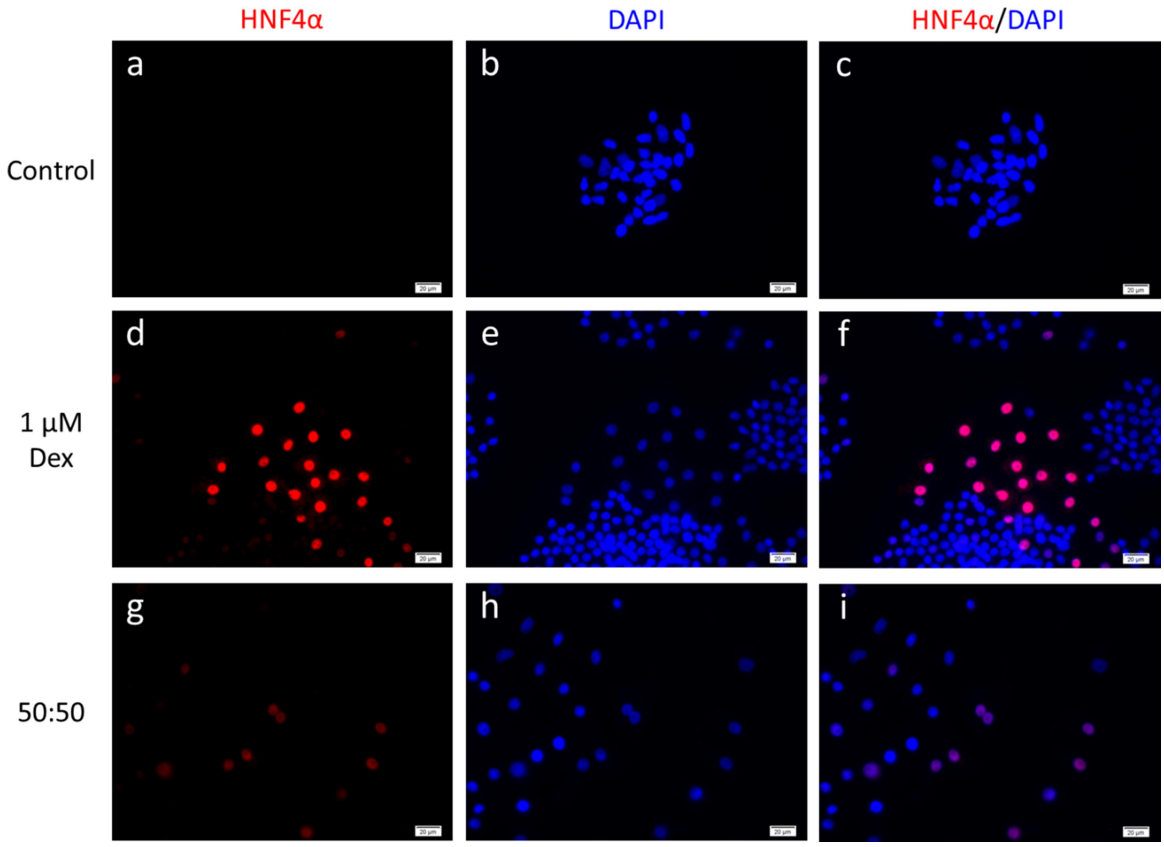

Figure 5.4 Expression of the transcription factor HNF4α in B13 cells cultured in different induction media. Cells were treated without (**a – c**) or with 1 µM Dex (**d – f**) or 50:50 (**g** – **i**) for 9 days. Cells were stained for the liver transcription factor HNF4α (red) and nuclei stained with DAPI (blue). Images (**c**), (**f**) and (**i**) are composites of (**a** & **b**), (**d** & **e**) and (**g** & **h**) respectively. Dex and 50:50-treated cultures contained cells positive for HNF4α expression. Scale bar = 20 µm.

The presence of hepatocyte markers in the Dex-treated and 50:50-treated cultures with reduction of amylase expression as seen in the B13 culture control suggests that the treatment had induced some cells to convert to an HLC phenotype. However, the presence of vacuolated cells and dead colonies in the 50:50-treated cultures, which were absent in the Dex-treated cultures, suggest that although this medium composition alone is able to induce transdifferentiation to HLCs, long term survival is less likely compared to the Dex-treatment alone.

5.2.2 Characterisation of HepatoZYME^{+}-based media as a post-induction of transdifferentiation treatment for B13 cells

Given the loss of cell viability visualised when solely using HepatoZYME^{+} or 50:50 as transdifferentiation induction and maintenance medium, further studies sought to determine the characteristics of B13 cultures that had already been induced to transdifferentiate to HLCs. These experiments utilised initial supplementation with 1 μM Dex and 10 ng/ml Oncostatin M (OSM) (referred to as 'Dex + OSM'). The combination of Dex + OSM in the transdifferentiation culture medium has previously shown enhancement of the transdifferentiation process and hepatic phenotype compared to supplementing the culture medium with Dex alone [130,132].

Previously, sole use of 50:50 medium was shown to be able to induce some B13 cells to convert to a flattened HLC morphology and express liver markers, whereas culture in complete HepatoZYME^{+} encouraged loss of cell viability. Previous work in the literature examining the transdifferentiation of B13 cells to HLCs under treatment with Dex + OSM have treated cells for up to 14 days with 80-90% of cells converting to HLCs after 7 days [237]. This provided an initial benchmark to compare the effect of the 50:50 culture medium on the B13 cultures.

B13 cells were initially treated for 7 days with complete B13 medium supplemented with Dex + OSM. After 7 days, the cultures either continued treatment with Dex + OSM or the medium was changed to the 50:50 composition. B13 cells cultured in complete B13 medium were used as a control. Initial experiments using HepatoZYME^{+} instead of 50:50 caused loss of culture viability (data not shown). Therefore, the initial investigation here was to assess the capability of the 50:50 composition to maintain conversion of the hepatic phenotype on pre-induced cells.

Morphological assessment of the cultures at 7, 10 and 14 days of treatment is shown in **Figure 5.5**. After 7 days of Dex + OSM treatment, the majority of cells had converted to a larger, flattened morphology in contrast to the control culture with the presence of binucleate cells indicative of HLCs. At this point, the culture medium was changed to the 50:50 composition. After 10 days of culture, the cells cultured only in Dex + OSM continued to present with flattened morphology with further binucleate development, with some cells taking on a more regular 'polygonal' shape.

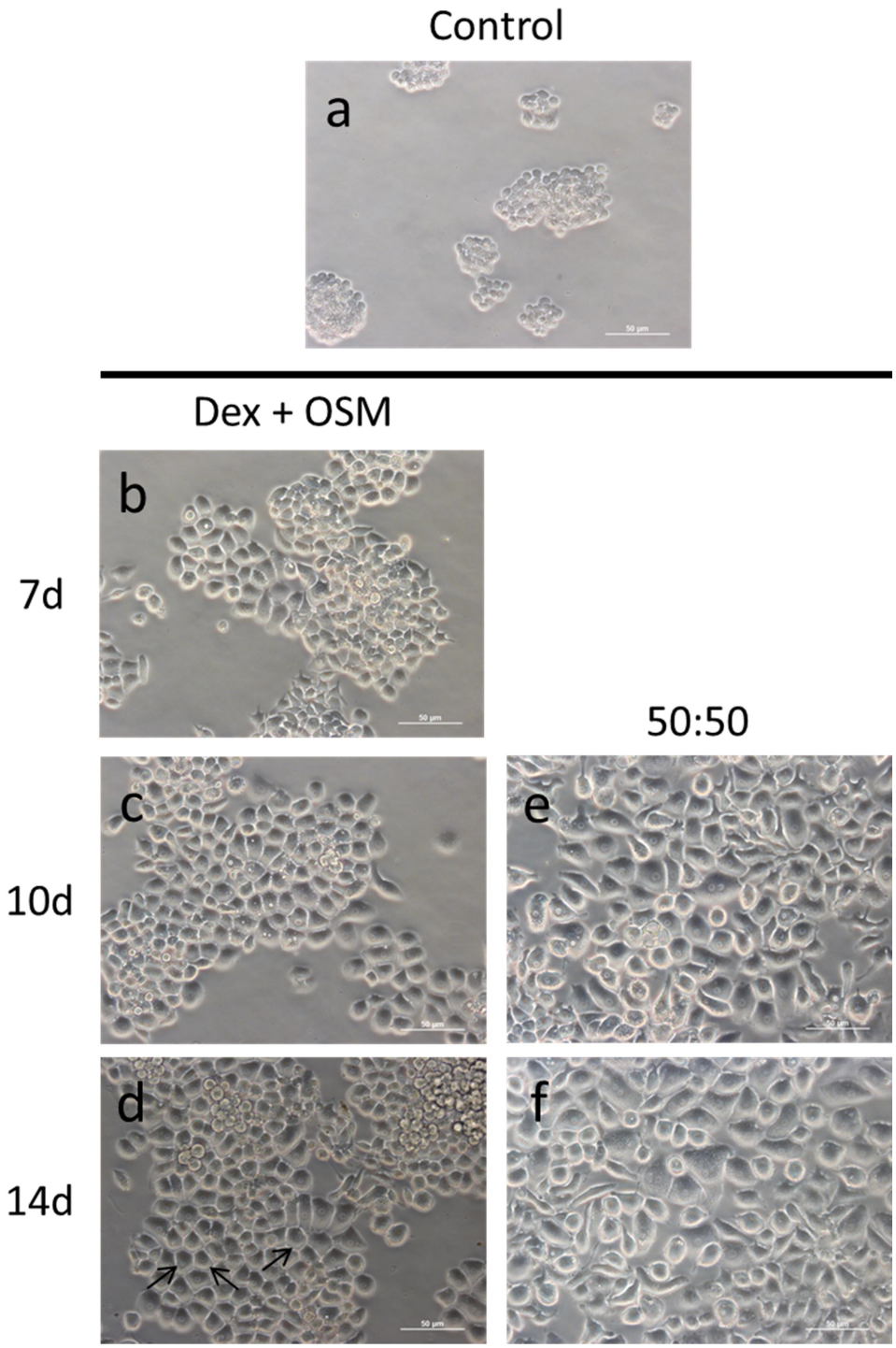

Figure 5.5 Morphology of B13 cells cultured in different transdifferentiation media for 14 days. Cells were treated with Dex + OSM only for 14 days (**b - d**) or initially treated with Dex + OSM for 7 days before changing culture medium to 50:50 for the remaining 7 days (**e** & **f**). Cell morphology is shown at 7 days (**b**), 10 days (**c** & **e**) and 14 days (**d** & **f**) of culture. Comparative B13 cell morphology control is shown after 4 days of culture (**a**). Arrows indicate examples of polygonal HLC morphology. Scale bar = 50 μm.

The cells cultured in the 50:50 composition, having been treated for 3 days since the switch from Dex + OSM medium, also contained cells with the binucleate trait, but appeared to be larger in size and less regular in shape. Distinctly elongated cells and vacuoles appeared to take up the majority of cytoplasmic space, similar to that observed in **Figure 5.1d**. After 14 days of culture, the Dex + OSM only cultures had retained their flattened, polygonal morphology in tight colonies as seen after 10 days, whereas the cells cultured in 50:50 were not in tight colonies and appeared more rounded. The cells were also elongated and irregularly shaped. Several cells were also observed to be multinucleate, possessing numbers of nuclei ranging from 2 to 6, as well as being highly vacuolated within the cytoplasm.

Immunofluorescent staining sought to identify and compare protein expression of pancreatic and liver markers within these cultures after 14 days of treatment. After 7 days of Dex + OSM treatment a mixed population of cells expressing the pancreatic marker amylase that contained both rounded B13 and flattened HLC morphologies was visible, although there were some flattened HLCs negative for amylase. By 14 days, expression of amylase appeared to be largely absent in Dex + OSM only-treated cells, particularly those possessing the enlarged, flattened HLC morphology. There was very sparse positive expression distributed in cells that did not display this morphological change. In contrast, the cultures where the medium had been changed to the 50:50 composition for the final 7 days displayed heterogeneity in terms of expression. Several cells showed elevated amylase expression compared to the B13 control, similar to that seen after the initial 7 days of treatment in Dex + OSM, but there was also a population of cells with reduced or negative amylase expression compared to the B13 control. Unlike the Dex + OSM only-treated cultures, the highly positive amylase expressing cells also displayed a flattened morphology rather than the smaller, rounded phenotype of B13 cells. (**Figure 5.6**).

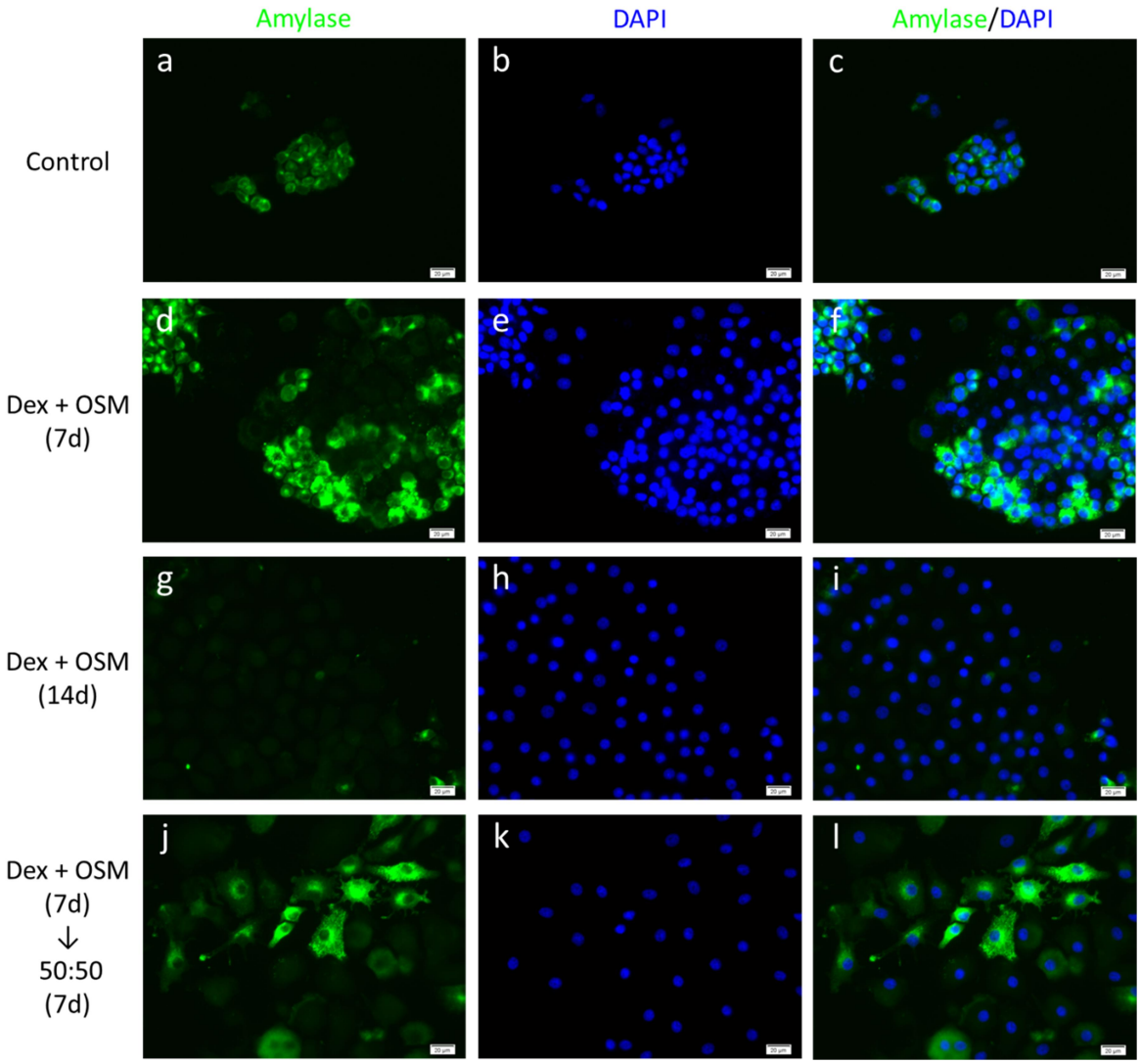

Figure 5.6 Expression of the pancreatic marker amylase in B13 cells cultured in different transdifferentiation media for 14 days. Cells were treated without (**a – c**) or with Dex + OSM only for 7 days (**d** – **f**) or 14 days (**g – i**); or with Dex + OSM for 7 days and 50:50 for a further 7 days (**j** – **l**). Cells were stained for the pancreatic marker amylase (green) and nuclei stained with DAPI (blue). Images (**c**), (**f**), (**i**) and (**l**) are composites of (**a** & **b**), (**d** & **e**), (**g** & **h**) and (**j** & **k**) respectively. Changing to the 50:50 composition presented with some cells showing upregulated amylase expression compared to the control after 14 days. The Dex + OSM-only condition presented with weak to largely absent expression of amylase after 14 days. Scale bar = 20 µm.

A double immunofluorescent stain for the functional markers GS and CPS-1, both enzymes involved in detoxification of ammonia by the liver, is shown in **Figure 5.7**. Expression of these enzymes was present in both Dex + OSM only-treated cultures at 7 days and 14 days and also where the medium had been changed to the 50:50 composition, with no visible increase or decrease in expression compared to the Dex + OSM only

medium. There was a visible heterogeneity in expression of these markers, with HLCs either showing positive for either one of these enzymes rather than simultaneously. As production of these liver enzymes is zonated along the porto-venous axis, this observed distribution is not unexpected, suggesting populations of periportal and perivenous hepatocytes in the culture.

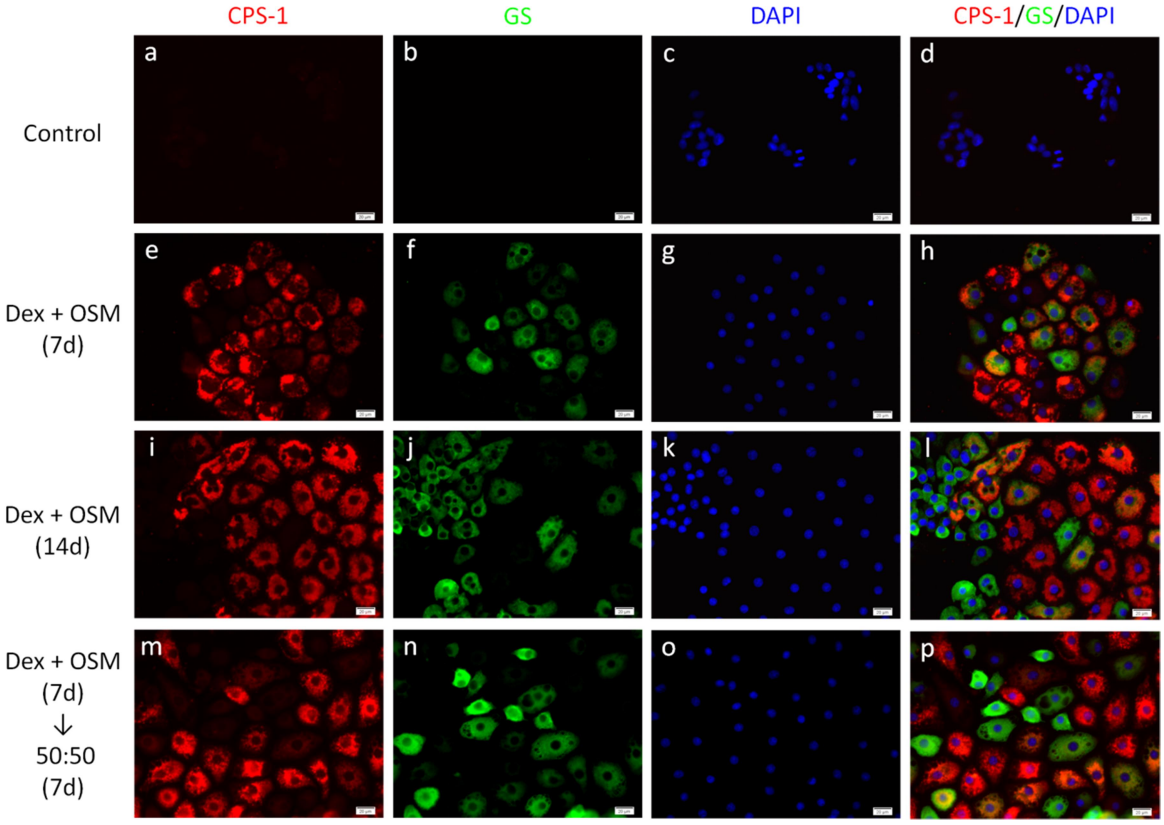

Figure 5.7 Expression of the hepatic markers GS and CPS-1 in B13 cells cultured in different transdifferentiation media for 14 days. Cells were treated without (**a – d**) or with Dex + OSM only for 7 days (**d - f**) or 14 days (**i - l**); or with Dex + OSM for 7 days and 50:50 for a further 7 days (**m - p**). Cells were stained for the ammonia detoxifying liver enzymes CPS-1 (red) and GS (green) and nuclei stained with DAPI (blue). Images (**d**), (**h**), (**l**) and (**p**) are composites of (**a - c**), (**e - h**), (**i - k**) and (**m - o**) respectively. GS and CPS-1 were expressed in the Dex + OSM-only and 50:50-treated cultures. Scale bar = 20 μm.

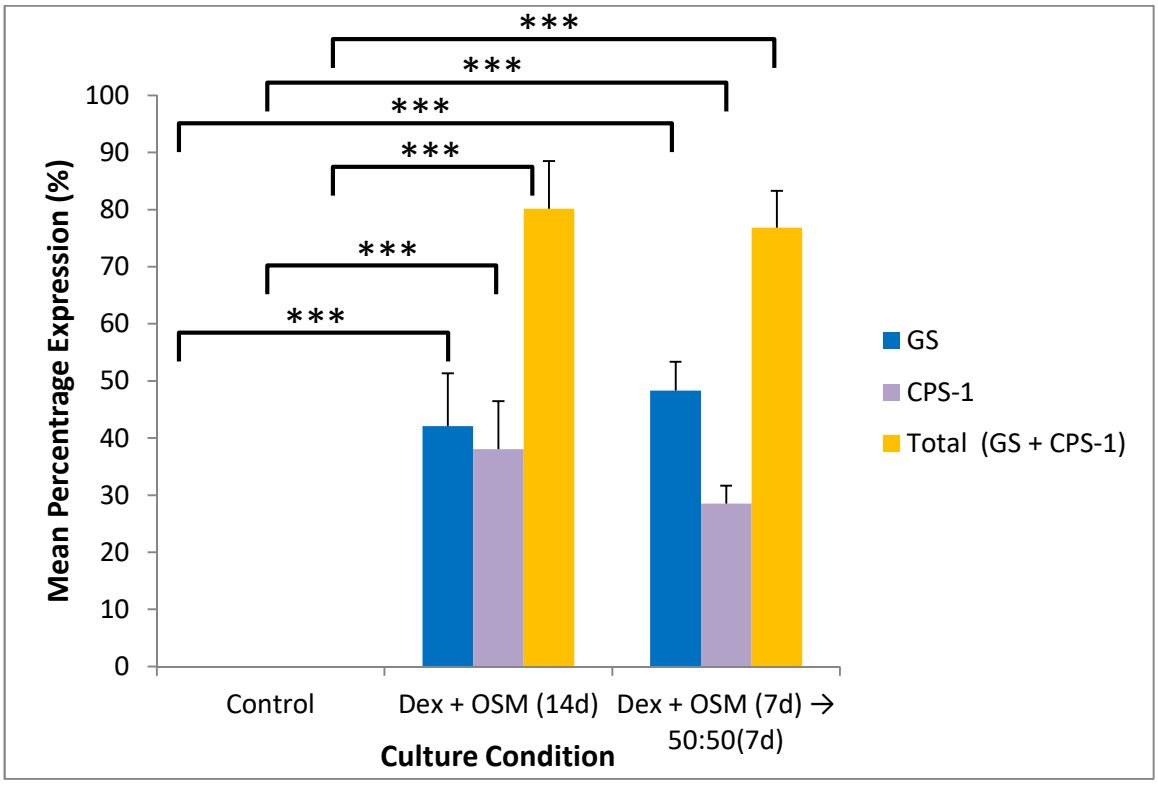

Figure 5.8 Mean percentage expression of GS and CPS-1 positive cells cultured in different transdifferentiation media for 14 days. Data is representative of three independent experiments. Statistical analysis was by a one-way ANOVA with Tukey's post-hoc tests. Error bars = + 1 SE; n = 3. All Dex-treated conditions were significantly different to the control (*** = $p < 0.001$), but not significantly different to each other in GS and CPS-1 expression ($p > 0.05$).

The percentages of cells staining positive for GS and CPS-1 after 14 days of culture were quantified by counting GS or CPS-1 DAPI-positive cells. The data were statistically compared between the different culture conditions using a one way ANOVA with Tukey's posthoc tests to determine whether there was any difference in expression levels between the culture conditions (**Figure 5.8**). Control cultures did not express either GS or CPS-1. Over 70% of cells in both the Dex + OSM only and 50:50 cultures appeared to be expressing either GS or CPS-1. No statistically significant differences was found between the total percentage of cells expressing both markers in the Dex + OSM treated cultures and the cells treated with 50:50, although the total expression in the cells treated with 50:50 did appear to be slightly lower than that of the Dex + OSM only treatment. Expression of GS in the 50:50 treated cells appeared to be slightly increased over Dex + OSM only treated cells, and CPS-1 expression appeared to be slightly reduced as well, but these differences were not found to be significant.

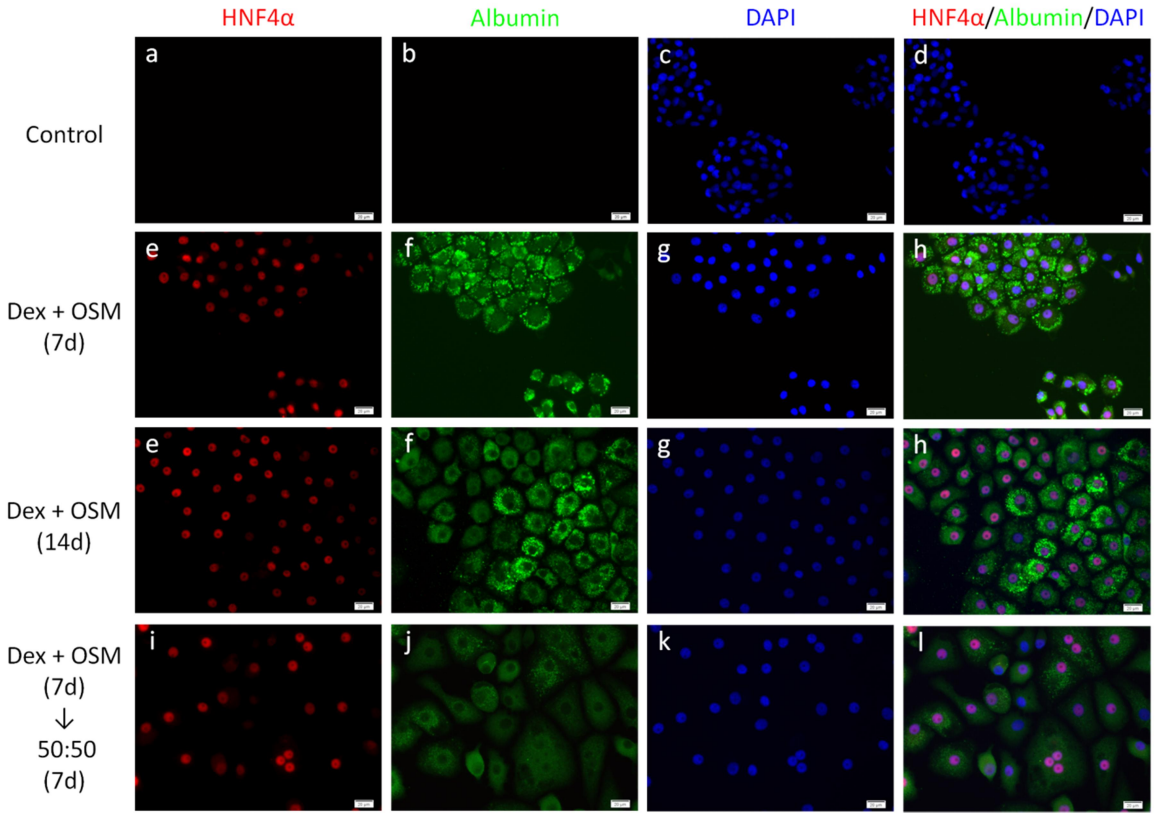

Figure 5.9 Expression of the hepatic markers HNF4α and albumin in B13 cells cultured in different transdifferentiation media for 14 days. Cells were treated without (**a – d**) or with Dex + OSM only for 7 days (**d - f**) or 14 days (**i - l**); or with Dex + OSM for 7 days and 50:50 for a further 7 days (**m - p**). Cells were stained for the liver transcription factor HNF4α (red), the liver plasma protein albumin (green) and nuclei stained with DAPI (blue). Images (**d**), (**h**), (**l**) and (**p**) are composites of (**a - c**), (**e - h**), (**i - k**) and (**m - o**) respectively. Both the Dex + OSM-only and 50:50 culture conditions showed dual expression of HNF4α and albumin in HLCs. Scale bar = 20 μm.

Figure 5.9 displays a double immunofluorescent stain of the liver enriched transcription factor HNF4α and albumin, a protein synthesised by hepatocytes. The Dex + OSM-treated cultures showed positive expression of both these liver markers in the same HLCs after 7 days and also at 14 days. Similarly, both markers were present where the medium had been changed to the 50:50 composition. However, albumin expression appeared to be weaker overall compared to the cultures treated continuously with Dex + OSM, but not completely absent as seen in the B13 cell control.

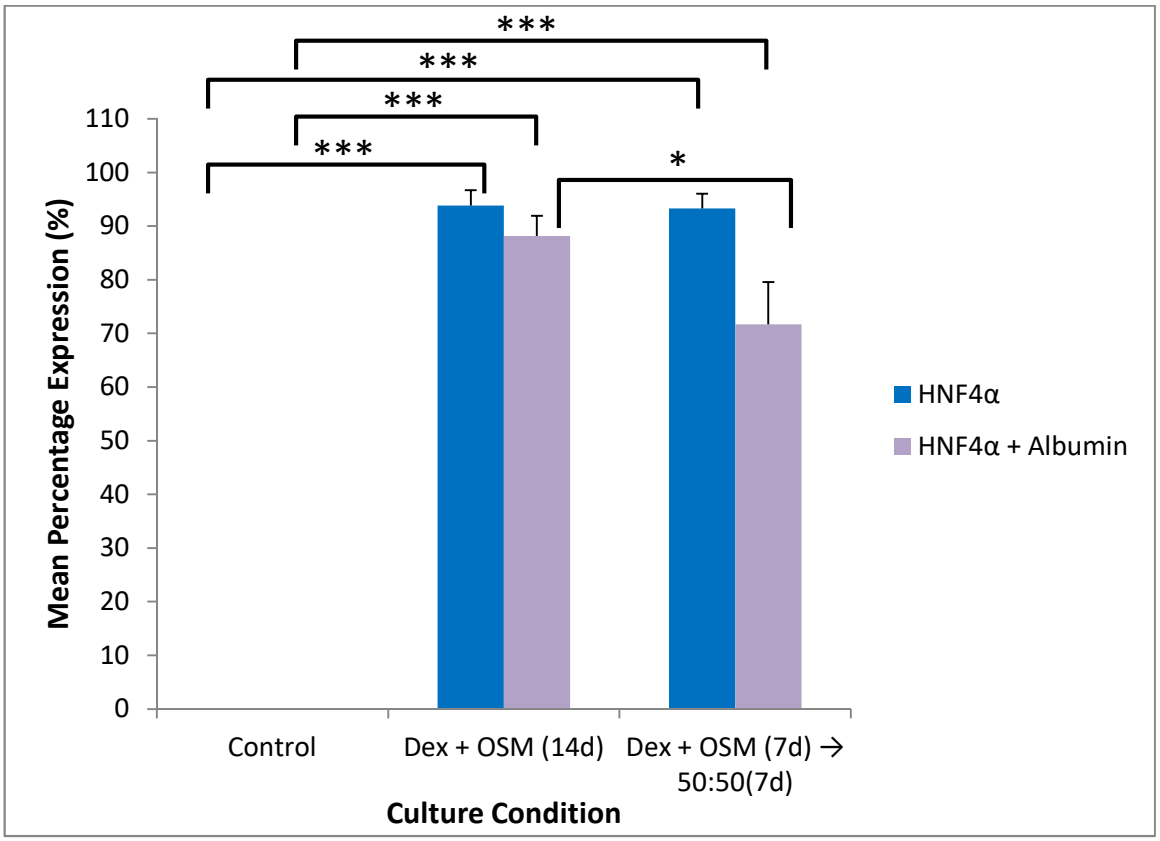

Figure 5.10 Mean percentage expression of HNF4α positive cells and HNF4α positive cells co-expressed with albumin cultured in different transdifferentiation media for 14 days. Data is representative of three independent experiments. Statistical analysis was by a one-way ANOVA with Tukey's post-hoc tests. Error bars = + 1 SE; n = 3; * = p = 0.014; *** = p < 0.001. All Dex-treated conditions were significantly different to the control. HNF4α expression was not significantly different between treated conditions, but Dex + OSM only treatment had a significantly percentage of cells positive for both HNF4α and albumin.

Quantification of mean percentage expression of HNF4α-positive cells and cells co-expressing both HNF4α and albumin is shown in **Figure 5.10**. In both populations of the Dex + OSM treated cells and the 50:50 treated cells, over 90% of cells were positive for HNF4α, but not all HNF4α positive cells were positive for albumin. The B13 control was negative for both markers. Statistical analysis by a one way ANOVA with Tukey's posthoc tests found that the percentage of cells expressing both HNF4α and albumin was significantly lower in the 50:50 treated culture compared to using Dex + OSM only. Furthermore, multinucleate cells with 6 nuclei were also visible in the 50:50 cultures only, staining positively for HNF4α and albumin (**Figure 5.11**).

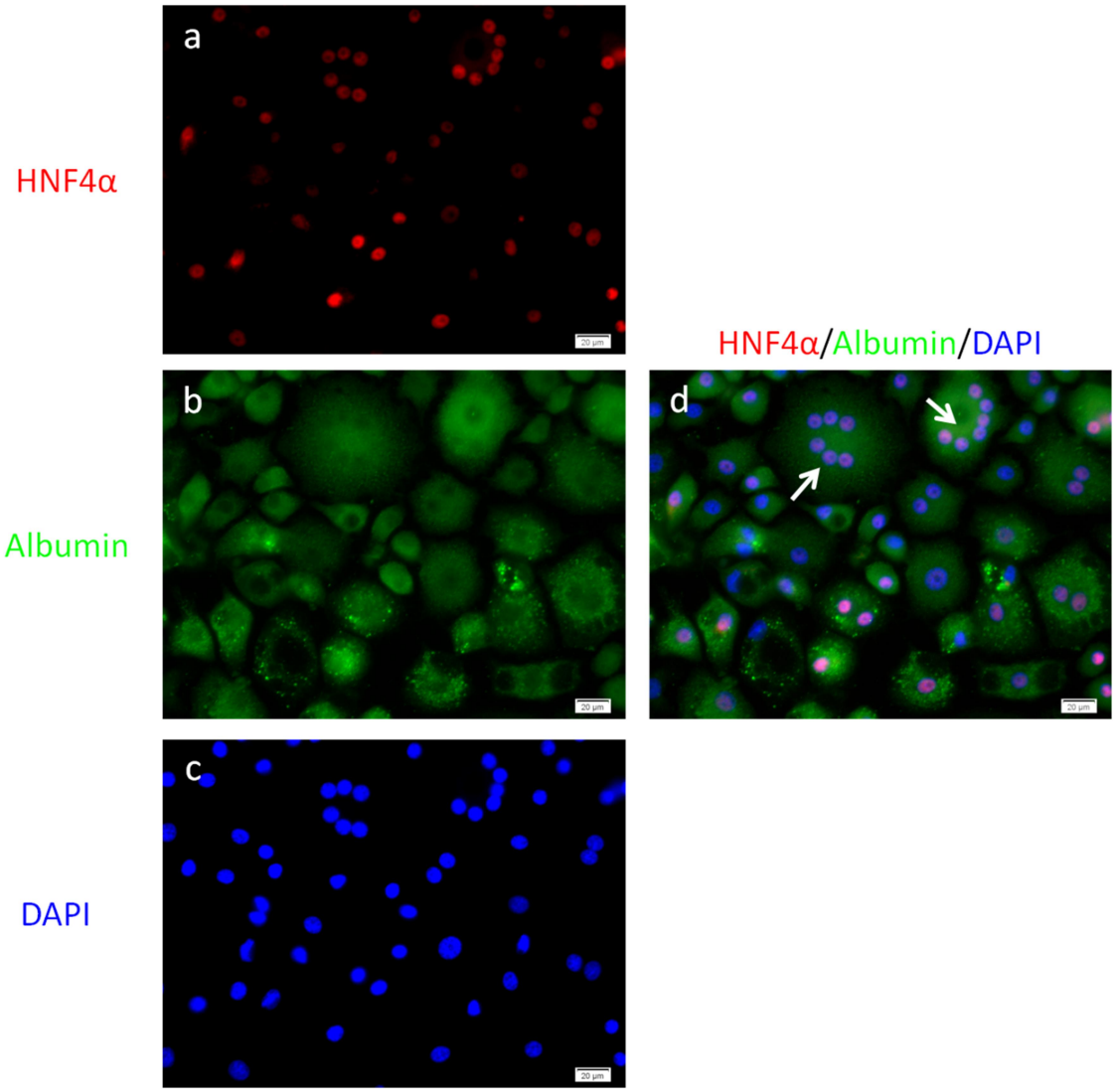

Figure 5.11 Mononucleate, binucleate and multinucleate cells expressing the hepatic markers HNF4α and albumin. B13 cells were treated with Dex + OSM only for 7 days and then 50:50 for a further 7 days. Cells were stained for the liver transcription factor HNF4α (red), the liver specific protein albumin (green) and nuclei stained with DAPI (blue). Image (**d**) is a composite of images (**a - c**). The field of view contained mononucleate, binucleate and multinucleate cells. Arrows indicate presence of cells possessing 6 nuclei.

To examine whether the increase in nuclei beyond the binucleate feature seen in cultures where the medium was changed to the 50:50 composition could be correlated to possible mitotic activity, immunofluorescent staining for the mitotic marker phospho-histone H3 (PH3) was performed and quantified by the mean percentage expression for each culture condition after 14 days of treatment. **Figure 5.12** shows positive expression for PH3 in the

B13 control, whereas expression appeared negative in the Dex + OSM only-treated cultures and also in the 50:50-treated cultures.

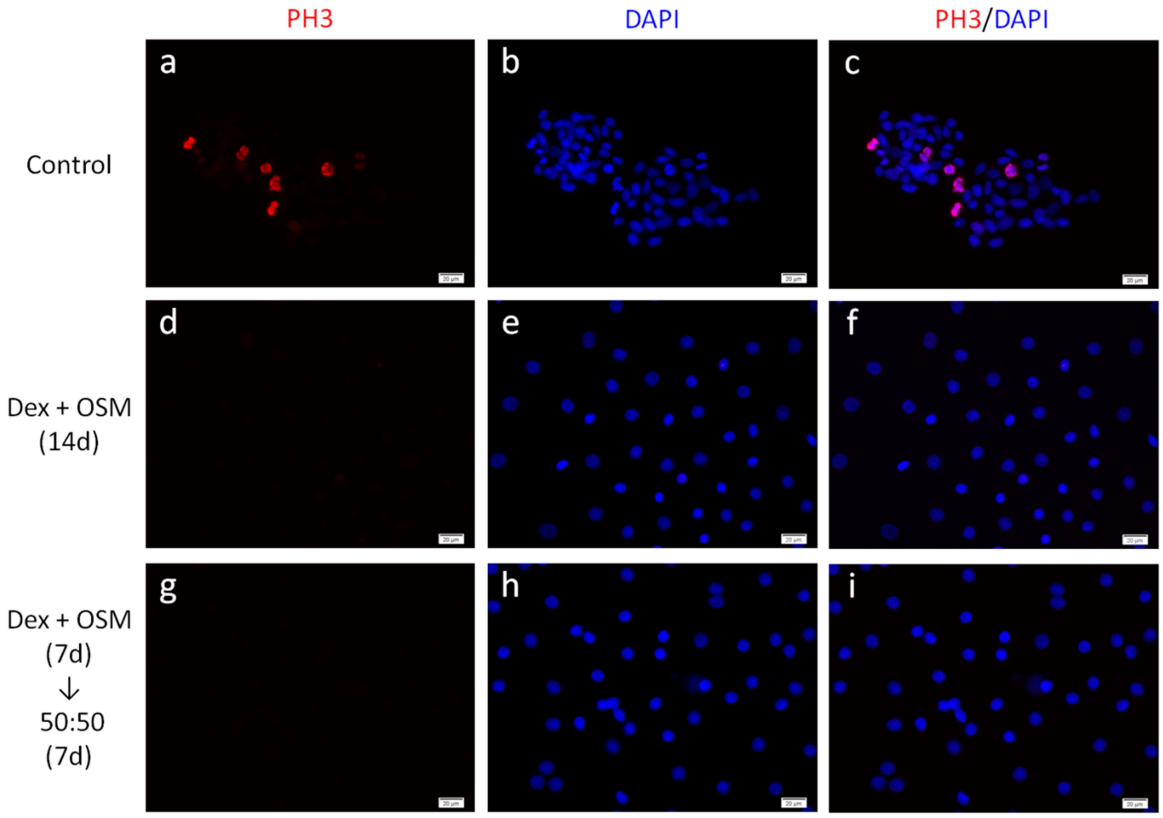

Figure 5.12 Expression of the mitotic marker PH3 in B13 cells cultured in different transdifferentiation media for 14 days. Cells were treated without (**a – c**) or with Dex + OSM for 14 days (**d – f**) or with Dex + OSM for 7 days and 50:50 for a further 7 days (**g** – **i**). Cells were stained for the mitotic marker PH3 (red) and nuclei stained with DAPI (blue). Images (**c**), (**f**) and (**i**) are composites of (**a** & **b**), (**d** & **e**) and (**g** & **h**) respectively. PH3 was expressed in the control but absent from the Dex + OSM-only and 50:50 treated cultures. Scale bar = 20 μm.

Calculation of the mean percentage expression of PH3 showed that on average fewer than 10% of DAPI positive cells were also positive for PH3 expression in the control (mean = 6.50%, SE = 1.21), but this was a statistically significant difference compared to the other treatment conditions which had no PH3 positive cells ($p < 0.001$). In addition, there was no significant difference between the Dex + OSM only and 50:50 treated cultures ($p > 0.05$).

5.2.3 Characterisation of transdifferentiated HLCs maintained in HepatoZYME$^+$-based media

It has been shown in previous work that B13 cells can be maintained in transdifferentiation media of Dex + OSM-only culture media for at least 14 days [130,131,222,238], and Dex-only culture media for 21 days [131]. In both of these conditions, the cultures converted to the HLC phenotype. In this section, further experiments increased the total culture time to 21 days, with initial induction and maintenance of transdifferentiation using Dex + OSM occurring over 14 days. This was done to ensure the presence of mature liver markers and loss of pancreatic expression as previously shown over 14 days in the Dex + OSM-only cultures. After 14 days in Dex + OSM-only medium, the cells either continued to be maintained in Dex + OSM or the culture medium was changed to HepatoZYME$^+$ medium or the 50:50 composition for a further 7 days of culture. The presence of pancreatic and liver markers was subsequently characterised. Although previous cultures of non-induced B13 cells in HepatoZYME$^+$ had caused a distinct deterioration of cell viability in less than 5 days (**Section 5.2.1**), its effect upon stable colonies of transdifferentiated HLCs was unknown.

Figure 5.13 shows that after 14 days of culture in Dex + OSM, the culture largely consists of enlarged, flattened regular polygonal cells indicative of HLC morphology, prior to changing the culture media to HepatoZYME$^+$ or 50:50. Binucleate cells were also visible. At 17 days of culture, this morphology is continued in the Dex + OSM only-treated cultures, whereas the cells maintained in HepatoZYME$^+$ have a rounded appearance 3 days post-change, losing the tight junctions previously present. Some cells retained a flattened appearance but had become even more enlarged and less regular in shape. In contrast, the cells maintained in 50:50 appeared to be larger compared to the Dex + OSM only culture after 3 days, with a more regular 'polygonal' shape, but also retaining clear tight junctions between cells (**Figure 5.13g**). However, there was also a small population of cells that had lost the polygonal HLC morphology, tending towards a more rounded, enlarged and irregular shape similar to that seen in the HepatoZYME$^+$ culture, with loss of the tight junctions between cells.

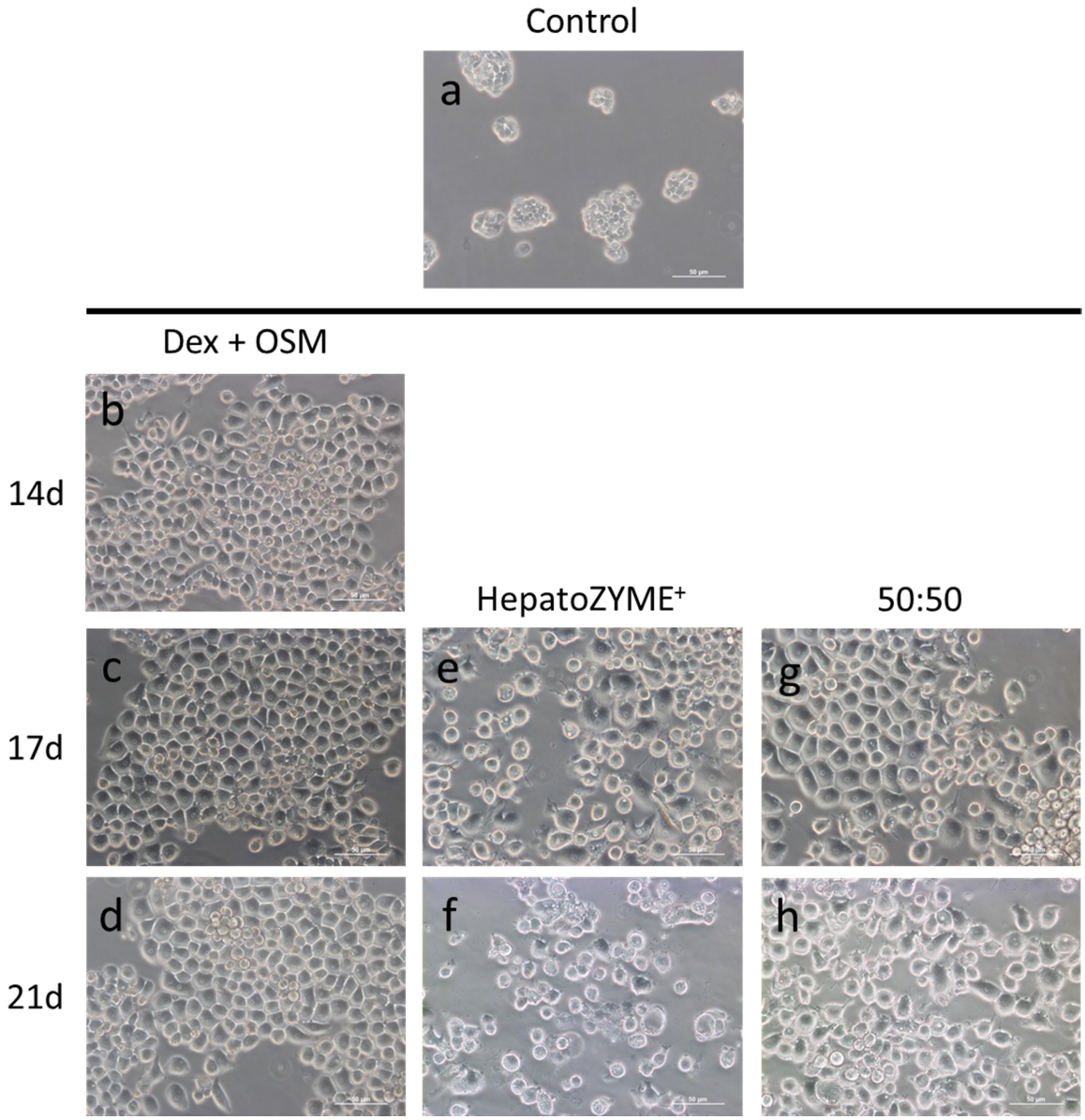

Figure 5.13 Morphology of transdifferentiated HLCs maintained in different transdifferentiation media after 21 days. Cells were treated with Dex + OSM only for 21 days (**b - d**) or initially treated with Dex + OSM for 14 days before changing culture medium to HepatoZYME^{+} (**e** & **f**) or 50:50 (**g** & **h**) for the following 7 days. Cell morphology is shown at 14 days (**b**), 17 days (**c - g**) and 21 days (**d - h**) of culture. Comparative B13 cell morphology control is shown after 4 days of culture (**a**). Scale bar = 50 µm.

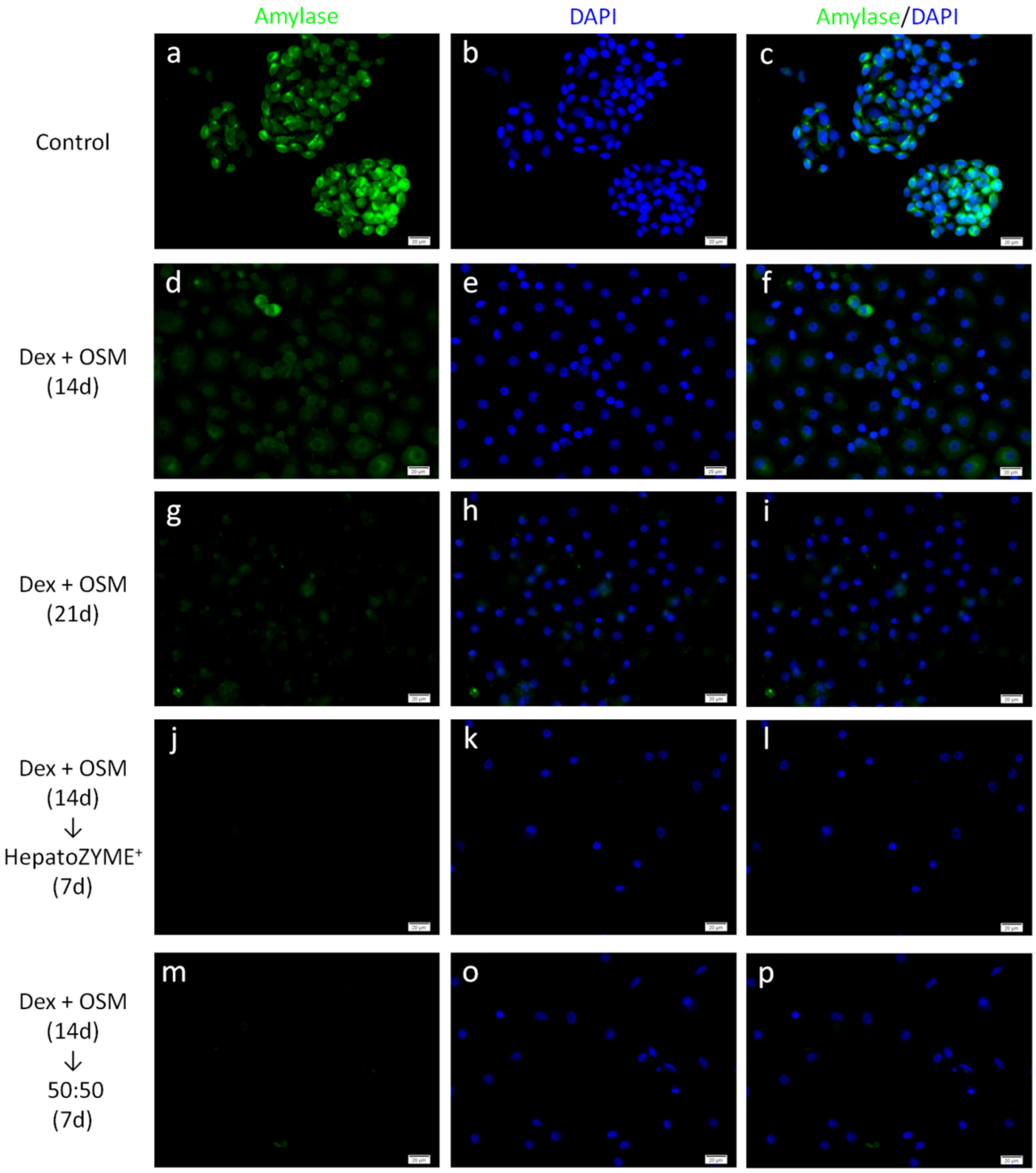

Figure 5.14 Expression of the pancreatic marker amylase in B13 cells cultured in different transdifferentiation media for 21 days. Cells were treated without (**a – c**) or with Dex + OSM only for 14 days (**d** – **f**) or 21 days (**g – i**); or with Dex + OSM for 14 days and HepatoZYME^{+} (**j** – **l**) or 50:50 (**m** – **p**) for a further 7 days. Cells were stained for the pancreatic marker amylase (green) and nuclei stained with DAPI (blue). Images (**c**), (**f**), (**i**), (**l**) and (**p**) are composites of (**a** & **b**), (**d** & **e**), (**g** & **h**), (**j** & **k**) and (**m** & **p**) respectively. Expression of amylase after 21 days of culture in the treated conditions is largely absent. Scale bar = 20 μm.

The presence of the pancreatic marker amylase was investigated at 14 days and 21 days. In the Dex + OSM only culture at 14 days, there was evidence of sporadic yet weak expression in very few cells. In general for all treatment conditions, after 21 days of culture amylase expression was largely inhibited (**Figure 5.14**).

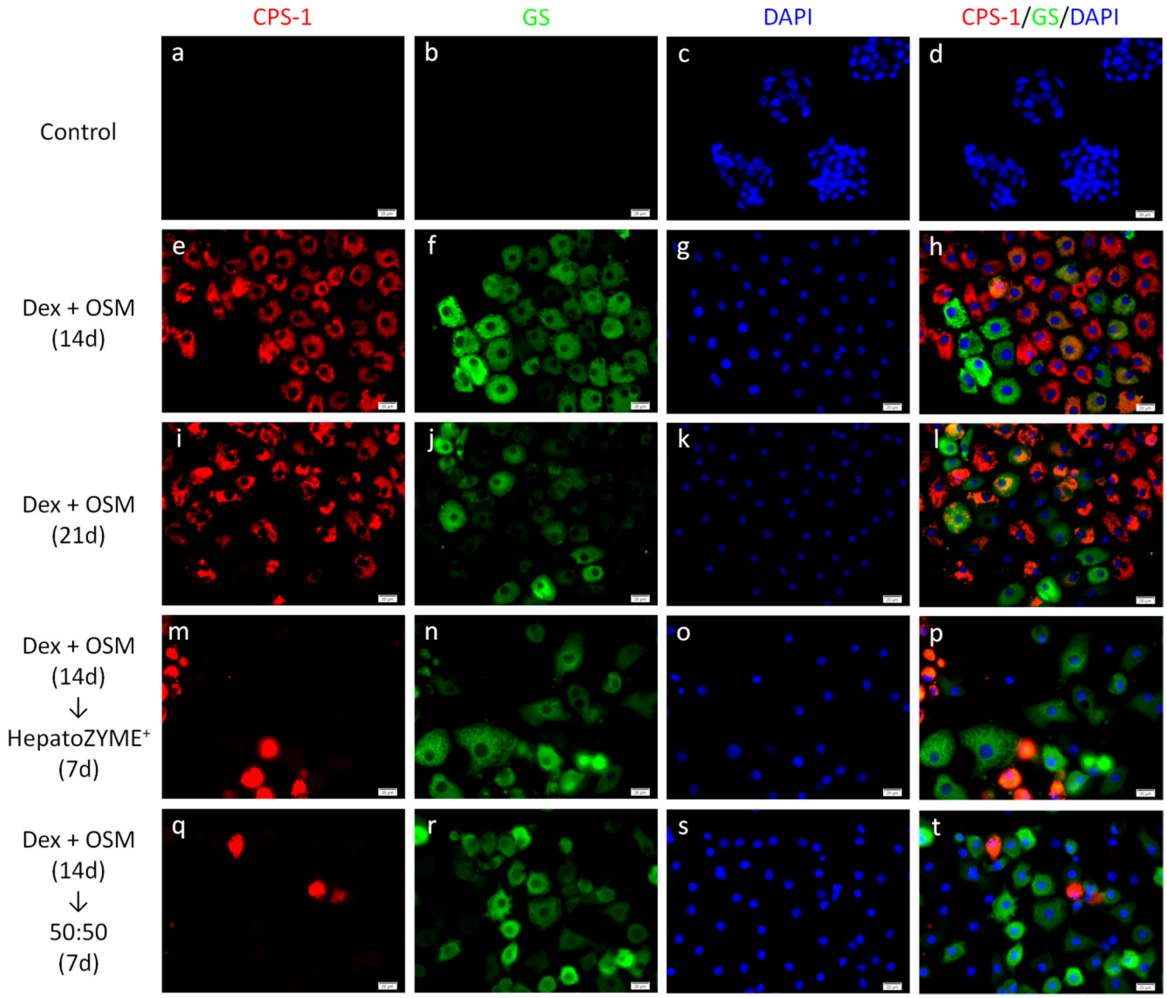

Figure 5.15 Expression of the hepatic markers GS and CPS-1 in B13 cells cultured in different transdifferentiation media for 21 days. Cells were treated without (**a – d**) or with Dex + OSM only for 14 days (**d - f**) or 21 days (**i - l**); or with Dex + OSM for 14 days and HepatoZYME^{+} (**m - p**) or 50:50 (**q - t**) for a further 7 days. Cells were stained for the ammonia detoxifying liver enzymes CPS-1 (red) and GS (green) and nuclei stained with DAPI (blue). Images (**d**), (**h**), (**l**), (**p**) and (**t**) are composites of (**a - c**), (**e - h**), (**i - k**), (**m - o**) and (**q - t**) respectively. GS and CPS-1 were expressed in all treated cultures but not the control. Rounded cell morphology is visible in the HepatoZYME^{+} and 50:50-treated cultures. Scale bar = 20 µm.

Staining for the liver markers GS and CPS-1 demonstrated that after 21 days of culture, the Dex + OSM only treated cells retained GS and CPS-1 expression beyond 14 days with

cells expressing one or the other enzyme. Cells treated with HepatoZYME^{+} or the 50:50 composition also presented with positive GS and CPS-1 staining, including the cells that had taken on a rounded or irregular morphology. (**Figure 5.15**).

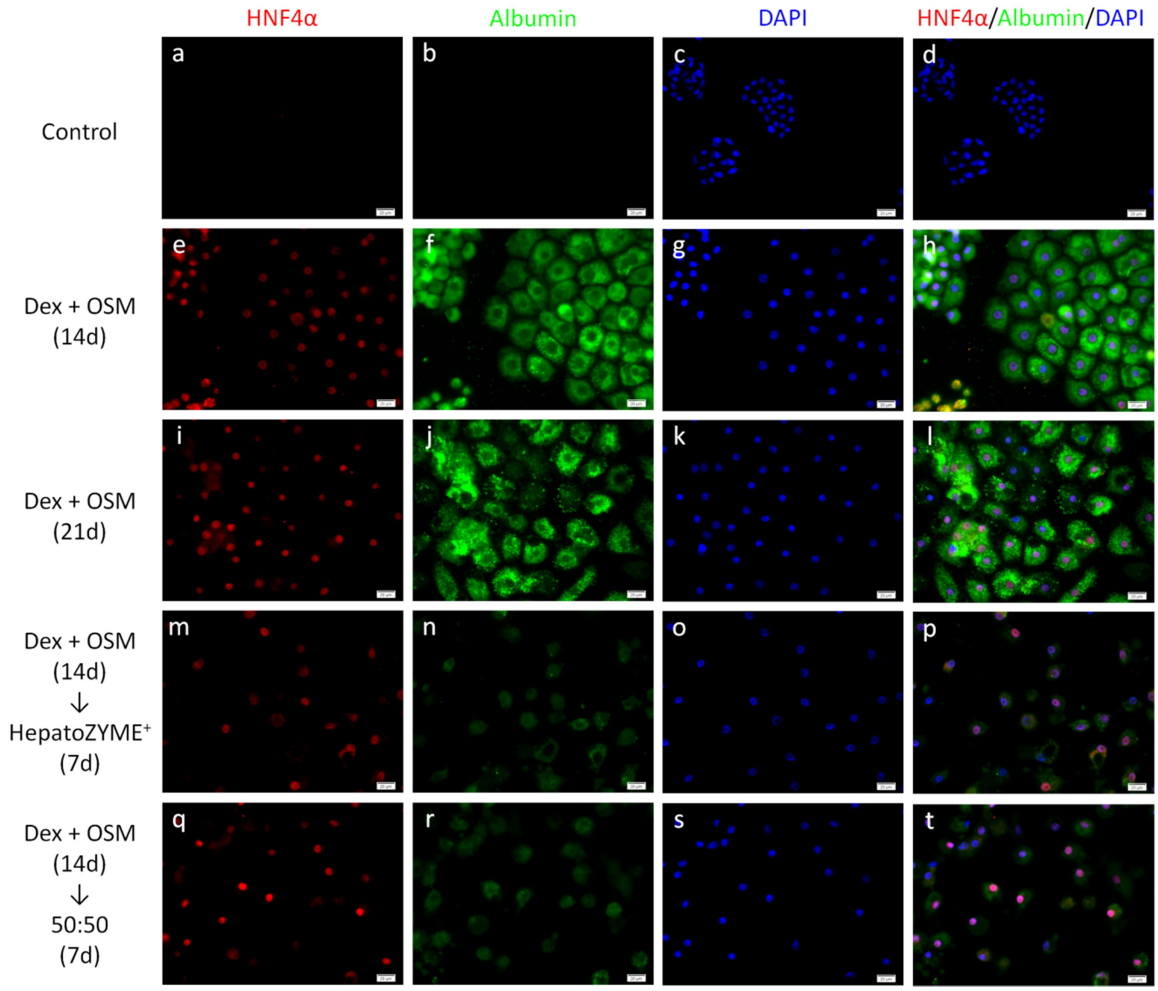

Figure 5.16 Expression of the hepatic markers HNF4α and albumin in B13 cells cultured in different transdifferentiation media for 21 days. Cells were treated without (**a – d**) or with Dex + OSM only for 14 days (**d - f**) or 21 days (**i - l**); or with Dex + OSM for 14 days and HepatoZYME^{+} (**m - p**) or 50:50 (**q - t**) for a further 7 days. Cells were stained for the liver transcription factor HNF4α (red), the liver specific protein albumin (green) and nuclei stained with DAPI (blue). Images (**d**), (**h**), (**l**), (**p**) and (**t**) are composites of (**a - c**), (**e - h**), (**i - k**), (**m - o**) and (**q - t**) respectively. All treatment conditions apart from the control had positive HNF4α and albumin expression.

HNF4α was continually expressed under all transdifferentiation maintenance conditions up to 21 days of culture even where the cells had adapted to a rounded irregular appearance.

However, expression of albumin appeared to be reduced after the culture medium was changed to HepatoZYME^{+} or 50:50 (**Figure 5.16**).

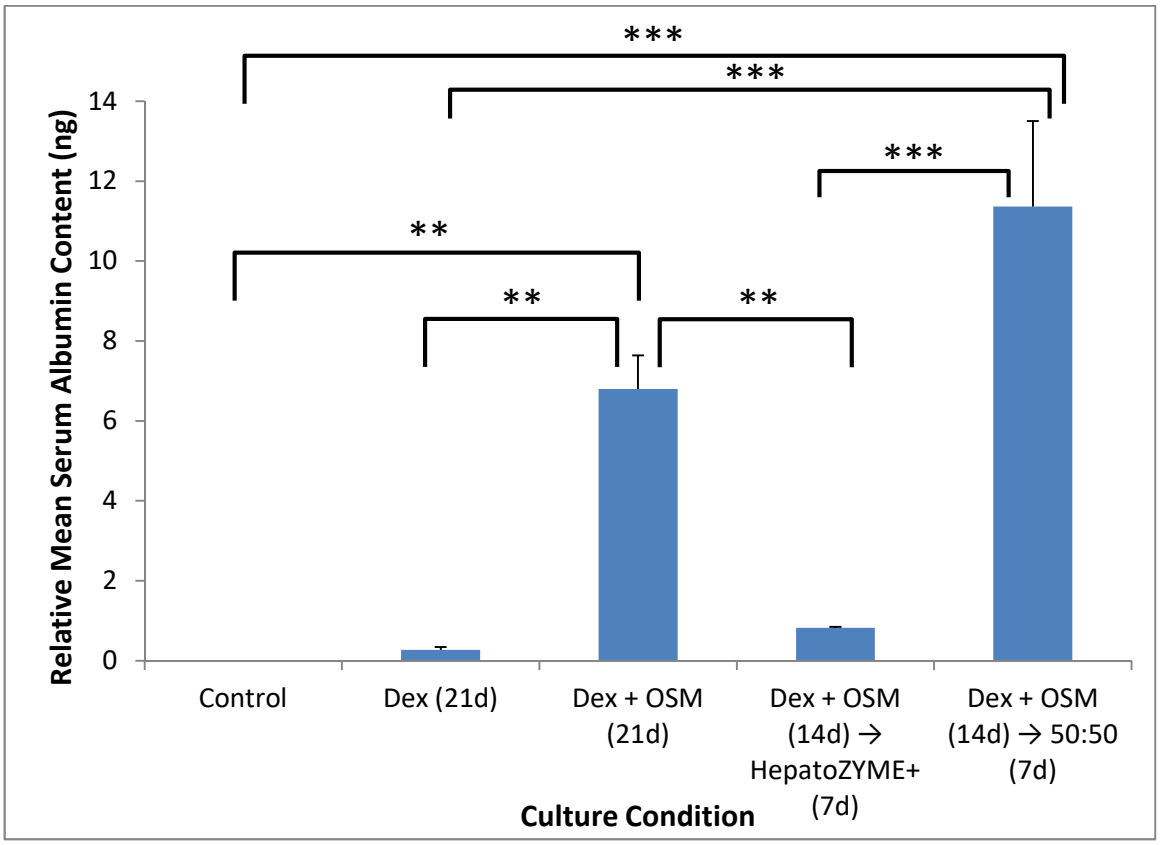

Figure 5.17 Relative mean secreted serum albumin content over 24 hr from B13 cells cultured in different transdifferentiation media for 21 days. Data were normalised per µg total cellular protein content and is representative of three independent experiments. Statistical analysis was by a one-way ANOVA with Tukey's post-hoc tests. Error bars = + 1 SE; n = 3; ** = $p < 0.01$; *** = $p < 0.001$.

To further compare the functional capacity of these cultures, the amount of albumin secreted by the cells into the culture medium after 24 hr was quantified using an enzyme-linked immunosorbent assay (ELISA) specific to rat albumin and normalised per µg total cellular protein content (**Figure 5.17**). Mean total cellular protein content of each culture condition is shown in **Table 5.1**. B13 cells in complete B13 maintenance medium were used as a negative control due to their pancreatic phenotype and cultured for 7 days only. In addition to the previously analysed medium compositions, B13 cells supplemented with 1 µM Dex were also measured for albumin secretion levels after 21 days of culture as an additional comparative element due to its ability to induce transdifferentiation.

Table 5.1 Mean total cellular protein content of B13 cells cultured in different transdifferentiation media for 21 days.

Culture Condition	Mean Total Cellular Protein Content (μg)
Control (7d)	723.36 ± 77.62
Dex (21d)	585.11 ± 61.32
Dex + OSM (21d)	407.76 ± 23.48
Dex + OSM (14d) → HepatoZYME^{+} (7d)	207.83 ± 31.08
Dex + OSM (14d) → 50:50 (7d)	444.27 ± 26.16

± 1 SE; n = 3

Compared to the other Dex treated samples, switching to HepatoZYME^{+} after 14 days resulted in reduced total cellular protein content at the end of the 21 day culture period. The Dex only treated culture had higher total protein content than all the Dex + OSM treated cultures. Dex + OSM only and where the culture medium was switched to 50:50 had similar total cellular protein content after 21 days.

All treated samples had detectable albumin content within the culture medium after 24 hours, whereas there was none present in the control. Changing to the 50:50 composition for the final 7 days of culture appeared to increase the amount of albumin secreted compared to continuing with Dex + OSM for the full 21 days. However, the difference between these two conditions was not found to be statistically significant after analysis with a one-way ANOVA and Tukey's post-hoc tests ($p > 0.05$). The levels of albumin secreted from the Dex + OSM only-treatment and from changing to the 50:50 treatment were judged to be significantly higher compared to the B13 cell control and Dex-only treated culture (Dex + OSM only = $p < 0.01$; 50:50 = $p < 0.001$); and also where the Dex + OSM treatment was changed to HepatoZYME^{+} (Dex + OSM only = $p < 0.01$; 50:50 = $p < 0.001$). Treatment with HepatoZYME^{+} did appear to show marginally greater albumin secretion than Dex treatment alone. However, no statistically significant difference was found between these two conditions, nor was any difference highlighted when they were both compared against the B13 cell control ($p > 0.05$).

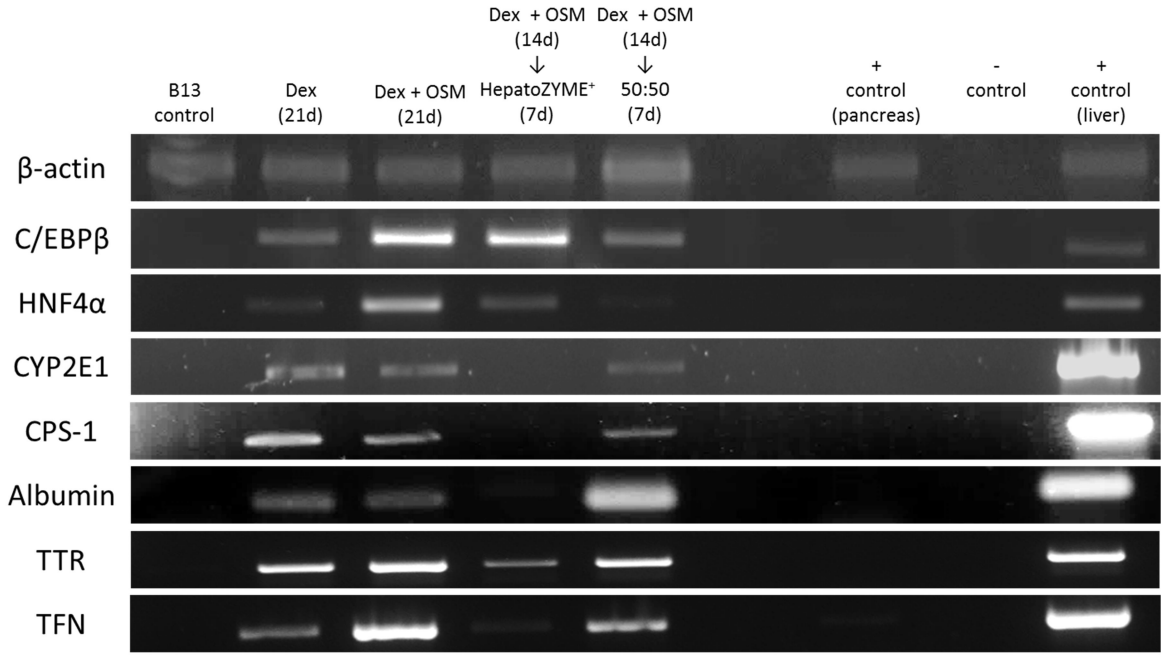

Figure 5.18 Gene expression of liver markers in transdifferentiated HLCs cultured in different transdifferentiation media for 21 days. Cells were treated with Dex only for 21 days, Dex + OSM only for 21 days; or with Dex + OSM for 14 days and HepatoZYME^{+} or 50:50 for a further 7 days. Gene expression was analysed using RT-PCR. Liver markers – C/EBPβ, HNF4α, CYP2E1, CPS-1, albumin, transthyretin (TTR) and transferrin (TFN). Reference gene – β-actin. The negative control contained no cDNA. Adult rat pancreas and liver cDNA were used as positive primary controls for their respective tissue markers. B13 cells cultured in complete B13 medium only were used as the untreated control.

RT-PCR was utilised to examine the presence of hepatic markers at the mRNA level. (**Figure 5.18**). Gene expression of liver specific markers was only observed in the transdifferentiated cultures and not the B13 cell control, although the relative levels of expression for each of the markers was different under the different conditions. Expression of the transcription factors C/EBPβ and HNF4α appeared upregulated in the Dex + OSM only culture and also where the medium had been changed to HepatoZYME^{+}, in contrast to Dex only-treated cells and where the medium was changed to 50:50. Positive expression of functional markers CYP2E1 and CPS-1 was similar between the Dex only, Dex + OSM only and 50:50 conditions, with weak to absent expression in the HepatoZYME^{+} condition. Albumin was also expressed in a similar fashion in these conditions, although appearing slightly upregulated in the 50:50 culture compared to the Dex only and Dex + OSM only conditions. In the case of TTR and TFN, the genes for two transport proteins synthesised

by the liver, gene expression was strongest in the Dex + OSM only culture. In order from highest to lowest, this was followed by 50:50, Dex only and finally the HepatoZYME^{+}-treated cells.

5.3 Discussion

The research aims for this Chapter were to investigate whether a potentially novel culture medium (HepatoZYME^{+}) could be utilised for the induction and maintenance of transdifferentiated HLCs from the B13 pancreatic cell line. This was done through characterisation of the culture medium on cell behaviour was performed by way of examining the effects on cell morphology, protein and gene expression in comparison with existing Dex-based transdifferentiation culture media to determine the most suitable medium composition for inducing transdifferentiation in the B13 cells and maintaining a stable hepatic phenotype.

5.3.1 HepatoZYME^{+}-based media for the induction of B13 cell transdifferentiation to HLCs

Attempts at culturing the B13 cell line in HepatoZYME^{+} alone were largely unsuccessful, as it was clear that the cells were unable to thrive in the culture medium as they were visibly shrivelling, highly vacuolated and detaching from the culture surface after the first 2 days of treatment. The 50:50 cultures were more successful, as although they eventually displayed the same loss of colony viability seen in the HepatoZYME^{+} cultures, the rate of cell deterioration, vacuole development and detachment from the culture surface was slower. A small population of cells in the 50:50 culture appeared to have developed a flatter, enlarged hepatocyte-like morphology distinct from the rounded, smaller control B13 cells. This behaviour was also visible in the cultures treated with Dex only. Immunofluorescent staining for hepatic markers after 9 days showed that the cultures were heterogeneous in expression for cells positive for HNF4α and CPS-1. The change to a flatter, enlarged HLC morphology and appearance of these markers have been shown to be present at this time point in other transdifferentiation studies where Dex was used as the induction factor [130,131,218,236], thus suggesting that the 50:50 culture medium is able to induce expression of these hepatic markers within a similar time frame. The presence of

the pancreatic marker amylase observed in both the Dex only cells as well as the 50:50 cultures at this time point is not unexpected as amylase expression has been observed to be initially upregulated upon glucocorticoid treatment, further than that normally seen in untreated B13 cells, before a gradual loss of expression occurs. Amylase expression is generally absent by 14 days of culture in the transdifferentiation medium, indicating the requirement of loss of the pancreatic phenotype for conversion to the HLC state [130,131,218].

Although these experiments suggested that the 50:50 culture composition has the potential to induce transdifferentiation of B13 cells to a hepatic phenotype, the gradual deterioration in cell viability over time means that this culture condition is unsuitable as a method for generating transdifferentiated HLCs as they cannot be maintained beyond the short term. This is not an improvement over established Dex-based transdifferentiation protocols. As the loss of viability was observed in the HepatoZYME^{+} and 50:50 treated cultures only, it is possible to infer that the composition of HepatoZYME^{+} may be the cause.

5.3.2 HepatoZYME^{+}-based media for the maintenance of transdifferentiated HLCs

Given that the 50:50 composition had shown capacity in causing HLC phenotypic changes to the B13 cell line, its effects on B13 cells that had been pre-induced to transdifferentiate to HLCs were assessed.

For B13 cells that had been cultured in the transdifferentiation induction medium Dex + OSM for 7 days before changing to 50:50 for a further 7 days, a clear morphological change was apparent. Prior to changing the medium, the Dex + OSM treated cells had adopted a flatter, enlarged polygonal appearance with some binuclear cells within the population for the first 7 days of culture. Where Dex + OSM was utilised for the full 14 days of culture, a change to a hepatocyte-like morphology was apparent, with the majority of B13 cells taking on an enlarged, flattened appearance. This is consistent with previous reports utilising these treatment conditions [130,132,133]. Where the medium was changed to 50:50 after 7 days of initial culture in Dex + OSM, the morphology was more irregular, with some cells increasing in size but losing their polygonal appearance, tending towards a more rounded one with vacuoles within the cytoplasm for the following 7 days. The cells

were also dissociating from each other and also from the culture surface, which was not seen in the Dex + OSM only cultures.

Notably, there was strong amylase expression in a small proportion of cells treated with 50:50 for 7 days alongside cells that appeared negative. The strong expression is in contrast to what was observed in the Dex + OSM only culture, which showed some amylase expression at 7 days but was negligible after 14 days. The behaviour seen in the 50:50 culture is in contrast to what has previously been observed with regards to the regulation of amylase expression during the transdifferentiation process with Dex-based treatment. As previously mentioned, in the early stages of glucocorticoid culture of B13 cells, there is enhancement of amylase expression which then decreases over prolonged exposure to the glucocorticoid with eventual loss of amylase expression and gain of hepatic markers [130,131]. In addition to the glucocorticoid Hydrocortisone, HepatoZYME^{+} contains the cytokine HGF, which has been shown to inhibit amylase content in the AR42J parent line [217] and in combination with Dex, significantly reduce amylase expression after only 5 days compared to supplementing with Dex alone [131]. Hydrocortisone is a less potent glucocorticoid than Dex. Furthermore, the concentration of HGF in the 50:50 medium was 5 ng/ml compared to the 10 ng/ml utilised in the study by Burke et al in 2006, which reported that HGF and Dex together reduced amylase expression significantly [131]. It has been previously shown in the AR42J parent line that the extent of amylase secretion upregulation from Dex stimulation is dose-dependent [217,239,240]. Secondly, previous investigations by Tosh et al and Fairhall et al note that removal of glucocorticoid stimulation does not appear to cause reversal of phenotype in transdifferentiating HLCs [218,241]. Thus, a possible explanation for the persistent amylase expression is that as Hydrocortisone is a less potent glucocorticoid compared to Dex and the HGF concentration is reduced compared to previous studies, this may reduce the extent of the eventual downregulatory effect on amylase compared to the combination of higher concentration Dex and HGF in the culture medium. It may be that prolonged maintenance in 50:50 beyond 7 days would eventually show complete loss of amylase expression and therefore the pancreatic phenotype, although further studies may be confounded by the increasing loss of viability in the culture. Notably, immunofluorescent staining for amylase in cells cultured for 7 days in 50:50 after 14 days of culture in Dex + OSM showed negative expression for this marker, suggesting that once the HLC phenotype is fully established, the pancreatic phenotype has been lost and changing to

50:50 does not subsequently upregulate amylase protein. However, a quantitative method of determining amylase secretion levels into the culture supernatant, such as the Phadebas colorimetric assay, would allow for increased understanding combined with the visual methods applied here as to the extent that amylase activity has changed in these cells between the different culture media.

Immunofluorescent staining also established that the change of medium to 50:50 did not cause a complete loss of protein expression of hepatocyte specific markers in HLCs. GS and CPS-1 staining were not co-expressed within the cell, reflecting the zonated distribution of expression seen in the liver where CPS-1 is only expressed in periportal hepatocytes and perivenous hepatocytes only express GS as previously reported [4,218]. This behaviour was also observed where the cultures were treated with Dex + OSM for 14 days and cultured for a further 7 days in 50:50 or HepatoZYME^{+}.

Statistical analysis of percentage cell expression showed that there were no significant differences between GS, CPS-1 and total GS and CPS-1 expression between treating cells with the Dex + OSM only treatment for 7 days and changing to the 50:50 composition for 7 more days. Although cell counting based on images is a useful method of determining percentage cell expression, given the visible deterioration of the culture in the 50:50 culture, further work to analyse this could involve combination of a secondary method for assessing mean percentage expression, such as fluorescent activated cell sorting, functional assays measuring ammonia detoxification and GS and CPS-1 specific ELISAs to provide further clarity as to how the culture media has affected expression against function.

HNF4α expression was also similar between these two treatments, being expressed in the majority of cells. However, co-expression with albumin was statistically found to be reduced in the 50:50 treated cells compared to Dex + OSM, where nearly all HNF4α positive cells were also positive for albumin. A possible reason for this is the loss of viability of the culture, as the culture medium was changed at the critical time when albumin would normally be upregulated. HNF4α is normally upregulated within the first 2 days of exposure to Dex treatment, whereas albumin is a marker that appears approximately 7-9 days after instigating transdifferentiation [130,131].

To further investigate the extent of active function in the different cultures as percentage expression only refers to the quantity of cells that are positive for that marker, quantitative

analysis was sought. The rat albumin ELISA was utilised to compare the amount of serum albumin secreted into the culture supernatant from cells treated using two established methods of B13 transdifferentiation to HLCs (Dex only and Dex + OSM only for 21 days) and from culturing in Dex + OSM for 14 days before changing to HepatoZYME^{+} or 50:50 for the following 7 days. From comparing the serum albumin content in the medium of the Dex only and Dex + OSM cultures, the Dex + OSM only culture was significantly increased compared to the Dex only culture, reflecting the result obtained by Shen et al in 2000 that showed a higher percentage cell expression of albumin in Dex + OSM treatment compared to Dex only treatment over 14 days of culture [130] and other studies reporting an increased population of B13 cells undergoing transdifferentiation to HLCs alongside enhancement of the hepatic phenotype [132,218]. Serum albumin was detected in the culture medium of cells treated with HepatoZYME^{+}, although it was significantly reduced compared to the Dex + OSM only culture and not significantly different from the Dex only culture. In contrast, the 50:50 medium was found to have the highest albumin content compared to the other conditions. However, this was not found to be statistically different from that of the Dex + OSM culture. It is possible that albumin secretion was further enhanced due to the presence of HGF in the 50:50 culture media, as this effect from HGF has previously been observed on addition to primary rat hepatocytes in culture [242] and also in the maturation of foetal mouse liver in combination with OSM [243]. This may have also affected the albumin secretion measured in the HepatoZYME^{+}-treated cell medium.

As the heterogeneity in population with regards to transdifferentiated hepatocytes is more apparent in Dex only-treated cultures compared to Dex + OSM treated cells, the total protein content will contain a combination of HLCs and non-transdifferentiated B13 cells unaffected by the transdifferentiation treatment which may still be undergoing proliferation. Although this normalisation is representative of the effect of Dex only treatment on a population of cells, it does not directly reflect the albumin secretion capability of only the HLCs within the population. Normalisation to cells expressing a liver specific marker would allow for a more direct comparative understanding of the functionality of the HLCs within these different cultures. Notably, the mean total cellular protein content measured for normalisation of the HepatoZYME^{+} culture was approximately half as much as that of the Dex + OSM culture after 21 days. This infers a possible loss of culture viability similar to that seen in earlier experiments, which may

augment loss of cell function such as reduced albumin secretion capability. In contrast, the 50:50 culture did not show reduced total cellular protein in comparison, displaying similar levels to the Dex + OSM culture. However, being less potent than HepatoZYME^{+} and considering the loss of culture coherency observed in previous experiments, a similar, eventual loss of viability is possible, albeit at a reduced rate of deterioration. Therefore, a further point of investigation could utilise viability studies such as analysis of caspase-3 activity and lactate dehydrogenase release alongside metabolic studies using as MTT or the colorimetric resazurin assay alamarBlue. This would allow comparison between the different culture conditions to determine if HepatoZYME^{+} based media increases apoptotic activity and affects metabolic function in correlation with the reductions in total cellular protein and secretory activity seen here.

RT-PCR was used to look at gene expression of hepatic markers after pre-treatment in Dex or Dex + OSM only for 14 days and then treatment with HepatoZYME^{+} or 50:50 for a further 7 days, compared to 21 days in Dex or Dex + OSM only. Notably, extracted RNA quantities from the HepatoZYME^{+} and 50:50 treated cultures were found to be lower compared to the other conditions. This may have been affected by overall culture viability. The hepatic markers were only detected in the positive liver control and the transdifferentiated culture extracts, but not the pancreatic controls, in agreement with previous studies [130,131,244]. The transcription factors C/EBPβ and HNF4α were upregulated the most under the Dex + OSM only treatment, but the HepatoZYME^{+} treated cells also showed strong expression compared to Dex only treatment and the 50:50 culture. The observed increase in C/EBPβ and HNF4α in HepatoZYME^{+} may be due to the increased concentration of HGF and OSM present in the culture medium, which has been previously shown to cause increased expression of these two factors in transdifferentiating B13 cells [130–132], or further unknown factors present within the proprietary basal medium. The weaker expression within the 50:50 culture may be related to only having half the concentration of the factors contained with HepatoZYME^{+} and reduced glucocorticoid potency, and the Dex only culture including no additional growth factors. Expression of functional markers CYP2E1, CPS-1, albumin, TTR and TFN was the weakest within the HepatoZYME^{+} culture compared to the Dex only and Dex + OSM only conditions. The 50:50 sample showed slightly elevated albumin expression, which correlates with the observation from serum albumin protein quantification. Although these results confirm that hepatic markers remain upregulated after changing culture medium,

which is in agreement with the protein expression of markers seen from immunofluorescent staining, there appear to be relative differences in the level of gene expression depending on the culture medium used. Expression of C/EBPβ in the positive liver control was reduced in comparison with all the Dex treated cultures. C/EBPβ is normally upregulated during early liver development [245] and is induced in B13 cells as the 'master switch' between a pancreatic and hepatic phenotype during transdifferentiation [130]. Therefore, the lower expression in the control may be attributed to primary adult liver possessing a more mature phenotype than the transdifferentiated HLCs at this time point. Expression of CYP2E1 and CPS-1 were found to be upregulated in the control liver compared to the transdifferentiated cultures, although expression of TTR and TFN in the control liver was similar to that of the Dex + OSM only culture. This suggests that the transdifferentiated HLCs are comparable in presence of expression to control liver. However, the variation in expression levels may be related to the relative maturity of the transdifferentiated cultures compared to the control liver. Further quantification using qRT-PCR would assist further in comparatively confirming mRNA levels with statistical analysis to examine the gene level differences between the different conditions.

A significant point of interest observed in the 50:50 cultures was the presence of not only binucleate cells, which are present in Dex-based cultures, but large, multinucleate cells that were expressing hepatic markers. A distinguishing feature of hepatocytes is that the population is heterogeneous for mononucleate or binucleate cells. In physiology, changes in the liver parenchyma during postnatal growth are characterised by increases in hepatocyte polyploidisation [246]. It has been suggested that the formation of binucleate cells in hepatocytes is due to incomplete cytokinesis [247,248], and that polyploidy is a protective measure against cellular stress and damage [249,250]. Given the apparent loss of culture viability observed in these experiments, this may have been a stimulatory factor in the appearance of these multinucleate cells if the culture medium contained a cytotoxic factor, or was absent for a factor essential for survival. Although hepatocytes and transdifferentiated HLCs are generally non-proliferative under normal physiological conditions, it was found that HGF in the presence of Dex, enhanced by the presence of non-essential amino acids, was able to induce a small population of transdifferentiated HLCs to proliferate [131]. In liver regeneration, HGF is known as a mitogen, so the presence of this growth factor may have influenced the presence of multiple nuclei as it was part of the supplementation in the 50:50 medium. Although all treated cultures apart

from the proliferating B13 cell control were negative for PH3, a marker of mitosis, further work could examine other cell cycle phase markers, such as cyclin D1 (G_1) and cyclin B1 (G_2/mitosis) to explore whether the culture medium has influenced cells to actively enter the cell cycle. Despite this, it is doubtful that the multinucleate cells would be able to survive long term.

To identify the likely causative agent or agents behind the overall loss of viability, further understanding of the composition of HepatoZYME$^+$ is required. HGF and OSM are cytokines that have previously been used as additional culture supplements in maturation media for embryonic liver tissue and in complete B13 DMEM-based transdifferentiation media, positively enhancing the hepatic phenotype [130–132,243]. The concentrations utilised in HepatoZYME$^+$ and 50:50 are within the range utilised in previous studies. Both Dex and Hydrocortisone have been shown to act upon the glucocorticoid receptor to induce transdifferentiation [130], but Dex is considered to be 25 times more potent in effect than Hydrocortisone [251,252]. Therefore, as the concentration of Hydrocortisone in HepatoZYME$^+$ is 10 μM, the concentration of Dex to achieve equivalent glucocorticoid activity would be 400 nM; in the 50:50 culture medium, the equivalent concentration is 200 nM Dex. The 1 μM concentration utilised in the Dex-treated cultures is comparatively 2.5 times more potent than the Hydrocortisone present in HepatoZYME$^+$, and 5 times more potent than that within the 50:50 medium. Transdifferentiation of B13 cells to HLCs has been previously achieved using concentrations of Dex as low as 10 nM, a glucocorticoid concentration much less potent than that contained in HepatoZYME$^+$ or 50:50 [130,238,253]. As B13 cells displayed some morphological change and upregulation of hepatic markers similar to that observed in HLCs when culturing using 50:50, it is possible to infer that as the Hydrocortisone content of the 50:50 medium is within the reported range of glucocorticoid concentrations used to induce transdifferentiation, the Hydrocortisone, HGF and OSM within the medium are unlikely to be the overarching causative factors for the observed loss of cell viability.

Notably, HepatoZYME$^+$ is serum-free and due to the proprietary nature of the basal medium HepatoZYME-SFM, it is unknown what other supplementation is involved beyond that stated here. It is possible that the lack of FBS to aid cell adhesion to the culture surface affected cell viability, as additional experiments using different serum concentrations in DMEM-based Dex-supplemented transdifferentiation media revealed

low to negligible B13 cell attachment, survival and transdifferentiation where there was no serum present. A stable culture with transdifferentiated cells was able to be established with a minimum of 5% (v/v) FBS and was able to be cultured for up to 60 days (data not shown). The 50:50 culture medium contained 5% (v/v) FBS by virtue of being HepatoZYME^{+} diluted with the complete B13 culture medium. This may have improved its survival beyond that of complete HepatoZYME^{+}, due to the presence of adhesion proteins from the FBS and dilution of the unknown factors contained within the proprietary basal medium. However, as the loss of culture stability was still occurring, this suggests that the contents of HepatoZYME-SFM itself are likely to be the issue, be it missing an essential factor required for the B13 cells and transdifferentiated HLCs to thrive, or a combination of factors at a concentration too toxic for them to survive. From this, additional experimental controls to clarify the effects of the HepatoZYME^{+} and 50:50 media would aid understanding of which component within the culture media is responsible for overall loss of viability when using HepatoZYME^{+}-based media or the induction of transdifferentiation observed with the 50:50 culture medium. This approach would involve characterisation of the effects of each of the components individually and in combination upon the B13 cells and cells pre-induced to transdifferentiate. For example, for the 50:50 culture medium, this approach would involve variant cultures of the B13 cells solely with Hydrocortisone, HGF or OSM within the combined basal medium of HepatoZYME-SFM and complete DMEM, as well as culturing using these additives within complete DMEM in the absence of HepatoZYME-SFM. Examining these factors using this experimental method would allow for greater specificity as to the causative agents involved in inducing transdifferentiation and also the loss of culture viability.

5.4 Conclusion

The aim of the research described in this Chapter was to investigate and characterise the utility of different culture media to induce transdifferentiation in pancreatic B13 cells, and also whether the media are able to maintain or enhance the hepatic phenotype in B13 cells that have undergone transdifferentiation to HLCs. The focus was on the culture medium HepatoZYME^{+}, a hepatocyte maturation medium that has been reported to improve the hepatic phenotype of the directed differentiation of hESCs and iPSCs to HLCs and whether this could be translated over to the transdifferentiation of pancreatic cells to HLCs. Two

culture media were examined; complete HepatoZYME$^+$, and 50:50, a 1 in 2 dilution of HepatoZYME$^+$ with complete B13 culture medium. These were comparatively characterised alongside established Dex-based transdifferentiation media.

HepatoZYME$^+$ was unable to induce transdifferentiation in B13 cells, and instead, visible deterioration of the culture within 48 hr was observed with complete loss of cell viability by day 5. The 50:50 culture medium appeared to show morphological changes in the cells similar to that of HLCs and simultaneously observed in Dex-treated cells. Protein expression of hepatic markers, absent in untreated B13 cells, was also seen. Despite this, the 50:50 medium also suffered from a gradual loss of cell viability and morphological derangement not seen in the Dex-treated cells, and was unable to support a culture long term. Therefore, neither HepatoZYME$^+$ nor 50:50 are better than current transdifferentiation methods.

Subsequent studies showed that the 50:50 culture medium was able to maintain expression of hepatic markers in transdifferentiated HLCs initially cultured using Dex + OSM. Firstly, at an earlier stage of transdifferentiation, induction of hepatic markers was maintained, although amylase expression was also present. Culture viability appeared compromised as observed previously. As a maintenance medium for the later stage of transdifferentiation, initially, the 50:50 culture medium appeared to show an improved regularity in hepatocyte-like morphology but eventually, both HepatoZYME$^+$ cultures deteriorated as seen previously. Amylase expression was not upregulated in the presence of the HepatoZYME$^+$-based cultures once conversion had been established. Both HepatoZYME$^+$ and 50:50 were able to show protein expression of hepatic markers, but there was a distinct reduction in albumin secretion with HepatoZYME$^+$. In contrast, the 50:50 medium was comparable to the Dex + OSM culture medium. Hepatic gene expression was present, but the level of regulation for the HepatoZYME$^+$ and 50:50 was variable when compared to Dex-based media. Finally, it appeared that the 50:50 culture medium was able to generate multinucleate cells beyond the mononucleate and binucleate phenotype normally seen in hepatocytes and transdifferentiated hepatocytes.

To answer the research aims of this Chapter, it is possible to conclude that neither the HepatoZYME$^+$ culture medium, nor the 50:50 medium, are suitable for inducing transdifferentiation to HLCS, nor are they suitable for maintenance of transdifferentiated HLCS. Despite this, several interesting points regarding the biology of transdifferentiation

have been highlighted through the work in this Chapter. Firstly, the 50:50 culture was shown to be able to initiate morphological changes and upregulation of hepatic markers in untreated B13 cells similar to that observed in Dex-based induction media, suggesting that this formulation is able to induce some cells to convert to an HLC phenotype. Furthermore, as a maintenance medium, transdifferentiated HLCs did not show complete reversal of the hepatic phenotype, and appeared to be comparable to the established Dex + OSM protocol with regards to serum albumin function with 50:50. Finally, the appearance of multinucleate cells when culturing using 50:50 may be partially encouraged by a combination of glucocorticoid hormone and HGF, although further work in this area to examine the cell cycle signalling mechanisms behind this will be required.

The loss of viability in both HepatoZYME^{+} based protocols show that they are no improvement on current transdifferentiation protocols. However, to examine why the cultures would eventually deteriorate in such a manner, future work quantifying cell viability, metabolic and cytotoxicity studies could be utilised to investigate the causative factor for loss of culture stability in these media, thus informing modifications for a potentially improved set of culture conditions beyond that described here.

The experiments in this Chapter have shown that out of the investigated culture media, the established Dex + OSM culture medium is the optimal culture condition for transdifferentiation of B13 cells to HLCs, as it can induce and maintain the hepatic phenotype within a stable culture. Therefore, further work in this thesis will utilise this culture medium with the intention of inducing and maintaining transdifferentiation of B13 cells to HLCs cultured on the surface-treated phase inversion PX membranes developed in **Chapter 4**.

Chapter 6
Biocompatibility and transdifferentiation of pancreatic cells to hepatocyte-like cells on surface treated polystyrene flat sheet membranes

6.1 Introduction

6.1.1 Biocompatibility of PX membranes for bioartificial liver device design

Developing a suitable *in vitro* environment for cells that recapitulate normal cellular functions is essential for a bioartificial liver (BAL) device, particularly as the primary goal is to replace the function of a failing liver effectively. By using tissue engineering techniques, the culture scaffold and medium can be tailored specifically to the cell type. For example, an ideal scaffold for a BAL device would be nontoxic and support cell adhesion and normal hepatocyte function *in vitro*.

The results presented in **Chapter 4** have described and characterised a method for modifying the surface chemistry and wettability of phase inversion cast PS membranes to encourage a surface environment more conducive to cell culture (termed here PX membranes). Furthermore, the results presented in **Chapter 5** determined a suitable induction and maintenance cell culture medium for the transdifferentiation of the pancreatic B13 cell line to functional HLCs respectively (Dex + OSM). Therefore, it was necessary to bring these components together to assess the cell culture capabilities of PX membranes with the intention of potentially translating both biomaterial and cell source to BAL device design.

The ideal biomaterial should be able to promote initial cell attachment to the membrane surface through deposition of proteins that are adsorbed onto the biomaterial surface and subsequently interact with the extracellular matrix. The interaction between cell and substrate is termed 'focal adhesion' [254], the extent of which eventually leads to stimulation of cell spreading and subsequent proliferation or differentiation. Optimal levels of initial cell attachment will increase the proliferative and differentiating capacity of the cells and overall culture viability due to the presence of sufficient numbers of cells. Furthermore, it is not possible to rule out that the utility of PX membranes to support transdifferentiation of pancreatic cells to functioning HLCs may also be affected by biomaterial characteristics such as surface chemistry and wettability. In the case of mesenchymal stem cells, they have been shown to differentiate down various lineages based on the stiffness of the gel they are seeded upon [255,256].

6.1.2 Expanding the scope of biomaterial development for regenerative medicine

A promising step further would be to expand the scope of the biomaterial to be able to support culture of a variety of cell types. In comparison with traditional tissue culture flasks and stirred tank bioreactors, HFBs are able to expand a large population of cells whilst using a fraction of the volume of the former and latter methods [147,150]. Combining a biomaterial that can support multiple cell lines with the HFB makes it an attractive prospect in regenerative medicine for the scale up of cell therapies to clinical quantities, be it the production of cells or producing sufficient quantities of cellular products, such as growth factors. For example, one potential use involves the MG63 cell line, a human osteosarcoma cell line that is used as a bone tissue model [257,258]. Notably for liver tissue engineering, it is also posited as a potentially cost effective and limitless source of hepatocyte growth factor (HGF) [259] that could be utilised in various induction and maintenance media for hepatic differentiation and also transdifferentiation. The ability of PX membranes to support MG63 culture is therefore also of relevance to this Chapter.

6.1.3 Experimental aims and objectives

The experimental research described in this Chapter sought to investigate the biocompatibility of oxygen plasma treated PX phase inversion flat sheet membranes and the ability of B13 cells to convert to HLCs on this culture substrate. The research questions to be addressed were whether PX phase inversion membranes: a) are biocompatible in comparison with other established biomaterials; b) can support the transdifferentiation of B13 pancreatic cells to HLCs; and c) can retain bulk physical characteristics under transdifferentiation culture conditions. These are important factors in establishing whether PX phase inversion membranes can potentially be used as a HFB tissue culture scaffold for long term cell culture, such as that in a BAL device. PX membranes were fabricated using deionised water as the nonsolvent to initially cast PS membranes and were subsequently exposed to oxygen plasma using a capacitively coupled plasma chamber to increase surface wettability.

This Chapter is divided into three parts. Firstly, biocompatibility studies sought to compare PX membranes as developed in **Chapter 4** as a suitable substrate against established biomaterials – tissue culture polystyrene (TCPS) and poly(D,L-lactide-*co*-glycolide) (PLGA) phase inversion cast membranes. Two cell lines were utilised – rat pancreatic cells (B13), which are of great interest in this thesis due to their ability to transdifferentiate to functional HLCs [130,131,241,244]; and human osteosarcoma cells (MG63), an osteoblast-like cell that is a potentially limitless source of HGF [259]. Biocompatibility was characterised through analyses of both cell lines with regards to (i) quantification of cell attachment on the different biomaterial surfaces to identify the efficacy of the surface treatment used to generate PX membranes; (ii) cell viability by visualisation of a live/dead stain followed by quantification of live and dead cells on each culture substrate and (iii) assessing the utility of using cellular release of lactate dehydrogenase into the culture medium as a measure of viability.

The second part of the Chapter deals with investigating the utility of B13 cells to transdifferentiate to HLCs upon PX membranes, utilising the Dex + OSM treatment as investigated in **Chapter 5**. Transdifferentiation of pancreatic cells to HLCs was investigated through (i) determination of pancreatic and hepatic protein expression by indirect immunofluorescent staining on PX membranes and (ii) comparison of hepatic function of transdifferentiated HLCs on PX membranes against standard TCPS and PLGA

membranes. Functional characterisation was performed through quantification of serum albumin secretion.

Lastly, a comparative study into whether the transdifferentiation culture conditions exacts physical alterations in PX and PLGA membranes without cells present was performed by comparative measurements examining differences in membrane mass, culture surface area and volume over time.

6.2 Results

6.2.1 Cell attachment on PX membranes

Attachment studies were performed over a 6 hr period to compare four culture substrates – TCPS, untreated PS membranes, PLGA membranes and treated PS membranes (known as PX). Two different cell lines were utilised – rat pancreatic B13 cells and human osteosarcoma MG63 cells.

PS and PLGA membranes were cast as previously described in **Section 3.2** using the phase inversion immersion precipitation method. To create PX membranes, untreated PS membranes were exposed to oxygen plasma generated by a capacitively coupled plasma chamber as described in **Section 3.2.3**. Both PX and PLGA membranes were then prepared for cell culture by fixing them in autoclaved polycarbonate bioreactor modules and sterilising the membrane culture surface (1.9 cm^2) with 1% (v/v) antibiotic-antimycotic solution for 24 hours at 4˚C. The membrane culture surfaces were then washed in sterile PBS prior to cell inoculation (**Section 3.6.1**).

The bioreactors were seeded with B13 cells or MG63 cells at a density of 20,000 cells/cm^2. This parameter was selected as it has been utilised previously in similar cell attachment studies on both PLGA flat sheet and hollow fibre membranes [154,171,260]. The seeded bioreactors were then incubated at 37˚C for 6 hr under static conditions. The cells were then lysed prior to quantification with the PicoGreen dsDNA quantification assay as described in **Section 3.6.2**. Tissue culture polystyrene (TCPS) for adherent cells was used as a control biomaterial and seeded accordingly.

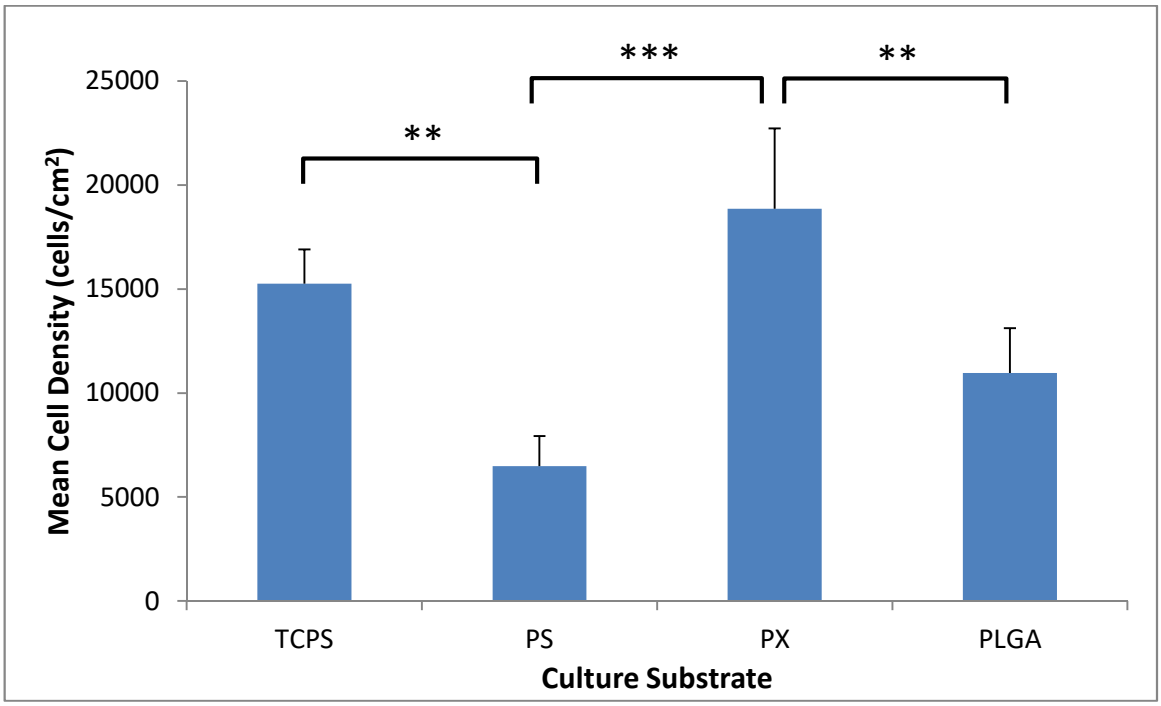

Figure 6.1 Mean cell densities of B13 cells seeded on different culture substrates after 6 hr culture. TCPS, PS, PX and PLGA membrane surfaces were seeded with B13 cells at a density of 20,000 cells/cm^2 each and cultured for 6 hr. Culture density of cells attached to the membrane surfaces was quantified by the PicoGreen dsDNA quantification assay. Statistical analysis was by way of a one-way ANOVA with Tukey's post hoc tests. Error bars = + 1 SE; n = 4; ** = p = 0.01; *** = p < 0.001. B13 cell attachment to PX was not significantly different to TCPS but was significantly higher than PS and PLGA.

Figure 6.1 shows the mean culture densities of B13 cells attached to the surfaces of different biomaterials 6 hr after seeding the bioreactors. Here, PX membranes appeared to have the highest mean cell attachment with a density similar to that of the initial seeding density, suggesting that the majority of the cells seeded had adhered to the culture substrate after 6 hr incubation. This was followed by TCPS, then in order: PLGA and PS. In contrast, there were significantly fewer cells attached to untreated PS membranes and PLGA membranes after 6 hr. Statistical analysis showed that there was no significant difference between TCPS and PX membranes with regards to the number of cells attached to the culture substrates, nor between TCPS and PLGA. Similarly, no significant difference was found between untreated PS and PLGA membranes. The higher attachment to PX membranes was found to be statistically significantly different when compared to cells attached to untreated PS and PLGA membranes.

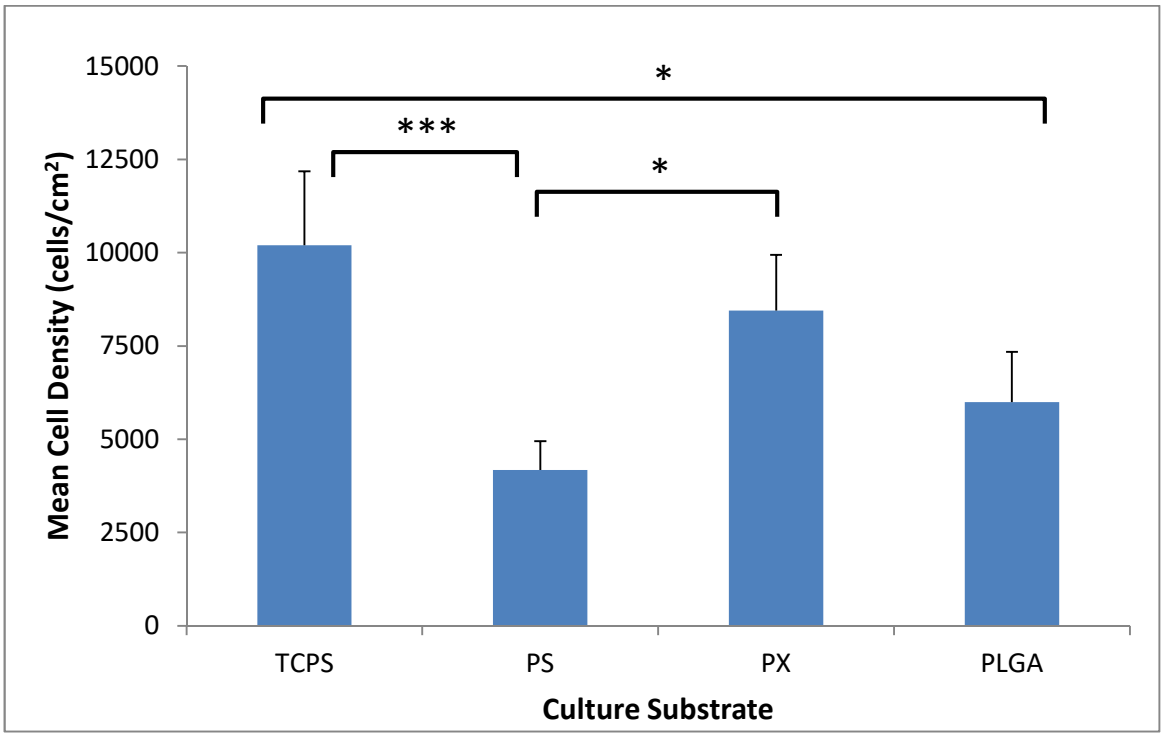

Figure 6.2 Mean cell densities of MG63 cells seeded on different culture substrates after 6 hr culture. TCPS, PS, PX and PLGA membrane surfaces were seeded with MG63 cells at a density of 20,000 cells/cm^2 each and cultured for 6 hr. Culture density of cells attached to the membrane surfaces was quantified by the PicoGreen dsDNA quantification assay. Statistical analysis was by way of a one-way ANOVA with Tukey's post hoc tests. Error bars = + 1 SE; n = 4; * = $p < 0.05$; *** = $p < 0.001$. MG63 cell attachment to PX membranes was not significantly different to TCPS or PLGA membranes but was significantly higher than PS membranes.

Figure 6.2 shows the mean cell densities of MG63 cells attached to different culture substrates after 6 hr incubation. With this cell line, TCPS was found to have the most cells attached to the culture surface, followed by the PX membrane; then in order, PLGA then untreated PS. Statistical analysis found no significant differences between TCPS and PX with regards to mean cell density, although no significant difference was found in attachment of cells between PX and PLGA membranes. PX membranes were found to have significantly higher MG63 cell attachment than that on PS membranes, whilst cell attachment to TCPS was found to be both significantly higher than both PLGA and PS membranes.

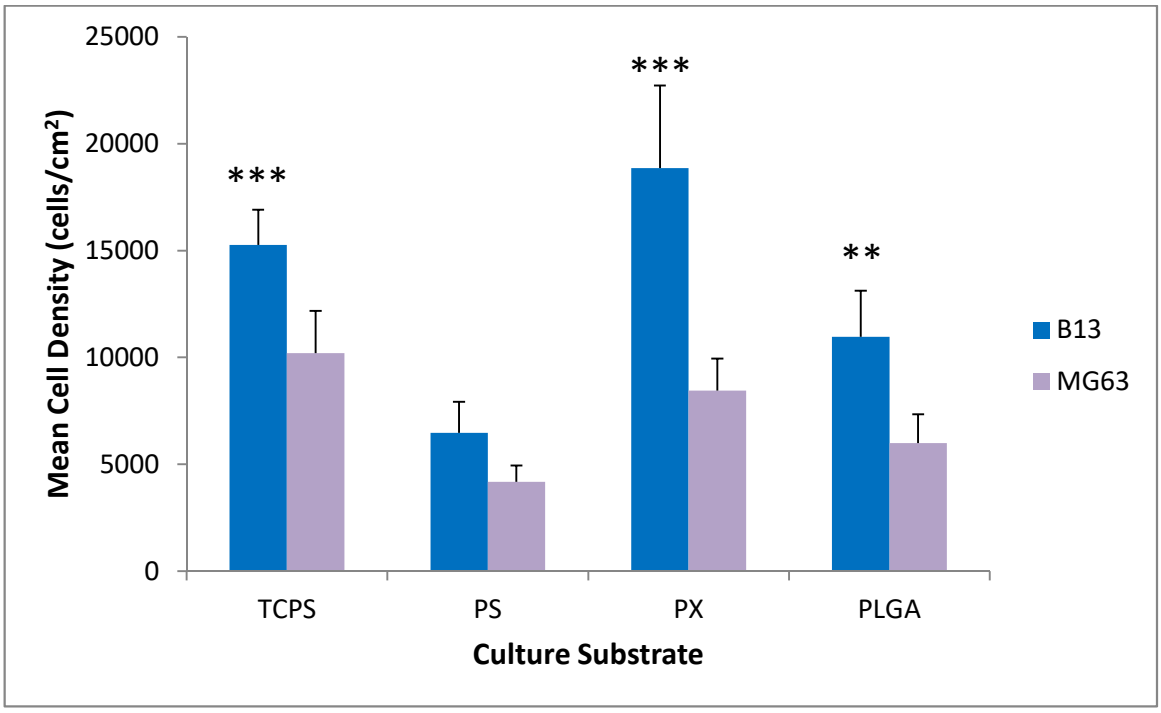

Figure 6.3 Comparison of mean cell densities between B13 and MG63 cells seeded on different culture substrates after 6 hr culture. TCPS, PS, PX and PLGA membrane surfaces were seeded with either B13 cells or MG63 cells at a density of 20,000 cells/cm^2 each and cultured for 6 hr. Culture density of cells attached to the membrane surfaces was quantified by the PicoGreen dsDNA quantification assay. Statistical analysis compared between cell lines per culture substrate using an independent samples Student's t-test for each substrate. Error bars = + 1 SE; n = 4; ** = p = 0.01; *** = p < 0.05. B13 cell attachment was found to be significantly higher than MG63 cell attachment on TCPS, PX and PLGA membranes but there were no significant difference between the two cell lines on PS membranes.

Compared to B13 cell attachment on all culture substrates, fewer MG63 cells overall had attached to each biomaterial surface 6 hr post seeding. Statistical analysis suggested that there were significant differences between attachment of the two cell lines on TCPS, PX and PLGA membranes with higher mean cell densities of B13 cells present than MG63 cells. Furthermore, there was no significant difference between the attachment capabilities of the different cell lines on PS membranes (**Figure 6.3**).

6.2.2 Cell viability on PX membranes

To culture cells on a biomaterial, it is essential that there is no loss of cell viability over time. Scaffold degradation can result in the release of breakdown products that may be

toxic to cells. Furthermore, the interaction between the cell membrane proteins and the surface chemistry of the biomaterial may not be amenable to normal cellular functions and may increase apoptotic behaviour.

Previously, PX membranes demonstrated an overall improvement of cells attaching to the membrane surface compared to untreated PS membranes. PX membranes appeared to be comparable to TCPS with regards to adhered cell densities of both the B13 and MG63 cell lines. Due to the low cell densities present on PS membranes, further studies sought to investigate the viability of cells cultured on PX membranes in comparison to TCPS and PLGA membranes only. To distinguish between live and dead cells a fluorescent stain utilising calcein AM and ethidium homodimer-1 was applied to B13 and MG63 cells that had been cultured for 48 hr on the aforementioned substrates, as described in **Section 3.6.3**.

Figure 6.4 depicts fluorescent visualisation of B13 cells on TCPS, PX and PLGA membranes. All biomaterial surfaces showed the presence of attached cells. There was a high proportion of B13 cells showing positive for calcein AM metabolism on all substrates, suggesting that the culture populations were metabolically active and therefore viable. There was very low incidence of ethidium homodimer-1 binding to nucleic acids with no cell colonies showing positive, only single isolated cells. These observations suggested negligible cell death within the cultures after 48 hr.

The cells stained with calcein AM and ethidium homodimer-1 were further quantified and analysed by comparing the mean percentage live or dead cells between the different culture substrates (**Figure 6.5**). All culture substrates showed overall mean viable cells of greater than 98% of the culture population, with less than 1.5% of cells dead. B13 cells cultured on PX membrane surfaces appeared to have the greatest mean percentage of live cells, reaching over 99.5%, followed by TCPS and PLGA, both with means over 98.5%. PLGA appeared to have a slightly higher percentage of dead cells in certain areas of the membrane. This suggested with greater variation in the results, given the larger standard error. When taking the standard error into account, the overall culture viability was still above 97.5% at the lower bound. Furthermore, statistical analyses found that there were no significant differences in B13 cell viability between the different culture substrates.

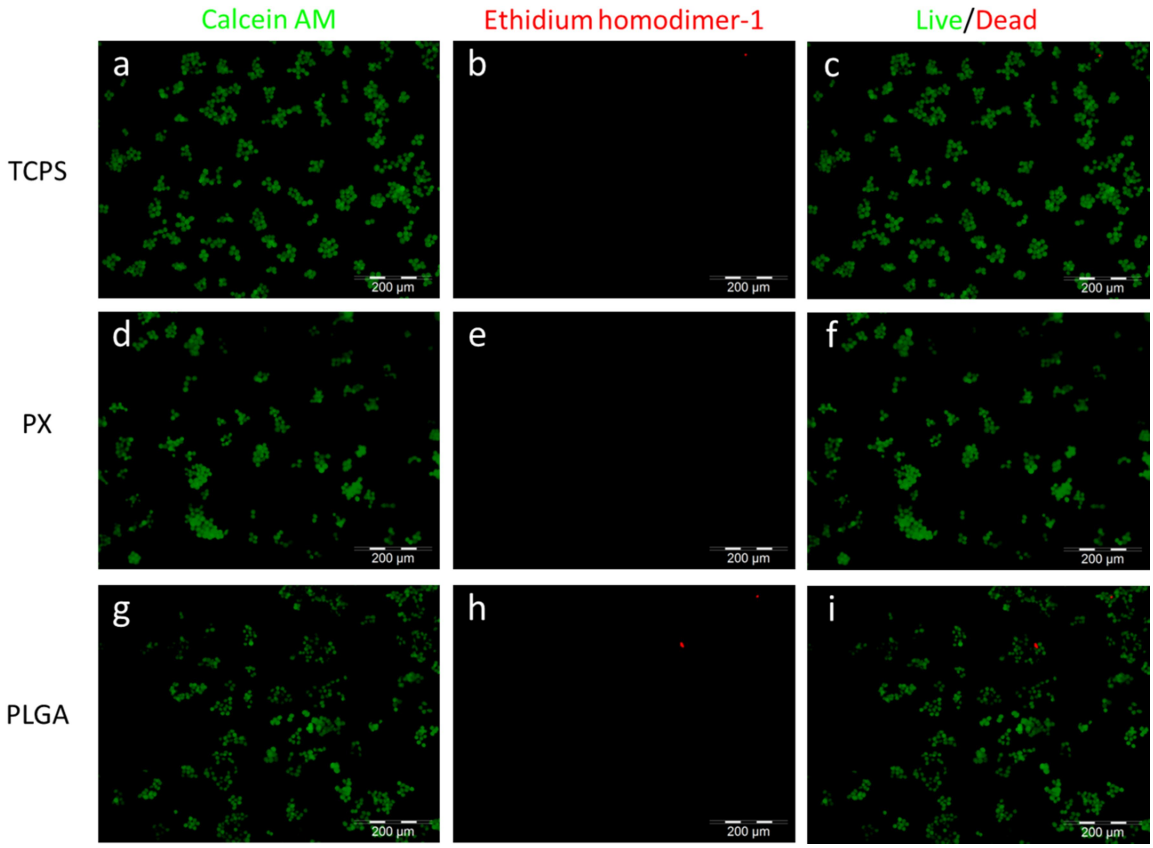

Figure 6.4 Viability of B13 cells seeded on TCPS, PX and PLGA membranes after 48 hr culture. TCPS (**a - c**), PX (**d - f**) and PLGA (**g - i**) membrane surfaces were seeded with B13 cells, stained after 48 hr culture and visualised by fluorescent microscopy. Live cells positive for calcein AM metabolism are shown in green (**a**, **d**, **g**); dead cells positive for ethidium homodimer-1 are shown in red (**b**, **e**, **h**). Images (**c**), (**f**) and (**i**) are composites of (**a** & **b**), (**d** & **e**) and (**g** & **h**) respectively. Scale bar = 200 µm.

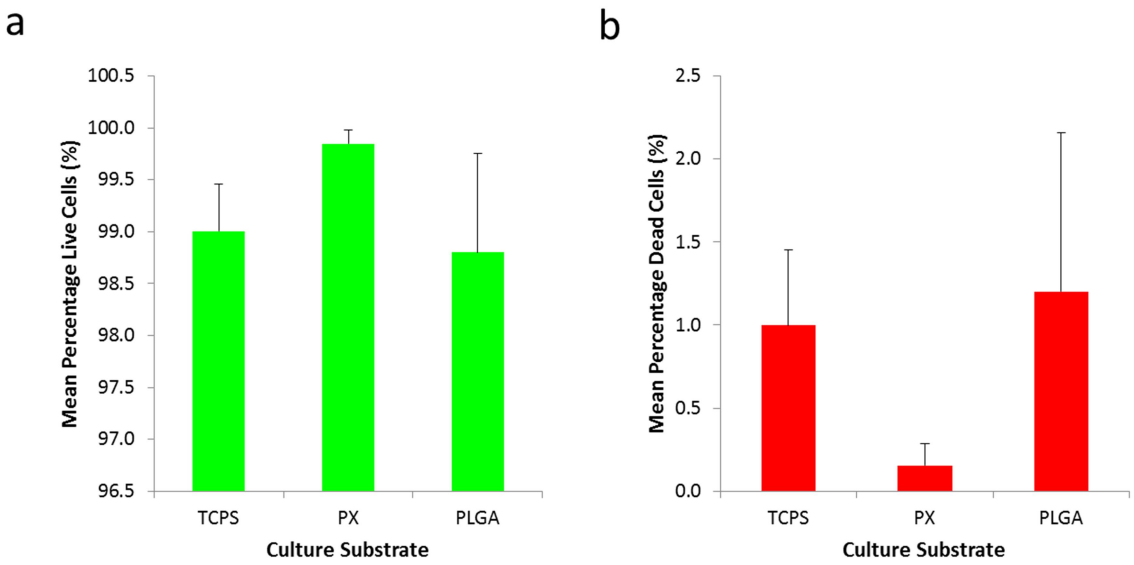

Figure 6.5 Mean percentage live and dead B13 cells seeded on different culture substrates after 48 hr culture. Statistical analyses were by way of a one-way ANOVA with Tukey's post hoc tests. (**a**) Mean percentage live cells; (**b**) mean percentage dead cells. Error bars = + 1 SE; n = 3; $p > 0.05$. No significant differences in viability were found between the different culture substrates after 48 hr of culture.

Upon similar investigation of the MG63 cell line, cells appeared to be attached to all culture substrates after 48 hr, as previously observed with the B13 cell line. The high proportion of positive staining for calcein AM metabolism and single, isolated cells staining positive in sparse quantities for ethidium homodimer-1 upon the different culture substrates as previously mentioned was also observed in the MG63 cell line (**Figure 6.6**).

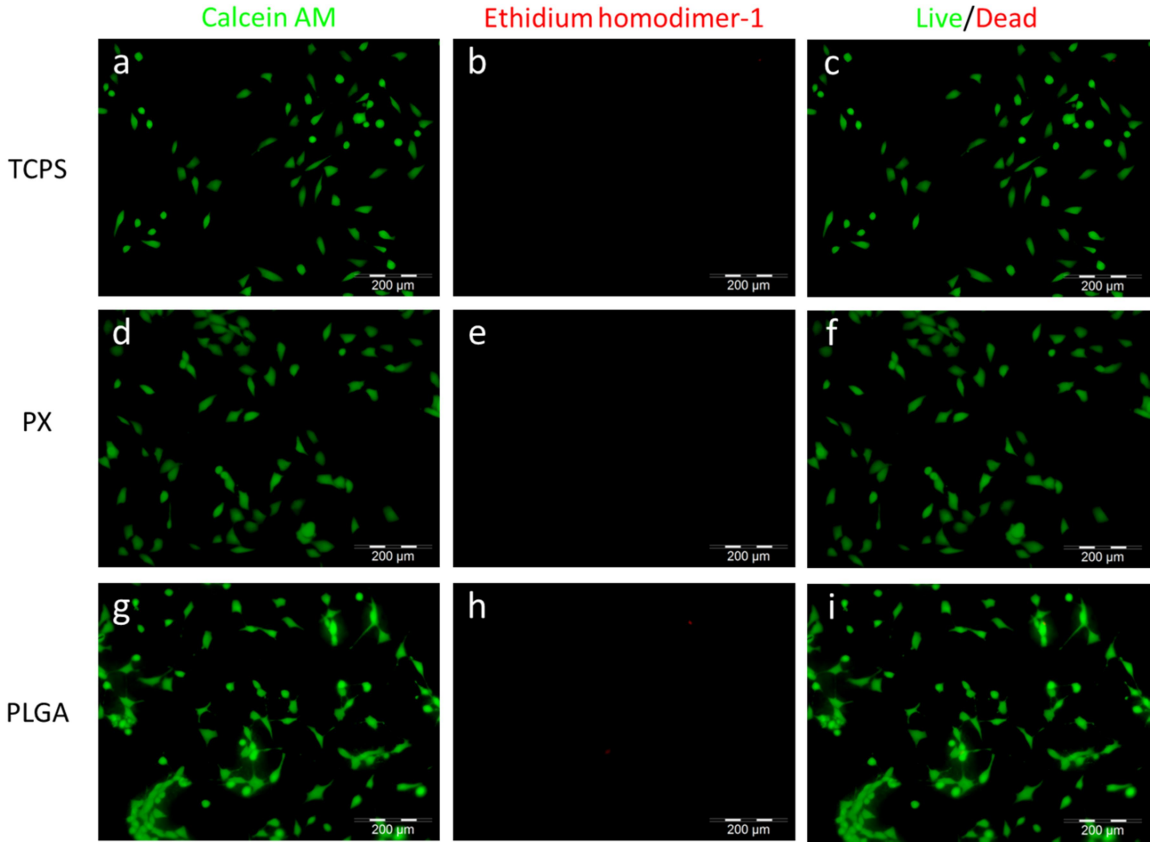

Figure 6.6 Viability of MG63 cells seeded on TCPS, PX and PLGA membranes after 48 hr culture. TCPS (**a - c**), PX (**d - f**) and PLGA (**g - i**) membrane surfaces were seeded with MG63 cells, stained after 48 hr culture and visualised by fluorescent microscopy. Live cells positive for calcein AM metabolism are shown in green (**a**, **d**, **g**); dead cells positive for ethidium homodimer-1 are shown in red (**b**, **e**, **h**). Images (**c**), (**f**) and (**i**) are composites of (**a** & **b**), (**d** & **e**) and (**g** & **h**) respectively. Scale bar = 200 µm.

Figure 6.7 shows quantification of stained live and dead MG63 cells by mean percentage of live and dead cells. Upon all culture substrates, the mean percentage of live cells in the culture population was found to be at least 96%. TCPS and PX had similar percentages of live cells with both reaching means of over 99%. In contrast, MG63 cultures on PLGA appeared to have a greater proportion of dead cells present, with a mean of over 3% dead cells within the culture population compared to just over 0.5% in the TCPS and PX cultures.

Statistical analysis comparing the different culture substrates suggested that there was no significant difference between the proportions of live and dead cells on TCPS and PX. However, both substrates were judged to be significantly different when compared with the

PLGA cultures. Based on the statistical analyses, the PLGA MG63 culture appeared to be less viable in comparison with cells seeded upon TCPS and PX.

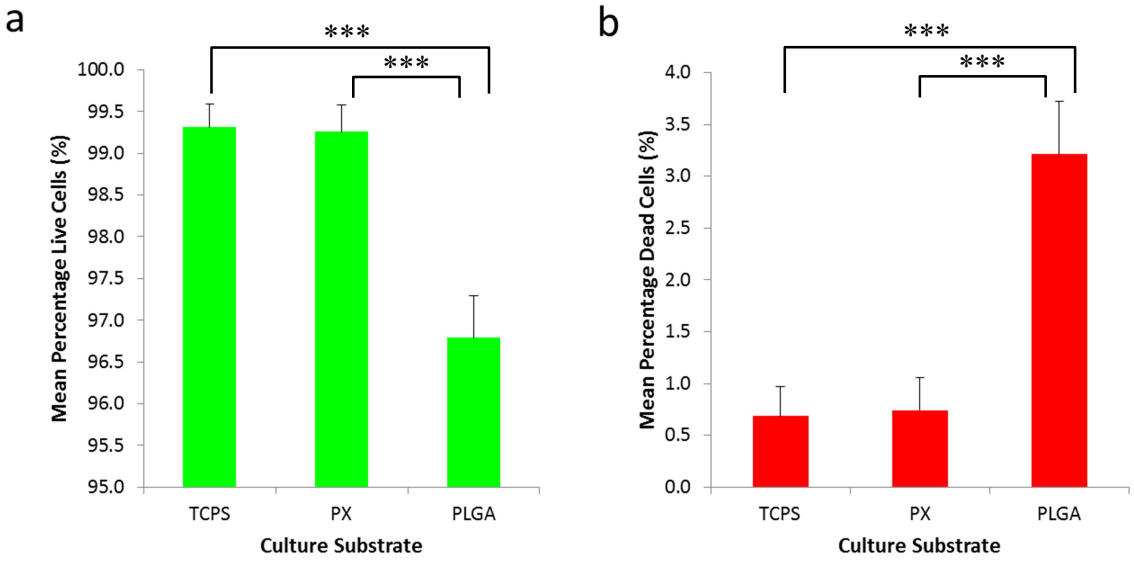

Figure 6.7 Mean percentage live and dead MG63 cells seeded on different culture substrates after 48 hr culture. Statistical analyses were by way of a one-way ANOVA with Tukey's post hoc tests. (**a**) Mean percentage live cells; (**b**) mean percentage dead cells. Error bars = + 1 SE; n = 3; *** = $p < 0.001$. Mean percentage live and dead cells on TCPS and PX were found to be statistically significantly different to PLGA ($p < 0.001$), but were not found to be significantly different from each other ($p > 0.05$).

A comparative analysis between mean percentage live and dead B13 and MG63 cells on the different culture substrates is shown in **Figure 6.8**. Statistical analysis using an independent samples Student's t-test suggested that there was no significant difference between the two cell lines with regards to their mean percentage live and dead cells on TCPS and PX membranes. However, a small significant difference was found between the two cell lines when culturing on PLGA, suggesting that B13 cells have a greater proportion of live cells compared to MG63 cells when both are cultured on PLGA membranes. The increased error bars of both PLGA cultures compared to TCPS and PX suggest an increased variability in cell viability on the surface of PLGA membranes compared to TCPS and PX.

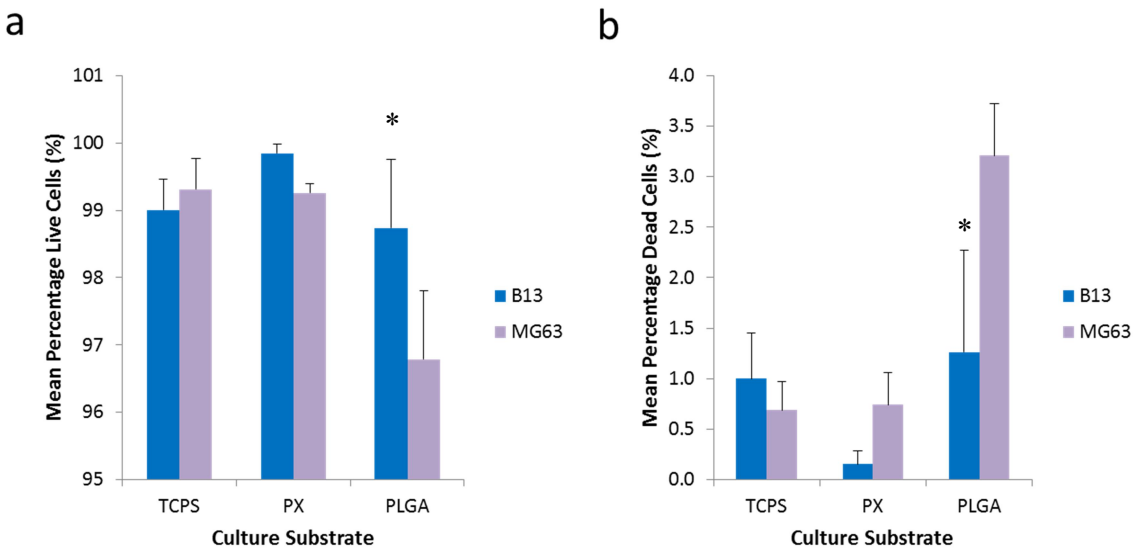

Figure 6.8 Comparison between mean percentage live and dead B13 and MG63 cells seeded on different culture substrates after 48 hr culture. Statistical analyses between cell lines were by way of independent samples Student t-tests for each substrate. (**a**) Mean percentage live cells; (**b**) mean percentage dead cells. Error bars = + 1 SE; n = 3; * = p = 0.05. B13 and MG63 cells appeared to show a small significant difference between their live and dead cells on PLGA. No significant differences were found between live and dead B13 and MG63 cells cultured on TCPS and PX.

A second, quantifiable method for assessing cell death was sought to compare with the results previously obtained through visual quantification. Initial experiments looked at the utility of measuring the release of the cytosolic enzyme lactate dehydrogenase (LDH) into the culture medium. LDH is released upon damage to the cell membrane, a signifier of cell death. The assay utilises a colorimetric approach to measure absorbance from the formation of a red formazan product in the culture medium. This is directly proportional to the LDH content in the culture medium. Percentage cytotoxicity is then reported based on comparison of the measured LDH content against the maximum LDH content determined from whole culture lysis.

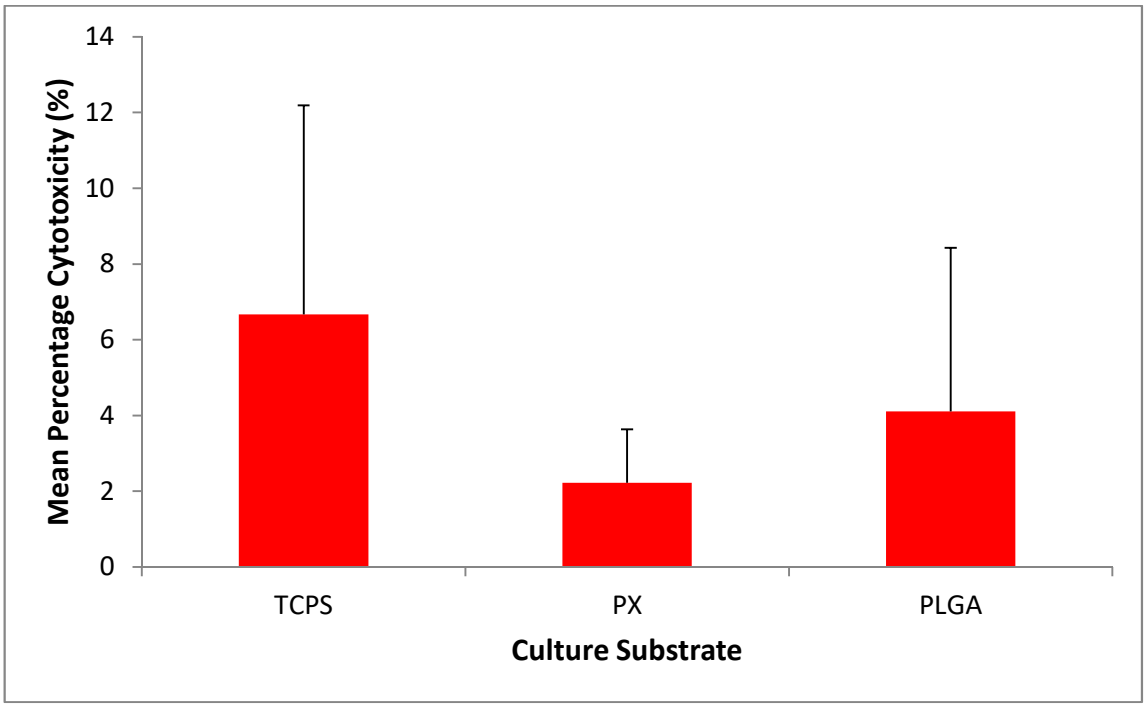

Figure 6.9 Mean percentage cytotoxicity based on LDH release from MG63 cells seeded on different culture substrates after 48 hr culture. Statistical analysis was by a one-way ANOVA with Tukey's post hoc tests. Error bars = + 1 SE; n = 3; $p > 0.05$. No significant differences in cytotoxicity were found between the culture substrates.

Initial experiments utilising the MG63 cell line for LDH release analysis are shown in **Figure 6.9**. The results obtained here suggested that the cells cultured on the PX membrane had the lowest incidence of LDH present in the culture medium, followed by PLGA. In contrast to the results obtained from the live/dead stain, TCPS had the highest incidence of LDH release. Despite this, statistical analysis found that there was no significant difference between LDH release in the cultures on all different substrates as expected from the large error bars.

However, initial experiments utilising this assay on the B13 cell line were unable to quantify the mean percentage cytotoxicity in these cultures. This was due to the presence of large background interference measured in the culture media, which confounded subsequent calculation of the mean percentage cytotoxicity. Further analyses with no-cell cultures suggested that the composition of the culture medium may be the causative agent (data not shown). In addition, this may also account for the larger standard errors from the means as shown for the MG63 analysis.

6.2.3 Transdifferentiation of pancreatic cells to hepatocyte-like cells on PX membranes

The ideal biomaterial should be able to facilitate good cell adhesion to the biomaterial surface and support stable cell viability within the culture. **Sections 6.2.1** and **6.2.2** established the ability of PX membranes to support cell adhesion and promote cell viability in two different cell lines at a level comparable to TCPS.

Furthermore, the ability of a cell to differentiate or transdifferentiate into a different cell type can be affected by the characteristics of the scaffold material it is cultured upon. Therefore, the aim of this part of the Chapter is to establish whether the B13 cell line can be induced to transdifferentiate to HLCs on PX membranes and determine their functional capability compared to TCPS and PLGA membranes.

Immunofluorescent staining for protein expression of pancreatic and hepatic markers was used to visualise B13 cells cultured on PX membranes that had been treated with the Dex + OSM transdifferentiation medium for 14 days. Cultures on glass coverslips were used as a phenotypic control. **Figure 6.10** shows immunofluorescent staining for the pancreatic marker amylase in B13 cells. Untreated B13 cells cultured on PX membranes presented with cells on the culture surface that were positive for amylase expression, similar to the untreated B13 cells cultured on glass coverslips. After treatment with Dex + OSM for 14 days, the cells appeared to have taken on a flattened, enlarged morphology on both substrates, similar to that previously reported in B13 transdifferentiation to HLCs. Furthermore, amylase expression was largely absent in these treated cells.

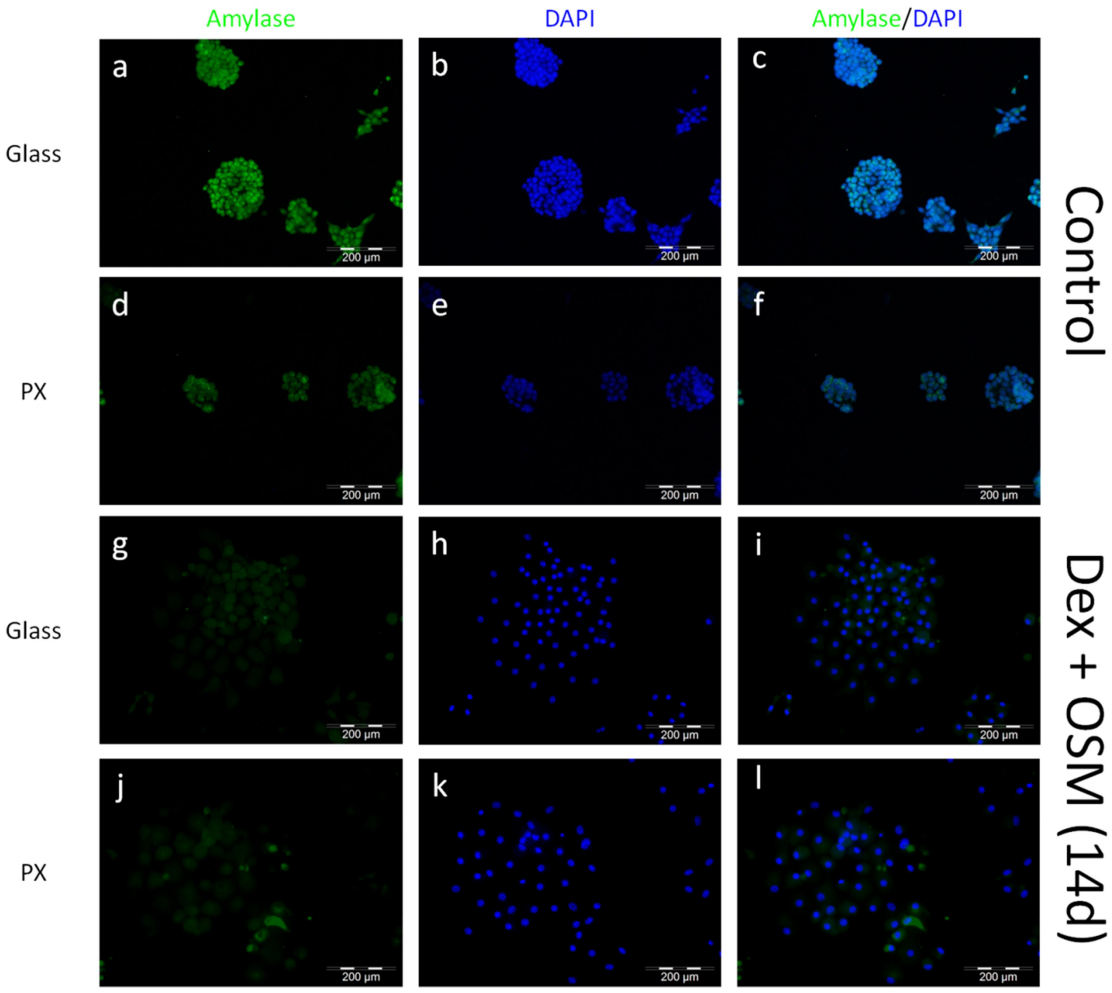

Figure 6.10 Expression of the pancreatic marker amylase in B13 cells cultured on different culture substrates for 14 days. Cells were cultured on glass coverslips or PX membranes and treated with the Dex + OSM transdifferentiation culture medium for 14 days. Controls were fixed after 4 days. Cells were stained for the pancreatic marker amylase (green) and nuclei stained with DAPI (blue). (**a – b**; **g - i**) Glass; (**d – f**; **j - l**) PX. Images (**c**), (**f**), (**i**) and (**l**) are composites of (**a** & **b**), (**d** & **e**), (**g** & **h**) and (**j** & **k**) respectively. Scale bar = 200 µm. Untreated B13 controls displayed amylase expression on both substrates. Dex + OSM treated cells on both substrates showed morphologically flattened cells with comparatively weak to absent amylase expression.

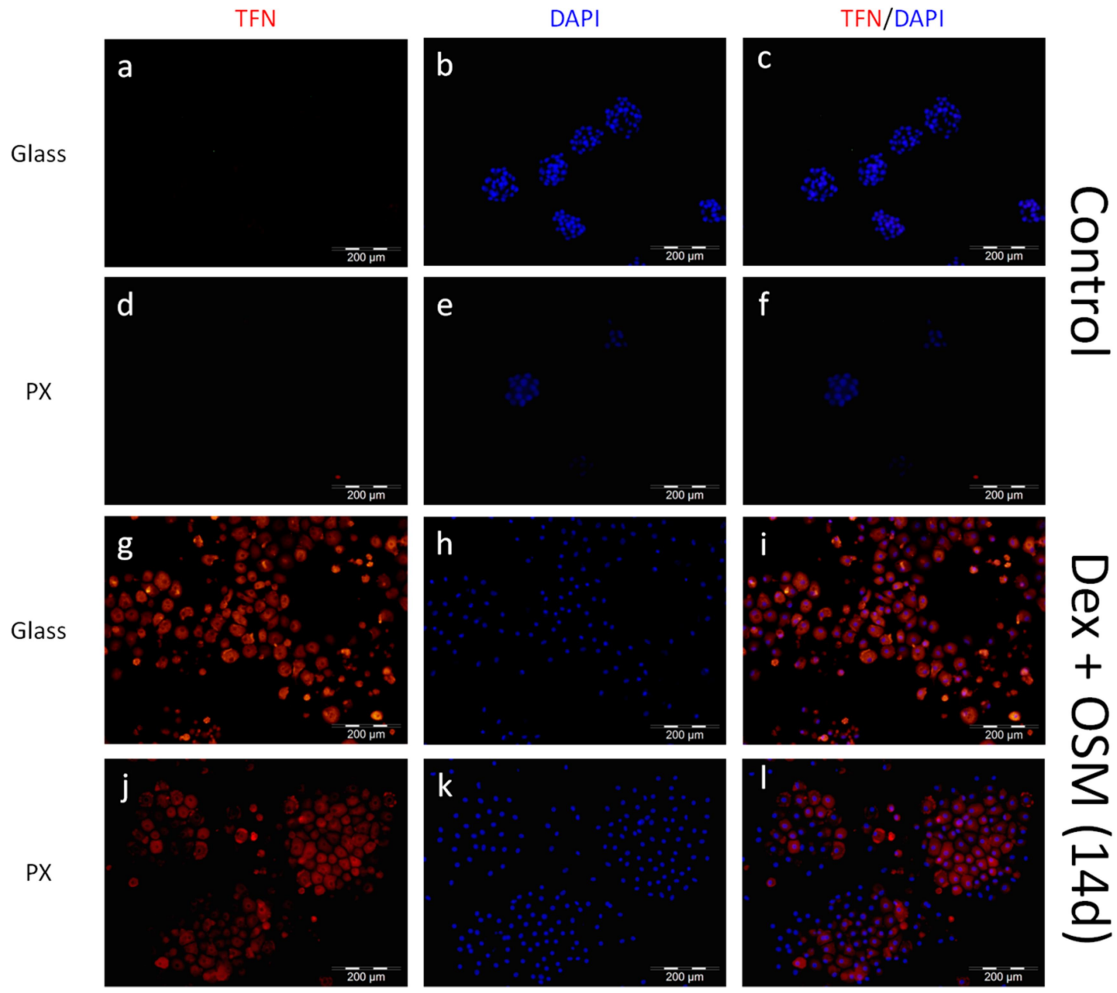

Figure 6.11 Expression of the hepatic transporter protein TFN in B13 cells cultured on different culture substrates for 14 days. Cells were cultured either on glass coverslips or PX membranes and treated with the Dex + OSM transdifferentiation culture medium for 14 days. Controls were fixed after 4 days. Cells were stained for the hepatic transporter protein TFN (red) and nuclei stained with DAPI (blue). (**a – b**; **g - i**) Glass; (**d – f**; **j - l**) PX. Images (**c**), (**f**), (**i**) and (**l**) are composites of (**a** & **b**), (**d** & **e**), (**g** & **h**) and (**j** & **k**) respectively. Scale bar = 200 µm. TFN was absent from the control cultures. Dex + OSM treated cells had an enlarged, flattened morphology and demonstrated expression of TFN on both substrates.

To assess the presence of hepatic markers, immunofluorescent staining was used to look at expression of the hepatic transporter protein TFN in both cultures (**Figure 6.11**). Expression of TFN was absent in the untreated B13 controls on both glass coverslips and the PX membrane. However, after 14 days of Dex + OSM treatment, TFN expression was clearly apparent in cells presenting with the flattened, enlarged morphology on both culture substrates.

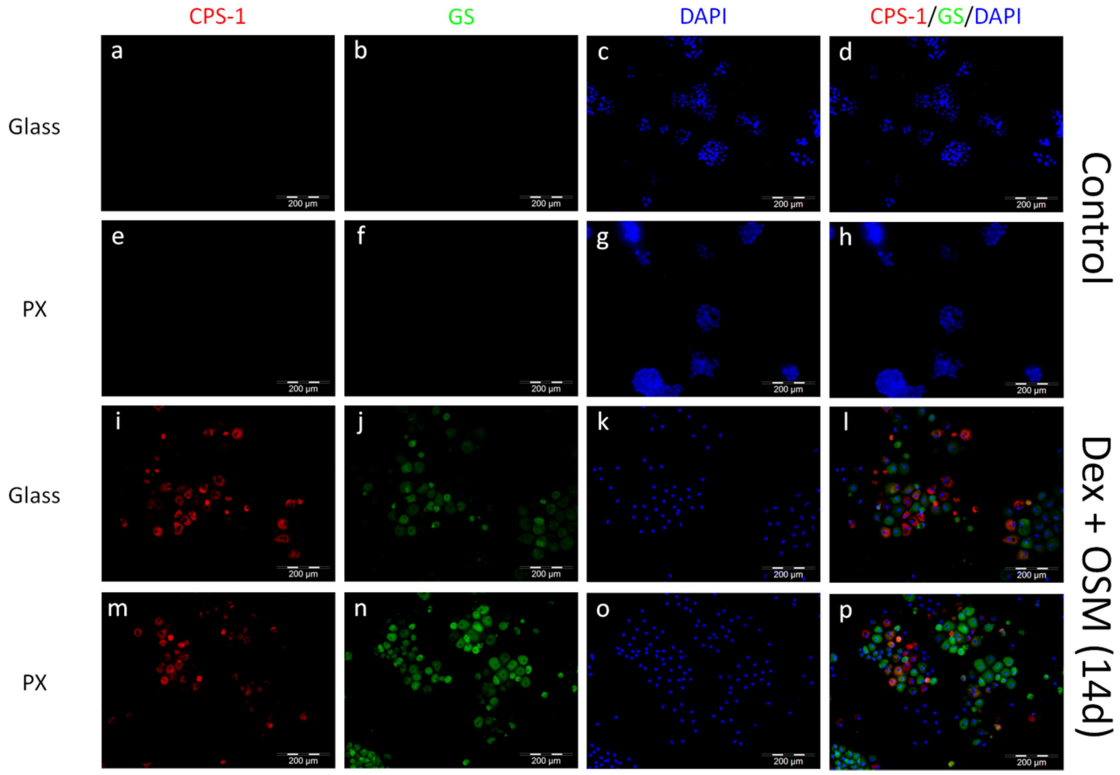

Figure 6.12 Expression of the ammonia detoxifying enzymes GS and CPS-1 in B13 cells cultured on different culture substrates for 14 days. Cells were cultured either on glass coverslips or PX membranes and treated with the Dex + OSM transdifferentiation culture medium for 14 days. Controls were fixed after 4 days. Cells were stained for the ammonia detoxifying enzymes CPS-1 (red) and GS (green). Nuclei were stained with DAPI (blue). (**a – d**; **i - l**) Glass; (**e – h**; **m - p**) PX. Images (**d**), (**h**), (**l**) and (**p**) are composites of (**a - c**), (**e - g**), (**i - k**) and (**m - o**) respectively. Scale bar = 200 µm. GS and CPS-1 were absent from the control cultures. Dex + OSM treated cells had an enlarged, flattened morphology and demonstrated expression of GS and CPS-1 on both substrates.

Protein expression of the ammonia detoxifying enzymes GS and CPS-1 is shown in **Figure 6.12**. Similarly to the expression of TFN, GS and CPS-1 expression is only present in the Dex + OSM treated cells cultured on both substrates, with staining positive in the flattened cells only. The control cultures were both negative for GS and CPS-1 expression, regardless of culture substrate.

As PX membranes appeared to be able to support induction of transdifferentiation of B13 cells to HLCs, further analysis was performed to gain a better understanding of the functional capability of HLCs cultured on PX membranes. Here, the secretion of serum albumin was compared between B13 cells induced to transdifferentiate on TCPS, PX and

PLGA membranes after 14 days of culture. Serum albumin was then quantified over a 24 hr period using a rat albumin ELISA as previously described (**Section 3.9.2**) and reported as mean serum albumin content per million cells over 24 hr.

Serum albumin secretion was not detected from B13 cell controls seeded on TCPS, PX and PLGA that were not treated with Dex + OSM. In contrast, detectable serum albumin was found in the Dex + OSM treated cultures (**Figure 6.13**).

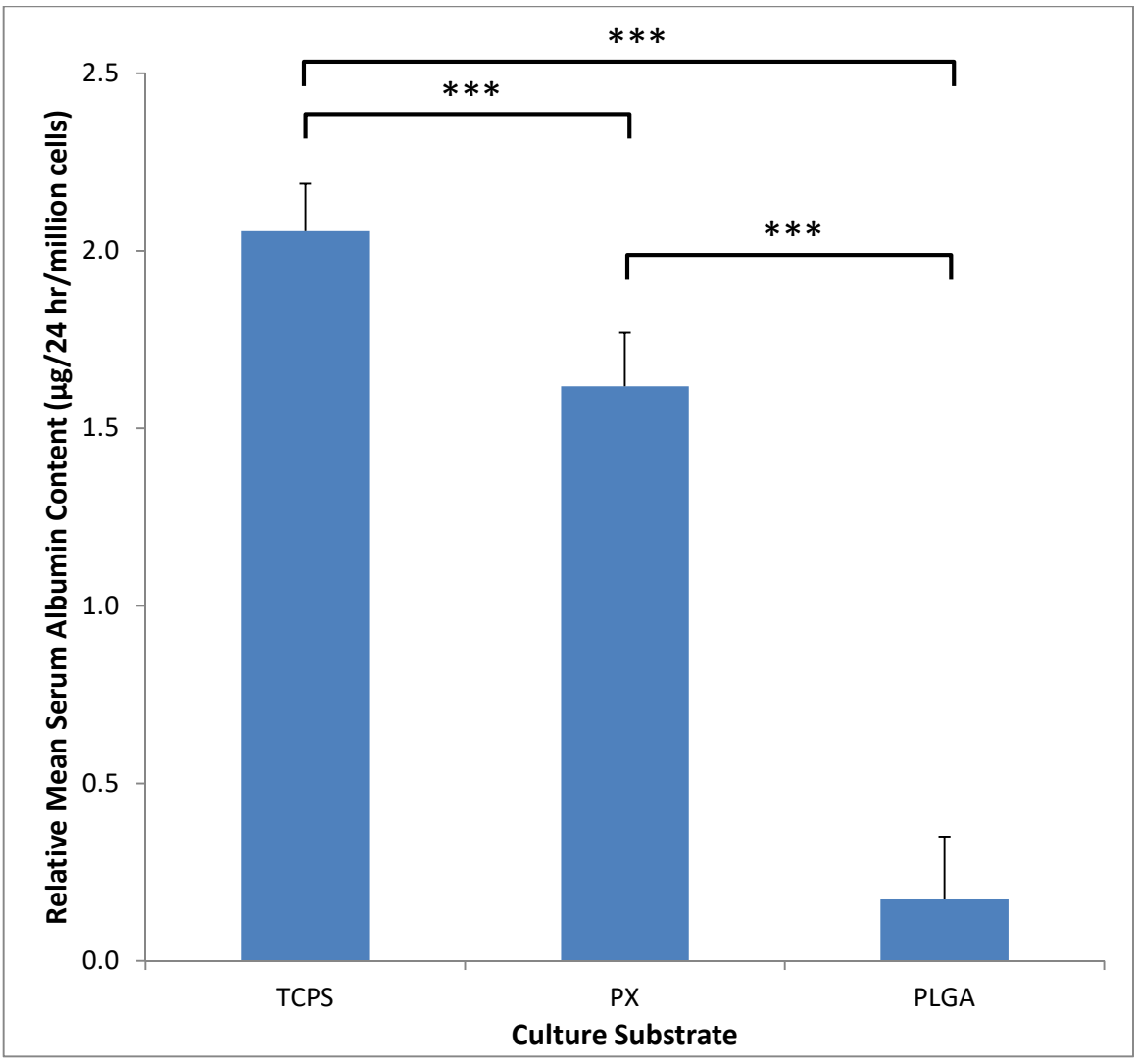

Figure 6.13 Relative mean secreted serum albumin content over 24 hr from B13 cells treated with Dex + OSM on different culture substrates for 14 days. Data were normalised per million cells and is representative of three independent experiments. Statistical analysis was by a one-way ANOVA with Tukey's post-hoc tests. Error bars = + 1 SE; n = 3; *** = $p < 0.001$.

Figure 6.13 shows the relative mean serum albumin content of Dex + OSM treated B13 cells cultured on different substrates. Dex + OSM treated cells on TCPS had the highest

mean serum albumin secretion, followed by cells treated on PX, which had a secretion efficacy of over 75% of the TCPS culture. In contrast, Dex + OSM treated cells on PLGA had far lower mean serum albumin content than the other two biomaterial surfaces.

Statistical analyses comparing the Dex + OSM treated cultures to each other found that the content on TCPS was significantly higher than both PX and PLGA ($p < 0.001$). The increased albumin content of PX compared to PLGA was also found to be significantly higher ($p < 0.001$).

Further analyses comparing untreated B13 cells to their Dex + OSM treated counterparts on each substrate was done by independent samples Student's t-test. The increased serum albumin secretion in Dex + OSM treated cells on TCPS and PX was both found to be significantly different ($p < 0.001$) compared to the control cells on those substrates. However, the albumin secretion from Dex + OSM treated cells on PLGA was not found to be significantly different from the untreated culture on PLGA ($p > 0.05$).

6.2.4 Characterisation of PX and PLGA membrane bulk under transdifferentiation culture conditions

A structurally stable culture scaffold is a necessity for tissue culture. A culture scaffold that is fit for purpose should be able to support a culture for as long as required. Although B13 cells seeded on PLGA membranes have previously been shown to be able to attach to the culture surface after 6 hr and have good viability after 48 hr of culture, it was observed in the 14 day transdifferentiation cultures on PLGA that serum albumin secretion from B13 cells treated with Dex + OSM on PLGA membranes were found to be greatly reduced relative to cultures on TCPS and PX membranes and not significantly different from untreated B13 cells on PLGA.

Visually, at the end of the transdifferentiation culture period, PLGA membranes appeared to show deformity in structure. **Figure 6.14** shows a representative image of a PLGA membrane fixed within the bioreactor after 15 days in culture, alongside a PX membrane used for culture at the same time. The available culture surface area on the PLGA membrane appears to have receded from the edge of the well. In comparison, the PX

membrane has shown no visible change in size and remains covering the bottom of the well.

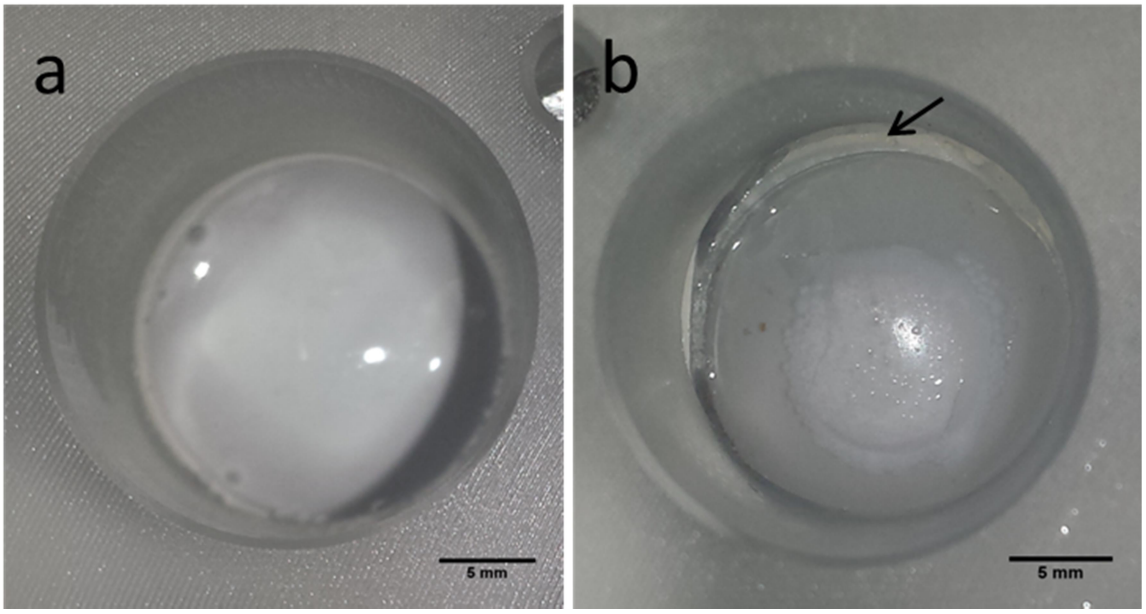

Figure 6.14 PX and PLGA membrane macrostructures after 14 days under transdifferentiation culture conditions. (**a**) PX membrane; (**b**) PLGA membrane. Black arrow shows receding edge of the PLGA membrane, a feature absent in the PX membrane. Scale bar = 5 mm.

Further experiments were performed to examine whether the transdifferentiation culture conditions alone could contribute to a change in membrane bulk in both PX and PLGA membranes in the absence of cells. To address this, 22 x 22 mm square samples of PX and PLGA membranes were sterilised over 24 hr at 4˚C with 1% (v/v) antibiotic-antimycotic as previously described (**Section 3.6.1**) in standard TCPS 6-well plates. After sterilisation, the membranes were gently washed with sterile PBS and complete B13 culture medium was added, ensuring that the membrane surface was completely covered by the culture medium. The samples were then incubated for 24 hr at 37˚C, before the medium was then changed to the Dex + OSM culture medium for the following 14 days. Therefore, membranes were under culture conditions for a total of 15 days.

Membranes were measured for dimensions (length, width and depth) using a micrometer and weighed before undergoing the sterilisation process and subsequent incubation. Measurements were taken at the culture time points of 3 days, 8 days and 15 days after the membrane had been removed from the culture medium, washed carefully with PBS and

dried using a desiccator to eliminate residual moisture mass. Further to this, each time point was compared to the pre-culture dimensions and mass of the membrane and the mean percentage change calculated.

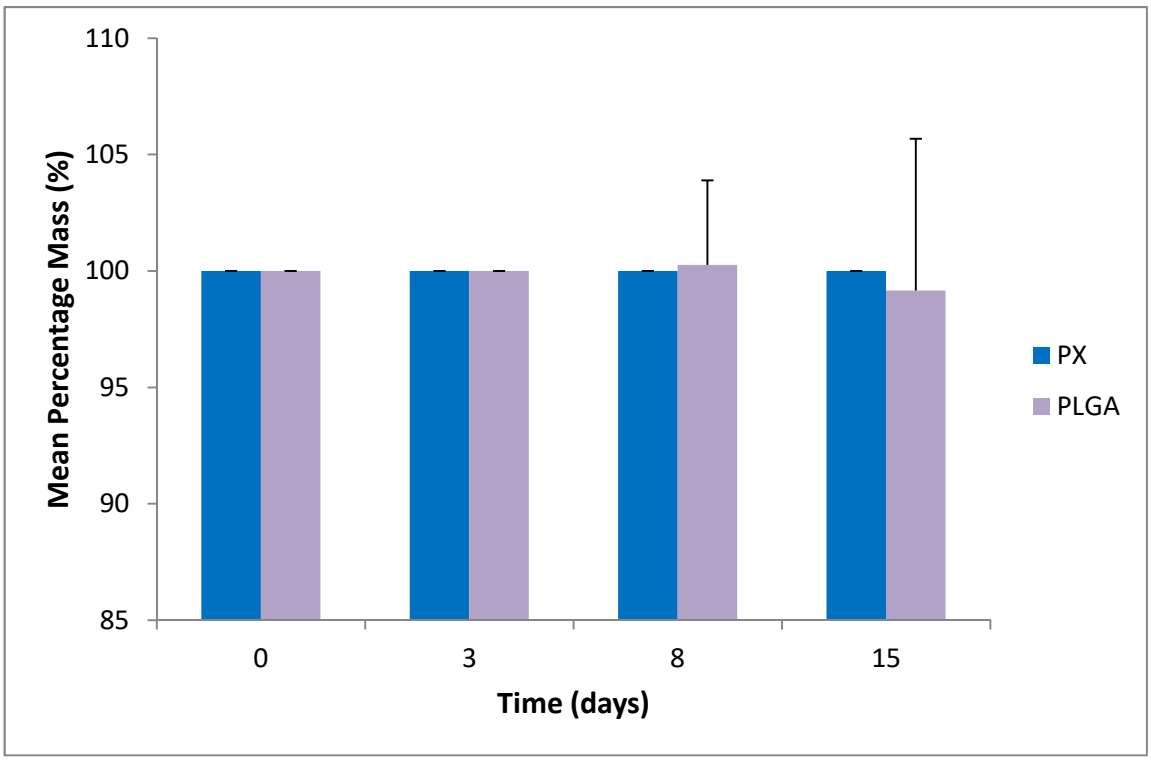

Figure 6.15 Mean percentage change of mass of PX and PLGA membranes under B13 transdifferentiation culture conditions without cells at 3, 8 and 15 days. PX and PLGA membranes were prepared for undergoing the culture conditions for transdifferentiation of B13 cells to HLCs and incubated for 3, 8 and 15 days with the transdifferentiation culture medium at 37˚C in 5% CO_2. Membranes were weighed at the specified time point and compared to the original membrane mass prior to entering culture conditions and the mean percentage change of mass calculated. Statistical analysis was by a one-way ANOVA with Tukey's post hoc tests for comparing within membranes and with independent samples Student's t-tests for comparing between membranes at the same time point. Error bars are for PLGA only as PX membranes showed no change in mass at any time point. Error bars ± 1 SE; n = 3; $p > 0.05$. No significant differences in mass were found between membranes or between time points.

Comparison of PX and PLGA membrane mass demonstrated that there was negligible change in mass between the lengths of incubation and also prior to undergoing transdifferentiation culture conditions (**Figure 6.15**). PX membranes in particular showed no change at all in mass comparing prior to incubation with each time point. PLGA

membranes showed a minor reduction in mass although this was deemed to be not statistically significant ($p > 0.05$).

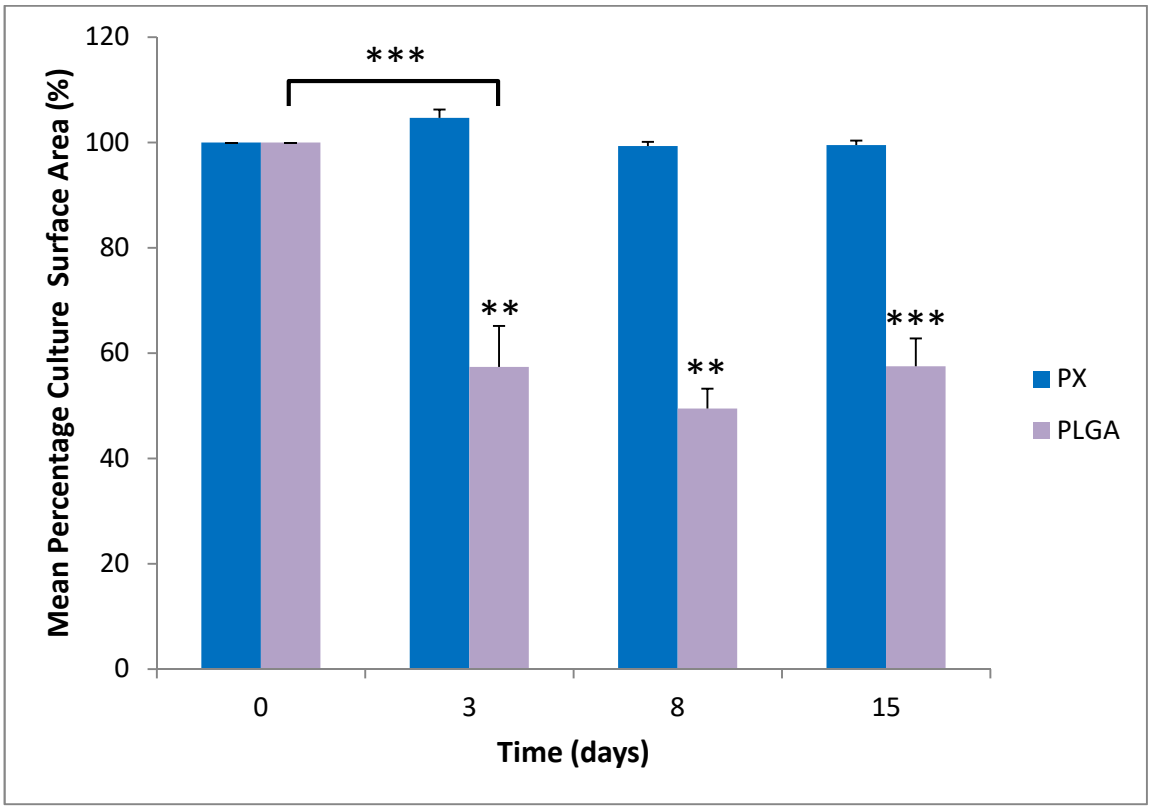

Figure 6.16 Mean percentage available culture surface area of PX and PLGA membranes under B13 transdifferentiation culture conditions without cells at 3, 8 and 15 days. PX and PLGA membranes were prepared for undergoing the culture conditions for transdifferentiation of B13 cells to HLCs and incubated for 3, 8 and 15 days with the transdifferentiation culture medium at 37˚C in 5% CO_2. Membrane culture surface area was measured at the specified time point and compared to the original membrane surface area prior to entering culture conditions and the mean percentage change of surface area calculated. Statistical analysis was by a one-way ANOVA with Tukey's post hoc tests for comparing within membranes and with independent samples Student's t-tests for comparing between membranes at the same time point. Error bars = + 1 SE; n = 3; ** = $p < 0.01$; *** = $p < 0.001$. PLGA membranes displayed a significant reduction in culture surface area after 3 days incubation.

Despite finding no significant changes in mass within the culture conditions for either polymer membrane, as mentioned previously it was observed visually that the PLGA membranes appeared to have undergone physical deformation, appearing smaller in size than what was seen prior to entering culture conditions. Therefore, the available culture surface area was also measured at each time point and compared. Comparisons of available

culture surface areas at different time points for each membrane type is shown in **Figure 6.16**.

PX membranes did not display a significant variation in culture surface area during any time point of the culture period ($p > 0.05$). PLGA membranes, in contrast, appeared to have lost approximately 40% of the original available culture surface area after 3 days in culture. Statistical analysis was able to confirm that after 3 days under culture conditions, the decrease in PLGA membrane culture surface area was a significant difference ($p < 0.001$). However, beyond this time point, there was no further significant change in PLGA membrane culture surface area the longer the incubation time ($p > 0.05$).

Comparisons between PX and PLGA membranes demonstrated that the reductions in PLGA membrane surface area compared to PX membranes at the same time point were also statistically significant differences – 3 days ($p < 0.01$); 8 days ($p < 0.01$) and 15 days ($p < 0.001$).

6.3 Discussion

The research aims for this Chapter were to investigate the biocompatibility of PX flat sheet membranes developed in **Chapter 4**, to determine if the biomaterial is suitable for tissue culture. Characterisation of PX membranes was studied through comparison with established biomaterials – TCPS and PLGA. Cell attachment and viability of two different cell lines (B13 and MG63) were assessed as well as the utility of the pancreatic B13 cell line to transdifferentiate to HLCs on PX membranes. Furthermore, the effects of transdifferentiation culture conditions without cells on the physical structures of PX and PLGA membranes were also examined.

6.3.1 Attachment of B13 and MG63 cell lines to PX membranes

For adherent cell culture, it is important to ensure that the biomaterial of choice provides a suitable environment for anchorage dependent interactions to occur. The phase inversion PS membranes initially developed in **Chapter 4** possessed a hydrophobic surface. Hydrophobicity is a trait that has previously been shown to not encourage attachment of cells to biomaterial surfaces [168,183,192,193]. Furthermore, in HFB for tissue

engineering applications, a more hydrophilic surface encourages hydraulic permeability and greater transfer of nutrients through the membrane wall [168]. Therefore, additional surface treatment by way of oxygen plasma exposure modification to alter the membrane surface chemistry was utilised. This was found to reduce hydrophobicity of the membrane surface to create a scaffold more conducive for adherent cell culture (PX membranes). In addition, different cell lines may favour various combinations of biomaterial characteristics over others with regards to attachment, viability and functional capacity. A greater quantity of cells adhering to biomaterial surfaces will facilitate cell spreading and subsequent proliferation and differentiation. For tissue engineering purposes, this feature is positive for producing large batches of cells quickly [171].

Both the B13 and MG63 cells attached to both PS and PX membranes after 6 hr. However, there were noticeable differences in the overall numbers attached. PX membranes were found to have significantly higher cell attachment than PS membranes. This suggested that the addition of oxygen functional groups to the membrane surface via the oxygen plasma surface treatment was successful in encouraging a greater number of cells to attach through the reduction in surface hydrophobicity. This behaviour is consistent with previous cell studies on oxygen plasma treated PS films with human foetal osteoblastic cells, mouse fibroblast cells and human umbilical vein endothelial cells [203,209,210].

With regards to the B13 cell line, the numbers of cells attached to the PX membrane was found to be comparable to TCPS with nearly all the seeded cells attached to the membrane surface. Notably, cell attachment on phase inversion PLGA membranes was lower than both TCPS and PX, and found to be comparable to that of untreated PS membranes. This suggests that the PX biomaterial possesses a more favourable attachment surface than PLGA membranes in the case of the B13 cell line, particularly as PLGA is a hydrophobic polymer [193].

The MG63 cell line similarly showed low cell attachment on untreated PS membranes. However, PX membranes showed reduced attachment of MG63 cells compared to TCPS, although this was not a statistically significant reduction. MG63 cells cultured on PLGA membranes also appeared to show attachment comparable to that of PX membranes. This observation is in contrast with B13 cell attachment, which overall, had higher attachment than MG63 cells on all substrates bar PS membranes. These differences in attachment behaviour suggest a degree of variation between cell lines in how suitable a particular

biomaterial is for purpose. For example, a previous study by Ellis and Chaudhuri utilising primary human bone derived cells demonstrated that PLGA flat sheet membranes with a similar lactide:glycolide ratio (72:25) had comparable attachment to TCPS within the first 6 hr [171]. This contrasts the results shown here for both cell lines on PLGA. It is possible that additional factors beyond surface chemistry, such as membrane surface roughness, may also influence adsorption and folding of adhesion proteins on to the biomaterial surface, the result of which may favour one cell type over another [261]. Indeed, phase inversion PLGA membranes have previously been shown to possess a rough surface morphology visible under SEM [171,175,260,262].

These results suggest that the oxygen plasma surface treated PX membranes were successful in improving cell attachment of both B13 and MG63 cells compared to untreated PS membranes. PX membranes have an attachment capacity comparable to TCPS for B13 cells, which is a positive attribute for utilising this biomaterial for transdifferentiation to HLCs. Furthermore, this biomaterial is also able to support attachment of MG63 cells, albeit at a reduced efficiency. However, to expand and explore the scope of PX membranes with regards to other cell lines and aid future development, a further point of investigation could be to examine the effects of surface roughness and substrate stiffness between the different culture substrates with regards to improving cell attachment, as well as the study of other cell lines originating from different tissues. Additional surface treatments on the membrane, such as increasing oxygen plasma treatment time and power beyond that utilised in this thesis, could be assessed for any subsequent changes in surface morphology through SEM and surface roughness and substrate stiffness by AFM. Cell attachment of different cell lines originating from different tissues could then be assessed in comparison with untreated PX membranes. The effect of substrate stiffness on different cell types could be further assessed through measurement of cell spreading area on the membrane surface as an indicator of adhesion strength and type, particularly as stiffness is a factor involved in efficacy of attachment, proliferation and differentiation, especially with regards to how the substrate stiffness relates to the environment of native tissue [254].

6.3.2 Viability of B13 and MG63 cell lines on PX membranes

Given the low cell attachment of PS membranes compared to PX membranes, further studies into B13 and MG63 cell viability were performed only on TCPS, PX and PLGA membranes. This was done primarily through comparative analysis of calcein AM metabolism of live cells and binding of ethidium homodimer-1 to nucleic acids in dead cells.

After 48 hr of culture both B13 and MG63 cells were shown to be attached to all culture substrates. Furthermore, the cells showed excellent viability with metabolically active cells and very low numbers of dead cells. No infection was detected on the polymer substrates, suggesting that treatment with the antibiotic-antimycotic solution previously recommended for sterilising PLGA membranes prior to culture is also a suitable treatment for sterilisation of PX membranes [175].

Notably, MG63 cells cultured on PLGA membranes appeared to have a significantly higher percentage of dead cells than those found on TCPS and PX. B13 cells also showed a slight increase in the numbers of dead cells on PLGA although this was not deemed statistically significant. The hydrophobic nature of PLGA may have influenced this behaviour, as a previous study by Chang et al reported that culturing MG63 cells on a hydrophobic surface demonstrated lower proliferative capacity and enhanced apoptotic behaviour at 48 hr when compared to a hydrophilic surface. This behaviour was observed to be due to reduced cell adhesion and subsequent spreading on the culture surface, causing insufficient activation of the Ras pathway by fibroblast growth factor-1 (FGF-1) [263]. The Ras pathway is involved in modulating the cell cycle and also rearrangement of the actin cytoskeleton [263–265]. In contrast to the PLGA utilised in this Chapter, the study by Chang et al utilised hydrophobic PS as an experimental substrate. Although the PLGA used in this Chapter is hydrophobic due to the lactide majority within the polymer, the glycolide contained within the polymer is hydrophilic [171]. This factor may reduce the hydrophobicity of the culture substrate beyond that utilised in the study by Chang et al and hence comparatively lessen the detrimental effects of PLGA surface wettability on the MG63 cells. Given the reduced PLGA attachment and viability seen with B13 cells, examination of these signalling factors with this cell line on PLGA may be a further point of investigation by comparing apoptotic behaviour with activation of Ras from initial attachment and proliferation over time.

Further analysis of cell viability was attempted by examining LDH release into the culture medium after 48 hr. LDH is released when there is damage to the cell membrane – a signifier of cell death. However, although it was possible to calculate release for MG63 cells, which were found to have low cytotoxicity, this was not possible for B13 cells. It was found that experimental sample measurements being measured as lower or identical to the spontaneous LDH release control, thus confounding calculation of percentage cytotoxicity. Although this may suggest very low or negligible cytotoxicity in B13 cells to the extent of being identical to the spontaneous LDH release control, which would agree with the results obtained by calcein AM and ethidium homodimer-1 analyses, it was also found that the FBS utilised in the cell culture medium gave a very high background which may have interfered with the controls. Notably, this effect was reduced in the MG63 cultures.

It is posited that as the MG63 culture medium utilised heat inactivated FBS, this factor may have reduced the confounding background effect seen in the B13 cells, which used non-heat inactivated FBS. A study by Thomas et al in 2015 showed a 50% reduction in background when using heat inactivated FBS as part of the culture medium used in the LDH assay [266]. A potential solution would be to switch to serum-free medium to quantify LDH release over 48 hr to completely avoid the background effect, although this may increase loss of viability in B13 cells as previously described in **Chapter 5**. Reduction of FBS may also avoid issues with too much background, although a different solution would be to utilise a method that is largely unaffected by the contents of the culture medium, such as the colorimetric resazurin assay alamarBlue.

Therefore, these results have shown that at 48 hr, B13 and MG63 cells cultured on PX membranes have good viability that is comparable with TCPS. Cultures on PLGA were also found to be viable. Although the studies in this Chapter found high overall viability in all cell lines on all substrates, this was only assessed up to 48 hr. Therefore, extending the culture period beyond 48 hr for proliferative and viability studies would help establish whether there is similar behaviour as reported here for both cell lines. Also, additional methods for assessing apoptotic behaviour could help gain a better understanding of changes in cell viability, such as staining with annexin V. This method detects phosphatidylserines that appear on the membrane surface in early apoptosis. As positive staining for ethidium homodimer-1 and release of LDH are factors indicative of loss of

membrane integrity which occurs later in apoptosis and therefore may not have been fully assessed in the time frame examined here, annexin V would be able to detect apoptotic behaviour in cells at an earlier time point [267].

6.3.3 Transdifferentiation of the B13 cell line to HLCs on PX membranes

Previously, the work in **Chapter 5** had demonstrated the greater efficiency of the Dex + OSM transdifferentiation culture medium to induce conversion of the B13 cell line to HLCs over solely using Dex as the inducing agent.

Here, treatment of B13 cells with Dex + OSM on PX membranes over 14 days induced transdifferentiation towards a hepatic phenotype. There was a distinct loss of the pancreatic phenotype shown through loss of expression of the pancreatic marker amylase replicating that observed on glass. Furthermore, expression of the hepatic markers TFN, CPS-1 and GS were found to be induced in the Dex + OSM treated cultures and not the untreated samples on all culture substrates. This is a significant observation as firstly, it shows that the loss of pancreatic phenotype coincides with induction of hepatic markers as previously described in the literature [130,131]; but secondly, the culturing of B13 cells on PX membranes in complete B13 culture medium alone does not induce transdifferentiation of B13 cells to HLCs. Therefore, this suggests that PX membranes can be utilised for homogenous cell expansion, and with the right treatment conditions, potentially be used to support the differentiation of one cell type to another as displayed here. However, it is not possible to fully ascertain the degree of transdifferentiation between the two substrates from the immunofluorescent staining alone. Examination of induction of hepatic markers and quantification of functional markers over time would be able to determine if the different cultures reach similar levels of transdifferentiation at the same time points.

Notably, the transdifferentiated HLCs cultured on PX membranes were also able to demonstrate functional capability of secreting serum albumin into the culture medium, with none detected from untreated B13 cells on all substrates. However, the amount secreted was found to be reduced when compared to transdifferentiated HLCs cultured on TCPS. It is possible that this may have been affected by the number of cells attached to the membrane surface, as these are relative albumin quantities. PX displayed a higher overall attached cell number than TCPS (data not shown). It has previously been reported that too

high a cell density can slow the rate of transdifferentiation and expression of hepatic markers [236,237]. Therefore, there is the possibility that there were fewer transdifferentiated HLCs at the right stage of maturity to express and secrete albumin on PX membranes at this time point. Further work will need to examine the transdifferentiation efficacy on PX membranes utilising different initial seeding densities. Although it is apparent that there are HLCs actively secreting albumin on PX membranes, the culture viability at this stage on all substrates is not known. Although the PicoGreen assay is widely utilised in the literature as a method of calculating cell number, a limitation is that it does not discriminate between live or dead cells and therefore quantifies all dsDNA present. Additional comparison with a metabolic assay to quantify viable cell number, such as the MTT assay, would be more informative to equate the albumin secretion results to living cells only.

Notably, relative to reported serum albumin secretion from primary rat hepatocytes cultured on TCPS, the amount secreted from the transdifferentiated HLCs cultured on TCPS is lower by at least 10-fold [96,268,269]. This difference suggests that although transdifferentiated HLCs as previously reported have a similar range of functions to primary rat hepatocytes, the lower level of secretion may reflect a less mature hepatic phenotype in the transdifferentiated HLCs. A comparative culture with primary rat hepatocytes on the different substrates with functional quantification would inform this assessment further. To add further clinical applicability, as the B13 model of transdifferentiation to HLCs can be translated to human pancreatic cells, further study into whether this reduction in albumin secretion would similarly occur when compared to adult primary human hepatocytes would also be useful.

Interestingly, B13 cells induced to transdifferentiate on PLGA membranes showed presence of serum albumin in the culture medium but this was greatly reduced in comparison with the serum albumin secretion of cells cultured on TCPS and PX. This was also accompanied by low overall calculated cell number compared to TCPS and PX. It is possible that the low cell number calculated is due to fewer cells surviving culture on PLGA. As mentioned previously, the measured dsDNA content from the PicoGreen assay does not distinguish between live or dead cells. Measurement of metabolic activity on all culture substrates, such as by the MTT assay, in combination with the calculated cell number would be able to confirm whether cells on PLGA had reduced metabolic activity.

Another possibility is that the reduced serum albumin secretion from cells cultured on PLGA is due to fewer cells undergoing transdifferentiation. Detection of the pancreatic marker amylase through visualisation by immunofluorescence after 14 days of transdifferentiation treatment combined with a quantitative method such as the Phadebas colorimetic assay would confirm whether the pancreatic phenotype is still prevalent in the cells. An additional quantitative hepatic marker assay, such as measurement of cytochrome P450 activity would also further determine the presence of hepatic transdifferentiation alongside the results obtained from serum albumin secretion. Although the serum albumin result here suggests that some cells on PLGA may be able to transdifferentiate to HLCs, the low attachment and functional secretion means that for translating to hollow fibre membrane culture, it is unsuitable. The PX biomaterial would be more suitable as it has displayed improved attachment and functionality compared to PLGA.

Furthermore, PLGA membranes displayed a deformation in structure after the full 15 days of treatment, which was further replicated under no-cell culture conditions. In comparison, PX membranes showed no change in structure. Although PLGA is a biodegradable polymer, no significant change in overall mass was found as significant degradation is reported to occur beyond the time point of these experiments [270]. However, it has been noted in the literature that wetting of PLGA, such as by culture medium, can cause the polymer to plasticise through lowering of its glass transition temperature and effectively shrink [271]. A study by Kim et al showed differences in glass transition temperatures between dry versus wet PLGA (75:25 lactide:glycolide) membranes, ranging from 45.2˚C dry to 37.3˚C wet [262]. As culture conditions are at 37˚C, it is possible that the change in morphology is due to reduction in glass transition temperature. Further viability studies would be useful in determining whether there is a gradual increase in cell death concurrent with changes in topography, contributing to the low overall cell number and function. Changes in culture surface area and topography during the culture period are potentially going to affect the proliferative and differentiation capacities of the cells and produce unwanted heterogeneity in the resultant product. Therefore, based on these results, the PX biomaterial is the optimum choice for translating the transdifferentiation of B13 cells to HLCs to a HFB setting.

6.4 Conclusion

The aim of the research in this Chapter was to investigate the biocompatibility of PX membranes. This was characterised initially through attachment capacity and viability of the rat pancreatic B13 and human osteosarcoma MG63 cells in comparison with TCPS and PLGA, two established biomaterials. PX membranes showed improved cell attachment of both cell lines compared to that of untreated PS membranes, suggesting that the oxygen plasma surface treatment developed in **Chapter 4** was effective. Furthermore, PX membranes were able to support B13 and MG63 cell attachment with good viability after 48 hr. Attachment and viability of B13 and MG63 cells on PX membranes were also found to be comparable to equivalent cultures on TCPS.

PX membranes were also able to support transdifferentiation of the B13 cell line to HLCs with loss of the pancreatic phenotype, induction of hepatic markers and adoption of a flattened, enlarged HLC morphology after 14 days of treatment with Dex + OSM. In addition, the secretion capacity of serum albumin from transdifferentiated HLCs was also retained on PX membranes, although reduced when compared to cultures on TCPS. There was no observed change in PX membrane structure, unlike PLGA membranes which demonstrated distinct deformation.

In conclusion, these results demonstrate that the PX biomaterial is biocompatible, with comparable cell attachment and viability to TCPS and ability to support transdifferentiation of pancreatic cells to HLCs. These results are very encouraging for eventually translating the PX biomaterial to a HFB setting. However, there is scope for further optimisation of PX membrane biocompatibility, such as modification of membrane surface roughness to improve cell attachment, viability and function, particularly with the requirement for a fully porous membrane to facilitate nutrient and waste transfer during cell culture.

Chapter 7
Conclusions and Future Work

7.1 Conclusions

The research in this thesis has focused on the design of a potential interim support therapy for liver failure – the bioartificial liver (BAL) device. The concept of the BAL device is to utilise hepatocytes or hepatocyte-like cells (HLCs) housed within a suitable bioreactor with the purpose of replicating normal liver functions. The purpose of this treatment is to bridge patients with liver failure to transplantation or to aid liver regeneration. Although some BAL device designs have reached clinical trials, none are currently in full clinical use as there is currently no significant difference in patient survival when comparing BAL device therapy with standard medical treatments. The two major challenges to producing a clinically viable BAL device are sourcing suitable hepatocytes or HLCs that can recapitulate *in vivo* hepatocyte functionality; and secondly, providing a suitable culture environment within the bioreactor for the cells to effectively function as hepatocytes or HLCs.

This thesis focused on two main research areas integral to BAL device design – firstly, the development of novel polystyrene (PS) phase inversion membranes to be used as a cell culture scaffold in a hollow fibre bioreactor (HFB) – a bioreactor configuration that resembles the architecture of the physiological liver. Although PS is widely used as a 2D cell culture substrate, it has yet to be reported as a biomaterial for phase inversion hollow fibre membrane cell culture purposes. Secondly, HLCs generated from the transdifferentiation of pancreatic cells were considered as a potential cell source for BAL devices due to their wide hepatic functionality. The culture medium HepatoZYME^{+} was reported to improve the hepatic phenotype in human embryonic and induced pluripotent stem cell differentiation. However, the effect of this culture medium on the transdifferentiation of pancreatic cells to HLCs was not known, and was selected as a potential method of improving upon current transdifferentiation protocols.

Therefore, the core research aims were as follows:

1. To develop and characterise a system for fabricating phase inversion PS membranes suitable for HFB cell culture using a flat sheet membrane model.

2. To improve upon the phenotype of transdifferentiated HLCs by characterising and comparing the HepatoZYME^{+} and "50:50" culture media against established Dex-based transdifferentiation protocols.

3. To characterise and compare the biocompatibility of the developed phase inversion polystyrene membranes with established biomaterials and investigate the utility of transdifferentiating pancreatic cells to HLCs on the developed biomaterial.

Chapter 4 investigated the development of PS flat sheet membranes. Using a PS-NMP polymer-solvent casting dope, it was found that ternary systems utilising either deionised water or 70% (v/v) IMS as nonsolvents were able to cast PS flat sheet membranes, using the phase inversion immersion precipitation method. Both systems yielded asymmetrical membranes with a nonporous top skin layer over a highly porous substructure. This indicated that these ternary systems alone were unable to produce completely porous membranes. Oxygen plasma treatment was identified as a suitable method for increasing PS membrane hydrophilicity. Membranes treated with oxygen plasma were denoted as "PX", to distinguish them from the more hydrophobic untreated PS membranes.

Oxygen plasma treatment with the inductively coupled plasma chamber generated surface pores on 70% (v/v) IMS cast PS membranes only. This change in physical structure is in agreement with the literature where plasma treatment has been utilised to etch material surfaces. However, this observation was not replicated using the capacitively coupled plasma chamber, suggesting that further work may be required to optimise the oxygen plasma treatment method for generating surface pores, such as varying plasma power and exposure time. Additional work into examining the mechanical effects of the plasma treatment method upon the membrane structure and also substrate stiffness would also aid further characterisation of the suitability of the biomaterial as a culture substrate, particularly as substrate stiffness is a factor affecting cultured cell behaviour.

The research in **Chapter 5** examined the utility of the culture media HepatoZYME$^+$ and a diluted variant, "50:50", to induce transdifferentiation of pancreatic B13 cells to HLCs and furthermore maintain the hepatic phenotype. The work here determined that overall, HepatoZYME$^+$ based media was no improvement over Dex-based transdifferentiation media as both an induction and maintenance treatment due to loss of viability. The 50:50 variant similarly showed overall culture deterioration but was able to show some induction of hepatic markers and a change in morphology to a HLC phenotype. Furthermore, 50:50 maintained expression of hepatic markers in cells that had already been induced to transdifferentiate using Dex + OSM at both early and later stages. Importantly, loss of the pancreatic phenotype was maintained after changing from Dex + OSM to HepatoZYME$^+$ based cultures. In addition, secretion of the hepatic protein albumin appeared to be increased beyond that of Dex + OSM treated cells upon changing the culture medium to 50:50. Culture with 50:50 was observed to generate multinucleate cells, although the stability of these cells long term is questionable. Overall, the Dex + OSM treatment was determined to be the optimum transdifferentiation medium for stable induction, maintenance and viability.

The biocompatibility of PX membranes developed using the PS-NMP-water ternary system and treated with oxygen plasma was assessed in **Chapter 6**. Treatment with 1% (v/v) antibiotic-antimycotic was found to be suitable for sterilising PX membranes. The pancreatic B13 and human osteosarcoma MG63 cell lines displayed improved attachment to PX membranes over untreated PS, confirming that the oxygen plasma surface treatment had generated a surface more conducive to cell culture. B13 cell attachment on PX was comparable to that of TCPS and greater than that of PLGA. MG63 cell attachment on PX was comparable to TCPS. After 48 hr culture cell viability was high for both cell lines on TCPS, PX and PLGA.

The B13 cell line retained a pancreatic phenotype when maintained in complete B13 culture medium upon PX membranes. When treated with the Dex + OSM transdifferentiation culture medium, the cells converted to HLCs on PX. These cells demonstrated the utility to secrete serum albumin, although this utility was reduced relative to TCPS. B13 cells induced to transdifferentiate on PLGA membranes showed greatly reduced serum albumin secretion function and overall cell attachment. Furthermore, PLGA

appeared to show signs of plasticising and deformation under transdifferentiation culture conditions, a feature not observed in PX membranes.

In conclusion, the PX membranes developed in this thesis were determined to be the preferential biomaterial for translation to HFB cell culture compared to PLGA and also displayed some comparability with TCPS. Furthermore, as transdifferentiated HLCs showed hepatic functionality on PX membranes, they have the potential to be utilised as a cell source for a BAL device utilising PX hollow fibre membranes.

7.2 Future work

7.2.1 Short term aims

Generation of a porous polystyrene membrane surface

This work has established PX membranes as scaffolds able to support cell culture. For translation of this work to a HFB setting, further optimisation of the membrane structure should be performed to create a porous surface layer, allowing for the mass transfer of nutrients from medium flowing intraluminally to the cells cultured on the fibre surface. The research in **Chapter 4** noted the potential of oxygen plasma as an etching agent. However, this was not found to be a universal effect as it was only observed when using the inductively coupled plasma chamber with the PS-NMP-70% (v/v) IMS ternary system. Therefore, further optimisation of the plasma treatment method as a physical surface modifier may be performed by comparing the effects of different plasma generation methods, power and time exposure with regards to their effects upon membrane structure, surface chemistry and wettability. One approach would be to investigate additional plasmas to treat the membrane surface. Argon and nitrogen plasmas have been utilised to etch polymer surfaces as well as modify the surface wettability for cell culture [184,201,209]. Further work would be required to assess whether differences in surface chemistry from utilising different plasmas or a combination of plasmas will affect overall biocompatibility due to addition of different functional groups compared to oxygen plasma treatment, such as C=N. From a process point of view, a single method that can affect surface wettability, chemistry and morphology would be ideal. However, with this

approach, finding a balance between wettability, biocompatibility and issues with overexposure causing bulk weakening of the overall membrane structure will require careful optimisation.

Another potential method of increasing membrane surface porosity would be to treat PS membrane surfaces prior to plasma treatment with sodium hypochlorite (NaClO). This is often used as a disinfection agent in tissue culture as well as for the removal of adsorbed proteins from haemodialysis membranes [272]. It has previously been shown to increase porosity of pure and blended polyethersulfone membranes [273,274] as well as poly(vinyl alcohol)-PLGA blended membranes [275]. However, as these increases in porosity are reported as coinciding with a weakening of membrane mechanical structure, development of an appropriate concentration of NaClO will be required. Furthermore, careful attention should also be given to changes in surface chemistry from this treatment which may affect overall wettability and biocompatibility, as NaClO is an oxidising agent.

The incorporation of a porogen as part of the membrane manufacture process is a further approach that is independent of altering polymer chemistry. Here, a porogen such as sodium chloride could be incorporated into the dope solution [276,277]. The dope is then cast in a nonsolvent bath as per the immersion precipitation method. As the membrane precipitates, the porogen dissolves and is subsequently leached out to generate pores [278]. The pore sizes and overall porosity can be controlled by the size of the salt crystals as well as the weight percentage of salt contained within the casting dope. Therefore, this is an economical approach that can potentially be tailored to specific cell requirements, as well as allowing tight control over the MWCO at the surface for separating specific products within the culture medium. Again, further characterisation of membrane tensile strength, substrate stiffness and structure will be required to ensure that such an additive does not lead to a weak and unsuitable hollow fibre membrane structure.

Improvement of the hepatic phenotype in transdifferentiated hepatocyte-like cells

Although HepatoZYME^{+} was deemed an unsuitable culture medium for the transdifferentiation of B13 cells to HLCs, further work to confirm that the basal medium

HepatoZYME-SFM as the causative agent could be performed by reducing the dilution of the basal medium in comparison with viability studies. If possible, quantitative ELISAs to examine hepatic function would also be useful in determining whether HepatoZYME-SFM in more dilute, nontoxic concentrations can benefit conversion to the hepatic phenotype. This can be combined with gene expression data to assess upregulation of hepatic genes.

Another approach to transdifferentiating B13 cells to HLCs in serum-free medium would be to characterise its proliferation and transdifferentiation using Panserin 401 as a basal medium. Panserin 401 has previously shown to be successful in culturing the parent line AR42J, which encouraged increased zymogen formation under treatment with Dex, indicating a push towards a more exocrine phenotype [279]. Culture with the B13 subclone has yet to be characterised in the literature, and characterisation could be done using the methods already utilised in this thesis, such as immunofluorescent staining for protein expression. This could be further complemented with Western blotting. In addition, functional quantification of pancreatic and hepatic markers and gene expression through PCR would provide a comprehensive profile. Certainly, given the increased cell death observed in the HepatoZYME^{+} culture, further viability studies would also complement this work.

Biocompatibility of surface treated polystyrene membranes with different cell types

The flat sheet membrane model as developed could be utilised for further biocompatibility studies. As the research in **Chapter 6** has shown that the adherent B13 and MG63 cell lines can be supported on the PX biomaterial, examining a range of other cell lines would expand their scope at being able to be translated to a HFB culture setting with this biomaterial. This is an attractive prospect due to the increased expansion capability of this culture method compared to traditional flask culture methods. Furthermore, assessment of other hepatocyte functions of transdifferentiated HLCs cultured on PX membranes, such as xenobiotic responsiveness, could be compared to other hepatocyte-like cell lines such as HepG2, C3A, HepaRG, and also primary hepatocytes. As the B13 cell line can also convert into insulin producing β-cells [217] and ductal cells [222], this utility on PX membranes could also be assessed.

7.2.2 Long term aims

Development and characterisation of porous polystyrene hollow fibre membranes

As a flat sheet membrane model for fabricating PX membranes has been developed, this needs to be translated to a HFB system. Therefore, the initial long term aim would be to determine if the parameters for casting established in the flat sheet membrane model can be utilised for casting hollow fibre membranes. Furthermore, once an efficient method for generating fully porous membranes has been established, further characterisation of the hollow fibre membrane will be required with regards to the bioreactor design. Investigations such as water and gas permeability of the membrane will be important in determining how porous the membrane walls are with regards to optimisation of medium flow rate and nutrient diffusion across the membrane wall.

Transdifferentiation of pancreatic cells to hepatocyte-like cells in a polystyrene hollow fibre bioreactor system

Once PX hollow fibre membranes have been established, it will be necessary to establish whether B13 cell culture and transdifferentiation to HLCs can be translated from a 2D static system to the 3D flow configuration of the HFB. Initially, a suitable seeding density and method of seeding will need to be established, as an issue with static seeding upon hollow fibres is non-uniform distribution across the membrane and reduced attachment, thus requiring the use of rotational seeding or oscillating perfusion methods to gain better uniformity and attachment [280,281]. Furthermore, as too low or too high a density can influence the transdifferentiation efficacy and overall culture viability, characterisation of attachment, viability, proliferative capacity and transdifferentiation utility will be essential for determining the correct operating methods for this cell line. Comparison with other hepatocyte-like cell lines and also primary hepatocytes will be necessary to establish the quality of transdifferentiated HLCs in a BAL device setting. Responsiveness to xenobiotics and subsequent analysis of cytochrome P450 activity would be useful in use of this system

as an *in vitro* drug toxicity model. As the B13 cell line is a rat pancreatic line, further work utilising a human pancreatic cell source would be more clinically relevant [134,135].

Determination of operating conditions for polystyrene hollow fibre bioreactor cell culture utilising different cell types

As there is the possibility of expanding the scope of this biomaterial to different tissue types for large scale cell expansion, such as the use of MG63 cells to generate HGF and the differentiation of stem cells down different lineages for cell therapies [150,172,282–285], determination of ideal operating conditions for specific cell types is important for bioreactor design optimisation. In the case of the BAL device, this is necessary to ensure that the environment mimics normal physiological conditions as closely as possible. Mathematical models will be useful in tailoring the system to a specific cell type [164]. In particular, as some hepatic functionality within hepatocytes is zonated depending on oxygen and nutrient gradients down the porto-venous axis, replicating this as closely as possible will further optimise BAL device design to provide a more *in vivo* like response [53,83].

To conclude, the overarching goal of this thesis was to develop a novel biomaterial and utilise a novel cell source for BAL device design, based upon a HFB system, using tissue engineering techniques. This research has elucidated the development of a biocompatible phase inversion membrane (PX) that can support functional transdifferentiated HLCs and has potentially expanded the scope of the design to support different cell types for large scale expansion. The ultimate long term aim would now be to develop an optimised BAL device design in an *in vivo* setting utilising the developments contributed by the research in this thesis.

References

1. Zakim D, Boyer TD. Hepatology: A Textbook of Liver Disease. 4th ed. Philadelphia; 2003.

2. Shier D, Butler J, Lewis R. Hole's Human Anatomy and Physiology. 11th ed. New York: McGraw-Hill; 2007.

3. Online Encyclopaedia Britannica. liver: anterior and posterior views [Internet]. 2003. Available from: http://www.britannica.com/EBchecked/media/68633/Anterior-and-posterior-views-of-the-liver

4. Burke ZD, Tosh D. The Wnt/beta-catenin pathway: master regulator of liver zonation? BioEssays. 2006;28(11):1072–7.

5. Malarkey DE, Johnson K, Ryan L, Boorman G, Maronpot RR. New Insights into Functional Aspects of Liver Morphology. Toxicol Pathol. 2005;33(1):27–34.

6. Perseghin G, Regalia E, Battezzati A, Vergani S, Pulvirenti A, Terruzzi I, et al. Regulation of glucose homeostasis in humans with denervated livers. J Clin Invest. 1997;100(4):931–41.

7. Juza RM, Pauli EM. Clinical and surgical anatomy of the liver: A review for clinicians. Clin Anat. 2014;27(5):764–9.

8. Kandilis AN, Koskinas J, Tiniakos DG, Nikiteas N, Perrea DN. Liver regeneration: Focus on cell types and topographic differences. Eur Surg Res. 2010;44(1):1–12.

9. Ordovás L, Park Y, Verfaillie CM. Stem cells and liver engineering. Biotechnol Adv. Elsevier Inc.; 2013;31(7):1094–107.

10. Gao B, Radaeva S, Park O. Liver natural killer and natural killer T cells: immunobiology and emerging roles in liver diseases. J Leukoc Biol. 2009;86:1–16.

11. Colnot S, Perret C. Liver Zonation. In: Monga SPS, editor. Molecular Pathology of Liver Diseases. Boston, MA: Springer US; 2011. p. 7–15.

12. Kinugasa A, Thurman RG. Differential effect of glucagon on gluconeogenesis in periportal and pericentral regions of the liver lobule. Biochem J. 1986;236(2):425–30.

13. Benhamouche S, Decaens T, Godard C, Chambrey R, Rickman DS, Moinard C, et al. Apc tumor suppressor gene is the "zonation-keeper" of mouse liver. Dev Cell. 2006;10(6):759–70.

14. Burke ZD, Reed KR, Phesse TJ, Sansom OJ, Clarke AR, Tosh D. Liver zonation occurs through a beta-catenin-dependent, c-Myc-independent mechanism. Gastroenterology. AGA Institute American Gastroenterological Association; 2009;136(7):2316-2324-3.

15. Katoonizadeh A, Nevens F, Verslype C, Pirenne J, Roskams T. Liver regeneration in acute severe liver impairment: a clinicopathological correlation study. Liver Int. 2006;26(10):1225–33.

16. Marudanayagam R, Shanmugam V, Gunson B, Mirza DF, Mayer D, Buckels J, et al. Aetiology and outcome of acute liver failure. HPB. 2009;11(5):429–34.

17. Nevens F, Laleman W. Artificial liver support devices as treatment option for liver failure. Best Pract Res Clin Gastroenterol. Elsevier Ltd; 2012;26(1):17–26.

18. Williams R, Aspinall R, Bellis M, Camps-Walsh G, Cramp M, Dhawan A, et al. Addressing liver disease in the UK: A blueprint for attaining excellence in health care and reducing premature mortality from lifestyle issues of excess consumption of alcohol, obesity, and viral hepatitis. Lancet. 2014;384(9958):1953–97.

19. British Liver Trust. Facts about liver disease [Internet]. 2012. Available from: http://79.170.44.126/britishlivertrust.org.uk/home-2/media-centre/facts-about-liver-disease/

20. Effiong K, Osinowo A, Pring A. Deaths from liver disease - Implications for end of life care in England. 2012.

21. Martin E. K, Allen, England NHS. Annual Report on Liver Transplantation: Report for 2014/2015. 2015.

22. Boudjema K, Bachellier P, Wolf P, Tempé J-D, Jaeck D. Auxiliary Liver Transplantation and Bioartificial Bridging Procedures in Treatment of Acute Liver Failure. World J Surg. 2002;26:264–74.

23. Bañares R, Catalina MV, Vaquero J. Molecular Adsorbent Recirculating System and Bioartificial Devices for Liver Failure. Clin Liver Dis. Elsevier Inc; 2014;18(4):945–56.

24. Chamuleau RA, Poyck PP, van de Kerkhove M-P. Bioartificial Liver: Its Pros and Cons. Ther Apher Dial. 2006;10(2):168–74.

25. Stange J, Ramlow W, Mitzner S, Schmidt R, Klinkmann H. Dialysis against a recycled albumin solution enables the removal of albumin-bound toxins. Artif Organs. 1993;17(9):809–13.

26. Stange, Mitzner, Risler, Erley, Lauchart, Goehl, et al. Molecular Adsorbent Recycling System (MARS): Clinical Results of a New Membrane-Based Blood Purification System for Bioartificial Liver Support. Artif Organs. 1999;23(4):319–30.

27. Sen S, Davies NA, Mookerjee RP, Cheshire LM, Hodges SJ, Williams R, et al. Pathophysiological effects of albumin dialysis in acute-on-chronic liver failure: A randomized controlled study. Liver Transplant. 2004;10(9):1109–19.

28. Donati G, La Manna G, Cianciolo G, Grandinetti V, Carretta E, Cappuccilli M, et al. Extracorporeal Detoxification for Hepatic Failure Using Molecular Adsorbent Recirculating System: Depurative Efficiency and Clinical Results in a Long-Term Follow-Up. Artif Organs. 2014;38(2):125–34.

29. Tsipotis E, Shuja A, Jaber BL. Albumin Dialysis for Liver Failure: A Systematic Review. Adv Chronic Kidney Dis. Elsevier Ltd; 2015;22(5):382–90.

30. Hassanein TI, Tofteng F, Brown RS, McGuire B, Lynch P, Mehta R, et al. Randomized controlled study of extracorporeal albumin dialysis for hepatic encephalopathy in advanced cirrhosis. Hepatology. 2007;46(6):1853–62.

31. Bañares R, Nevens F, Larsen FS, Jalan R, Albillos A, Dollinger M, et al. Extracorporeal albumin dialysis with the molecular adsorbent recirculating system

in acute-on-chronic liver failure: The RELIEF trial. Hepatology. 2013;57(3):1153–62.

32. Jalan R, Schnurr K, Mookerjee RP, Sen S, Cheshire L, Hodges S, et al. Alterations in the functional capacity of albumin in patients with decompensated cirrhosis is associated with increased mortality. Hepatology. 2009;50(2):555–64.

33. Sauer IM, Goetz M, Steffen I, Walter G, Kehr DC, Schwartlander R, et al. In vitro comparison of the molecular adsorbent recirculation system (MARS) and single-pass albumin dialysis (SPAD). Hepatology. 2004;39(5):1408–14.

34. Sponholz C, Matthes K, Rupp D, Backaus W, Klammt S, Karailieva D, et al. Molecular adsorbent recirculating system and single-pass albumin dialysis in liver failure – a prospective, randomised crossover study. Crit Care. Critical Care; 2015;20(1):2.

35. Falkenhagen D, Strobl W, Vogt G, Schrefl A, Linsberger I, Gerner FJ, et al. Fractionated Plasma Separation and Adsorption System: A Novel System for Blood Purification to Remove Albumin Bound Substances. Artif Organs. 1999;23(1):81–6.

36. Rifai K, Ernst T, Kretschmer U, Bahr MJ, Schneider A, Hafer C, et al. Prometheus® – a new extracorporeal system for the treatment of liver failure. J Hepatol. 2003;39(6):984–90.

37. Oppert M, Rademacher S, Petrasch K, Jörres A. Extracorporeal Liver Support Therapy With Prometheus in Patients With Liver Failure in the Intensive Care Unit. Ther Apher Dial. 2009;13(5):426–30.

38. Rocen M, Kieslichova E, Merta D, Uchytilova E, Pavlova Y, Cap J, et al. The Effect of Prometheus Device on Laboratory Markers of Inflammation and Tissue Regeneration in Acute Liver Failure Management. Transplant Proc. Elsevier Inc.; 2010;42(9):3606–11.

39. Rifai K. Removal selectivity of Prometheus: A new extracorporeal liver support device. World J Gastroenterol. 2006;12(6):940.

40. Evenepoel P, Laleman W, Wilmer A, Claes K, Maes B, Kuypers D, et al. Detoxifying Capacity and Kinetics of Prometheus® – A New Extracorporeal

System for the Treatment of Liver Failure. Blood Purif. 2005;23(5):349–58.

41. Vienken J, Christmann H. How Can Liver Toxins be Removed? Filtration and Adsorption With the Prometheus System. Ther Apher Dial. 2006;10(2):125–31.

42. Stadlbauer V, Krisper P, Aigner R, Haditsch B, Jung A, Lackner C, et al. Effect of extracorporeal liver support by MARS and Prometheus on serum cytokines in acute-on-chronic liver failure. Crit Care. 2006;10(6):R169.

43. Kribben A, Gerken G, Haag S, Herget–Rosenthal S, Treichel U, Betz C, et al. Effects of Fractionated Plasma Separation and Adsorption on Survival in Patients With Acute-on-Chronic Liver Failure. Gastroenterology. 2012;142(4):782–789.e3.

44. Khuroo MS, Khuroo MS, Farahat KLC. Molecular adsorbent recirculating system for acute and acute-on-chronic liver failure: A meta-analysis. Liver Transplant. 2004;10(9):1099–106.

45. Stutchfield BM, Simpson K, Wigmore SJ. Systematic review and meta-analysis of survival following extracorporeal liver support. Br J Surg. 2011;98(5):623–31.

46. Zheng Z, Li X, Li Z, Ma X. Artificial and bioartificial liver support systems for acute and acute-on-chronic hepatic failure: A meta-analysis and meta-regression. Exp Ther Med. 2013;6(4):929–36.

47. Saliba F, Camus C, Durand F, Mathurin P, Letierce A, Delafosse B, et al. Albumin Dialysis With a Noncell Artificial Liver Support Device in Patients With Acute Liver Failure. Ann Intern Med. 2013;159(8):522.

48. Olin P, Hausken J, Foss A, Karlsen TH, Melum E, Haugaa H. Continuous molecular adsorbent recirculating system treatment in 69 patients listed for liver transplantation. Scand J Gastroenterol. 2015;50(9):1127–34.

49. Rittler P, Ketscher C, Inthorn D, Jauch K-W, Hartl WH. Use of the molecular adsorbent recycling system in the treatment of postoperative hepatic failure and septic multiple organ dysfunction - preliminary results. Liver Int. 2004;24(2):136–41.

50. van de Kerkhove MP, Hoekstra R, Chamuleau RAFM, van Gulik TM. Clinical

Application of Bioartificial Liver Support Systems. Ann Surg. 2004;240(2):216–30.

51. van Wenum M, Chamuleau RA, van Gulik TM, Siliakus A, Seppen J, Hoekstra R. Bioartificial livers in vitro and in vivo : tailoring biocomponents to the expanding variety of applications. Expert Opin Biol Ther. 2014;14(12):1745–60.

52. Berthiaume F, Maguire TJ, Yarmush ML. Tissue Engineering and Regenerative Medicine: History, Progress, and Challenges. Annu Rev Chem Biomol Eng. 2011;2(1):403–30.

53. Davidson AJ, Ellis MJ, Chaudhuri JB. A theoretical approach to zonation in a bioartificial liver. Biotechnol Bioeng. 2012;109(1):234–43.

54. Kunisaki SM, Fauza DO. Current State of Clinical Application. In: Principles of Tissue Engineering. Third Edit. Elsevier; 2007. p. 1189–200.

55. Demetriou AA, Brown RS, Busuttil RW, Fair J, McGuire BM, Rosenthal P, et al. Prospective, Randomized, Multicenter, Controlled Trial of a Bioartificial Liver in Treating Acute Liver Failure. Ann Surg. 2004;239(5):660–70.

56. Rozga J, Podesta L, LePage E, Morsiani E, Moscioni AD, Hoffman A, et al. A Bioartificial Liver to Treat Severe Acute Liver Failure. Ann Surg. 1994;219(5):538–46.

57. Mullon C, Pitkin Z. The HepatAssist® Bioartificial Liver Support System: clinical study and pig hepatocyte process. Expert Opin Investig Drugs. 1999;8(3):229–35.

58. Pryor II HI, Vacanti JP. The promise of artificial liver replacement. Front Biosci. 2008;13(13):2140.

59. Wang S, Nagrath D. Liver Tissue Engineering. In: Burdick JA, Mauck RL, editors. Biomaterials for Tissue Engineering Applications. Vienna: Springer Vienna; 2011. p. 389–419.

60. Millis JM, Cronin DC, Johnson R, Conjeevaram H, Conlin C, Trevino S, et al. Initial experience with the modified extracorporeal liver-assist device for patients with fulminant hepatic failure: system modifications and clinical impact. Transplantation. 2002;74(12):1735–46.

61. Ellis AJ, Hughes RD, Wendon JA, Dunne J, Langley PG, Kelly JH, et al. Pilot-controlled trial of the extracorporeal liver assist device in acute liver failure. Hepatology. 1996;24(6):1446–51.

62. Hillebrand DJ, Frederick RT, Williams WW, Brown Jr RS, Napotilano LM, Te HS, et al. Safety and Efficacy of the Extracorporeal Liver Assist Device (ELAD®) in Patients With Acute on Chronic Liver Failure. J Hepatol. European Association for the Study of the Liver; 2010;52(Supplement 1):S323–4.

63. Thompson JA, Subramanian RM, Al-khafaji A, Reich DJ, Nicholas R Mac, Hassanein TI, et al. LB-1 The Effect of Extracorporeal C3a Cellular Therapy in Severe Alcoholic Hepatitis - The Elad Trial. Hepatology. 2015;62(6):1379A–1399A.

64. Karvellas CJ, Subramanian RM. Current Evidence for Extracorporeal Liver Support Systems in Acute Liver Failure and Acute-on-Chronic Liver Failure. Crit Care Clin. 2016;32(3):439–51.

65. Diekmann S, Bader A, Schmitmeier S. Present and future developments in hepatic tissue engineering for liver support systems : State of the art and future developments of hepatic cell culture techniques for the use in liver support systems. Cytotechnology. 2006;50:163–79.

66. Sauer IM, Gerlach JC. Modular Extracorporeal Liver Support. Artif Organs. 2002;26(8):703–6.

67. Sauer IM, Zeilinger K, Obermayer N, Pless G, Grünwald A, Pascher A, et al. Primary human liver cells as source for modular extracorporeal liver support - a preliminary report. Int J Artif Organs. 2002;25(10):1001–5.

68. Mazariegos G V., Patzer JF, Lopez RC, Giraldo M, DeVera ME, Grogan TA, et al. First Clinical Use of a Novel Bioartificial Liver Support System (BLSS)+. Am J Transplant. 2002;2(3):260–6.

69. Mazariegos G V, Kramer DJ, Lopez RC, Obaid Shakil A, Rosenbloom AJ, DeVera M, et al. Safety Observations in Phase I Clinical Evaluation of the Excorp Medical Bioartificial Liver Support System after the First Four Patients. ASAIO J.

2001;47(5):471–5.

70. van de Kerkhove MP, Poyck PPC, Deurholt T, Hoekstra R, Chamuleau RAFM, van Gulik TM. Liver Support Therapy: An Overview of the AMC-Bioartificial Liver Research. Dig Surg. 2005;22(4):254–64.

71. Poyck PPC, Hoekstra R, Vermeulen JLM, van Wijk ACWA, Chamuleau RAFM, Hakvoort TBM, et al. Expression of Glutamine Synthetase and Carbamoylphosphate Synthetase I in a Bioartificial Liver: Markers for the Development of Zonation in vitro. Cells Tissues Organs. 2008;188(3):259–69.

72. Nibourg GAA, Boer JD, van der Hoeven T V., Ackermans MT, van Gulik TM, Chamuleau RAFM, et al. Perfusion flow rate substantially contributes to the performance of the HepaRG-AMC-bioartificial liver. Biotechnol Bioeng. 2012;109(12):3182–8.

73. Van De Kerkhove MP, Di Florio E, Scuderi V, Mancini A, Belli A, Bracco A, et al. Phase I clinical trial with the AMC-bioartificial liver. Int J Artif Organs. 2002;25(10):950–9.

74. Hoekstra R, Nibourg GAA, van der Hoeven T V, Ackermans MT, Hakvoort TBM, van Gulik TM, et al. The HepaRG cell line is suitable for bioartificial liver application. Int J Biochem Cell Biol. Elsevier Ltd; 2011;43(10):1483–9.

75. Nibourg GAA, Chamuleau RAFM, van der Hoeven T V, Maas M a W, Ruiter AFC, Lamers WH, et al. Liver progenitor cell line HepaRG differentiated in a bioartificial liver effectively supplies liver support to rats with acute liver failure. PLoS One. 2012;7(6):e38778.

76. Poyck PP, Pless G, Hoekstra R, Roth S, van Wijk AC, Schwartlander R, et al. In vitro comparison of two bioartificial liver support systems: MELS CellModule and AMC-BAL. Int J Artif Organs. 2007;30(3):183–91.

77. Pless G. Bioartificial Liver Support Systems. In: Maurel P, editor. Hepatocytes. Totowa, NJ: Humana Press; 2010. p. 511–23.

78. Gu J, Shi X, Ren H, Xu Q, Wang J, Xiao J, et al. Systematic review: extracorporeal bio-artificial liver-support system for liver failure. Hepatol Int. 2012;6(4):670–83.

79. Zheng Z, Li X, Li Z, Ma X. Artificial and bioartificial liver support systems for acute and acute-on-chronic hepatic failure: A meta-analysis and meta-regression. Exp Ther Med. 2013;6:929–36.

80. Zhao L-F, Pan X-P, Li L-J. Key challenges to the development of extracorporeal bioartificial liver support systems. Hepatobiliary Pancreat Dis Int. The Editorial Board of Hepatobiliary & Pancreatic Diseases International; 2012;11(3):243–9.

81. Tsiaoussis J. Which hepatocyte will it be? Hepatocyte choice for bioartificial liver support systems. Liver Transplant. 2001;7(1):2–10.

82. Morsiani E, Brogli M, Galavotti D, Pazzi P, Puviani AC, Azzena GF. Biologic liver support: Optimal cell source and mass. Int J Artif Organs. 2002;25(10):985–93.

83. Davidson AJ, Ellis MJ, Chaudhuri JB. A theoretical method to improve and optimize the design of bioartificial livers. Biotechnol Bioeng. 2010;106(6):980–8.

84. Hu C, Li L. In vitro culture of isolated primary hepatocytes and stem cell-derived hepatocyte-like cells for liver regeneration. Protein Cell. Higher Education Press; 2015;6(8):562–74.

85. Fraczek J, Bolleyn J, Vanhaecke T, Rogiers V, Vinken M. Primary hepatocyte cultures for pharmaco-toxicological studies: at the busy crossroad of various anti-dedifferentiation strategies. Arch Toxicol. 2013;87(4):577–610.

86. Hamilton GA, Westmorel C, George AE. Effects of medium composition on the morphology and function of rat hepatocytes cultured as spheroids and monolayers. Vitr Cell Dev Biol - Anim. 2001;37(10):656–67.

87. Lang R, Stern MM, Smith L, Liu Y, Bharadwaj S, Liu G, et al. Three-dimensional culture of hepatocytes on porcine liver tissue-derived extracellular matrix. Biomaterials. Elsevier Ltd; 2011;32(29):7042–52.

88. Skardal A, Smith L, Bharadwaj S, Atala A, Soker S, Zhang Y. Tissue specific synthetic ECM hydrogels for 3-D in vitro maintenance of hepatocyte function. Biomaterials. 2012;33(18):4565–75.

89. Thomas RJ, Bhandari R, Barrett DA, Bennett AJ, Fry JR, Powe D, et al. The Effect

of Three-Dimensional Co-Culture of Hepatocytes and Hepatic Stellate Cells on Key Hepatocyte Functions in vitro. Cells Tissues Organs. 2005;181(2):67–79.

90. Abu-Absi SF, Hansen LK, Hu W-S. Three-dimensional co-culture of hepatocytes and stellate cells. Cytotechnology. 2004;45(3):125–40.

91. Godoy P, Hewitt NJ, Albrecht U, Andersen ME, Ansari N, Bhattacharya S, et al. Recent advances in 2D and 3D in vitro systems using primary hepatocytes, alternative hepatocyte sources and non-parenchymal liver cells and their use in investigating mechanisms of hepatotoxicity, cell signaling and ADME. Arch Toxicol. 2013;87(8):1315–530.

92. Bhogal RH, Hodson J, Bartlett DC, Weston CJ, Curbishley SM, Haughton E, et al. Isolation of primary human hepatocytes from normal and diseased liver tissue: a one hundred liver experience. PLoS One. 2011;6(3):e18222.

93. Tolosa L, Bonora-Centelles A, Teresa Donato M, Pareja E, Negro A, López S, et al. Steatotic liver: a suitable source for the isolation of hepatic progenitor cells. Liver Int. 2011;31(8):1231–8.

94. Terry C, Mitry RR, Lehec SC, Muiesan P, Rela M, Heaton ND, et al. The Effects of Cryopreservation on Human Hepatocytes Obtained From Different Sources of Liver Tissue. Cell Transplant. 2005;14(8):585–94.

95. Donato MT, Castell J V., Gómez-Lechón MJ. Characterization of drug metabolizing activities in pig hepatocytes for use in bioartificial liver devices: comparison with other hepatic cellular models. J Hepatol. 1999;31(3):542–9.

96. Langsch A, Giri S, Acikgöz A, Jasmund I, Frericks B, Bader A. Interspecies difference in liver-specific functions and biotransformation of testosterone of primary rat, porcine and human hepatocyte in an organotypical sandwich culture. Toxicol Lett. 2009;188(3):173–9.

97. Poyck PPC, Hoekstra R, van Wijk ACWA, Attanasio C, Calise F, Chamuleau RAFM, et al. Functional and morphological comparison of three primary liver cell types cultured in the AMC bioartificial liver. Liver Transplant. 2007;13(4):589–98.

98. Cowan PJ, D'Apice AJ. The coagulation barrier in xenotransplantation:

incompatibilities and strategies to overcome them. Curr Opin Organ Transplant. 2008;13(2):178–83.

99. Schrem H, Kleine M, Borlak J, Klempnauer J. Physiological incompatibilities of porcine hepatocytes for clinical liver support. Liver Transplant. 2006;12(12):1832–40.

100. Pitkin Z, Mullon C. Evidence of Absence of Porcine Endogenous Retrovirus (PERV) Infection in Patients Treated with a Bioartificial Liver Support System. Artif Organs. 1999;23(9):829–33.

101. Di Nicuolo G, Kerkhove M-P, Hoekstra R, Beld MGHM, Amoroso P, Battisti S, et al. No evidence of in vitro and in vivo porcine endogenous retrovirus infection after plasmapheresis through the AMC-bioartificial liver. Xenotransplantation. 2005;12(4):286–92.

102. Di Nicuolo G, D'Alessandro A, Andria B, Scuderi V, Scognamiglio M, Tammaro A, et al. Long-term absence of porcine endogenous retrovirus infection in chronically immunosuppressed patients after treatment with the porcine cell-based Academic Medical Center bioartificial liver. Xenotransplantation. 2010;17(6):431–9.

103. Wang Y, Susando T, Lei X, Anene-Nzelu C, Zhou H, Liang LH, et al. Current development of bioreactors for extracorporeal bioartificial liver (Review). Biointerphases. 2010;5(3):FA116.

104. Chen G, Palmer A. Hemoglobin regulates the metabolic, synthetic, detoxification, and biotransformation functions of hepatoma cells cultured in a hollow fiber bioreactor. Tissue Eng Part A. 2010;16(10):3231–40.

105. Zhang S, Liu T, Chen L, Ren M, Zhang B, Wang Z, et al. Bifunctional polyethersulfone hollow fiber with a porous, single-layer skin for use as a bioartificial liver bioreactor. J Mater Sci Mater Med. 2012;23(8):2001–11.

106. Zhang S-C, Liu T, Wang Y-J. Porous and single-skinned polyethersulfone membranes support the growth of HepG2 cells: A potential biomaterial for bioartificial liver systems. J Biomater Appl. 2012;27(3):359–66.

107. Coward SM, Legallais C, David B, Thomas M, Foo Y, Mavri-Damelin D, et al. Alginate-encapsulated HepG2 Cells in a Fluidized Bed Bioreactor Maintain Function in Human Liver Failure Plasma. Artif Organs. 2009;33(12):1117–26.

108. Chamuleau RAFM, Deurholt T, Hoekstra R. Which Are the Right Cells to be Used in a Bioartificial Liver? Metab Brain Dis. 2005;20(4):327–35.

109. Nyberg SL, Remmel RP, Mann HJ, Peshwa M V, Hu WS, Cerra FB. Primary hepatocytes outperform Hep G2 cells as the source of biotransformation functions in a bioartificial liver. Ann Surg. 1994;220(1):59–67.

110. Mavri-Damelin D, Eaton S, Damelin LH, Rees M, Hodgson HJF, Selden C. Ornithine transcarbamylase and arginase I deficiency are responsible for diminished urea cycle function in the human hepatoblastoma cell line HepG2. Int J Biochem Cell Biol. Elsevier Ltd; 2007;39(3):555–64.

111. Mavri-Damelin D, Damelin LH, Eaton S, Rees M, Selden C, Hodgson HJF. Cells for bioartificial liver devices: The human hepatoma-derived cell line C3A produces urea but does not detoxify ammonia. Biotechnol Bioeng. 2008;99(3):644–51.

112. Darnell M, Schreiter T, Zeilinger K. Cytochrome P450-dependent metabolism in HepaRG cells cultured in a dynamic three-dimensional bioreactor. Drug Metab Dispos. 2011;39:1131–8.

113. Nibourg GAA, Hoekstra R, van der Hoeven T V., Ackermans MT, Hakvoort TBM, van Gulik TM, et al. Increased hepatic functionality of the human hepatoma cell line HepaRG cultured in the AMC bioreactor. Int J Biochem Cell Biol. Elsevier Ltd; 2013;45(8):1860–8.

114. van Wenum M, Adam AAA, Hakvoort TBM, Hendriks EJ, Shevchenko V, van Gulik TM, et al. Selecting Cells for Bioartificial Liver Devices and the Importance of a 3D Culture Environment: A Functional Comparison between the HepaRG and C3A Cell Lines. Int J Biol Sci. 2016;12(8):964–78.

115. Gerets HHJ, Tilmant K, Gerin B, Chanteux H, Depelchin BO, Dhalluin S, et al. Characterization of primary human hepatocytes, HepG2 cells, and HepaRG cells at the mRNA level and CYP activity in response to inducers and their predictivity for

the detection of human hepatotoxins. Cell Biol Toxicol. 2012;28(2):69–87.

116. Gilbert SF. Developmental Biology. 9th ed. Sunderland, MA: Sinauer Associates; 2010.

117. Hay DC, Zhao D, Ross A, Mandalam R, Lebkowski J, Cui W. Direct Differentiation of Human Embryonic Stem Cells to Hepatocyte-like Cells Exhibiting Functional Activities. Cloning Stem Cells. 2007;9(1):51–62.

118. Shan J, Schwartz RE, Ross NT, Logan DJ, Thomas D, Duncan SA, et al. Identification of small molecules for human hepatocyte expansion and iPS differentiation. Nat Chem Biol. 2013;9(8):514–20.

119. Siller R, Greenhough S, Naumovska E, Sullivan GJ. Small-molecule-driven hepatocyte differentiation of human pluripotent stem cells. Stem Cell Reports. The Authors; 2015;4(5):939–52.

120. Chen Y, Soto-Gutierrez A, Navarro-Alvarez N, Rivas-Carrillo JD, Yamatsuji T, Shirakawa Y, et al. Differentiation of Human Embryonic Stem Cells to Hepatocytes Using Deleted Variant of HGF and Poly-amino-urethane-Coated Nonwoven Polytetrafluoroethylene Fabric. Cell Transplant. 2006;15(10):865–71.

121. Szkolnicka D, Farnworth SL, Lucendo-Villarin B, Storck C, Zhou W, Iredale JP, et al. Accurate prediction of drug-induced liver injury using stem cell-derived populations. Stem Cells Transl Med. 2014;3(2):141–8.

122. Baxter M, Withey S, Harrison S, Segeritz CP, Zhang F, Atkinson-Dell R, et al. Phenotypic and functional analyses show stem cell-derived hepatocyte-like cells better mimic fetal rather than adult hepatocytes. J Hepatol. European Association for the Study of the Liver; 2015;62(3):581–9.

123. Sauer V, Roy-Chowdhury N, Guha C, Roy-Chowdhury J. Induced Pluripotent Stem Cells as a Source of Hepatocytes. Curr Pathobiol Rep. 2014;2(1):11–20.

124. Behbahan IS, Duan Y, Lam A, Khoobyari S, Ma X, Ahuja TP, et al. New approaches in the differentiation of human embryonic stem cells and induced pluripotent stem cells toward hepatocytes. Stem Cell Rev. 2011;7(3):748–59.

125. Aurich I, Mueller LP, Aurich H, Luetzkendorf J, Tisljar K, Dollinger MM, et al. Functional integration of hepatocytes derived from human mesenchymal stem cells into mouse livers. Gut. 2007;56(3):405–15.

126. Aurich H, Sgodda M, Kaltwasser P, Vetter M, Weise A, Liehr T, et al. Hepatocyte differentiation of mesenchymal stem cells from human adipose tissue in vitro promotes hepatic integration in vivo. Gut. 2009;58(4):570–81.

127. Palakkan AA, Hay DC, Pr AK, Tv K, Ross JA. Liver tissue engineering and cell sources: Issues and challenges. Liver Int. 2013;33(5):666–76.

128. Augello A, Kurth TB, De Bari C. Mesenchymal stem cells: a perspective from in vitro cultures to in vivo migration and niches. Eur Cells Mater. 2010;20:121–33.

129. Corbett JL, Tosh D. Conversion of one cell type into another: implications for understanding organ development, pathogenesis of cancer and generating cells for therapy: Figure 1. Biochem Soc Trans. 2014;42(3):609–16.

130. Shen C-N, Slack JMW, Tosh D. Molecular basis of transdifferentiation of pancreas to liver. Nat Cell Biol. 2000;2(12):879–87.

131. Burke ZD, Shen C-N, Ralphs KL, Tosh D. Characterization of liver function in transdifferentiated hepatocytes. J Cell Physiol. 2006;206(1):147–59.

132. Kurash JK, Shen C-N, Tosh D. Induction and regulation of acute phase proteins in transdifferentiated hepatocytes. Exp Cell Res. 2004;292(2):342–58.

133. Wang RY-L, Shen C-N, Lin M-H, Tosh D, Shih C. Hepatocyte-Like Cells Transdifferentiated from a Pancreatic Origin Can Support Replication of Hepatitis B Virus Hepatocyte-Like Cells Transdifferentiated from a Pancreatic Origin Can Support Replication of Hepatitis B Virus. J Virol. 2005;79(20):13116–28.

134. Sumitran-Holgersson S, Nowak G, Thowfeequ S, Begum S, Joshi M, Jaksch M, et al. Generation of hepatocyte-like cells from in vitro transdifferentiated human fetal pancreas. Cell Transplant. 2009;18(2):183–93.

135. Fairhall EA, Wallace K, White SA, Huang GC, Shaw JA, Wright SC, et al. Adult human exocrine pancreas differentiation to hepatocytes – potential source of a

human hepatocyte progenitor for use in toxicology research. Toxicol Res (Camb). 2013;2(1):80.

136. Shen C-N, Seckl JR, Slack JMW, Tosh D. Glucocorticoids suppress β-cell development and induce hepatic metaplasia in embryonic pancreas. Biochem J. 2003;375:41–50.

137. Yu C-B, Pan X-P, Li L-J. Progress in bioreactors of bioartificial livers. Hepatobiliary Pancreat Dis Int. 2009;8(2):134–40.

138. Yang TH, Miyoshi H, Ohshima N. Novel cell immobilization method utilizing centrifugal force to achieve high-density hepatocyte culture in porous scaffold. J Biomed Mater Res. 2001;55(3):379–86.

139. Chen J-P, Lin C-T. Dynamic seeding and perfusion culture of hepatocytes with galactosylated vegetable sponge in packed-bed bioreactor. J Biosci Bioeng. 2006;102(1):41–5.

140. Selden C, Spearman CW, Kahn D, Miller M, Figaji A, Erro E, et al. Evaluation of Encapsulated Liver Cell Spheroids in a Fluidised-Bed Bioartificial Liver for Treatment of Ischaemic Acute Liver Failure in Pigs in a Translational Setting. Yamamoto M, editor. PLoS One. 2013;8(12):e82312.

141. Erro E, Bundy J, Massie I, Chalmers S-A, Gautier A, Gerontas S, et al. Bioengineering the Liver: Scale-Up and Cool Chain Delivery of the Liver Cell Biomass for Clinical Targeting in a Bioartificial Liver Support System. Biores Open Access. 2013;2(1):1–11.

142. De Bartolo L, Salerno S, Curcio E, Piscioneri A, Rende M, Morelli S, et al. Human hepatocyte functions in a crossed hollow fiber membrane bioreactor. Biomaterials. Elsevier Ltd; 2009;30(13):2531–43.

143. Palakkan AA, Raj DK, Rojan J, Raj R.G. S, Anil Kumar PR, Muraleedharan C, et al. Evaluation of Polypropylene Hollow-Fiber Prototype Bioreactor for Bioartificial Liver. Tissue Eng Part A. 2013;19(9–10):1056–66.

144. Sullivan JP, Gordon JE, Bou-Akl T, Matthew HWT, Palmer AF. Enhanced oxygen delivery to primary hepatocytes within a hollow fiber bioreactor facilitated via

hemoglobin-based oxygen carriers. Artif Cells Blood Substitutes Immobil Biotechnol. 2007;35(6):585–606.

145. De Bartolo L, Jarosch-Von Schweder G, Haverich A, Bader A. A Novel Full-Scale Flat Membrane Bioreactor Utilizing Porcine Hepatocytes: Cell Viability and Tissue-Specific Functions. Biotechnol Prog. 2000;16(1):102–8.

146. Vinci B, Duret C, Klieber S, Gerbal-Chaloin S, Sa-Cunha A, Laporte S, et al. Modular bioreactor for primary human hepatocyte culture: Medium flow stimulates expression and activity of detoxification genes. Biotechnol J. 2011;6(5):554–64.

147. Ellis MJ, Jarman-Smith M, Chaudhuri JB. Bioreactor systems for tissue engineering: a four-dimensional challenge. In: Chaudhuri JB, Al-Rubeai M, editors. Bioreactors for Tissue Engineering. Dordrecht: Springer; 2005. p. 1–16.

148. Storm MP, Sorrell I, Shipley R, Regan S, Luetchford KA, Sathish J, et al. Hollow Fiber Bioreactors for In Vivo-like Mammalian Tissue Culture. J Vis Exp. 2016;(111):1–12.

149. Bokhari M, Carnachan RJ, Cameron NR, Przyborski SA. Culture of HepG2 liver cells on three dimensional polystyrene scaffolds enhances cell structure and function during toxicological challenge. J Anat. 2007;211(4):567–76.

150. Wung N, Acott SM, Tosh D, Ellis MJ. Hollow fibre membrane bioreactors for tissue engineering applications. Biotechnol Lett. 2014;36(12):2357–66.

151. Underhill GH, Khetani SR, Chen AA, Bhatia SN. Liver. In: Principles of Tissue Engineering. Elsevier; 2007. p. 707–31.

152. Yamazoe H, Iwata H. Efficient generation of dopaminergic neurons from mouse embryonic stem cells enclosed in hollow fibers. Biomaterials. 2006;27(28):4871–80.

153. Dai J, Zhang G-L, Meng Q. Interaction between hepatocytes and collagen gel in hollow fibers. Cytotechnology. 2009;60:133–41.

154. Ellis MJ, Chaudhuri JB. Poly(lactic-co-glycolic acid) Hollow Fibre Membranes for use as a Tissue Engineering Scaffold. Biotechnol Bioeng. 2007;96(1):177–87.

155. Li J, Pan J, Zhang L, Guo X, Yu Y. Culture of primary rat hepatocytes within

porous chitosan scaffolds. J Biomed Mater Res. 2003;67A(3):938–43.

156. Zhao Y, Xu Y, Zhang B, Wu X, Xu F, Liang W, et al. In Vivo Generation of Thick, Vascularized Hepatic Tissue from Collagen Hydrogel-Based Hepatic Units. Tissue Eng Part C Methods. 2010;16(4):653–9.

157. Jain E, Damania A, Kumar A. Biomaterials for liver tissue engineering. Hepatol Int. 2014;8(2):185–97.

158. Shiraha H, Koide N, Hada H, Ujike K, Nakamura M, Shinji T, et al. Improvement of serum amino acid profile in hepatic failure with the bioartificial liver using multicellular hepatocyte spheroids. Biotechnol Bioeng. 1996;50(4):416–21.

159. Mulder M. Basic Principles of Membrane Technology. 2nd ed. Dordrecht: Kluwer Academic Publishers; 2003.

160. Nedredal GI, Amiot BP, Nyberg P, Luebke-Wheeler J, Lillegard JB, McKenzie TJ, et al. Optimization of mass transfer for toxin removal and immunoprotection of hepatocytes in a bioartificial liver. Biotechnol Bioeng. 2009;104(5):995–1003.

161. Stockmann HB, Hiemstra CA, Marquet RL, IJzermans JN. Extracorporeal perfusion for the treatment of acute liver failure. Ann Surg. 2000;231(4):460–70.

162. Xu Q, Sun X, Qui Y, Zhang H, Ding Y. The Optimal Hepatocyte Density for a Hollow-Fiber Bioartificial Liver. Ann Clin Lab Sci. 2004;34(1):87–93.

163. Patzer JF. Oxygen Consumption in a Hollow Fiber Bioartificial Liver - Revisited. Artif Organs. 2004;28(1):83–98.

164. Shipley RJ, Davidson AJ, Chan K, Chaudhuri JB, Waters SL, Ellis MJ. A Strategy to Determine Operating Parameters in Tissue Engineering Hollow Fiber Bioreactors. Biotechnol Bioeng. 2011;108(6):1450–61.

165. Catapano G, Di Lorenzo MC, Volpe C Della, De Bartolo L, Migliaresi C. Polymeric membranes for hybrid liver support devices: The effect of membrane surface wettability on hepatocyte viability and functions. J Biomater Sci Polym Ed. 1996;7(11):1017–27.

166. Jacobs T, Morent R, Geyter N, Dubruel P, Leys C. Plasma Surface Modification of

Biomedical Polymers: Influence on Cell-Material Interaction. Plasma Chem Plasma Process. 2012;32(5):1039–73.

167. Bellis SL. Advantages of RGD peptides for directing cell association with biomaterials. Biomaterials. Elsevier Ltd; 2011;32(18):4205–10.

168. Meneghello G, Parker DJ, Ainsworth BJ, Perera SP, Chaudhuri JB, Ellis MJ, et al. Fabrication and characterization of poly(lactic-co-glycolic acid)/polyvinyl alcohol blended hollow fibre membranes for tissue engineering applications. J Memb Sci. 2009;344(1–2):55–61.

169. De Bartolo L, Morelli S, Bader A, Drioli E. Evaluation of cell behaviour related to physico-chemical properties of polymeric membranes to be used in bioartificial organs. Biomaterials. 2002;23(12):2485–97.

170. Makadia HK, Siegel SJ. Poly Lactic-co-Glycolic Acid (PLGA) as biodegradable controlled drug delivery carrier. Polymers (Basel). 2011;3(3):1377–97.

171. Ellis MJ, Chaudhuri JB. Human bone derived cell culture on PLGA flat sheet membranes of different lactide:glycolide ratio. Biotechnol Bioeng. 2008;101(2):369–77.

172. Morgan SM, Tilley S, Perera S, Ellis MJ, Kanczler J, Chaudhuri JB, et al. Expansion of human bone marrow stromal cells on poly-(DL-lactide-co-glycolide) (PDLLGA) hollow fibres designed for use in skeletal tissue engineering. Biomaterials. 2007;28(35):5332–43.

173. Morgan SM, Ainsworth BJ, Kanczler JM, Babister JC, Chaudhuri JB, Oreffo ROC. Formation of a human-derived fat tissue layer in P(DL)LGA hollow fibre scaffolds for adipocyte tissue engineering. Biomaterials. Elsevier Ltd; 2009;30(10):1910–7.

174. Ye H, Xia Z, Ferguson DJP, Triffitt JT, Cui Z. Studies on the use of hollow fibre membrane bioreactors for tissue generation by using rat bone marrow fibroblastic cells and a composite scaffold. J Mater Sci Mater Med. 2007;18(4):641–8.

175. Shearer H, Ellis MJ, Perera SP, Chaudhuri JB. Effects of Common Sterilization Methods on the Structure and Properties of Poly(D,L Lactic-Co-Glycolic Acid) Scaffolds. Tissue Eng. 2006;12(10):2717–27.

176. Peng N, Widjojo N, Sukitpaneenit P, Teoh MM, Lipscomb GG, Chung TS, et al. Evolution of polymeric hollow fibers as sustainable technologies: Past, present, and future. Prog Polym Sci. Elsevier Ltd; 2012;37(10):1401–24.

177. Strathmann H, Kock K. The formation mechanism of phase inversion membranes. Desalination. 1977;21(3):241–55.

178. Young TH, Chen LW. Pore formation mechanism of membranes from phase inversion process. Desalination. 1995;103(3):233–47.

179. Ellis MJ. Development of a novel hollow fibre membrane for use as a tissue engineered bone graft scaffold [PhD Thesis]. University of Bath, UK; 2005.

180. Bandyopadhyay A, Basak CG. Studies on photocatalytic degradation of polystyrene. Mater Sci Technol. 2007;23(3):307–14.

181. Han CD. Rheology and Processing of Polymeric Materials, Volume 1 - Polymer Rheology. Oxford University Press. Oxford University Press; 2007.

182. Knovel Sampler. Knovel. Knovel; 2003.

183. Curtis AS, Forrester J V, McInnes C, Lawrie F. Adhesion of Cells to Polystyrene Surfaces. J Cell Biol. 1983;97(5 Pt 1):1500–6.

184. Baker SC, Atkin N, Gunning PA, Granville N, Wilson K, Wilson D, et al. Characterisation of electrospun polystyrene scaffolds for three-dimensional in vitro biological studies. Biomaterials. 2006;27(16):3136–46.

185. Jouyban A, Fakhree MAA, Shayanfar A. Review of Pharmaceutical Applications of N-Methyl-2-Pyrrolidone. J Pharm Pharm Sci. 2010;13(4):524–35.

186. Miguel BS, Ghayor C, Ehrbar M, Jung RE, Zwahlen RA, Hortschansky P, et al. N-Methyl Pyrrolidone as a Potent Bone Morphogenetic Protein Enhancer for Bone Tissue Regeneration. Tissue Eng Part A. 2009;15(10):2955–63.

187. Dufresne M, Bacchin P, Cerino G, Remigy JC, Adrianus GN, Aimar P, et al. Human hepatic cell behavior on polysulfone membrane with double porosity level. J Memb Sci. Elsevier; 2013;428:454–61.

188. Eenink MJD, Feijen J. Biodegradable hollow fibres for the controlled release of hormones. J Control Release. 1987;6:225–47.

189. Diban N, Haimi S, Bolhuis-Versteeg L, Teixeira S, Miettinen S, Poot A, et al. Hollow fibers of poly(lactide-co-glycolide) and poly(ε-caprolactone) blends for vascular tissue engineering applications. Acta Biomater. Acta Materialia Inc.; 2013;9(5):6450–8.

190. Chung TS, Teoh SK, Hu X. Formation of ultrathin high-performance polyethersulfone hollow-fiber membranes. J Memb Sci. 1997;133(2):161–75.

191. Altankov G, Grinnell F, Groth T. Studies on the biocompatibility of materials: Fibroblast reorganization of substratum-bound fibronectin on surfaces varying in wettability. J Biomed Mater Res. 1996;30(3):385–91.

192. Underwood PA, Steele JG, Dalton BA. Effects of polystyrene surface chemistry on the biological activity of solid phase fibronectin and vitronectin, analysed with monoclonal antibodies. J Cell Sci. 1993;104:793–803.

193. Mikos AG, Lyman MD, Freed LE, Langer R. Wetting of poly(L-lactic acid) and poly(DL-lactic-co-glycolic acid) foams for tissue culture. Biomaterials. 1994;15(1):55–8.

194. Ishaug-Riley SL, Crane-Kruger GM, Yaszemski MJ, Mikos AG. Three-dimensional culture of rat calvarial osteoblasts in porous biodegradable polymers. Biomaterials. 1998;19(15):1405–12.

195. Wung N. Improving hollow fibre bioreactors and cell seeding scaffolds for bioartificial liver design [MRes Dissertation, unpublished]. University of Bath, UK; 2012.

196. Peng N, Chung TS, Wang KY. Macrovoid evolution and critical factors to form macrovoid-free hollow fiber membranes. J Memb Sci. 2008;318(1–2):363–72.

197. Conrads H, Schmidt M. Plasma generation and plasma sources. Plasma Sources Sci Technol. 2000;9(4):441–54.

198. Bonaccurso E, Graf K. Nanostructuring effect of plasma and solvent treatment on

polystyrene. Langmuir. 2004;20(25):11183–90.

199. Wan Y, Qu X, Lu J, Zhu C, Wan L, Yang J, et al. Characterization of surface property of poly(lactide-co-glycolide) after oxygen plasma treatment. Biomaterials. 2004;25(19):4777–83.

200. Cui N-Y, Brown NMD. Modification of the surface properties of a polypropylene (PP) film using an air dielectric barrier discharge plasma. Appl Surf Sci. 2002;189(1–2):31–8.

201. Nakhowong R, Srikhirin T, Osotchan T. Surface Treatment of Polystyrene Films with Inductively Coupled Plasma System. Adv Mater Res. 2008;55–57:753–6.

202. Biazar E, Heidari M, Asefnejad A, Asefnezhad A, Montazeri N. The relationship between cellular adhesion and surface roughness in polystyrene modified by microwave plasma radiation. Int J Nanomedicine. 2011;6:631–9.

203. Yang SY, Kim E-S, Jeon G, Choi KY, Kim JK. Enhanced adhesion of osteoblastic cells on polystyrene films by independent control of surface topography and wettability. Mater Sci Eng C. Elsevier B.V.; 2013;33(3):1689–95.

204. Kular JK, Basu S, Sharma RI. The extracellular matrix: Structure, composition, age-related differences, tools for analysis and applications for tissue engineering. J Tissue Eng. 2014;5:1–17.

205. Natarajan V, Berglund EJ, Chen DX, Kidambi S. Substrate stiffness regulates primary hepatocyte functions. RSC Adv. Royal Society of Chemistry; 2015;5:80956–66.

206. Li W, Yao SY, Ma KM, Chen P. Effect of Plasma Modification on the Mechanical Properties of Carbon Fiber/Phenolphthalein Polyaryletherketone Composites. Polym Compos. 2013;16(2):101–13.

207. Shang J, Flury M, Harsh JB, Zollars RL. Comparison of different methods to measure contact angles of soil colloids. J Colloid Interface Sci. 2008;328(2):299–307.

208. Drelich J. Guidelines to measurements of reproducible contact angles using a

sessile-drop technique. Surf Innov. 2013;1(4):248–54.

209. Chen Y, Gao Q, Wan H, Yi J, Wei Y, Liu P. Surface modification and biocompatible improvement of polystyrene film by Ar, O2 and Ar + O2 plasma. Appl Surf Sci. Elsevier B.V.; 2013;265:452–7.

210. van Kooten TG, Spijker HT, Busscher HJ. Plasma-treated polystyrene surfaces: model surfaces for studying cell–biomaterial interactions. Biomaterials. 2004;25(10):1735–47.

211. Occhiello E, Cinquina P, Garbassi F, Guido I, Spa D. Hydrophobic recovery of oxygen-plasma-treated polystyrene. Polymer (Guildf). 1992;33(14):3007–15.

212. Jokinen V, Suvanto P, Franssila S. Oxygen and nitrogen plasma hydrophilization and hydrophobic recovery of polymers. Biomicrofluidics. 2012;6(1):16501–1650110.

213. Burke ZD, Tosh D. Therapeutic potential of transdifferentiated cells. Clin Sci. 2005;108(4):309–21.

214. Tosh D, Slack JMW. How Cells Change Their Phenotype. Nat Rev Mol Cell Biol. 2002;3(3):187–94.

215. Rao M, Dwivedi R, Subborao V. Almost total conversion of pancreas to liver in the adult rat: a reliable model to study transdifferentiation. Biochem Biophys Res Commun. 1988;156(1):131–6.

216. Paner GP, Thompson KS, Reyes C V. Hepatoid carcinoma of the pancreas. Cancer. 2000;88(7):1582–9.

217. Mashima H, Shibata H, Mine T, Kojima I. Formation of insulin-producing cells from pancreatic acinar AR42J cells by hepatocyte growth factor. Endocrinology. 1996;137(9):3969–76.

218. Tosh D, Shen C-N, Slack JMW. Differentiated properties of hepatocytes induced from pancreatic cells. Hepatology. 2002;36(3):534–43.

219. Wu SY, Hsieh CC, Wu RR, Susanto J, Liu TT, Shen CR, et al. Differentiation of Pancreatic Acinar Cells to Hepatocytes Requires an Intermediate Cell Type.

Gastroenterology. 2010;138(7):2519–30.

220. Lardon J, De Breuck S, Rooman I, Van Lommel L, Kruhøffer M, Orntoft T, et al. Plasticity in the adult rat pancreas: transdifferentiation of exocrine to hepatocyte-like cells in primary culture. Hepatology. 2004;39(6):1499–507.

221. Lardon J, Huyens N, Rooman I, Bouwens L. Exocrine cell transdifferentiation in dexamethasone-treated rat pancreas. Virchows Arch. 2004;444(1):61–5.

222. Al-Adsani A, Burke ZD, Eberhard D, Lawrence KL, Shen C-N, Rustgi AK, et al. Dexamethasone treatment induces the reprogramming of pancreatic acinar cells to hepatocytes and ductal cells. PLoS One. 2010;5(10):e13650.

223. Marek CJ, Cameron GA, Elrick LJ, Hawksworth GM, Wright MC. Generation of hepatocytes expressing functional cytochromes P450 from a pancreatic progenitor cell line in vitro. Biochem J. 2003;370(Pt 3):763–9.

224. Vega ME, Giroux V, Natsuizaka M, Liu M, Klein-Szanto AJ, Stairs DB, et al. Inhibition of notch signaling enhances transdifferentiation of the esophageal squamous epithelium towards a Barrett's-like metaplasia via KLF4. Cell Cycle. 2014;13(24):3857–66.

225. Fléjou J-F. Barrett's oesophagus: from metaplasia to dysplasia and cancer. Gut. 2005;54 Suppl 1:i6-12.

226. Burke ZD, Tosh D. Barrett's metaplasia as a paradigm for understanding the development of cancer. Curr Opin Genet Dev. 2012;22(5):494–9.

227. Fairhall EA, Charles MA, Wallace K, Schwab CJ, Harrison CJ, Richter M, et al. The B-13 hepatocyte progenitor cell resists pluripotency induction and differentiation to non-hepatocyte cells. Toxicol Res (Camb). 2013;2(5):308–20.

228. Hang H, Shi X, Gu G, Wu Y, Ding Y. A simple isolation and cryopreservation method for adult human hepatocytes. Int J Artif Organs. 2009;32(10):720–7.

229. Shen L, Hillebrand A, Wang DQ-H, Liu M. Isolation and primary culture of rat hepatic cells. J Vis Exp. 2012;(64):1–4.

230. Heathman TRJ, Stolzing A, Fabian C, Rafiq QA, Coopman K, Nienow AW, et al.

Serum-free process development: Improving the yield and consistency of human mesenchymal stromal cell production. Cytotherapy. Elsevier Inc; 2015;17(11):1524–35.

231. Jung S, Panchalingam KM, Wuerth RD, Rosenberg L, Behie LA. Large-scale production of human mesenchymal stem cells for clinical applications. Biotechnol Appl Biochem. 2012;59(2):106–20.

232. Williams DJ, Thomas RJ, Hourd PC, Chandra A, Ratcliffe E, Liu Y, et al. Precision manufacturing for clinical-quality regenerative medicines. Philos Trans A Math Phys Eng Sci. 2012;370(1973):3924–49.

233. Szkolnicka D, Zhou W, Lucendo-Villarin B, Hay DC. Pluripotent stem cell-derived hepatocytes: potential and challenges in pharmacology. Annu Rev Pharmacol Toxicol. 2013;53:147–59.

234. Cameron K, Lucendo-Villarin B, Szkolnicka D, Hay DC. Serum-Free Directed Differentiation of Human Embryonic Stem Cells to Hepatocytes. Protoc Vitr Hepatocyte Res. 2015;1250:1–390.

235. Szkolnicka D, Farnworth SL, Lucendo-Villarin B, Hay DC. Deriving functional hepatocytes from pluripotent stem cells. Curr Protoc Stem Cell Biol. 2014;2014(August):1g.5.1-1g.5.12.

236. Eberhard D, Neill KO, Burke ZD, Tosh D. In Vitro Reprogramming of Pancreatic Cells to Hepatocytes. In: Ding S, editor. Cellular Programming and Reprogramming: Methods and Protocols. Totowa, NJ: Humana Press; 2010. p. 285–92.

237. Shen C-N, Tosh D. Transdifferentiation of Pancreatic Cells to Hepatocytes. In: Maurel P, editor. Hepatocytes. 1st ed. New York: Humana Press; 2010. p. 273–80.

238. Wallace K, Marek CJ, Hoppler S, Wright MC. Glucocorticoid-dependent transdifferentiation of pancreatic progenitor cells into hepatocytes is dependent on transient suppression of WNT signalling. J Cell Sci. 2010;123(Pt 12):2103–10.

239. Logsdon CD, Moessner J, Williams JA, Goldfine ID. Glucocorticoids increase amylase mRNA levels, secretory organelles, and secretion in pancreatic acinar

AR42J cells. J Cell Biol. 1985;100(4):1200–8.

240. Logsdon CD, Perot KJ, McDonald AR. Mechanism of glucocorticoid-induced increase in pancreatic amylase gene transcription. J Biol Chem. 1987;262(32):15765–9.

241. Fairhall EA, Charles MA, Probert PME, Wallace K, Gibb J, Ravindan C, et al. Pancreatic B-13 Cell Trans-Differentiation to Hepatocytes Is Dependent on Epigenetic-Regulated Changes in Gene Expression. PLoS One. 2016;11(3):e0150959.

242. Yamaoka M, Hirata K, Ogata I, Tomiya T, Nagoshi S, Mochida S. Enhancement of albumin production by hepatocyte growth factor in rat hepatocytes : distinction in mode of action from stimulation of DNA synthesis. Liver. 1998;18(1):52–9.

243. Kamiya A, Kinoshita T, Miyajima A. Oncostatin M and hepatocyte growth factor induce hepatic maturation via distinct signaling pathways. FEBS Lett. 2001;492(1–2):90–4.

244. Wallace K, Fairhall EA, Charlton KA, Wright MC. AR42J-B-13 cell: An expandable progenitor to generate an unlimited supply of functional hepatocytes. Toxicology. 2010;278(3):277–87.

245. Westmacott A, Burke ZD, Oliver G, Slack JMW, Tosh D. C/EBPα and C/EBPβ are markers of early liver development. Int J Dev Biol. 2006;50(7):653–7.

246. Gentric G, Desdouets C. Polyploidization in liver tissue. Am J Pathol. American Society for Investigative Pathology; 2014;184(2):322–31.

247. Guidotti JE, Brégerie O, Robert A, Debey P, Brechot C, Desdouets C. Liver cell polyploidization: A pivotal role for binuclear hepatocytes. J Biol Chem. 2003;278(21):19095–101.

248. Margall-Ducos G, Celton-Morizur S, Couton D, Brégerie O, Desdouets C. Liver tetraploidization is controlled by a new process of incomplete cytokinesis. J Cell Sci. 2007;120(20):3633–9.

249. Anatskaya O V., Vinogradov AE. Genome multiplication as adaptation to tissue

survival: Evidence from gene expression in mammalian heart and liver. Genomics. 2007;89(1):70–80.

250. Duncan AW, Taylor MH, Hickey RD, Hanlon Newell AE, Lenzi ML, Olson SB, et al. The ploidy conveyor of mature hepatocytes as a source of genetic variation. Nature. Nature Publishing Group; 2010;467(7316):707–10.

251. Zoorob RJ, Cender D. A Different Look at Corticosteroids. Am Fam Physician. 1998;58(2):443–50.

252. Wishart DS, Tzur D, Knox C. Dexamethasone [Internet]. Human Metabolome Database Version 3.0. 2012. Available from: http://www.hmdb.ca/metabolites/HMDB30049

253. Probert PME, Chung GW, Cockell SJ, Agius L, Mosesso P, White SA, et al. Utility of B-13 Progenitor-Derived Hepatocytes in Hepatotoxicity and Genotoxicity Studies. Toxicol Sci. 2014;137(2):350–70.

254. Chang H-I, Wang Y. Cell Responses to Surface and Architecture of Tissue Engineering Scaffolds. In: Regenerative Medicine and Tissue Engineering - Cells and Biomaterials. 2011. p. 569–88.

255. Kim SH, Turnbull J, Guimond S. Extracellular matrix and cell signalling: The dynamic cooperation of integrin, proteoglycan and growth factor receptor. J Endocrinol. 2011;209(2):139–51.

256. Engler AJ, Sen S, Sweeney HL, Discher DE. Matrix Elasticity Directs Stem Cell Lineage Specification. Cell. 2006;126(4):677–89.

257. Díaz-Rodríguez L, García-Martínez O, Arroyo-Morales M, Rubio-Ruiz B, Ruiz C. Effect of acetaminophen (paracetamol) on human osteosarcoma cell line MG63. Acta Pharmacol Sin. 2010;31(11):1495–9.

258. Prouillet C, Mazière JC, Mazière C, Wattel A, Brazier M, Kamel S. Stimulatory effect of naturally occurring flavonols quercetin and kaempferol on alkaline phosphatase activity in MG-63 human osteoblasts through ERK and estrogen receptor pathway. Biochem Pharmacol. 2004;67(7):1307–13.

259. Meneghello G, Storm MP, Chaudhuri JB, De Bank PA, Ellis MJ. An investigation into the stability of commercial versus MG63-derived hepatocyte growth factor under flow cultivation conditions. Biotechnol Lett. 2015;37(3):725–31.

260. Ellis MJ, Forsey R, Chaudhuri JB. Post-culture treatment protocols for PLGA membrane scaffolds. Biotechnol Lett. 2010;32(2):215–22.

261. Chim H, Ong JL, Schantz J-T, Hutmacher DW, Agrawal CM. Efficacy of glow discharge gas plasma treatment as a surface modification process for three-dimensional poly (D,L-lactide) scaffolds. J Biomed Mater Res A. 2003;65(3):327–35.

262. Kim SY, Kanamori T, Noumi Y, Wang P, Shinbo T. Preparation of Porous Poly (D,L-lactide) and Poly (D,L-lactide-co-glycolide) Membranes by a Phase Inversion Process and Investigation of Their Morphological Changes as Cell Culture Scaffolds. J Appl Polym Sci. 2004;92(4):2082–92.

263. Chang EJ, Kim HH, Huh JE, Kim IA, Seung Ko J, Chung CP, et al. Low proliferation and high apoptosis of osteoblastic cells on hydrophobic surface are associated with defective Ras signaling. Exp Cell Res. 2005;303(1):197–206.

264. Mettouchi A, Klein S, Guo W, Lopez-Lago M, Lemichez E, Westwick JK, et al. Integrin-specific activation of Rac controls progression through the G1 phase of the cell cycle. Mol Cell. 2001;8(1):115–27.

265. Jenzora A, Behrendt B, Small JV, Wehland J, Stradal TEB. PREL1 provides a link from Ras signalling to the actin cytoskeleton via Ena/VASP proteins. FEBS Lett. 2005;579(2):455–63.

266. Thomas MG, Marwood RM, Parsons AE, Parsons RB. The effect of foetal bovine serum supplementation upon the lactate dehydrogenase cytotoxicity assay: Important considerations for in vitro toxicity analysis. Toxicol Vitr. Elsevier B.V.; 2015;30(1):300–8.

267. Walker JM. Mammalian Cell Viability. 1st ed. Stoddart MJ, editor. Totowa, NJ: Humana Press; 2011.

268. Kurosawa H, Yuminamochi E, Yasuda R, Amano Y. Morphology and albumin

secretion of adult rat hepatocytes cultured on a hydrophobic porous expanded polytetrafluoroethylene membrane. J Biosci Bioeng. 2003;95(1):59–64.

269. Katsuki M, Kurosawa H, Amano Y. Enhancement of albumin secretion by short-term hypothermic incubation of primary rat hepatocytes. Biochem Eng J. 2004;20(2–3):137–41.

270. Holy CE, Dang SM, Davies JE, Shoichet MS. In vitro degradation of a novel poly(lactide-co-glycolide) 75/25 foam. Biomaterials. 1999;20(13):1177–85.

271. Pan Z, Ding J. Poly(lactide-co-glycolide) porous scaffolds for tissue engineering and regenerative medicine. Interface Focus. 2012;2(3):366–77.

272. Caillou S, Boonaert CJP, Dewez J-L, Rouxhet PG. Oxidation of Proteins Adsorbed on Hemodialysis Membranes and Model Materials. J Biomed Mater Res Part B Appl Biomater. 2008;84B:240–8.

273. Jung B, Joon KY, Kim B, Rhee HW. Effect of molecular weight of polymeric additives on formation, permeation properties and hypochlorite treatment of asymmetric polyacrylonitrile membranes. J Memb Sci. 2004;243(1–2):45–57.

274. Arkhangelsky E, Kuzmenko D, Gitis V. Impact of chemical cleaning on properties and functioning of polyethersulfone membranes. J Memb Sci. 2007;305(1–2):176–84.

275. Meneghello G, Ainsworth B, de Bank P, Ellis MJ, Chaudhuri J. Effect of polyvinyl alcohol and sodium hypochlorite on porosity and mechanical properties of PLGA hollow fibre membrane scaffolds. Eur Cells Mater. 2008;16(SUPPL. 3):82.

276. Mikos AG, Thorsen AJ, Czerwonka LA, Bao Y, Langer R, Winslow DN, et al. Preparation and characterization of poly(l-lactic acid) foams. Polymer (Guildf). 1994;35(5):1068–77.

277. Reignier J, Huneault MA. Preparation of interconnected poly(ε-caprolactone) porous scaffolds by a combination of polymer and salt particulate leaching. Polymer (Guildf). 2006;47(13):4703–17.

278. Mondal M, De S. Preparation, characterization, and performance of a novel hollow

fiber nanofiltration membrane. Polym Adv Technol. 2015;26(9):1155–67.

279. Rinn C, Aroso M, Prüssing J, Islinger M, Schrader M. Modulating zymogen granule formation in pancreatic AR42J cells. Exp Cell Res. 2012;318(15):1855–66.

280. Alvarez-Barreto JF, Linehan SM, Shambaugh RL, Sikavitsas VI. Flow perfusion improves seeding of tissue engineering scaffolds with different architectures. Ann Biomed Eng. 2007;35(3):429–42.

281. Godbey WT, Hindy SBS, Sherman ME, Atala A. A novel use of centrifugal force for cell seeding into porous scaffolds. Biomaterials. 2004;25(14):2799–805.

282. Housler GJ, Miki T, Schmelzer E, Pekor C, Zhang X, Kang L, et al. Compartmental Hollow Fiber Capillary Membrane–Based Bioreactor Technology for In Vitro Studies on Red Blood Cell Lineage Direction of Hematopoietic Stem Cells. Tissue Eng Part C. 2012;18(2):133–42.

283. Nold P, Brendel C, Neubauer A, Bein G, Hackstein H. Good manufacturing practice-compliant animal-free expansion of human bone marrow derived mesenchymal stroma cells in a closed hollow-fiber-based bioreactor. Biochem Biophys Res Commun. Elsevier Inc.; 2013;430(1):325–230.

284. Roberts I, Baila S, Rice RB, Janssens ME, Nguyen K, Moens N, et al. Scale-up of human embryonic stem cell culture using a hollow fibre bioreactor. Biotechnol Lett. 2012;34(12):2307–15.

285. Xue C, Kwek KYC, Chan JKY, Chen Q, Lim M. The hollow fiber bioreactor as a stroma-supported, serum-free ex vivo expansion platform for human umbilical cord blood cells. Biotechnol J. 2014;9(7):980–9.